

CONFERENCE

Compatibility of Propellants, Explosives and Pyrotechnics with Plastics and Additives

Picatinny Arsenal
Dover, New Jersey



DTIC QUALITY INSPECTED 4

December 3-4, 1974

DEPARTMENT OF DEFENSE
PLASTICS TECHNICAL EVALUATION CENTER
PICATINNY ARSENAL, DOVER, N. J.

AMERICAN DEFENSE PREPAREDNESS ASSOCIATION
NATIONAL HEADQUARTERS: Union Trust Building, Washington, D. C. 20005

19960229 043

PLASTIC
22870-22881

DEDICATION

This book is dedicated to Norman E. Beach, 1904 - 1973. Norman was a prominent figure in compatibility studies, first as chief of the Stability Laboratory at Picatinny Arsenal and then in compatibility data tabulation and publication. In this latter role, he served as editor in the DOD Plastics Technical Evaluation Center, also located at Picatinny Arsenal. A teacher, writer, artist, but in all, a man of great humanity, Norman Beach brought to any situation a positive attitude and a practical plan for accomplishment.

DISCLAIMER NOTICE



**THIS DOCUMENT IS BEST
QUALITY AVAILABLE. THE
COPY FURNISHED TO DTIC
CONTAINED A SIGNIFICANT
NUMBER OF PAGES WHICH DO
NOT REPRODUCE LEGIBLY.**

CONFERENCE

Compatibility of Propellants, Explosives
and
Pyrotechnics with Plastics and Additives

Picatinny Arsenal
Dover, New Jersey

December 3-4, 1974

(AMERICAN DEFENSE PREPAREDNESS ASSOCIATION)
NATIONAL HEADQUARTERS: Union Trust Building, Washington, D.C. 20005

PREFACE

The selection of materials to be used with explosives, propellants, and similar high energy compounds is generally based on the physical properties required of the resulting system. However, the ability to use a given material with a given high energy compound is ultimately determined by the compatibility of the two within the resulting system. There are two aspects of compatibility to be considered: the effect of the materials on the high energy compound, and the effect of the high energy compound on the materials.

Compatible materials are those that may be used in conjunction with high energy compounds and have no potential for interaction that could in a hazardous or environmentally unstable device. Traditionally, compatibility has been determined by predictive test techniques. For example, the effect of a high energy compound on a plastic material may be tested by exposing the plastic to the high energy compound at elevated temperatures, and at selected intervals removing samples and measuring properties considered critical to operation of the device. On the other hand, the effect of a material on the behavior of a high energy compound is not routinely determined and, in fact, has been the subject of extensive studies dating back to World War II. Mr. S. Axelrod of Picatinny Arsenal in his report, "Effects Produced Upon Explosives by Contact with Plastics, Report No. 1," dated December 1946, discusses use of the vacuum-stability test to evaluate compatibility. Miss Marjorie St. Cyr later published an early compilation of vacuum stability compatibility results in a report entitled, "Compatibility of Explosives with Polymers," dated March 1959. Also, several compilations of data have been published by PLASTECH, Sandia Labs. Picatinny Arsenal, and others. To this day, vacuum stability remains the most readily accepted test in predicting compatibility of materials with high energy compounds.

Many authors have noted the problems associated with determining compatibility by vacuum stability: the test takes too long to perform, it yields no kinetic data, and there is a propensity of some materials to absorb gasses, etc. Much work has been performed to correct these problems. The result has included a number of outgassing test variations as well as new techniques based on instrumental analysis. The goal has been a quantitative approach to compatibility testing that will allow meaningful statements as to the ability of a given system to perform reliably at some time in the future.

This conference is an attempt to review the current technology of evaluating the compatibility of materials with high energy compounds. The materials discussed here are plastics and related chemicals, but the test approaches are appropriate to all foreign ingredients including other high energy compounds. Hopefully, this conference will improve communications between the scientists studying the compatibility of materials and ultimately result in standardization of test techniques and data analysis.

The success of a conference such as this is dependent upon the authors willingness to publish the results of their work. Additionally, the support of Harrison C. Chandler, Jr., Firestone Tire and Rubber Company; Frank J. Lavacot, United Aircraft Corporation; Doug Ayer, Naval Ordnance Station, Indianhead; Harry Pebly, PLASTEC; and the American Defense Preparedness Association staff is gratefully acknowledged.

Frank Swanson
Honeywell Inc.
December 19, 1974

AGENDA

MONDAY, 2 DECEMBER 1974

1800 Registration - Lobby, Holiday Inn
to Parsippany, N. J.
2200

TUESDAY, 3 DECEMBER 1974

0815 Registration - Picatinny Arsenal Auditorium Lobby
0900 Opening Remarks - F. D. Swanson, Honeywell Inc. -
Program Chairman
0905 Welcome - Col. J. Holman, Commander, Picatinny Arsenal
0910 Keynote Address - W. Powers, Chief, Materials Engineering
Division, Picatinny Arsenal

SECTION I

GAS EVOLUTION TESTS FOR COMPATIBILITY

Session Chairman: Tom Massis, Sandia Laboratories

		<u>Page</u>
0930	"Compatibility of Plastic Gun Ammunition Components with Energetic Materials" - D. E. Ayner and S. E. Mitchell, Naval Ordnance Station, Indian Head, MD.	I-A-1 <i>ju</i>
1000	"Comparison of Analytical Techniques for Testing Compatibility of Plastics with High Energy Materials" - John H. Fossum and Walter Y. Wen, Honeywell Inc., Hopkins, MN.	I-B-1 <i>PL- 22871</i>
1030	"Long Term Compatibility Testing of Double Base Propellants" - Kenneth P. McCarty, Hercules Incorporated, Magna, UT.	I-C-1
1111	Coffee Break	
1115	"Recent Development in Vacuum Stability Testing" - William Merrick, Atomic Weapons Research Establishment, Aldermaston, United Kingdom	I-D-1
1145	"The Influence of Metals on the Thermal Decomposition of S-Triaminotrinitrobenzene (TATB)" - E. D. Loughran, E. M. Wewerka, R. N. Rogers, and J. K. Berlin, Los Alamos Scientific Laboratory, Los Alamos, NM.	<i>I-E-1</i> <i>ju</i>

*pl-22870 = add 420286
add 420287-420297*

1215

"Testing of Plastic, Composites, and Coatings for Use in Naval Ordnance" - Benjamin D. Smith, Naval Weapons Laboratory, Dahlgren, VA.

Page

I-F-1

1245

Luncheon

PL-22872

SECTION II

CHEMICAL KINETICS

Session Chairman: Al Camp, Naval Ordnance Station, Indian Head, MD.

Page

1400

"Compatibility and Chemical Kinetics" - R. N. Rogers, Los Alamos Scientific Laboratory

II-A-1

1430

"Pentaerythritol Tetranitrate (PETN) Stability and Compatibility" - D. M. Coleman, Monsanto Research Corporation, Miamisburg, OH. and R. N. Rogers, Los Alamos Scientific Laboratory

II-B-1

1500

"Chemical Degradation of Nitramine Explosives" - Suryanarayana Bulusu, Feltman Research Laboratory, Picatinny Arsenal

II-C-1

1530

Coffee Break

1545

"Effects of Dibutyl Tin Dilaurate on the Thermal Decomposition of RDX" - Gaylord J. Knutson and Russel M. Potter, Air Force Armament Laboratory, Elgin AFB, FL.

II-D-1

1645

"Explosive and Physical Properties of Polymer-Coated RDX" - Andrew F. Smetana and Thomas C. Castonina, Feltman Research Laboratory

PL-22873
II-E-1

1720

Return to motels

1900

Reception and Banquet - Holiday Inn

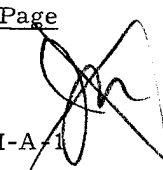
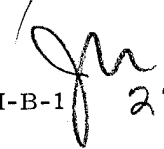
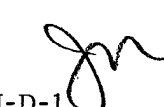
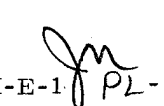
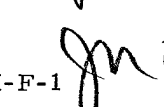
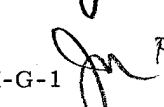
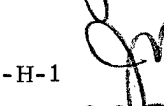
Honored guest and speaker will be Brig. General Robert Malley, Project Manager for Munitions Production Base Modernization and Expansion.

WEDNESDAY, 4 DECEMBER 1974

SECTION III

POLYMERS WITH ENERGETIC MATERIALS

Session Chairman: Raymond Rogers, Los Alamos
Scientific Laboratory

		Page
0830	"Elastomer Fluid Containment Materials for Energetic Liquid Rocket Propellants" - J. K. Sieron, Air Force Materials Laboratory, Wright Patterson AFB, OH.	III-A-1 
0900	"The Effect of Explosives and Propellants on the Tensile Properties of Polymers" - D. Sims and A. L. Stokoe, Explosives Research and Development Establishment, Waltham Abbey, United Kingdom	III-B-1  PL-22874
0930	"The Determination of Binder Degradation in Plastic-Bonded Explosives" - E. M. Wewerka, E. D. Loughran, and J. W. Williams, Jr., Los Alamos Scientific Laboratory	III-C-1
1000	"The High Explosive Compatibility of Some Rigid Polyurethane Foams" - E. R. Thomas, Atomic Weapons Research Establishment, Aldermaston, United Kingdom	III-D-1  PL-22875
1030	Coffee Break	
1045	"Response of Some Polyurethanes to Humid Environment" Henry P. Marshall and Larry Jensen, Lockheed Palo Alto Research Laboratory, Palo Alto, CA.	III-E-1  PL-22876
1115	"Effects of Additives on Polyacetals by TGA" - Albert S. Tompa and David M. French, Naval Ordnance Station, Indian Head, MD.	III-F-1  PL-22877
1145	"The Compatibility of PBX-9404 and Delrin" - Donald J. Gould, Thomas M. Massis, and E. A. Kjeldgaard, Sandia Laboratories, Albuquerque, NM.	III-G-1  PL-22878
1215	"Liquid, Heavily-Fluorinated Epoxy Resins for High Energy Applications" - James R. Griffith, Naval Research Laboratory, Washington, D. C.	III-H-1  PL-22879
1245	Luncheon	

SECTION IV

STABILITY OF ENERGETIC MATERIALS

Session Chairman: Harry Pebly, PLASTEC,
Picatinny Arsenal

Page

1400

"Long Term Effects of Silicone Oil on PETN" -
Henry S. Schuldt, Robert J. Burnett, Sandia Laboratories,
and Billy D. Faubson, Pantex AEC Plant, Amarillo, TX.

IV-A-1

1430

"The Effect of Humidity on the Performance of HNAB" -
Thomas M. Massis, Donald J. Gould, and William D.
Harwood, Sandia Laboratories

IV-B-1

1500

"Demonstration of Computer Compatibility Data Retrieval
Program" - Julian L. Davis, George Brincka, and
David W. Levi, Picatinny Arsenal

PL-22880
IV-C-1

1530

Coffee Break

1545

"Compatibilities of Plastics and Energetic Materials in
Small Caliber Ammunition" - Wilmer White, Frankford
Arsenal, Philadelphia, PA.

PL-22881
IV-D-1

1615

"Compatibility Testing Techniques for Gasless
Pyrotechnics" - Thomas M. Massis, David K. McCarthy,
Donald J. Gould, and B. D. McLaughlin, Sandia
Laboratories

IV-E-1

1645

"A New Highly Stable and Compatible Smokeless Rocket
Propellant" - A. T. Camp, E. R. Csanady, and P. R. Mosher,
Naval Ordnance Station, Indian Head, MD

IV-F-1

1715

Conference Summary

1730

Adjourn

PROGRAM COMMITTEE

Frank D. Swanson, Honeywell Inc., Program Chairman

Richard E. Harmon, PPG Industries, Chairman, Materials Division

Frank J. Lavacot, United Aircraft Corp., Chairman, Propellants & Explosives Sections

Harrison C. Chandler, Jr., Firestone Tire & Rubber Co., Chairman, Plastics Section

*Program Proceedings courtesy of Honeywell Inc.

THE COMPATIBILITY OF PLASTIC GUN AMMUNITION COMPONENTS WITH ENERGETIC MATERIALS

D. E. Ayer and S. E. Mitchell
Naval Ordnance Station
Indian Head, Maryland

ABSTRACT

Two Navy case studies concerning the compatibility of plastics with Navy propellants are discussed. The studies emphasize problems encountered with traditional compatibility tests and recommend general areas that should be pursued in order to improve these tests.

1. INTRODUCTION

This paper outlines the background, data generated, conclusions reached, and procedural details for two compatibility case studies conducted by the Gun Systems Engineering Division, Naval Ordnance Station, Indian Head, Md. One study concerned the determination of the compatibility of an adhesive used to affix a polyethylene foam wad in place above a propellant bed. The second study examined the compatibility of a polyurethane foam employed in the fabrication of ammunition components used with propellants.

The purpose of this paper is to reinforce the argument that there is a great need for systemization of compatibility testing and the creation of a central clearing house for the dissemination of compatibility data.

2. BACKGROUND

As the Navy's principal designer, developer, and evaluator of gun ammunition propelling charges, the

Naval Ordnance Station, Indian Head, is particularly concerned with the compatibility of energetic materials with plastics. Those plastic components of the gun ammunition propelling charge that are routinely evaluated for compatibility with propellants include: the cartridge case closure plug, the wad, cartridge case coatings, adhesives, and sealants. In addition, a number of other plastic materials examined in R&D programs have been evaluated for compatibility with propellants.

Indian Head has generated compatibility data with polymers and three types of gun propellants (single-base, double-base, and modified double-base), as well as black powder and pyrotechnic priming compositions. Those families of plastics that have been investigated include polyurethanes, epoxies, polyolefins, polyesters, vinyls, and polyamides, both with and without numerous combinations of additives.

The compatibility of a propellant/polymer combination is determined by employing a combination of test

techniques that include: differential thermal analysis, thermal gravimetric analysis, differential scanning calorimetry, Taliani nitrogen analysis, heat tests, vacuum stability testing, and surveillance testing, if time allows. All of these data are collected and a composite compatibility sheet is prepared.

The final decision on compatibility is always the responsibility of the project engineer. If the compatibility of a particular plastic/energetic material combination is in doubt, the project engineer will call for an informal conference of cognizant personnel from each of the special test areas in an effort to resolve the compatibility question. It is at this point that the dilemma often arises as to whether or not incompatibility exists. Generally, historical information as to the compatibility of a particular combination of materials is not available in the literature and the opinions of the individual specialists in attendance are often mixed.

3. DISCUSSION

The relative locations of plastic ammunition components employed in the propelling charge of conventional Navy ammunition appear in Figure 1. Two components, the plug and the adhesive, will be the subject of two interesting case studies on the compatibility question with which our office has dealt.

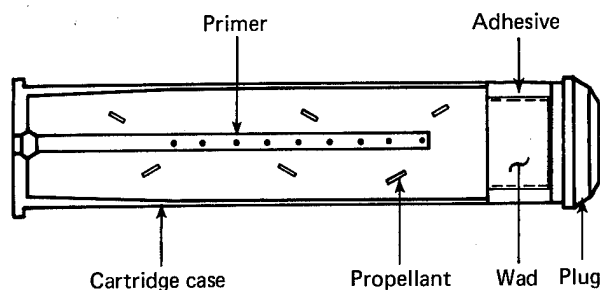


FIGURE 1. TYPICAL NAVY
PROPELLING CHARGE

3.1 THE PLUG

The cartridge case plug protects the lip of the cartridge case as the round is cycled through the gun's automatic handling system. It is important that the physical properties of the plug are not deleteriously affected by the propellants, owing to the extensive physical loads to which the plug is subjected. The rounds are typically cycled in a 5-inch rapid-fire mount from three stories below deck to the loading tray where they are rammed home in the gun breech at a velocity of 22 feet per second.

Cartridge case closure plugs are molded of polyurethane foam. A typical formulation is polyester/TDI (toluene diisocyanate) based, employing an η -methylmorpholine catalyst and is water blown.

Historically, polyurethane, similar to the foam system described above, has been rated as incompatible with many Army and Navy propellants.⁽¹⁾ Further, when Naval gun ammunition is assembled, propellant grains are often trapped between the plug and wad, creating a potential for the propellant to contact the plug. Therefore, the historical compatibility information becomes extremely important to the ammunition designer and must be verified.

In 1971 and 1972, interest in alternate polyurethane foam systems to that one traditionally used in cartridge case closure plugs prompted an extensive compatibility test effort. The classic vacuum stability test was complimented with additional compatibility test techniques including differential scanning calorimetry (DSC), differential thermal analysis (DTA), Taliani nitrogen analysis, and surveillance. Summaries of these test procedures are presented in Appendixes A through E.

The corresponding composite compatibility sheet for two double-base propellant formulations (Appendixes F and G) is presented in Table I. The conflicting subjective compatibility ratings that appear in Table

I were based on the data summarized in Table II.

It is the paradox created by the differing results shown here for the various tests that must be resolved. The problem is further emphasized with a case study concerning the compatibility of adhesive with propellants.

Table I

COMPOSITE COMPATIBILITY SHEET
POLYURETHANE FOAM CARTRIDGE CASE PLUG
MATERIAL WITH DOUBLE-BASE PROPELLANTS

Propellant technique	DTA	Taliani	Vacuum stability	DSC	80° C surveillance
M-26	I	I	I	C	C
SGP-20	I	-	I	M	C

Key:

C - Compatible

I - Incompatible

M - Marginal Compatibility

Table II

SUMMARY OF COMPATIBILITY TESTING SGP-20 AND M-26 WITH
POLYURETHANE FOAM PLUG MATERIAL

Material	DTA			Taliani slope	Vacuum stability reaction	DSC*	80° C surveillance (days)
	Temperature to ignition (°C)	Temperature at $\Delta T > 0$ (°C)	Breakaway temperature (°C)				
M-26 alone	151.0	135	120	0.97	-	-	49-151
SGP-20 alone	162.0	135	120	-	-	-	178-183
Plug + M-26	149.0	129	100	2.49	6.54	1.0	155
Plug + SGP-20	152.4	130	120	-	3.08	0.75	600

* Ratio of satisfactory to total no. test results based on statistical analysis of test data of control versus propellant plus plastic (including variance, parallelism, coincidence, and straight line fit).

3.2 THE ADHESIVE

The adhesive (noted in Figure 1) is used to affix both the wad and plug to the cartridge case. It further serves as a seal between the propellant and the atmosphere. The adhesive that has been documented for this use in nearly all Navy propelling charges is a one-part, ketone solvent, nitrile rubber based adhesive manufactured by 3M Company and designated Scotchgrip-1099 Brand Plastic Adhesive. This adhesive conforms to the requirements of government specifications MIL-A-13883, Type 1, and MMM-A-189A. Adhesive 1099 is routinely used in Navy ammunition depots to assemble components in 5-inch, 54-caliber; 5-inch, 38-caliber; and 8-inch, 55-caliber propelling charges.

In September of 1971, our office was informed that a number of 5-inch, 54-caliber propelling charges were loaded for fleet use employing adhesives other than the 1099, but in accordance with documentation that allowed use of an "equivalent" adhesive. Indian Head was tasked to determine the compatibility of the substitute adhesives with two single-base propellants, Pyro and NACO (Appendixes H and I), used in the fleet. The substitute adhesives used in the 5-inch assemblies are given in Table III.

As a preliminary screening method, vacuum stability testing was conducted on the adhesives. The results are outlined in Table IV. Based on results of the preliminary vacuum stability testing, Ultrabond 76-125C was designated as incompatible with single-

base propellants. Those rounds assembled with Ultrabond were classed in a "restricted" status until further verifying compatibility data could be generated.

Table III

ADHESIVES USED AS ALTERNATES TO 3M-1099

Adhesive	Type	Manufacturer
Loxite 703-487	Nitrile (acetone)	Firestone Tire and Rubber Co.
Ultrabond 76-125	Nitrile-phenolic (acetone)	General Adhesive and Chemical Co.
SC 840	Butadiene acrylonitrile (acetone)	H. B. Fuller Co.

Table IV

VACUUM STABILITY SCREENING OF ADHESIVES FOR COMPATIBILITY WITH SINGLE-BASE PROPELLANTS*

Adhesive	Reactivity with		Rating
	NACO	Pyro	
UB 76-125C	2.44	2.51	Incompatible
Lox 703-487	0.14	nil	Compatible
SC 840	0.07	nil	Compatible
3M-1099	nil	nil	Compatible

* Sample size of 0.5 gram propellant and 0.5 gram of adhesive.

Four subsequent duplicate vacuum stability tests were conducted on the Ultrabond plus single-base propellants with nearly identical results to those reported in Table IV. Further, as a compatibility check, DTA's were run on all the adhesives with NACO and Pyro propellant and those data are presented in Table V.

Based on the results of the DTA and vacuum stability testing, the Ultrabond was selected as requiring further evaluation. The Ultrabond was subjected to DSC analysis by Honeywell along with a sample of the standard adhesive 3M-1099. A statistical analysis of the test data led to the compatibility ratings assigned in Table VI.

Table V

DTA RESULTS ON SINGLE-BASE PROPELLANTS AND ADHESIVES

Sample	Breakaway temperature (°C)	Temperature to ignition (°C)	Rating
Pyro propellant alone	110-120	160-164	-
NACO propellant alone	110-120	159-162.5	-
UB 76-125 + NACO	112	160.1	Compatible
UB 76-125 + Pyro	110	155.5	Marginal
3M-1099 + Pyro	100	158.5	Compatible
3M-1099 + NACO	110	160.5	Compatible
Loxite 703-487 + NACO	110	160.5	Compatible
Loxite 703-487 + Pyro	110	156.7	Compatible
SC 840 + Pyro	100	154.0	Marginal
SC 840 + NACO	100	155.7	Marginal

Table VI

DSC STATISTICAL COMPATIBILITY RATING OF ADHESIVE WITH SINGLE-BASE PROPELLANTS

Adhesive	Propellant	Rating
3M-1099	NACO	Marginal
3M-1099	Pyro	Incompatible
UB 76-125	NACO	Compatible
UB 76-125	Pyro	Incompatible

With the problem of conflicting compatibility information, there was no recourse but to place all assemblies loaded with Ultrabond in a "hold" status. Further, it was necessary to report that all rounds of Navy gun ammunition in the fleet were loaded with an adhesive (3M-1099) whose compatibility with propellants was suspect. However, after a delay of 60 days required to conduct accelerated surveillance tests at 80° C, both adhesives were judged compatible with single-base Navy propellants. This was also borne out by the 65° C surveillance testing.

4. CONCLUSIONS AND RECOMMENDATIONS

The difficulties in determining the compatibility of plastics with energetic materials has been shown in the two Navy case studies presented here. There are numerous other similar examples of conflicting compatibility data that this office could cite that have perplexed Navy project engineers. It is, with these examples in mind, that we urge a reevaluation of even the basic meaning of the term compatibility and recommend that present test techniques be constructively criticized.

Chemical compatibility test techniques must be refined in order to be a meaningful tool for the project engineer. Further, more reliable compatibility test methods with shorter turn-around times on results must be found. A central clearing house for compatibility data, available to all the military services, must be established and supported. Finally, we must continue on an annual basis a forum for the exchange of information between cognizant individuals.

Appendix A

VACUUM STABILITY TEST PROCEDURE SUMMARY USED BY NAVAL ORDNANCE STATION, INDIAN HEAD, MD.

1. Weigh 5.00 grams of propellant and 0.50 gram of plastic into separate, clean, dry, test tubes.
2. Heat at 90° C for 48 hours under vacuum and measure volume of gas evolved in milliliters (ml).
3. Combine the same weights of each of the respective materials in a clean dry test tube and apply step 2.
4. Record the reactivity as the arithmetic difference between 3 and 2.

5. If the reactivity exceeds 5.00 ml, the materials are considered "incompatible." Reactivity in excess of 1.00 ml is a "marginally compatible" reading.

Appendix B

DIFFERENTIAL SCANNING CALORIMETRY PROCEDURE SUMMARY USED BY HONEYWELL, INC.

1. Cut 15-milligram (mg) sample from plastic test specimen and combine with 5 mg of the propellant; crimp into a standard DSC sample pan.
2. Scan sample as per standard DSC as used with a Perkin-Elmer Model DSC-1BU procedure, from room temperature to decomposition at heating rates of 80°, 40°, 20°, 10°, 5°, 2.5°, and 1.25° C/min.
3. The temperature at which the decomposition rate reached its peak exotherm is then recorded.
4. Corrected data from each propellant and propellant-plastic combination are then Fortran programmed to calculate activation energy, frequency factor, and reaction rate constant at any temperature. The program is also used to predict the extent of the decomposition reaction over any desired period of time at any temperature via the Arrhenius rate equation.
5. Steps 1 through 4 are repeated with a control sample (the propellant alone).
6. The criterion for judging a plastic/propellant combination to be compatible is that there be no statistical differences between the control and test sample data.

Appendix C

DIFFERENTIAL THERMAL ANALYSIS PROCEDURE SUMMARY USED BY THE NAVAL ORDNANCE STATION, INDIAN HEAD, MD.

1. Weigh and combine 1.8 grams of propellant and 0.2 gram of plastic to be evaluated into a test cell.
2. Heat the combination of plastic/propellant along with a reference sample of glass beads (of about the same volume as the test sample) at the rate of 1° C/min.
3. Plot the temperature of the sample minus the temperature of the reference versus the temperature of the reference sample.
4. The corresponding curve may be analyzed for slope, temperature to ignition, and breakaway temperature. This information is compared to similar information generated on the propellant alone, and a subjective decision as to the compatibility of the plastic/propellant combination is made.

Appendix D

AUTOMATIC TALIANI ANALYSIS PROCEDURE SUMMARY USED BY THE NAVAL ORDNANCE STATION, INDIAN HEAD, MD.

1. Weigh 1.00 gram of propellant and 0.10 gram of plastic into separate, clean, dry test tubes.
2. Flush with nitrogen and heat at atmospheric pressure (and at constant volume) and 110° C, for time required to generate 100-mm (Hg) pressure for a maximum of 5 hours.
3. Plot the pressure versus time of the test sample and repeat with the propellant alone.

4. The corresponding curves are analyzed for slope and a decision as to the compatibility of the propellant/plastic combination is made.

Appendix E

SURVEILLANCE PROCEDURE SUMMARY USED BY THE NAVAL ORDNANCE STATION, INDIAN HEAD, MD.

1. Weigh and combine 45 grams of propellant and 4.5 grams of plastic in a clean, dry 1/2-liter jar.
2. Heat the sample at 80° or 65.5° C and survey on a daily basis for observation of brown fumes.
3. Record and compare the number of days, from sample entry to fuming, with that of a standard (propellant alone).
4. A decision as to the compatibility is based on a comparison of the number of days that it takes the test sample to fume against the propellant alone.

Appendix F

M-26 PROPELLANT COMPOSITION

<u>Ingredient</u>	<u>Percentage</u>
Nitrocellulose	67.25 ± 1.80
Type*	I
Grade	C
Nitroglycerin	25.00 ± 1.00
Ethyl centralite	6.00 ± 0.50
Barium nitrate	0.75 ± 0.20
Potassium nitrate	0.70 ± 0.25
Graphite	0.30 ± 0.10
Total volatiles (max)	
Type I	2.00
Type II	1.50
Moisture (max)	0.70

* Type I: Cylindrical multiple-perforated grain.

(REF: MIL-STD-652A: Propellants, Solid)

Appendix G

SGP-20 PROPELLANT COMPOSITION

<u>Ingredient</u>	<u>Percentage</u>
Nitrocellulose (12.0)	46.0 \pm 1.25
Metriol trinitrate	38.5 \pm 1.00
Triethyleneglycol dinitrate	3.0 \pm 0.030
Dibutyl phthalate	8.1 \pm 0.50
Ethyl centralite	2.0 \pm 0.30
Basic lead carbonate	1.0 \pm 0.20
Potassium sulfate	1.3 \pm 0.20
Candelilla wax	0.1 \pm 0.05
Moisture	0.5 max

Appendix H

PYRO PROPELLANT COMPOSITION

<u>Ingredient</u>	<u>Percentage</u>
Nitrocellulose (12.6)	100.00 nominal
Diphenylamine	1.0 \pm 0.10
Basic lead carbonate	0.75 \pm 0.15
Total volatiles	5.0 max

Appendix I

NACO PROPELLANT COMPOSITION

<u>Ingredient</u>	<u>Percentage</u>
Nitrocellulose (12.0)	93.75 nominal
n-Butyl stearate	3.0 \pm 0.3
Ethyl centralite	1.0 \pm 0.2
Basic lead carbonate	1.0 \pm 0.2
Potassium sulfate	1.25 \pm 0.2
Water	3.0 max, 1.0 min
Total volatiles	5.0 max

REFERENCE

- (1) St. Cyr, Marjorie C., Compatibility of Explosives with Polymers with Addendums, TR 2595, Feltman Research and Engineering Laboratories, Picatinny Arsenal, Dover, New Jersey, March 1959.

BIOGRAPHIES

D. E. AYER: Born in Nashua, N. H., August 5, 1943. Received B. S. in Chemistry from Lowell Technological Institute in 1967. Has also attended the University of New Hampshire, George Washington University, and New York University. Employed by Sprague Electric Company in plastic R&D, 1963-1967; Naval Ordnance Station 1967 to present in pilot plant processing, plastic application, plastic ordnance component design. Presently plastics technologist in the Special Programs Department. Holder of patents in degradable plastics.

S. E. MITCHELL: Born in Olney, Ill., August 20, 1946. Received B. S. degree in Chemistry from Rose Polytechnic Institute in 1968. Employed by the Naval Ordnance Station, Indian Head, Md., from 1968 to the present in propellant R&D. Presently gun propellants technologist in the Special Programs Department.

A COMPARISON OF THE ANALYTICAL TECHNIQUES FOR TESTING THE COMPATIBILITY OF POLYMERS WITH HIGH ENERGY MATERIALS

John H. Fossum and Walter Y. Wen
Government and Aeronautical Products Division
Honeywell Inc.
Hopkins, Minnesota

ABSTRACT

Various methods have been used in our laboratories for testing the compatibility of polymers with high energy materials. These methods include the vacuum stability test, thermal methods, mass spectrometry, gas chromatography, chemiluminescence, colorimetry and spectrophotometry, and wet chemical methods. Often, using a combination of two or more of these methods has proven advantageous. This paper discusses the advantages and limitations of these methods.

1. INTRODUCTION

In the design and manufacture of devices containing high energy materials, such as propellants and explosives, it is critical that the materials used in the device be completely compatible with the high energy materials contained therein. Although much effort has been expended in developing methods for measuring compatibility, many of them have inherent shortcomings. Some examples of these shortcomings are that:

- (1) The method is empirical and based on unvalidated assumptions.
- (2) The method is not reproducible, especially from laboratory to laboratory.
- (3) The method is slow and cumbersome.
- (4) The method is too specific.
- (5) The definition of compatibility is arbitrary, etc.

This paper will describe the various methods used in Honeywell's Government and Aeronautical Products Division's (G&APD) laboratories to measure high energy material/polymer compatibility and will discuss their advantages and limitations

The methods to be discussed include vacuum stability techniques, thermal techniques (thermo-gravimetric analysis (TGA), differential scanning calorimetry (DSC), and differential thermal analysis (DTA), mass spectrometry, gas chromatography, chemiluminescence, colorimetry and spectrophotometry, and wet chemical methods. These methods have all been used with varying degrees of success. Often, a combination of two or more of the methods has increased the value of the data obtained.

2. EXPERIMENTAL METHODS

2.1 VACUUM STABILITY TEST

Glassware was built and Vacuum Stability Testing was conducted as described in MIL-STD-286B⁽¹⁾. Five grams of propellant were mixed with 0.5 gram of polymer. Both materials were ground in a Wiley mill and conditioned in a humidity room at 5 percent humidity. The mixture was heated to 90°C and maintained at that temperature, under vacuum, for 40 hours, after which the volume

of gas produced was measured.

2.2 THERMAL ANALYSIS TECHNIQUES

All materials tested by thermal methods were tested as received. The thermogravimetric equipment consisted of a Cahn RG electrobalance with a Perkin-Elmer furnace. A UU-1 program was employed and interfaced with a Honeywell H112 computer. The differential scanning calorimeter, a Perkin-Elmer model DSC 1B, was also interfaced with the Honeywell H112 computer. The differential thermoanalyzer was designed and built in Honeywell's Plastics Laboratory.

All thermogravimetric measurements were made in a nitrogen atmosphere, whereas the measurements taken with the differential scanning calorimeter and differential thermal analyzer were made in air. When conducting experiments in the computer-controlled mode, the data acquisition process was automatic. The details of this computer-controlled system have been described by Wen and Dole⁽²⁾.

2.3 MASS SPECTROMETRY

Most of the work on the mass spectrometry was conducted on a Dupont Model 21-492 medium resolution mass spectrometer interfaced with a Honeywell 716 computer. In studies involving the gas phase analysis of polymer and propellant mixtures, heated under controlled conditions, a limited amount of work has been done on a Honeywell-assembled quadrupole mass spectrometer equipped with a pulsed leak device.

The mass spectrometer was used in several modes of operation to measure material compatibility. The analysis of the rate of gas evolution and of the types of gas formed in an accelerated aging test under reduced pressure was carried out by mixing 5.0 grams of propellant with 0.5 gram of polymer in a Fisher-Porter tube. To

establish an internal standard, the tube was evacuated and backfilled with neon to a pressure of 20 Torr. The mixture was heated for two hours at 100°C, and the gas phase analyzed by directly introducing it into the mass spectrometer.

In a second mode of operation, a polymer/explosive mixture was placed in a capillary tube and inserted in the direct probe of the mass spectrometer. The probe was heated from 50°C to 600°C. Scans were made when change in total ion count indicated that increased amounts of materials were being given off. This method was modified in that the polymer and explosive were analyzed separately, before and after accelerated aging. In a third mode of operation, the effluent from the gas chromatograph was analyzed to identify those compounds formed during accelerated aging.

2.4 GAS CHROMATOGRAPHY

The analysis of the gases given off and pyrolysis products produced after accelerated aging was carried out in a Hewlett-Packard Model 7620A gas chromatograph equipped with electronic integrator. The gas chromatograph effluent splitter was connected to the mass spectrometer to permit identification of the various compounds separated. The detector was flame ionization, and the column used was 5 percent Carbowax 20M on Chromasorb G.

2.5 CHEMILUMINESCENCE

A McMillan Electronics Corporation chemiluminescent nitric oxide detector, Model 1400, with a minimum full-scale range of 100 ppm and a maximum full-scale range of 10,000 ppm, was used in the NO_x mode to determine the amounts of nitrogen oxides formed after accelerated aging of propellant/polymer mixtures. In these tests, one gram of propellant was mixed with 0.1 gram of polymer after grinding both

materials in a Wiley mill and conditioning them in the humidity room at 5% humidity. The mixture was placed in a Schwartz tube, and the tube evacuated. The tubes were heated to 100°F for one hour. After they cooled to room temperature, the tubes were filled to ambient pressure with dry nitrogen. The resulting mixture was then analyzed with the nitric oxide detector.

2.5 COLORIMETRY AND SPECTRO-PHOTOMETRY

The propellant and polymer were mixed and aged as described for the method of chemiluminescence. The gases produced were analyzed for nitrogen oxides by the Griess-Saltzman reaction as described in ASTM⁽³⁾.

2.6 WET CHEMICAL METHODS

The polymer was hydrolyzed chemically, before and after accelerated aging, and the reaction mixture analyzed by the gas chromatograph or gas chromatograph/mass spectrometer. For the polyurethane studied, the polymer was hydrolyzed by refluxing with phenethyl amine.

3. RESULTS AND DISCUSSION

A major difficulty in compatibility testing is the definition of compatibility. Small changes in decomposition rates may not be significant, even during prolonged storage periods of 10 or 20 years. In addition, incompatibility may affect either the polymer or the high energy material, or both. Over the years, more or less arbitrary standards of acceptability have been established; these probably define the term "compatibility" adequately.

3.1 VACUUM STABILITY METHOD

Although this method has been in use for nearly 100 years, it has serious disadvantages, some of which have been pointed out by Reich⁽⁴⁾ and Leutscher⁽⁵⁾. The method is based upon the

assumption that incompatibility will result in the formation of noncondensable gases. For a given system, this assumption may or may not be valid. Other disadvantages are long test times (40 hours) and poor reproducibility, especially between laboratories.

The vacuum stability method was used in our laboratories as a reference method in a study aimed at finding a faster, more reliable testing method. The study was performed for the Naval Ordnance Station at Indian Head, Maryland⁽⁶⁾.

3.2 THERMAL ANALYSIS TECHNIQUES

In general, the thermal decomposition kinetics of most explosives or propellants are extremely complex and their reaction mechanisms not clearly defined. Therefore, present analytical techniques for thermal analysis have been based on empirical methods. Leutscher⁽⁵⁾ assumed that if a chemical reaction occurred, heat would be produced. On this assumption, he designed a calorimeter to measure heat changes in a mixture of propellants and polymers while heating the mixture at 70°C for four days.

In thermogravimetric analysis, sample weight is monitored while heating at a programmed heating rate. It has been shown⁽²⁾ that if no reaction occurs between a high energy material and a polymer, when they are mixed and heated, the weight fraction remaining of a sample mixture can be calculated from Equation 1.

$$\alpha = \alpha_p + (1 - \gamma) \alpha_e \quad (1)$$

where α is the fraction of high energy material in the mixture, α_p is the fraction remaining in the control run of pure polymer, α_e is the fraction remaining in the control run of pure high energy material and γ is the fraction of the high energy material in the original mixture. If the polymer is compatible with the high energy material, the experimental curve of the mixture should overlap or somewhat, or lie underneath that calculated

from Equation 1. Obviously, Equation 1 is valid only when all measurements are performed with an identical heating rate.

Figure 1 shows the thermogravimetric curves of compatibility tests of two propellants, PYRO and NACO, with a polyurethane foam (Freeman Chemicals System 1732/1426). The results indicate that both PYRO and NACO have a thermal runaway temperature or deflagration point of approximately 445°K and that their mixtures with the foam deflagrate at slightly higher temperatures. At the deflagration point, about 10 percent of the original material has decomposed. The fact that the propellant-foam mixtures deflagrate at about the same temperature as the pure propellants suggests that the foam is compatible with both propellants, at least up to the thermal runaway temperature.

The differential scanning calorimeter measures the enthalpic effects of a material when it is heated. The compatibility criteria of this technique are based on the exotherm peak temperatures shown on the thermograms when a pure energetic material is compared with a mixture of this material with a polymer. A typical differential scanning calorimeter thermogram is shown in Figure 2. This curve measures the compatibility of EPON 815/U with Composition B. Pure Composition B showed an exotherm peak at 503°K. No observable enthalpy change was detected for EPON 815/U alone in the temperature range studied. The appearance of an exotherm peak at 487°K for the mixture indicates that the system is incompatible. The system had been tested by the vacuum stability method, and a value of 98.1 ml of gas evolved was reported⁽⁷⁾. According to current compatibility standards, this system would be considered to show excessive incompatibility. In using the differential scanning calorimeter for determining compatibility, it must be borne in mind that the peak temperature of an exotherm is affected by the heating rate and the effect is not necessarily linear. Nevertheless, the method is adequate for determining marginal compatibility of a system.

Differential thermal analysis also measures changes in enthalpy of a system during heating. Mixtures known to be compatible show a shift of the exotherm peak of 3°K or less. The curves obtained by differential thermal analysis of mixtures of NACO with methylene dianiline are shown in Figure 3. The shift in the exotherm peaks indicates that these materials are incompatible.

Table 1 summarizes the results by thermal analysis of some of the systems tested in our laboratories. Systems shown in this table represent both those with moderate incompatibility and those with excessive incompatibility, as measured by the vacuum stability test. Thus, the system Composition B/EPON 815/U has been reported to yield a net volume of 9.81 ml of gas and is thus considered excessively incompatible; whereas the system Composition B/Armstrong 6 was reported to yield a net volume of 4.77 ml and is thus considered to be moderately incompatible, when tested by the vacuum stability method⁽⁷⁾. These results indicate that thermal analysis methods can detect both moderate and excessive incompatibility. The weakness of the thermal techniques, however, is that they give no indication of the type of reaction occurring, or of the reaction products formed. In this respect, the methods are empirical.

3.3 MASS SPECTROMETRY

The mass spectrometer can be used in several ways to analyze high energy material/polymer compatibility. The mass spectrometer has the distinct advantage of identifying reaction products and characterizing starting materials. It thereby provides useful information for the more empirical methods.

During the study to find a faster method for determining the compatibility of PYRO and NACO with polyurethane foam⁽⁶⁾, the mass spectrometer was used in two ways: In the first method, it was used to show that when either of these two propellants is heated with an incompatible polyurethane foam,

nitric oxide is a major decomposition product. The second method utilized either the quadrupole or magnetic sector mass spectrometer to measure excessive nitric oxide production after accelerated aging. For quantitative determinations, neon was used as an internal standard.

Table 2 summarizes data obtained by various non-thermal methods for determining the compatibility of both compatible and incompatible polyurethane foams with NACO⁽⁶⁾.

A major difficulty encountered during this study was obtaining an incompatible foam. Incompatible foams were obtained by adding a large excess of the methyl morpholine catalyst to the polyurethane foam system. Although the results in the accompanying table show these foams to be moderately incompatible by the vacuum stability test, retest of the same material at the Naval Laboratories at Indian Head, Maryland gave results of over 6 ml of gas evolved for all systems containing excess catalyst. According to these results, the system would show excessive incompatibility.

It was originally hoped that a direct correlation could be obtained between the results from the vacuum stability test and those from other non-thermal methods. However, the variability of results obtained from the vacuum stability test prevented a correlation constant from being obtained. However, it is evident that an incompatible system shows a marked increase in the amount of nitric oxide formed in this system. By obtaining kinetic data, it may be possible to calculate an approximate change in shelf life of a given system due to incompatibility.

In other studies, the mass spectrometer, either by itself or coupled with the gas chromatograph, was used to measure pyrolysis products of the high energy material, and of the polymer before and after accelerated aging. Incompatibility can involve changes in either the polymer or the high energy material. Although the main concern is

usually whether the high energy material has been sensitized, changes in the polymer can also result in device malfunction. Therefore, this approach has the advantage of showing chemical reaction of either the polymer or the high energy material. The main difficulty encountered with this approach is interpreting the results of the pyrolysis. The problem is simplified, somewhat, by using the gas chromatograph to separate the pyrolysis products before mass spectrometer analysis, but this approach limits identification of the products to those sufficiently volatile to pass through the gas chromatograph.

In a study to evaluate the compatibility of Composition B with a battery electrolyte, the temperature at which violent reaction of Composition B occurred was measured using the direct probe of the mass spectrometer. For this method, a temperature-programmed probe is necessary to obtain reproducible results because the behavior of the high energy material depends upon the heating rate. The temperature at which this reaction occurs is easily determined by monitoring the total ion count, either from the computer readout or from the beam monitor. Examination of the scans at which a sudden increase in total ion count occurs shows the gaseous reaction products formed. This method is very similar to thermogravimetric analysis and has the advantage of giving information concerning the reaction products. The difference, of course, is that instead of measuring weight loss as in thermogravimetric analysis, one is measuring ion concentration by the evolution of volatile material in the ionization chamber of the mass spectrometer.

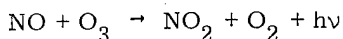
During this study it was found that after accelerated aging, the Composition B sensitized in that the temperature of sudden volatilization was lowered significantly. In addition, by accelerated aging of each of the components of the electrolyte with the Composition B, it was possible to determine those components having a sensitizing effect on the Composition B.

3.4 GAS CHROMATOGRAPHY

Should volatile decomposition products be formed during accelerated aging, they can be separated and measured with the gas chromatograph. If available, this instrumentation can be adapted readily for routine compatibility testing. Identification of the reaction products can be a problem, and, in this case, the use of the mass spectrometer in conjunction with the gas chromatograph is recommended.

3.5 CHEMILUMINESCENCE

If nitrogen oxides are the main products of decomposition during accelerated aging, the chemiluminescence method is ideal for routine compatibility testing. In evaluating various methods for rapid routine testing of NACO and PYRO with polyurethane foam⁽⁶⁾, this was the recommended method, for it is simple, rapid and does not require elaborate instrumentation. The chemiluminescence method is based on the reaction:



In the presence of an excess of ozone, the radiation intensity is directly proportional to the concentration of NO. NO_x concentrations may be obtained by catalytically converting any NO₂ which may be present to NO prior to analysis.

It was somewhat surprising in studying this system that NO was the primary product of decomposition. Very little NO₂ was formed, possibly because NO₂ is sufficiently acid to react with the inhibitor used with the propellant and form a nonvolatile salt. Such a reaction would also have an adverse effect on the use of the vacuum stability test to measure incompatibility.

The main limitation of this method of compatibility testing, of course, is that for the test to be valid an oxide of nitrogen must be formed in the decom-

position process. This limitation can inhibit the more general use of this test, but, when applicable, it is ideal.

The high sensitivity of this test, as well as some of the others we have used (such as mass spectrometry and gas chromatography), enables one to reduce the time required for accelerated aging tests. Whereas 40 hours and relatively large amounts of explosives are required for the vacuum stability test, 1 or 2 hours and much less material are required for these more sensitive methods.

3.6 COLORIMETRY AND SPECTROPHOTOMETRY

The use of these methods in our laboratories has been limited to employment of the Griess-Saltzman reaction for the detection and measurement of the oxides of nitrogen. In this respect, their applicability is similar to that of chemiluminescence. The advantage of these techniques is that special instrumentation is not required, as most laboratories have available some type of colorimeter or spectrophotometer. Their main disadvantage is the preparation and maintenance of the reagents required for the reaction.

3.7 WET CHEMICAL METHODS

These methods have had very limited use in our laboratories for compatibility testing. In general, they lack the sensitivity and speed of the various instrumentation methods.

One exception, however, is the use of wet methods to convert compounds having limited volatility to more volatile ones which can be easily tested by methods such as gas chromatography and mass spectrometry. An example of this approach is the hydrolysis of a polyurethane in phenethyl amine to give readily volatile monomers. This method will probably not show changes in molecular weight of a polymer during accelerated aging with a high energy material. However, other changes or

differences from one lot of polymer to another should be readily detected.

Should the hydrolysis product be a relatively non-volatile monomer, such as a carboxylic acid, it may be necessary to convert this material into a more volatile compound, such as an ester.

4. BIBLIOGRAPHY

- (1) MIL-STD-286B, 1 December 1967, Method 403.1, 2, "Vacuum Stability Tests (90 and 100°C)."
- (2) Wen, W. Y. and Dole, M., "Computer Techniques for Kinetic Studies in Thermal Analysis and Radiation Chemistry of High Polymers," Computers in Chemistry and Instrumentation, Vol. VI, J. S. Mattson, H. B. Mark, Jr., and H. C. MacDonald, Jr., ed, Marcel Dekker, New York, in progress, 1975.
- (3) 1973 Annual Book of ASTM Standards, D1607-69. "Standard Method of Test for Nitrogen Dioxide Content of the Atmosphere (Griess-Saltzman Reaction)," ASTM, Philadelphia, Pa, 1973 p 874.
- (4) Reich, L., "Compatibility of Polymers with Highly Energetic Materials by DTA," Thermochemica Acta 5, 433 (1973).
- (5) Leutscher, A., "Investigation into the Compatibility of Explosives in Mutual Contact," N74-26238 (Technol Lab RVO-TNO, Rijswijk, Neth) Dec 1973, p 34.
- (6) Fossum, J. H., Keller, R. P. and Wen, W. Y., "Accelerated Compatibility Test for the MK12 Plug and Propellants," Final Report: Contract No. N00174-74-C-0168, Naval Ordnance Station, Indian Head, Md., August 1974.

- (7) Beach, N. E., and St. Cyr, M. C., "Compatibility of Explosives with Polymers: A Guide to the Reactions Reported in Picatinny Arsenal Technical Report 2595, March 1959," Picatinny Arsenal, New Jersey, October 1970, p 6.

5. BIOGRAPHIES

5.1 JOHN H. FOSSUM

Dr. Fossum received the degree of Bachelor of Chemistry from the University of Minnesota and his PhD, with a major in organic chemistry and a minor in analytical chemistry, from the State University of Iowa. Over the past 35 years, he has had broad experience in research and development, in both organic and analytical chemistry as well as in technical management. Currently, he is principal chemist for the Government and Aeronautical Products Division of Honeywell Inc. In his current capacity, he is responsible for the technical adequacy of the output of the Division's chemical laboratory.

5.2 WALTER Y. WEN

Walter Y. Wen received a BS in Chemical Engineering from Cheng-Kung University Taiwan, in 1963; a PhD in Physical Chemistry from the University of Oregon in 1971. During 1972, he was a research associate in the Department of Chemistry at the University of Oregon and 1973 at Baylor University. His work at Baylor included areas such as radiation chemistry of polymers, laboratory automation techniques, and computer methods for analyzing complex kinetic problems. Currently he is a plastics engineer at the Government and Aeronautical Products Division of Honeywell Inc. He has been actively studying various data analysis techniques for thermal analysis, including differential scanning calorimetry, differential thermal analysis, thermogravimetric analysis, and thermomechanical analysis.

He is responsible for the development of computer-controlled thermal analysis equipment and data processing techniques at Honeywell's Plastics

Laboratory. He is also interested in techniques for testing mechanical properties of polymers under high loading rates.

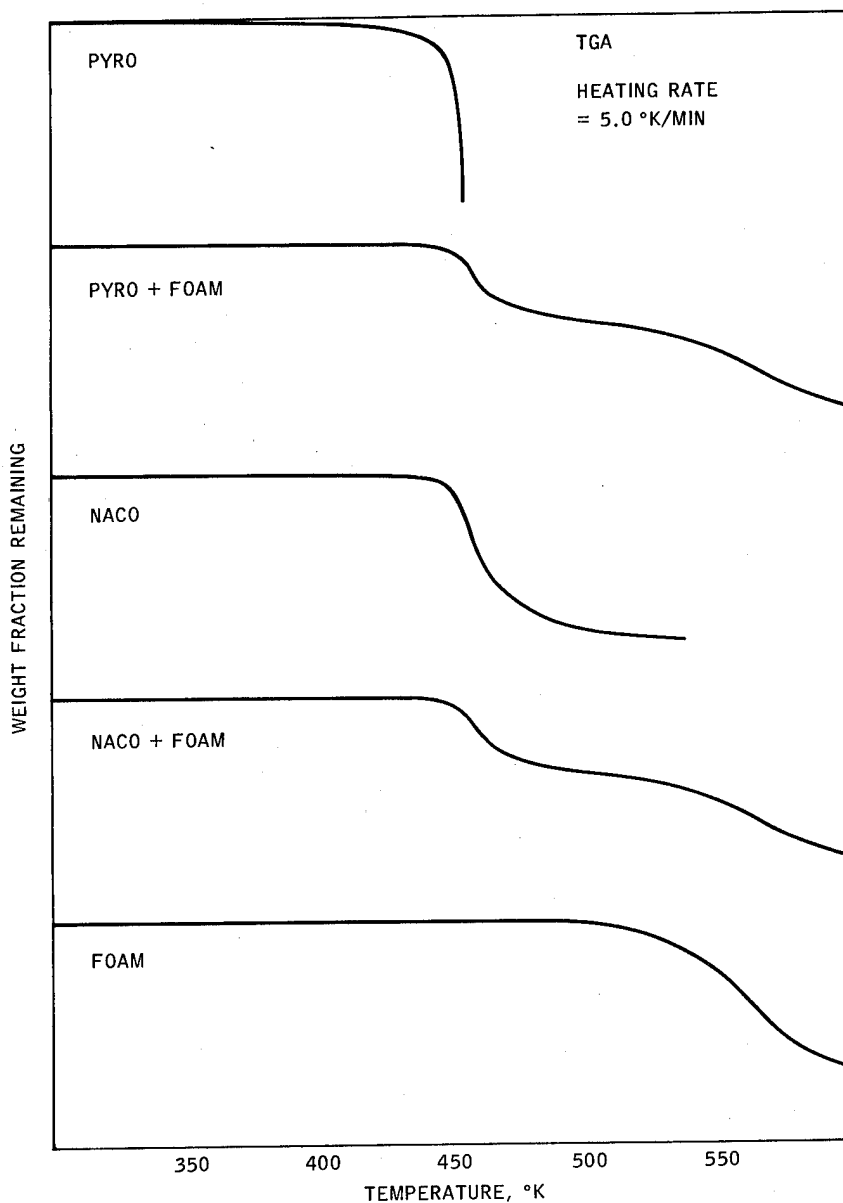


Figure 1. Thermogravimetric Curves for Compatibility Tests of PYRO and NACO with Polyurethane Foam

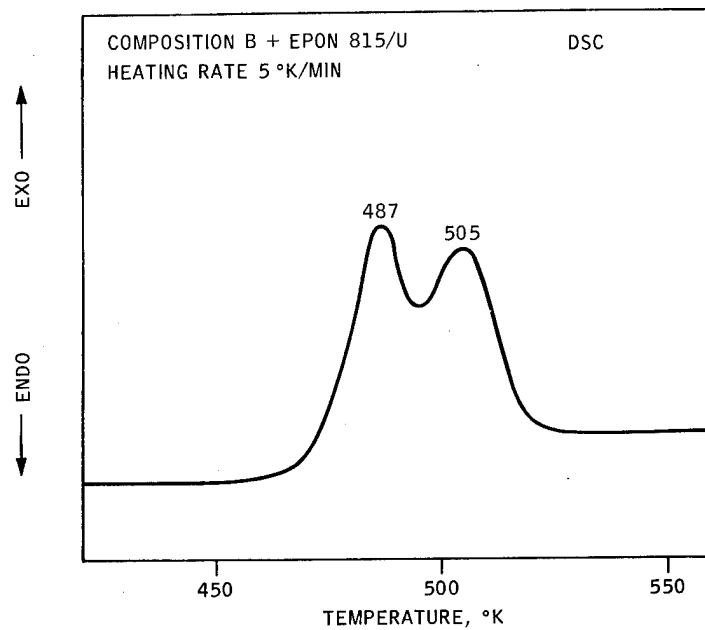


Figure 2. Differential Calorimeter Thermogram Showing Compatibility of EPON 815/U with Composition B

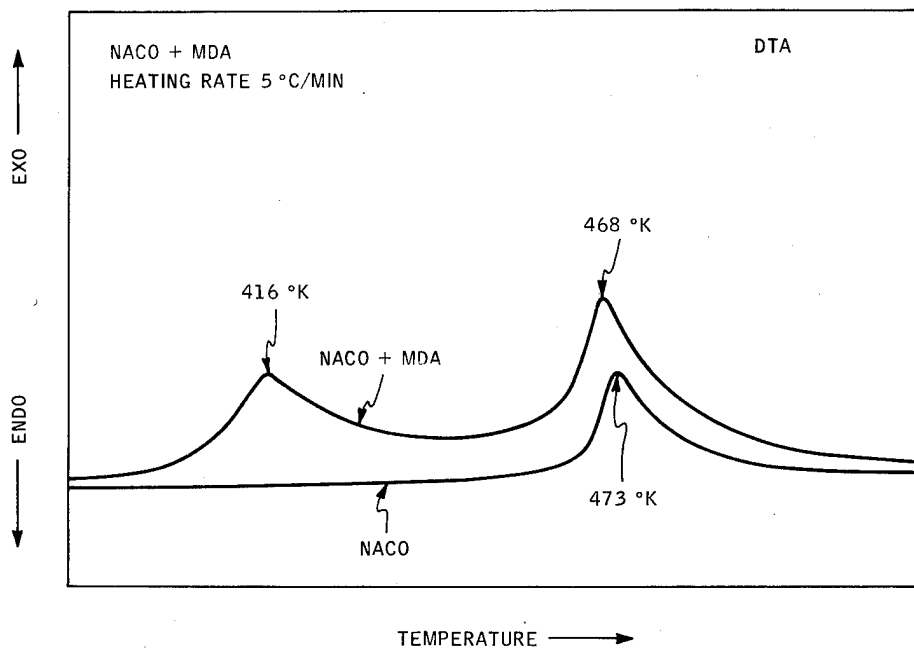


Figure 3. Curves from Differential Thermal Analysis of NACO/Methylene Dianiline Mixtures

Table 1. Results of Compatibility Test on High Energy Materials with Various Inactive Materials as Measured by TGA, DSC, and DTA.

<u>High Energy Material</u>	<u>Inactive Material</u>	<u>Test Method</u>	<u>Compatibility</u> ^a
NACO	MDA	DSC, DTA	-b
NACO	Polyurethane	TGA, DSC, DTA	+b
NACO	Teflon	TGA, DSC, DTA	+
PYRO	Teflon	TGA, DSC, DTA	+
PYRO	Polyurethane	TGA, DSC	+b
Composition B	Epon 815/U	DSC, DTA	-d
Composition B	Li Electrolyte	TGA, DSC	-c
Composition B	Armstrong 6/E	DSC, DTA	-d
Cyclotol	Caytur 22	TGA, DSC	-b

a - "+" compatible, "-" incompatible

b - Agrees with vacuum stability tests performed at Honeywell Inc.

c - Agrees with mass spectrometry tests performed at Honeywell Inc.

d - Agrees with vacuum stability tests of Reference 7

Table 2. Comparison of Compatibility Data by Various Methods

<u>System</u>	<u>Vacuum Stability</u>	<u>Griess-Saltzman Reaction</u>	<u>Chemiluminescence</u>	<u>Mass Spectrometry</u>
NACO + Correct Mix Polyurethane Foam (0.1% Catalyst)	-0.25 ml	.250 μ moles	.1 μ moles	Ratio Peak Heights AMU30/AMU20 1.32
NACO + Polyurethane Foam Containing Excess Catalyst				
6% Catalyst	2.1	.276	.670	2.08 (5% Catalyst)
7% Catalyst	2.2	----	.360	3.36
8% Catalyst	3.0	.312	.480	
9% Catalyst	2.5	.404	.510	3.27
10% Catalyst	3.6	.289	1.080	6.63

LONG TERM COMPATIBILITY TESTING OF DOUBLE-BASE PROPELLANTS

By Kenneth P. McCarty
Hercules Incorporated
Bacchus Works
Magna, Utah

ABSTRACT

Short term accelerated aging tests are useful for compatibility screening, but results can be misleading if applied to long-term aging. Several examples are presented where the normal high temperature gassing tests failed to detect double-base propellant incompatibility which showed up on longer term storage. Analysis of the mechanism of double-base propellant decomposition and a comparison of observed safe-life with stabilizer depletion times is used to show that stabilizer depletion measurement is an effective means of detecting long term propellant incompatibility.

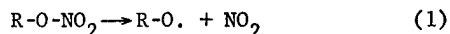
DISCUSSION

Short-term accelerated aging tests are useful for rapid detection of incompatible materials involving double-base rocket motor propellants. However, reactions that have low activation energies and hence low temperature dependence will not be observed in short-term high temperature compatibility testing. Longer term tests of temperatures approaching the use-temperature are needed. High temperature gassing tests such as the German tests, the Taliani, and the modified Taliani tests have been successfully used to avoid compatibility problems in the manufacture of double-base propellants and rocket motors containing double-base propellants. Materials of marginal compatibility may not be detected in high temperature gassing tests. Such incompatibility can be due to physical effects as well as chemical, as illustrated by the following examples. In one case an RTV rubber that showed good stability in the modified Taliani test (a measurement of the gas generated on 23 hour storage at 93.3° C or 200° F) showed a rapid loss of stabilizer because the stabilizer migrated from the propellant to the rubber. As a result, the safe life was

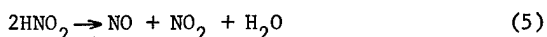
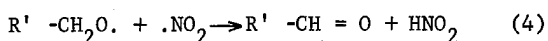
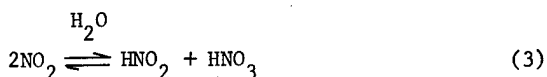
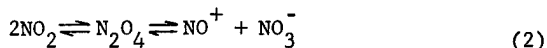
decreased. Chemical incompatibility was observed in a second case. Severe chemical degradation was observed in propellant in contact with a Teflon coating. The stabilizer content was observed to be much lower (0.2 percent) than expected from the temperature time history and in addition, a high concentration of stabilization product was observed at the surface. The bulk of the propellant was normal (0.54 percent stabilizer). The cause was traced to small amounts of soluble chromic acid on the surface of the Teflon. Such an incompatibility had not been observed previously, since the chromic acid is normally volatilized in the coating process. The incompatible condition was reproduced by intentionally modifying the coating process to leave soluble chromic acid on the Teflon surface. The modified Taliani test did not indicate incompatibility, but chemical degradation and rapid stabilizer depletion were observed as before. A routine check of Tefloned surfaces for soluble chromic acid prevented a recurrence of this condition.

The failure of high temperature gassing tests to detect long-term incompatibility can be understood

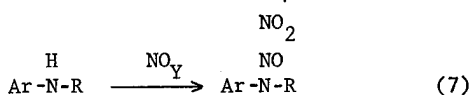
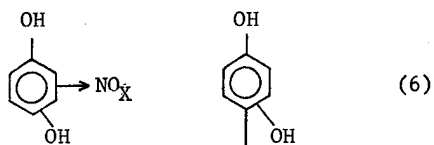
by examining the chemistry of double-base stabilization. The first step in the decomposition of double-base propellant is a breakdown of the nitrate ester to form nitrogen dioxide



a variety of nitrogen oxides and acids can be formed by subsequent reaction of the NO_2



The propellant decomposition is autocatalytic. If the nitrogen oxides are allowed to accumulate, rapid decomposition is observed. Effective stabilizers for double-base propellants are nitrating and nitrosating agents that scavenge the nitrogen oxides.



The exact form of the nitrating or nitrosating agent in the stabilization process has not been demonstrated. As long as an active stabilizer is present, no gas buildup is detected and autocatalytic decomposition is not observed.

Stabilizer depletion in double-base propellant is a pseudo zero order reaction. An Arrhenius plot of stabilizer depletion of typical double-base propellants shows that the activation energy is about 35 Kcal/mole which corresponds to the O- NO_2 bond energy in the nitrate ester. The results indicate that the nitrate ester decomposition is

the rate-determining step, as would be required for good stabilization. If the nitrogen oxide content is to be kept low, the reaction of the stabilizer with the nitrogen oxide must be faster than the rate of nitrogen oxide production by nitrate ester decomposition. Since the nitrate ester content is in excess, the rate of reaction does not change significantly during the life of the stabilizer and an apparent zero order reaction is observed.

As long as an active stabilizer is present no gas buildup is detected and autocatalytic decomposition is not observed. As is shown in the Arrhenius plot of stabilizer life in Figure 1, except at very high temperatures (over 100° C), runaway reaction and cookoff does not occur until the stabilizer is depleted. The time for the modified Taliani test (23 hours at 93.3° C) is also shown in Figure 1. The stabilizer will not be depleted and gases will not be evolved in this time at the normal nitrate ester decomposition rate. However, if an incompatible material is present, the nitrate ester will decompose more rapidly, the stabilizer will be depleted more rapidly, and a gas pressure will be observed in the modified Taliani test. Extrapolation of the modified Taliani conditions with an activation energy of 35 Kcal/mole (as shown in Figure 1) shows that the modified Taliani test is equivalent to 10 years at 100° F. However, if the activation energy is lower, the modified Taliani conditions represent considerably shorter times at use-temperatures. (For example, less than a year at 100° F for $E_a = 20$).

The activation energy for diffusion is about 10 Kcal/mole; therefore, rapid stabilizer loss due to diffusion at use-temperatures would not be detected by the modified Taliani tests as was observed with the RTV rubber. Chemical reactions leading to incompatibility may also have low activation energies as is evident in the case involving incompatibility with chromic acid.

A very effective method of avoiding long-term

compatibility problems with double-base propellants is to measure the stabilizer depletion rate. This method offers two major advantages: (1) Incompatibility can be detected early in the reaction thereby permitting safe life predictions from data at or near use temperature, and (2) stabilizer depletion measurements at a series of temperatures provide a means of extrapolation to lower temperatures. Hercules routinely ages "sandwiches" of propellant/casebond/insulator systems (or other materials that contact propellant) to determine stabilizer (and plasticizer) loss from the propellant. At selected time intervals, the stabilizer content is determined as a function of distance from the interface. This approach permits early detection of stabilizer migration or abnormally high stabilizer depletion rate due to chemical reaction to prevent problems in long-term aging.

Stabilizer depletion measurements at a series of temperatures will detect incompatibility regardless of the reason. If there is a direct incompatibility that could be a problem at use-temperatures, a higher than normal depletion rate or a low activation energy will be observed. This was the case with the chromic acid on the Teflon coating. The incompatibility existed but the stabilizer functioned as intended to prevent nitrogen oxide buildup and, in the process, prevented the

Dr. McCarty received a B.S. in Chemical Engineering from Lehigh University in 1949 and an M.S. in Chemistry in 1951. He then spent two years as a chemist with Trojan Powder Company, Allentown, Pennsylvania. At Edgewood Arsenal, with the U. S. Army, he performed technical investigations into the effects of solutions of monomolecular films. He was granted a Research Fellowship on Gaseous Diffusion at the University of Maryland from 1955 to 1959. This work led to a Ph. D. in Chemistry in 1961 at that institution.

modified Taliani test from detecting incompatibility. Stabilizer depletion measurements did detect incompatibility. If an inadequate stabilizer is used it will not scavenge all of the nitrogen oxides; the stabilizer depletion rate will be low. If the stabilizer itself tends to accelerate nitrate ester decomposition (as is the case for a strong aromatic amine) the stabilizer action will prevent gassing and hence no incompatibility will be indicated in the modified Taliani test, but a high stabilizer depletion rate will be observed. In a chemical reaction that does not involve the nitrate ester directly, but generates enough heat to be hazardous, stabilizer depletion measurements will still detect the potential problem. The heat generated will accelerate the nitrate ester decomposition and because of the high activation energy, the resulting increased stabilizer depletion rate will be readily apparent.

In summary, a combination of the modified Taliani test and stabilizer depletion measurements has been very successful for avoiding compatibility problems with double-base propellants. The modified Taliani test is an effective method of rapidly screening for compatibility and has ensured safety in propellant and rocket motor development. Longer term stabilizer depletion measurement has ensured adequate compatibility for the long storage times required in use.

In 1959, Dr. McCarty started his employment with Hercules as Senior Research Chemist at Allegany Ballistics Laboratory investigating propellant combustion problems. He was transferred to the Home Office, Wilmington, Delaware in 1962 as Technical Assistant to the Director of Development for the Chemical Propulsion Division.

In 1966, Dr. McCarty was transferred to Bacchus Works as Superintendent of Propellant and Process Development.

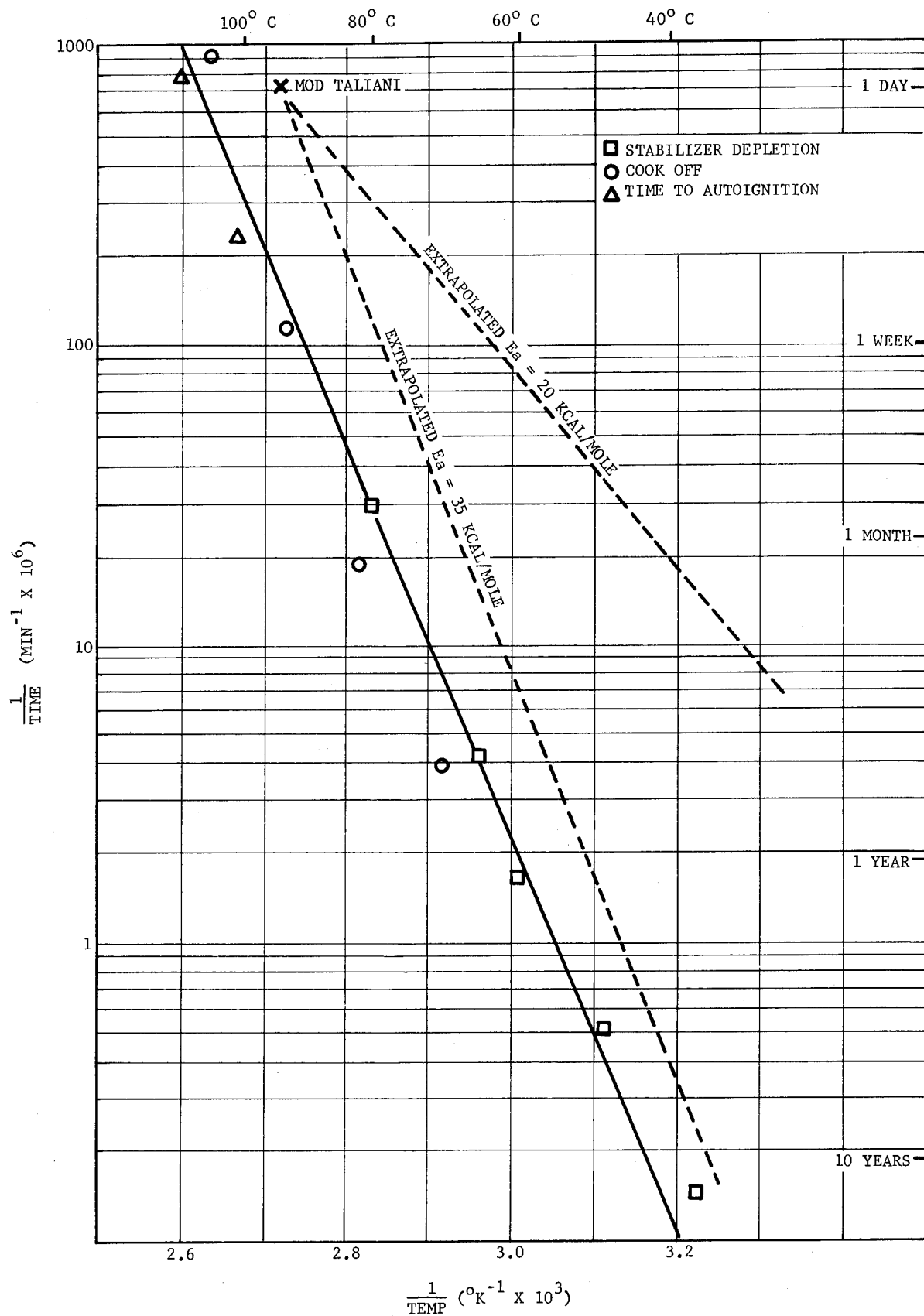


Figure 1. Safe Life

RECENT DEVELOPMENTS IN VACUUM STABILITY TESTING

W Merrick
Ministry of Defence (Procurement Executive)
Atomic Weapons Research Establishment
Aldermaston, England

ABSTRACT

The history of the development of the vacuum stability test in the UK is traced and reservations concerning the manner in which the test is variously applied to HE stability and compatibility testing are discussed. Recent developments have led to the updating of the apparatus in most UK establishments by the introduction of pressure transducers and in some cases data logging equipment. The modified equipment comprising heating tube and transducer assembly is compact and can be transferred after test to a vacuum rig which permits the separation, collection and identification (if required) of the liquid and gaseous products. This ancillary procedure is of value in comparing the chemical reactivity of materials where the products are liquid as well as gaseous. It may also provide better correlation between the physical and chemical properties of the material and its reactivity with explosives than the traditional gas only assessment.

1. INTRODUCTION

In the United Kingdom the assessment of the thermal stability of explosives or mixtures of explosives and other materials as in a compatibility test requires known weights of the explosives or the mixtures to be heated under certain specified physical conditions and the volumes of gas produced to be measured. The relevant specifications lay down limits for the quantities of gas allowed and these limits apply to the use of engineering materials in explosive assemblies. The underlying principle is that the evolution of gas is the accepted criterion for comparing the chemical instabilities of explosives in the vacuum stability test and of mixtures in a compatibility test. These tests work well in practice. They are quick and cheap to perform and the assessment of the results in terms of the relevant specification is in general unambiguous. For many years the results have been used to

assess the stability of explosives for both specification and research purposes and have been a significant factor, both inside and outside AWRE, in deciding if a particular material is sufficiently chemically unreactive and therefore 'compatible' to be incorporated safely in a given environment involving explosive. It has become accepted in the course of time that the amount of gas evolved on heating an explosive is the basic criterion of stability. It is one purpose of this paper to give some consideration to the philosophy involved in this type of stability testing and another to refer to a simple modification and extension of the apparatus so that it employs modern equipment and allows it to be used for assessing some of the non-gaseous products.

2. BACKGROUND

2.1 Early references to the routine use of a mercury manometer for explosive stability assessment was by Obermuller in 1904⁽¹⁾ and 1910⁽²⁾.

In the UK, Farmer published work in 1920⁽³⁾ in which he applied the technique to assessing the thermal stability of production batches of the explosive tetryl. The test was virtually the same as the present day test; the gas criterion was used and was almost ideally suited to the purpose. The volume of gas evolved was related to the small quantities of impurities in various batches of the explosive. It was found that small quantities of tetranitro phenyl methyl nitramine which could be present as an impurity in the trinitrophenyl methyl nitramine (tetryl) accelerated the decomposition of the tetryl at 100°C as well as decomposing 25 times as fast as tetryl itself. The test was simultaneously a test for the intrinsic stability of the tetryl and for the quality of the batch. Since the former is a constant the test becomes in practice a comparative one for the latter. This test was most satisfactory from both the theoretical and practical points of view because it was coupled with a limit on the volume of gas allowed which was specific for tetryl. The method has with equal justification been applied to the production control of other explosives. Such applications are thoroughly sound provided a corresponding limit on the gas evolution is applied which is specific for the explosive. This assumes that variations in the reactivity observed are due to the same impurities or crystal quality defects present in differing quantities and are related to the amount of explosive decomposed. The volume of gas is then an indicator of the amount of chemical decomposition and reaction which has taken place and therefore of the 'stability' of the sample.

2.2 If the test is now extended to make comparisons between the thermal stabilities of different explosives by comparing their respective gas evolutions, the original justification does not strictly apply. This is because different explosives do not produce the same gas volume for a given amount of decomposition, and moreover the ratio of gaseous to other decomposition products

varies for all explosives. The possibility of getting decomposition products other than gaseous ones should not be overlooked. It may be expected that the main decomposition products from an explosive are gaseous since the primary function of an explosive is to produce a large amount of hot gas quickly. However under the conditions of vacuum stability testing we have sometimes noticed the presence of condensates in the manometer tubes, the contribution of which to the quoted 'gas evolution' is somewhat fortuitous being dependent on the design of the apparatus and on the vapour pressure of the liquid. Some of this may be moisture or solvents from the explosives tested but these cannot be distinguished from products of reaction unless quantitative work is performed, including control samples. Variations in the gas composition from different explosives will also add to the errors of a gas volume measurement used as the basis for assessment of explosives decomposition.

2.3 The same basic criticism in comparing explosives by gas evolution applies to compatibility tests, the difference being one of degree rather than principle. In the standard UK compatibility test the sample contains 5% of deliberately added impurity - the impurity being the non-explosive material under test. Other testing establishments in some cases use 50% of non-explosive sample in the standard mix for testing.

2.4 The purpose of the present programme, of which this paper is intended to be an introduction, is to validate the test as far as possible by a study of those parameters referred to earlier and to develop a more meaningful test whilst retaining the speed and cheapness of the present test. It is hoped that such a test will be applicable routinely, if desired, to any solid explosive or mixture of explosive and adulterant.

3. RELATED WORK

3.1 The concept of total volatile products has

been appreciated in principle by many workers. There are many examples of investigations in which stability or chemical reactivity studies have been conducted so as to take account of these factors. In many cases this is also combined with the concept that volatile reactants shall not be removed from the reaction vessel by condensation in the cooler parts of the system and in these cases the reactants and the products are all kept at the test temperature. Provided the reaction vessel is sufficiently large to allow vaporisation of all the liquid products of the reaction at the test temperature, then such methods give reliable estimates of the total volatile products of the reaction. A well-known example of this type of test is the Taliani type apparatus^(4,5,6) in which the reaction is performed in air at a pressure somewhat above atmospheric. The apparatus is however complicated compared with the very simple vacuum stability apparatus and probably for this reason is not widely used whereas the vacuum stability test is a standard test in very many countries. A limitation of many of the designs of enclosed apparatus (and also of the standard vacuum stability apparatus) is that there is no provision for removal from the reaction vessel of the volatile contents nor for their separation into gas and volatile liquids so that they can be separately estimated and analysed. There are many examples of the totally enclosed versions of reactivity apparatus reported, but for the purpose of this paper no useful purpose would be served by attempting to provide detail or references to them. However some reference should perhaps be made to the simplest of all techniques - because of its simplicity- that of weighing a sample before and after heat treatment and its more recent extension to thermogravimetric analysis. Both these methods allow for the estimation of the total volatile products.

3.2 In its original and simplest form as published by A P Sy in 1903⁽⁷⁾ for nitrocellulose powders, losses of up to ten per cent were involved over a period of 68 days of heating. This is

however a very different case from its use as a stability or compatibility test for application to high explosives where small fractions of one per cent are looked for from quantities of sample of the order of 5 grams or smaller. Apart from the evident objection that all volatile products or even reactants are completely removed from the reaction zone, there are also the problems of weighing sufficiently accurately the small losses in weight from relatively large sample masses in a suitable containing vessel. If this were applied to a compatibility test on a mixture of explosive and sample six weighings would be involved for a complete assessment. This led to the introduction by Guichard⁽⁸⁾ in France in 1926 of a built-in automatic recording balance and the development in recent years into the sophisticated designs of thermogravimetric analysis apparatus^(9,10). Such apparatus is however expensive and although valuable for special investigations in no way competes with the simple vacuum stability test when large numbers are to be tested for compatibility with explosives.

3.3 There are of course concepts for dealing with compatibility problems other than evaluating the products of reaction such as methods dependent on the changes which occur in the explosive properties of a system or an explosive when heated, but these are outside the scope of this paper.

3.4 Having made the above brief survey of the various types of stability test it is perhaps worth while surveying the problem more generally, making some reference to the great deal of work done by many workers using modern techniques which lead to separation and/or identification of the products of reaction.

3.5 To start at the beginning it might be asked why the products of decomposition should be estimated when what one really wants to know in the general practice of stability testing and also in reaction kinetics (as distinct from work on reaction mechanisms) is how much explosive has

decomposed. Why not estimate the undecomposed explosive? The answer is clear and is that in spite of all the remarkable developments in analytical chemistry, it is still not possible to analyse with sufficient accuracy the total quantity of explosive left at the level of decomposition of interest for safety and compatibility purposes. Under conditions of more gross decomposition such as in the determination of velocity constants or reaction mechanisms there are certainly methods of sufficient accuracy but these problems are not of major interest in the context of this paper. To verify the sort of precision attainable some work was done at AWRE on the assay of one unadulterated explosive⁽¹¹⁾. The method was essentially a classical volumetric technique. The explosive chosen was PETN because it was considered that this explosive could probably be estimated with at least as good precision, and probably better, than the nitroaromatic or nitroamine type explosives. The details are noted in the Appendix A and this shows that for a discrimination of 0.1% at the 95% level of confidence 17 replicates would be required. It may well be that this precision could be improved but the results are a long way from being sufficiently precise to compete with the vacuum stability test. With the AWRE apparatus a change in pressure of 1 mm of mercury is equivalent to about 0.03 ml of gas or 10^{-3} per cent decomposition. Methods other than volumetric analysis can be used to estimate the total residual explosive but all suffer from the lack of adequate sensitivity; in particular, liquid and thin layer chromatography and, in suitable cases, gas chromatography. Methods for estimating the unreacted explosive have one further problem in common. They are complicated by the presence in the residue of all the products of reaction. Each method developed has to be specific for the particular explosive and in the case of compatibility tests would have to be suitable in the presence of the adulterant which is different in every case and is frequently of unknown and complicated composition.

3.6 It therefore follows that we are constrained to dealing with the products of decomposition. We

have already referred to the pressure measuring and gravimetric approaches to the problem but a large amount of work has been done using chromatographic techniques for separating and/or estimating the products of the reaction. With quantitative improvement, any one of these could conceivably lead to a new general approach for particular applications and it is worth while making some reference to these. Some of these techniques are already at or near to this stage.

3.7 Thin layer chromatography has been widely investigated by many workers^(12...25) and in some cases applied quantitatively. With eluents specially selected for the system and with modern quantitative instrumentation for dispensing micro-litre quantities of solutions which virtually eliminate creep-back and capillation errors⁽²⁶⁾ together with densitometer measurement of spot intensities, a great deal of useful work can be done on separating and identifying the products of decomposition. In suitable cases accuracies of the order of a few per cent can be achieved and since the method is essentially one for minute quantities of material this is a suitable accuracy for the small amounts of decomposition products involved. The identification of the constituents may be integral with the technique when the chemistry of the system is known, such as in the estimation of the dimer and trimer of PETN or of the lower nitrated penta-erythritols. Other techniques can also be applied to the spot after removal from the plate.

3.8 In applications where some suitable degree of volatility of the constituents is involved, gas chromatography has been pursued. This method is quantitative within the limits of the technique used and the response of the material, and can again give accuracies of a few percent. Because of the volatility limitation this technique has found application to DNT, TNT, PETN, glycol esters, NC^(27...32) rather than the essentially involatile nitramine explosives.

3.9 A promising technique which is also applicable to involatile explosives is liquid chromatography.

Useful information on the technique in general is given by the various manufacturers and an introduction to the technique is given in a book by Hadden and reviewed in Analytical Chemistry in 1973⁽³³⁾.

In all the above chromatographic techniques a spectroscopic method can be applied to the separated material. Mass spectrometry and infra red are the most selective^(34,35) but where applicable UV spectroscopy can be applied more quantitatively. Mass spectrometry and UV usually consume the least material.

3.10 The above general picture of the 'state of the art' in stability testing gives some impression of the present trends. All the methods are sound within their known limitations, but in spite of all these the very simple vacuum stability apparatus persists and shows no sign of being replaced. Indeed the reverse is true. The test is considered of sufficient interest to warrant a great deal of consideration being given under the auspices of NATO to bringing about a uniform detailed testing technique. This is because, although the basic technique is essentially the same in various countries and within a country, there are many variations in the conditions of use such as time and temperature, the quantity or composition of the explosive or the mixture, sample preparation and the formula used for sentencing etc. The work at AWRE has had one overriding premise - namely that any modified test which might be developed should include an assessment identical with the standard test. It is fortunate that this view was taken since the modification finally proposed will now be applicable to any revised NATO version of the test.

3.11 If then we accept that there is some value in adhering to the vacuum stability test with all its known disadvantages (which will not be discussed here because this is a separate and controversial topic on its own), we can proceed to the AWRE approach to the problem. In brief this has been to separate and determine the quantity of liquid and gaseous material in the reaction tube

and not the solids. For the purposes of this paper only essentially solid explosives have been considered. Now it is quite practicable to devise a single technique which will separate out from a mixture of solids, liquids and gases those components which are gaseous and liquid. Such a method can depend on the vapour pressure differences involved. This can be done irrespective of the chemical composition, and depends solely on adopting a practical definition of what is to be called 'liquid' and 'gas'. On the other hand it is not possible to have a single method applicable to any mixture for separating the solid decomposition products from the original solid reactants since this must depend on the chemistry of the various solid components present. These are all different and, except for the original explosive and in a few cases the sample, are unknown. This is a natural limitation of this type of system which has no simple solution.

3.12 The problem with the conventional VS apparatus is that it is cumbersome and awkward to handle and not designed to take off the products for separate examination. To overcome these defects a study was made of alternative methods of pressure measurement and as a result the mercury manometer has been replaced by a small pressure transducer. This modification at once makes the apparatus more portable and also updates it since it can then be used with data logging devices.

4. EXPERIMENTAL

4.1 The experimental technique for measuring gas and liquid products has been described at another Symposium in 1973⁽³⁶⁾ and will be available when the Proceedings are published. A general summary only of the apparatus will therefore be given here but some features of both the apparatus and the technique quoted at the earlier Symposium will be updated.

4.2 In the conventional apparatus we have a reaction tube and a mercury-filled manometer. In the

modified apparatus the manometer is replaced by a small pressure transducer⁽³⁶⁾. The two are connected by an adapter. At AWRE this is a simple glass adapter⁽³⁶⁾ with a side arm for evacuation. At other UK establishments various designs of metal adapters^(38,39,40), and in one case a PTFE (TEFLON) one⁽³⁷⁾, are in use or under development. In some cases these are fitted with pressure release safety valves^(37,39,40) and sometimes a rubber septum^(39,40). At the present time the various designs cannot be considered finalised. No problems have been found with the AWRE glass adapter which has no release valve and at present no rubber septum. The internal volume of the assembly should be the same as the conventional apparatus which it replaces, so that any autocatalytic effects due to decomposition products are the same as in the conventional apparatus. The output from the transducer is fed to a multi-point recorder in the AWRE apparatus but this is replaced by a digital voltmeter⁽³⁷⁾ or data logging equipment with print-out^(38,39) at some other UK establishments. A data logger is expected to be in use at AWRE in the near future. The output is interpreted as a volume of gas either by calculation from the recorder or digital voltmeter reading, or more simply as a direct print-out in the case of the data logger. Where the data logger is chosen to include individual channel adjustment for zero and sensitivity, the calibration can be made particularly easy and rapid. A known volume of dry air is introduced into the evacuated apparatus by means of an accurately calibrated gas syringe via the rubber septum in the adapter. The assembly is then placed in the usual heating bath to attain the normal working temperature differential. The sensitivity control on the data logger for the particular channel in use is then adjusted so that the read-out corresponds to the volume of air injected after correction to standard temperature and pressure. This procedure eliminates all calibration of the assembly for volume and temperature which is necessary for the recorder and DVM techniques⁽³⁹⁾. The procedure described so far corresponds to the conventional test.

4.3 The second and new procedure is now commenced. The assembly is removed from the heating bath and the tube cooled to minus 80°C, with a mixture of trichloroethylene and solid carbon dioxide, to obtain the pressure corresponding to the 'permanent gas'. The assembly is then transferred to a vacuum rig⁽³⁶⁾ and with the tube still kept cold the permanent gas is either evacuated to waste or is sampled. Any condensed material is then distilled out of the reaction tube and into a 'U' shaped tube packed with glass beads, by heating the reaction tube and cooling the 'U' tube to minus 80°C. The reaction tube and transducer assembly is then replaced by a preweighed and evacuated small tube⁽³⁶⁾ about 1 ml capacity fitted with a vacuum tap and joint (a 'cold finger condenser') which is cooled to minus 80°C. The cold bath is removed from the 'U' tube which is allowed to warm to room temperature and a back distillation commences into the cold finger and when this is complete the cold finger is weighed. The whole process is monitored by a Pirani gauge. Care must be taken at the final stage not to overcool the cold finger condenser so as to avoid condensation on the 'wrong' side of the tap. Quantitative recovery of milligram quantities of solvents was achieved by this technique with a wide range of solvents from the ethyl alcohol ($v_p = 5.3 \text{ KN/m}^2$ or 40 mm Hg) to gamma butyro lactone ($v_p = <0.01 \text{ KN/m}^2$ or $<0.1 \text{ mm Hg}$) and with weights from a few mg to tens of mg.

4.4 It may be useful to other workers interested in this part of the technique to note here that a considerable amount of development work preceded the final technique as described above. Before the introduction of the transducer, the reaction was performed in a sealed vacuum stability reaction tube with no pressure measuring device and at the end of the heating period this was transferred to a vacuum rig. The permanent gas was then measured by a volumetric-pressure technique while keeping the tube cold to retain condensible matter. The latter was then expanded into known volumes until it was completely gaseous and its pressure measured. The volume was then converted to a hypothetical 'gas volume' at NTP - under which conditions it was

in fact likely to be liquid. Subsequent to this the transducer was introduced for measurement of the gas and the liquid portion again measured by the expansion technique. This latter technique had the attraction that both the gas and liquid were assessed as volumes and were therefore additive. It was found however that although the methods could be operated to give satisfactory results they required a more complicated vacuum rig and a higher standard of vacuum technique than we felt was viable for general use. The method also did not produce a condensed sample of the liquid for identification purposes.

4.5 In the present technique the gas is assessed as a volume and the condensibles as a weight. If additivity of units is required the permanent gas can be analysed and its weight calculated or alternatively can be assumed to have some average density typical of the gases obtained from high explosives. Additivity is then achieved on a weight basis and this is of course relevant to calculation of percentage decomposition from the known weight of explosive taken.

5. RESULTS

5.1 The first part of the practical procedure, in which the mercury manometer is replaced by the transducer and the pressure readings interpreted as gas, has been applied to 47 mixtures involving 9 different high explosives and 13 different non-explosive adulterants. The results were compared statistically with corresponding data from the standard manometer test. This showed that the two methods produced comparable results⁽³⁶⁾.

5.2 The complete procedure including separation of the gas and condensible matter has been applied to 4 unadulterated explosives and 2 adulterated. The experimental figures are shown in Appendix B together with the results from a standard manometer test. Appendix C then shows an assessment of the total information available from the two types of test. No analysis of the permanent gas has been done from either set of results, and to calculate

the weight of the gas a weight of 2 mg per 1 ml of gas has been assumed. This is an approximately correct figure for the mixture of gases from PETN and RDX decomposition and is sufficiently near for the purpose for the other gas mixtures.

For the manometer test, the figures give a volume aggregate from the $1\frac{1}{2}$ h to $41\frac{1}{2}$ h readings of what is usually termed 'gas', plus material of unknown molecular weight. The latter is usually assumed to comprise water, solvent and other volatiles. Since the sample in the evacuated reaction tube takes a considerable time to reach the test temperature the amount of gas from the thermal decomposition in the initial 0 to $1\frac{1}{2}$ hour period should normally be negligible.

For the transducer test the figures give an assessment of the permanent gas as that which is not condensible at -80°C and a weight assessment of the condensible matter. The results show that RDX and HMX produce little or no 'volatile' matter other than permanent gas and the two methods thus give comparable results. In the case of PETN particularly at 120°C and for the mixture of Composition B and polycarbonate a large proportion of the gas volume in the conventional method is accountable for as liquid as shown in the last column of the table. It is considered that the breakdown into gas/liquid constituents which the new technique provides is a more objective analysis of the decomposition behaviour. The transducer test which gives a permanent gas volume and a weight condensate is in general a much closer approximation to the percentage weight decomposition of an explosive than that given by the usual volumetric stability test, although both fail to estimate solid decomposition products.

6. CONCLUSIONS

6.1 A new approach to vacuum stability testing is proposed incorporating a pressure transducer which can with ancillary apparatus produce a more objective assessment of the total products than the conventional manometer test. The method can at the

same time reproduce the normal test figure obtained from the conventional apparatus.

6.2 The technique should be of general applicability to thermal stability and compatibility testing of essentially solid materials and possibly liquids. The application of the method so far has given sufficient confidence to warrant its application to samples obtained routinely so that the degree of contribution from liquid components produced in reaction can be assessed.

ACKNOWLEDGMENTS

Acknowledgments are due to Mr J L Seymour for much of the development work on this topic and for much valuable discussion; and to Mr W V Chappell for most of the testing. The author also wishes to thank the Director, AWRE for permission to publish this work. Crown copyright reserved.

REFERENCES

1. J. OBERMULLER, MITT. BERL. BEZIRKUER, Ver. deutsch. Chem 1, 30 (1904).
2. J. OBERMULLER and B PLEUS, Z. ges. Schiess- u Sprengstoff 5 121 (1910).
3. FARMER, J. Chem Soc 1920. 117 1432 and 1603.
4. URBANSKI, Chemistry and Technology of Explosives, Pergamon Press 1965 Vol 2 page 28.
5. TALIANI, Gazz. chim. ital 51 1, 184 (1921).
6. GOUJON, Mém l'artill. Franc. 8 837 (1929).
7. SY, J. Amer. Chem. Soc. 25 549 (1903).
8. GUICHARD, Bull. soc. chim. France 19 1113 (1926).
9. Explosivestoffe, 1965 13 (8) 205.
10. URAKAWA, J. Ind. Expl. Soc. Japan, March 1967, 28 146-9.
11. WELCH - unpublished work.
12. J. Chromat. Dec 1967 31 pp 551-556. (NG, PETN and others).
13. J. Chromat. Dec 1967 31 pp 606-608 (nitrate esters - 2 dimensional technique).
14. Explosivestoffe, Sept 1966 p 193 (NG and nitroaromatics).
15. Explosivestoffe, Feb 1967 15 25-33 (nitrate esters and nitroaromatics).
16. Explosivestoffe, 1966 15 (nitrate esters and nitroaromatics).
17. Explosivestoffe, Feb 1962, 33-37 (nitrate esters and nitro bodies).
18. Anal. Chem. 36 No. 12 Nov 1964 2301-3 (PETN and related products).
19. J. Chromat. Nov 1967 31 120-7 (nitroaromatics).
20. Infcción Quím analit pura apl Ind, 1966 20 (4) 108-114 (nitrate esters and nitroaromatics).
21. J. Chromat. 1966 24 (1) 236-238 (aromatic compounds).
22. Nature, 216 5121 (1967) pp 1168-70 (a review).
23. Explosivestoffe 1967 15 (2) 25-33 (2 dimensional TLC of nitroaromatics).
24. Explosivestoffe, Jan 1971 (PETN).
25. J. Chromat. 38 (1968) 508-14 (polynitro aromatics).
26. Quantitative Paper and Thin Layer Chromatography - E J Shellard, Chapter 1, Academic Press 1968.
27. Anal. Chem. Sept 1967 39 (11) pp 1315-18 (TNT and DNT).
28. Anal. Chem. 36 No. 12 Nov 1964 2301-3 (PETN and related materials).
29. Mem. Poud. 1964-5 (1966) 46-47, 164-189 (aromatics).
30. J. Ind. Expl. Soc. Japan March 1967. 28 146-9 (pentolite).
31. Anal. Chem. Sep 1967 39 (11) p 1315-18 (TNT and DNT).
32. J. Chromat. Dec 1967 31 551-556 (glycol esters, NC, PETN).
33. Anal. Chem. Vol 45 No. 2 Feb 1973 p 213A.
34. Anal. Abs. 7 2353 (1960) (di-PETN in PETN by I.R.).
35. Ind. Chim. Belg. 325 (1967) 647-50 (HMX decomposition by mass spectrometer).
36. MERRICK and SEYMOUR: 'Third Symposium on Chemical Problems connected with the Stability of Explosives', Ystad, Sweden, May 1973, sponsored by the Sektionen für Detonikoch Förbränning. Secretary Tekn lic Stig Johansson, Box 608, 55102, Jonkoping, Sweden.

37. UNPUBLISHED: Ministry of Defence, Royal Armament Research and Development Establishment, Fort Halstead, London, England.
38. UNPUBLISHED: Ministry of Defence, Experimental Research and Development Establishment, Waltham Abbey, Essex, England.
39. UNPUBLISHED: Ministry of Defence, Materials Quality Assurance Directorate, Royal Arsenal, Woolwich SE18, London, England.
40. HOLLAND: Compatibility assessment by vacuum stability tests: The use of pressure transducers. Technical Report No. 74/5, May 1974. Imperial Metal Industries Limited, Summerfield Research Station, Kidderminster, Worcestershire, England.

BIOGRAPHY

Bill Merrick was born and educated in Manchester, England and is an Associate of the Royal Institute of Chemistry. The early part of his career was concerned with Dyestuffs at Imperial Chemical Industries but during the war he was engaged on munitions work. Since 1954 he has been at AWRE Aldermaston mostly in the Explosives Division but more recently in the Chemistry Division. His main activities have been concerned with analytical chemistry, microscopy, climatic trials and explosives safety testing with a special interest in impact sensitiveness and thermal stability. He was a joint author of a paper in 1963 to the Sensitiveness and Hazards Conference at ERDE England and of a paper in 1973 on explosive stability testing at Ystad, Sweden.

APPENDIX A

Reproducibility of an Assay on PETN

The determinations were by reduction with ferrous ammonium sulphate dissolved in sulphuric acid according to the conditions described by Scott and Furman but substituting the colorimetric end point by a conductometric end point using platinum and tungsten electrodes. The end point was sensitive to 0.01 ml of 0.3N ferrous ammonium sulphate. The estimate of the standard deviation (S) from 17 results was 0.15% and the derived statistical parameters shown in the table were calculated.

<u>Number of Tests</u>	<u>Standard Error</u>	<u>Precision</u>	<u>Accuracy 95% Confidence Limits</u>	<u>Least Significant Difference</u>
N	$\frac{S}{\sqrt{N}}$	$\pm \frac{2S}{\sqrt{N}}$	$\pm \frac{St}{\sqrt{N}}$	$S.t.\sqrt{\frac{2}{N}}$
17	0.036%	0.072%	0.077%	0.11%
5	0.067%	0.134%	0.186%	0.22%

APPENDIX B

Table of Results

SAMPLE	Temperature and Duration of test		Mercury Manometer		Transducer + vacuum treatment		
			0 to 1½ h	0 to 41½ h or 72 h	calculated from HOT reading	from -80°C reading	liquid
	°C	hours	(ml)	(ml)	(ml)	(ml)	(mg)
5 g RDX	120°	41½	0.1	0.6	0.6	0.3	0.2
5 g HMX	120°	41½	none	0.1	0.1	0.1	none
5 g TETRYL	120°	72	0.6	large	large	large	3.8
5 g PETN	100°	41½	0.9 0.6	1.6 1.4	1.6 1.4	0.1 none	3.2 1.6
5 g PETN	120°	41½	2.8 2.6	4.7 4.2	4.7 4.2	2.0 2.1	5.7 4.0
1 g PETN Treated Sample A	100°	41½	-	1.0	-	0.7	0.3
1 g PETN Treated Sample B	100°	41½	-	9.0	-	8.4	5.6
0.25 g "PC"*	120°	41½	0.1	0.3	0.5	0.5	none
5 g COMP.B + "PC"	120°	41½	0.5	1.2	1.4	0.8	2.5

*PC = polycarbonate

APPENDIX C

Assessment of Results

	Manometer Test			Transducer Test + vacuum treatment			
	Vol of gas <u>ml</u>	TOTAL Information					TOTAL Information
		Vol x 2 = wt of gas <u>mg</u>	Vol of volatiles at 1½ h <u>ml</u>	Vol of gas at -80°C <u>ml</u>	Vol x 2 = wt of gas <u>mg</u>	wt of liquid <u>mg</u>	
RDX	0.5	1.0	0.1	0.3	0.6	0.2	0.8
HMX	0.1	0.2	none	0.1	0.2	none	0.2
PETN 100°C	0.7 0.8	1.4 1.6	0.9 0.6	0.1 none	0.2 none	3.2 1.6	3.4 1.6
PETN 120°C	1.9 1.6	3.8 3.2	2.8 2.6	2.0 2.1	4.0 4.2	5.7 4.0	9.7 8.2
PC	0.2	0.4	0.1	0.5	1.0	none	1.0
PC + COMP.B	0.7	1.4	0.5	0.8	1.6	2.5	4.1

THE INFLUENCE OF METALS ON THE THERMAL DECOMPOSITION OF s-TRIAMINOTRINITROBENZENE (TATB)

E. D. Loughran, E. M. Wewerka, R. N. Rogers, and J. K. Berlin*
University of California, Los Alamos Scientific Laboratory
Los Alamos, New Mexico 87544

ABSTRACT

Although s-triaminotrinitrobenzene (TATB) possesses unusually high thermal stability for an organic explosive, the rate of gas evolution at elevated temperatures appears to be increased markedly by the presence of copper, iron, or brass. Aluminum in the same experimental environment produces little or no effect on the gas evolution rate. This paper presents the results of various experiments in which attempts were made to evaluate the magnitude of the effects and to elucidate the mechanism of the thermal degradation of TATB both in the pure state and in the presence of the aforementioned metals.

1. INTRODUCTION

TATB and TATB compositions have been under study at LASL for a number of years. Interest in this compound as a secondary explosive stems mainly from its relatively high thermal stability and its insensitivity to initiation by friction and impact. Although it is not as energetic an explosive (calculated for $\rho_o = 1938 \text{ kg/m}^3$; $P_{CJ} = 313 \text{ kbar}$, $D = 7970 \text{ m/s}$) as the widely used HMX and RDX formulations, it is sufficiently powerful for use in certain weapon applications where the size of the explosive system is not severely restricted and the stability characteristics of TATB are a desirable feature of the design.

We are aware of very little published work on the thermal decomposition of TATB. NOL first became interested in its potential as a heat-resistant explosive in the 1950's

and reported briefly on its properties⁽¹⁾. Several laboratories have investigated specific properties of the compound in more detail, e.g., molecular structure^(2,3,4), vapor pressure⁽⁵⁾, shock Hugoniot⁽⁶⁾, etc. Serious evaluation of the thermal stability of TATB and its formulations began at LASL in 1965 and has continued at various levels of activity to this date.

2. BACKGROUND

Our first estimates of the thermal stability of TATB were obtained in short-term, high-temperature tests, i.e., vacuum stability tests at 260°C and DSC studies and Henkin time-to-explosion tests at still higher temperatures. Although kinetics constants determined by the DSC method (analyzing only the most rapid observable portion of the decomposition reaction) correctly predicted the critical tempera-

*Present address: Chemistry Dept, U of Illinois, Urbana, IL.

ture determined in the Henkin test, extreme environmental requirements imposed upon several proposed system designs prompted us to initiate long-term stability tests at the temperatures of interest. It was from these experiments that a striking incompatibility between brass and TATB was observed, initiating further studies into the TATB thermal decomposition mechanism.

3. EXPERIMENTAL

The TATB used in the work reported herein was prepared at LASL by an improved process based on the NOL synthesis⁽¹⁾ that resulted in a higher purity product. The purity level was greater than 99%, the major impurity being NH_4Cl .

Long-term gas-evolution studies were performed on samples of powder, pressed pellets, and Henkin cells sealed in Pyrex ampoules filled with a cover gas of dry air or argon. The sealed ampoules were stored in temperature-controlled ovens at 177 or 204°C for various lengths of time. After removal from the ovens, the ampoules were opened on a CEC 21-103 mass spectrometer inlet system where gas volumes were measured and mass spectra of the gases obtained. In several instances the solid residue remaining in the ampoules was removed, weighed, and analyzed by several techniques including CHN analysis, x-ray diffraction, and mass spectrometry.

The sealed-ampoule studies necessarily produced results that reflected processes occurring in a closed environment, including back reactions of gaseous products with the solid and product reactions in the gas phase. In the hope of elucidating primary reaction mechanisms, several experimental techniques were employed that

rapidly removed the gaseous products from the reaction zone, namely thermal gravimetric analysis (duPont Model 950 TGA), pyrolysis, and pyrolysis/TOFMS (Perkin-Elmer Pyrolysis Accessory/Bendix MA-2 time-of-flight mass spectrometer). In all these methods, helium was used as the carrier gas with flow rates ranging from 0.2 to 0.8 cm^3/s . A simple flow-splitter was incorporated into the heated effluent line of the pyrolysis accessory to reduce the flow into the mass spectrometer to an acceptable level ($\sim 2\%$ of the total effluent). Pure TATB samples and TATB/metal mixtures were contained either in open platinum boats or sealed aluminum DSC cells for the TGA and pyrolysis studies. In several instances, small perforations were made in the sealed DSC cells, and various metal powders were layered over the TATB in the open boats. The techniques of data collection and reduction were more or less conventional for these experimental methods and will not be detailed here.

4. RESULTS AND DISCUSSION

Table I contains gas evolution data typical of the results obtained in the sealed-ampoule experiments. Mass spectral analyses showed that the major gaseous product ($> 50\%$) was CO_2 ; lesser amounts of N_2 , CO , and H_2O were also present. For those samples where extensive decomposition had occurred, a white residue formed on the inner ampoule surface upon removal from the oven. This substance (representing about 20% of the total weight loss) was identified by x-ray analysis as ammonium bicarbonate. Sealed brass Henkin cells (containing TATB), exposed to 204°C in Pyrex ampoules for one week, had a bluish deposit on the cell surface that was identified, also by x-ray analysis, as $(\text{NH}_3)_4\text{CuCO}_3$. Table II summarizes the weight-loss data obtained on a

TABLE I

Total-Evolved Gas from Sealed Ampoule
Surveillance of TATB Contained
in Henkin Cells

Henkin Cell Material ^a	Storage Time (wk)	Temp (°C)	Total Evolved Gas ^b (cm ³ /g, STP)
Brass	1	177	14
	2	177	35
Aluminum	1	177	0.3
Brass	4 days	204	162
Aluminum	4 days	204	1.0
	1	204	1.6
	2	204	5.4

^aCells contained approximately 0.25 g of powdered TATB.

^bIncludes N₂, N₂O, NO, CO, CO₂, and H₂.

TABLE II

Percent Weight Loss of TATB
After 14 Days at 204°C

Container	Weight Loss (%)
Pyrex Ampoule	1 ^a
Al Henkin Cell	2
Brass Henkin Cell	50
Vacuum Stability (200°C)	0.6 ^a
DSC Predicted	1.4

^aCalculated from measured gas volumes and assuming a molecular weight for the gas of 38.

number of sealed Henkin cells and Pyrex ampoules after storage for two weeks at 204°C. Again this information is presented as an example of the magnitude of the effect observed with these particular experimental conditions.

The point of interest in these data is the pronounced difference between the rates of gas evolution from the two different cell

materials. The TATB contained in aluminum cells decomposed at a rate comparable to that observed with bulk material sealed in Pyrex ampoules, whereas the TATB sealed in brass cells decomposed quite rapidly. The results (to be discussed in more detail in the oral presentation) led us to investigate more thoroughly the TATB decomposition reaction. Subsequently, extensive use was made of the flow techniques (described in the experimental section) in the hope of obtaining some information about the primary decomposition products and the reaction mechanism.

Since the sublimation rate of TATB is moderately high at the temperatures that make the use of the flow techniques practical, quantitation of the thermal decomposition reaction was somewhat difficult. However, it was felt that comparative observations were meaningful and useful in attempting to unravel the mechanisms operative in the systems studied. On comparing TGA weight-loss curves for pure TATB with those for TATB/metal mixtures, very little difference in the rate of weight loss was observed for isothermal runs in the 320-360°C temperature range. However, DTA curves for the Cu/TATB and Fe/TATB mixtures, obtained at a heating rate of 0.66°C/s (40°C/min), showed an exothermic reaction occurring at temperatures 50° to 75°C lower than the major decomposition exotherm in pure TATB. Aluminum appeared to have little, if any, effect on the DTA curve for TATB. The pyrolysis/-TOFMS results indicated that the thermal decomposition reaction occurring below about 450°C gave CO₂, NO, HCN, C₂N₂ and a mass 43 component (possibly cyanic acid) in roughly equal amounts. Lesser quantities of N₂, CO, and H₂O were also observed. The rates of gas evolution, as recorded by the mass spectrometer total-ion monitor, were significantly higher at a given pyrolysis

temperature for samples of the Cu/TATB and Fe/TATB mixtures than for the Al/TATB and pure TATB samples.

5. CONCLUSION

We have observed a marked acceleration in the rate of thermal decomposition of TATB in contact with copper and iron by several experimental methods. Aluminum, under the same conditions, appears to have little or no effect. Although all the details of the reaction are not yet explained in terms of a reaction mechanism, the experimental results at this point indicate that a reaction occurs between the gaseous components (TATB vapor and/or decomposition products) and the metals, either to produce a reaction catalyst or to remove an inhibitor from the system. Copper and iron are relatively strong reducing substances, and we believe that similar metals would also accelerate the TATB decomposition. Information such as that obtained in this study can be of practical significance when considering TATB for a particular weapon application.

6. ACKNOWLEDGMENT

The authors wish to express their appreciation to Dr. H. H. Cady of WX-2 for his assistance in collecting the TGA, DTA and x-ray data cited in this paper.

7. REFERENCES

- (1) Kaplan, L. and Taylor, F., Jr., "Process Development Study of 1,3,5-triamino-2,4,6-trinitrobenzene," NAVORD report 6017, March 1958 (Confidential report).
- (2) Cady, H. H. and Larson, A. C., *Acta Cryst.* 18, 485 (1965).
- (3) O'Connell, A. M., Rae, A.I.M., and Maslen, E. N., *Acta Cryst.* 21, 208 (1966).
- (4) Deopura, B. L. and Gupta, V. D., *J. Chem. Phys.* 54, 4013 (1971).
- (5) Rosen, J. M. and Dickinson, C., "Vapor Pressures and Heats of Sublimation of Some High Melting Organic Explosives," NOLTR report 69-67, April 1969.
- (6) Coleburn, N. L. and Liddiard, T. P., Jr., *J. Chem. Phys.* 44, 1929 (1966).

TESTING OF PLASTIC, COMPOSITES, AND COATINGS FOR USE IN NAVAL ORDNANCE

Benjamin D. Smith
Naval Surface Weapons Center
Dahlgren Laboratory
Dahlgren, Virginia 22448

ABSTRACT

Plastics, composites and coatings have found increased usage in Naval Ordnance applications for reasons of: ease of construction, and maintenance; lightweight but structurally strong construction; corrosion and erosion protection; and cook-off protection in fire situations. In order to be accepted for use in the fleet these materials which come into contact with explosives as well as with the final ordnance item have to satisfy the test requirements of "Safety and Performance Tests for Qualification of Explosives", NAVORD publication OD 44811 volume 1. Such tests as vacuum stability, differential thermal analysis, and accelerated weight loss (thermogravimetric analysis) for mixtures of explosives and plastics are routinely performed. However, additional tests are often desirable to enable the researcher to select the best suited material, particularly for "unconventional" applications. Examples of such applications include: interior ordnance liners designed to increase the cook-off time in a fire; plastic beakers to contain explosive charges; plastic heat shielding for ordnance in a fire situation; coatings to protect ship decks from rocket exhaust; and plenum chambers to channel rocket, exhaust gases overboard in case of accidental rocket firing in storage magazines. We have used a variety of test methods; i.e., static firing of a missile with the exhaust impinging on plastic and composite samples, polarized light microscopy, comparing the heat evolved in differential scanning calorimetry for mixtures of explosive and plastic liner materials versus the explosive itself, and field cook-off tests. The results of our testing program will be discussed.

1. INTRODUCTION

The Dahlgren Laboratory routinely performs the standard compatibility tests of plastics and composites with explosives and propellants; vacuum stability, and temperature stability, DSC and TGA. We have modified and expanded these tests to help solve a variety of safety, performance and quality control problems associated with Naval ordnance hardware.

2. MISSILE EXHAUST DEFEATING MATERIALS

2.2 DECK COATING MATERIALS

During firing tests of standard missile blast test vehicles at the NASA Wallops Island facility, candidate deck coating and plenum chamber materials were fastened on blast doors which were positioned twelve inches from, and normal to, the missile exhaust nozzle. This simulated the most hazardous exhaust impingement conditions that could exist in a normal missile launch aboard ships. The data collected included the temperature of the back side of the candidate deck coating material and documentation of the erosion. From such tests, the deck coating material Dyna-Therm E-345, was

identified and is now widely used in the fleet to defeat the heat, blast and erosion of the exhaust plume. Left unprotected, the decks, superstructure, doors, launcher systems, and other equipment such as guns and radar antennae may suffer erosion and material degradation from the heat and blast of the missile exhaust plume. For example, the exhaust plume from a single missile launch will erode away an area between 18 and 24 inches in diameter and a minimum depth of 1/4 inch from a typical 5456 aluminum, unprotected, superstructure.

2.3 MAGAZINE PROTECTION

During a normal, on deck missile launch, the deck is exposed to the exhaust plume for only a few milliseconds. If the missile is accidentally actuated in the magazine, the combustion process can be either propulsive or non-propulsive burning; i.e., the burning can range from a low order conflagration to a full 30 second propulsion burn. The missile exhaust from the Standard Missile has a mass flow rate of 90 pounds per second, of which approximately 38 pounds per second are alumina, Al_2O_3 , and 17 pounds per second are hydrochloric acid, HCl. The temperature of the exhaust reaches several thousand degrees and can cause the temperatures of bare, unprotected metal to exceed 1000°F in less than 0.5 seconds and can burn through 9 inches of steel. With the development of the Standard Missile, new methods were investigated to defeat the erosive problems associated with missile exhausts. Merely increasing the capacity of the CO_2 extinguishing system

and installing higher pressure water injection and sprinkler systems provided only marginal solutions at best. A plenum chamber system which defeats, controls, and allows the venting overboard of the exhaust gases has been developed and is used in the fleet. The plenum chamber is constructed from an ablative material which not only defeats the missile exhaust but also has allowed the Navy to realize substantial cost and weight savings.

2.4 PLENUM CHAMBER

Figure 1 shows a three-port plenum chamber section constructed from HAVEG-41. It is placed in the bottom of the magazine with the nozzles of three missiles inserted into the three openings. If a missile accidentally ignites, the exhaust blows out the protective metal discs and the exhaust gases are directed overboard. Blow out discs prevent the ignition of additional missiles by the exhaust from the first missile. The steel brackets on the ends of the plenum chamber serve to support and to join the plenum chamber sections. The pipes for the high pressure water injection system are located underneath the plenum chamber. Figure 2 shows the interior of a single-port plenum chamber which was subjected to four missile tests which ranged from a fly-away to a full-up missile burn in a passive-dry condition. Even after the four missile firing tests, the plenum chamber is in excellent condition and could be used again. Plenum chambers constructed from the ablative material HAVEG-41 are now in use in the fleet. The screening methods applied to candidate ablative materials included using an acetylene torch, placing candidate mater-

ials on the blast doors and conducting launch tests, and soaking samples in hydrochloric acid (HCl) and sulfuric acid (H₂SO₄).

3. COMPATIBILITY OF MISSILE PROPELLANTS AND JP-5 FUEL

The effort to develop protective deck coatings and plenum chambers underscores the ability of missile exhaust to erode materials. However, the safety and performance of missiles are also important. For example, what compatibility and performance problems arise if JP-5 fuel is spilled and comes into contact with missile propellants? Besides the standard laboratory tests, we have used two other laboratory tests. First, we have used a Mettler Hot-Stage and a Zeiss polarizing microscope equipped with a 35mm camera to record dimensional changes, swelling, and changes in the physical appearance of various missile propellants exposed to JP-5 vapors as a function of time at 120°F. A glass ring was epoxied to a glass slide. A microtomed section of the propellant, an electron calibration grid, and a section of glass filter paper saturated with JP-5 fuel were placed inside the glass ring chamber. A glass cover slip was placed on top of the glass ring and sealed with a polyglycol. The glass slide was placed on a Mettler FP Hot Stage which held the temperature at 120°F. Photographs were taken of the electron microscope grid and the propellant over a 48-hour period, Figure 3. The rate of swelling was determined by projecting the slides and comparing the dimensions of the propellant against the electron microscope grid. Table 1 summarizes the

swelling, percent increase in the area, and the results of vacuum stability tests of three propellants and a silicone rubber. To establish if the swelling is only a physical absorption of the JP-5 or if chemical degradation of the propellant also occurs, vacuum stability tests were also performed. The increase in the volume of gas parallels the swelling but all volumes are below the accepted maximum value of 2 cc/g/48 hours. The vacuum stability tubes used in these tests had an extra outlet over which a rubber septum was placed. A gas tight syringe equipped with a special lock valve was used to withdraw gas samples which were analyzed on a Carle Model 8000 Portable Gas Chromatograph for oxides of nitrogen, carbon monoxide, carbon dioxide, hydrogen cyanide, nitrogen and oxygen. Although the gas chromatograph was calibrated to detect concentrations of these gases as low as 10 parts per million, only nitrogen and oxygen were detected. The only color change observed was that the JP-5 became a pale yellow when it was placed in contact with the nitrocellulose propellant. Therefore, it was determined that the missile propellants tested are compatible with JP-5 and that the swelling of the propellant is a physical absorption. The effect of swelling on the performance of the missile propellants will have to be determined by closed bomb (pressure vs. time) experiments and firing tests. The tests were also performed on an inert silicone rubber which is used in some missiles. It exhibited the greatest degree of swelling but there is no evidence for chemical degradation.

4. COMPATIBILITY OF EXPLOSIVES AND PLASTIC

MISSILE WARHEAD CASES

The replacement of a metallic missile warhead with a fiberglass-reinforced, phenol-formaldehyde plastic case permitted a 25-pound weight savings and the elimination of 24 metal parts. A one-step phenolic resin is used to eliminate possible compatibility problems with the explosive. Two-step phenolic resins contain paraformaldehyde or hexamethylenetetramine. The latter will, when heated, out-gas ammonia which tends to sensitize explosives. If one-step phenolic resin is stored at room temperature for several months, it loses its tackiness and plasticity under molding conditions. Cases molded from overaged resin which has been stored at room temperature develop cracks in the finished warhead case and uneven distribution of the glass fibers is found. Such resins are already partially polymerized before the molding operation. As part of the quality control effort, we analyzed two samples of phenolic resin, one, from which specification cases could be molded, and which had been stored at 40°F for one month and was moist and tacky. The other sample, which had unsatisfactory molding properties and was dry and friable, had been stored at the same temperature for nine months and had exceeded its shelf life. The analysis procedure consisted of dissolving and decanting off the phenolic resin, determining the weight percent of glass fibers in the resin, and then, by microscopic examination, determining the fiber length (1/2 inch), fiber diameter (8.9-9.0 μ m), and the refractive index (N_D^{25} 1.5504). Both

resin samples contained only glass fibers and had not been contaminated with other fibers such as asbestos. No differences between the two resins could be detected using thermogravimetric, infrared, and mass spectrometry analyses. In conclusion, the storage temperature and shelf life recommended by the resin manufacturer have to be strictly observed to assure acceptable, crack-free missile warhead cases.

5. PLASTIC BEAKERS FOR USE IN LARGE CALIBER

NAVAL PROJECTILES

Large caliber naval projectiles being developed utilize a plastic beaker into which a plastic bonded explosive (PBX) is poured and allowed to cure. Figure 4 shows a plastic bonded explosive with strips of five different plastics laid across the explosive. The five plastics, which are candidate beaker materials, are high density polyethylene, cross-linked polyethylene, nylon 12, ethylcellulose, and low density polyethylene (left to right). The slide was placed in the microscope hot stage and heated at 1°C/min. When a temperature of 150°C was reached, the binder of the PBX began to degrade and the low and high density polyethylenes had melted. The Nylon 12 melted at 167°C and the RDX, which appears as crystals in the binder matrix melts at 195°C. At 195°C, both the cross-linked polyethylene and the ethyl cellulose are soft but intact and, therefore, are considered candidate beaker materials. No compatibility problems were detected.

Ethyl cellulose has been used to fabricate beakers into which the PBX has been cased. Figure 5 shows

the interface of the ethyl cellulose beaker and the explosive. No voids are detected either at the interface or in the cast explosive. The crystalline material is RDX. The magnification is 12.5 X. Figure 6 shows the interior of the ethyl cellulose beaker after it had been stripped away from the explosive. Several crystals of RDX still adhere to the ethyl cellulose and indentations on the surface of the beaker were caused by other crystals of RDX. The binder of the PBX wetted and adhered to the ethyl cellulose, forming a void free interface between the beaker and the explosive. No compatibility problems were observed.

6. INTERIOR LINERS FOR WARHEADS TO PROVIDE COOK-OFF PROTECTION

The final area of research to be discussed is interior liners for ordnance items which will react in an endothermic manner with the explosive if the ordnance item is engulfed in a JP-5 fire. Sufficient time, before a violent reaction occurs, would allow the fire to be extinguished and/or the ordnance item to be jettisoned. Historically, asphaltic hot melt and thickened asphaltic hot melt have been used in bombs. However, asphaltic hot melts react exothermically with TNT and RDX-based explosives. Various new liner materials have been screened in the laboratory by the classical screening techniques; thermogravimetric analysis, differential thermal analysis, and vacuum stability. Promising formulations have been used to line small pipe bombs; i.e., pipes of four-inch diameter by six inches in length with

two end caps. Figure 7 pictures a test pipe bomb. After mica insulation is wrapped around the bomb, approximately nine feet of 1/4 inch heating ribbon is wrapped around the exterior and this is covered by fiber glass insulation. Applying 18 amps from a 208 volt line gives a 4°F/sec. heat rise in the interior of the bomb which simulates the heating rate experienced in a JP-5 fire. Table 2 lists the times to a violent reaction. The classical asphaltic hot melt offers only limited protection; i.e., 2 minutes and 25 seconds. The addition of the sulfur-containing heterocyclic S-trithiane to asphaltic hot melt offers marginal improvement. Combination of the S-trithiane with the plastisol Denflex offers the greatest protection; i.e., a cook-off time of 9 minutes and 11 seconds. The bomb liner formulations based on the silicon R631 resin, which requires the evaporation of an aromatic solvent, and the combination of the plastisol Denflex with the antioxidant CA044 do not offer sufficient protection to warrant additional testing but larger scale cook-off tests are planned for formulations based on the plastisol and S-trithiane mixture.

7. SUMMARY

The Naval Surface Weapons Center, Dahlgren Laboratory, has used standard laboratory tests in programs designed to improve the performance and safety of Naval ordnance and has developed specialized test methods where the specification procedures were inadequate for the problem.



FIGURE 1. THREE PORT PLENUM CHAMBER WITH HIGH PRESSURE
WATER INJECTION SYSTEM



FIGURE 2. INTERIOR OF PLENUM CHAMBER WHICH HAS BEEN SUBJECTED TO FOUR MISSILE FIRING TESTS.

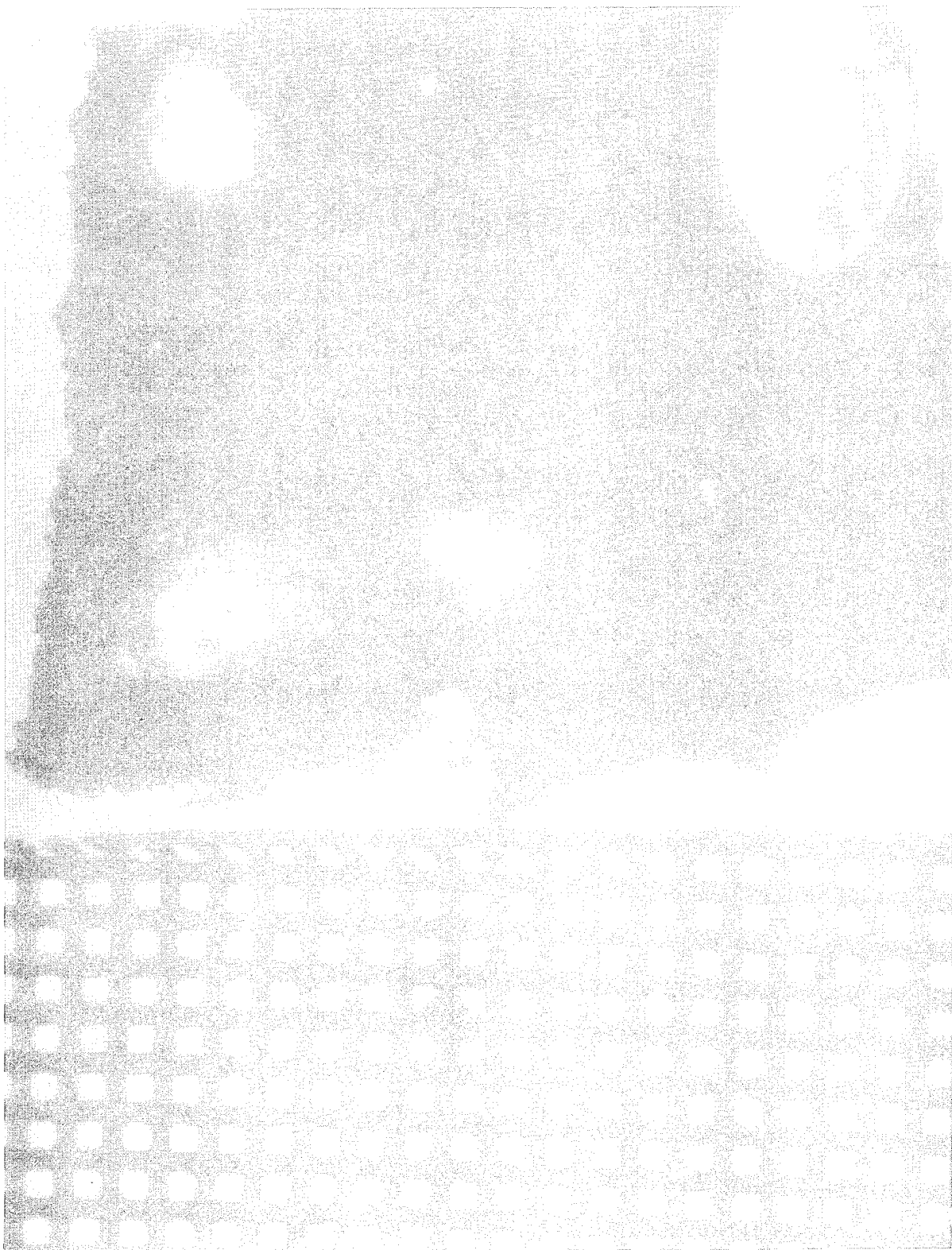


FIGURE 3. RATE OF SWELLING TESTS OF MISSILE PROPELLANT EXPOSED TO JP-5 FUEL.



FIGURE 4. COMPATIBILITY TESTS OF PLASTIC BONDED EXPLOSIVES AND FIVE PLASTICS BY MICROSCOPIC EXAMINATION.



FIGURE 5. INTERFACE OF ETHYL CELLULOSE BEAKER AND PLASTIC BONDED EXPLOSIVES



FIGURE 6. INTERIOR OF THE ETHYL CELLULOSE BEAKER AFTER IT HAS BEEN STRIPPED AWAY FROM THE PBX.

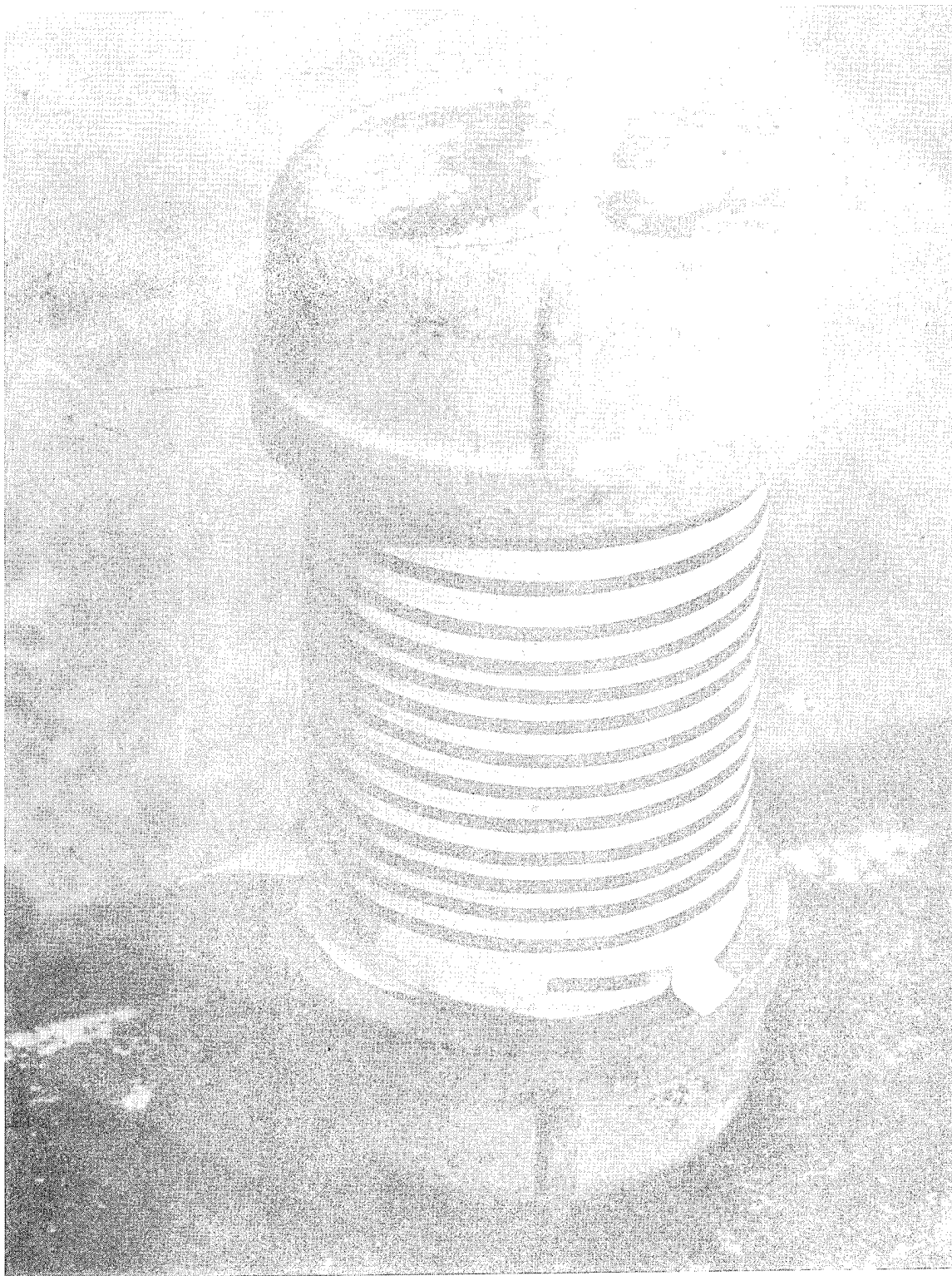


FIGURE 7. PIPE BOMB FOR TESTING INTERIOR LINERS.

TABLE 1

SWELLING BY MICROSCOPE TEST AND VACUUM STABILITY
TEST OF VARIOUS MATERIALS EXPOSED TO JP-5

MATERIAL	SWELLING, PERCENT INCREASE IN THE AREA	VACUUM STABILITY TEST*	
		cc/g/48 HRS.	COLOR CHANGE GASES DETECTED**
NITROCELLULOSE - NITROGLYCERINE PROPELLANT	1.1	.0074	CLEAR TO PALE YELLOW N ₂ , O ₂
AMMONIUM PERCHLORATE - POLYURETHANE - ALUMINIUM PROPELLANT	16.4	.1131	NONE N ₂ , O ₂
AMMONIUM PERCHLORATE - POLYBUTADIENE PROPELLANT	22.9	.1149	NONE N ₂ , O ₂
SILICONE RUBBER	60.6	-.0355	NONE N ₂ , O ₂

*TEST PERFORMED AT 120°F.

**OXIDES OF NITROGEN, CO, CO₂, HCN, H₂ AND O₂ WERE TESTED FOR, USING 12 FOOT BY 1/8 INCH PORAPAK Q,
SILICA GEL AND MOLECULAR SEIVE COLUMNS.

TABLE 2

LINER COMPOSITION	COOK OFF TIMES	
	HEATED MIN., SEC.	REACTIONS MIN., SEC.
65% DENFLEX 35% S-TRITHIANE	9:11	9:11
50% SILICONE R631 50% 450 WAX	7:30	N.R.*
50% SILICONE R631 50% CAO 44	5:46	8:17
50% SILICONE R631 50% MELAMINE	5:46	5:46
69% DENFLEX 31% CAO 44	5:00	5:00
75% ASPHALTIC HOT MELT 25% S-TRITHIANE	2:50	2:50
90% ASPHALTIC HOT MELT 10% S-TRITHIANE	2:28	2:28
100% ASPHALTIC HOT MELT	2:25	2:25
*NO REACTION		

COMPATIBILITY AND CHEMICAL KINETICS

R. N. Rogers
University of California, Los Alamos Scientific Laboratory
Los Alamos, New Mexico 87544

ABSTRACT

Several small-scale thermochemical methods have been developed at Los Alamos for the determination of the stability of explosives, and these methods have been applied to the detection of materials that are incompatible with explosives. What follows is an historically oriented review of small-scale compatibility work at Los Alamos.

1. INTRODUCTION

I define incompatibility very broadly as unwanted time-dependent chemical or physical processes that occur in a system in response to the environment or mutual proximity of materials. The definition purposely includes both stability and compatibility (the ability of materials to retain their normal properties when in contact or vapor-phase communication with one another).

Our Laboratory originally used vacuum stability, Taliani, and impact sensitivity tests to detect incompatible systems; however, none of those methods could be used to obtain reliable quantitative data that would allow prediction of extents of degradation as a function of time. Therefore, we have attempted to develop quantitative methods for the measurement of unperturbed degradation rates and the changes caused by admixture with other materials.

In work with explosives-containing weapons, we recognize two types of incompatibility⁽¹⁾.

Incompatibility of Type I includes all of those conditions that cause a weapon to fail to operate as designed, that is, it is a function category. Incompatibility of Type II includes all of those conditions leading to the appearance of hazards. In planning our program on the study of compatibility, we decided that it was most important to consider hazards first.

2. DETECTION OF THERMAL HAZARDS

The fabrication of our explosives required the pressing of preheated thermoplastic-bonded explosives; therefore, the first hazard-related problem we considered was that involving self heating to explosion.

The lowest constant surface temperature above which a thermal explosion is produced is called the critical temperature, T_m , and a relatively simple expression has been derived^(2,3,4) for T_m in terms of the related chemical and physical parameters. The expression is

$$\frac{E}{T_m} = R \ln \left[\frac{a^2 \rho Q Z E}{T_m^2 \delta \lambda R} \right] \quad (1)$$

where R is the gas constant, a is the radius of a sphere or cylinder or the half-thickness of a slab, ρ is the density, Q is the heat of reaction during the self-heating process, Z is the pre-exponential and E is the activation energy from the Arrhenius expression, λ is the thermal conductivity, and δ is the shape factor (0.88 for infinite slabs, 2.00 for infinite cylinders, and 3.32 for spheres). The usefulness of the expression for the calculation of T_m has been verified^(4,5,6); however, accurate values for the kinetics constants were required for reliable use of the expression.

Differential thermal analysis⁽⁷⁾, using Kissinger's method for data analysis⁽⁸⁾, and pyrolysis (later called effluent gas analysis)⁽⁹⁾ were the first methods attempted for the determination of kinetics constants. The time-to-explosion method of Henkin and McGill⁽¹⁰⁾ was known to give low results, but it provided an excellent method for the detection of hazardous incompatible systems⁽¹⁾ and a method for checking the accuracy of kinetics constants determined by other means⁽⁵⁾.

The advent of the differential scanning calorimeter (DSC) gave us better methods for the estimation of kinetics constants^(10,11,12), but the first methods could be applied only to homogeneous systems. Since our most important explosives melt with decomposition as they self heat to explosion, more general DSC methods were developed^(13,14,15). We have recently showed that the kinetics constants obtained by the isothermal DSC method⁽¹⁴⁾ can be used to calculate accurate critical temperatures,

and we believe that the work on thermal hazards of unperturbed systems is largely finished. Perturbed reactions that show first-order or pseudo-first-order relationships between time and active mass can be studied in the same way as unperturbed reactions.

Time-to-explosion test. A time-to-explosion test provides an excellent method for the detection of incompatible systems, but its most important function is to provide a direct test for the accuracy of kinetics constants determined by other means. The test is used to obtain an experimental value for the critical temperature of a system, and that value is checked against the value calculated from equation (1).

The method now in use at Los Alamos is a compromise between accuracy of specification of sample dimensions and geometry and violence of reaction. The test was designed to be a routine laboratory test rather than a firing-site operation.

The sample, usually 40 mg of the explosive component, is pressed into a DuPont E-83 aluminum blasting-cap shell with a hollow, skirted plug (Fig. 1). A conical punch is used, and the plug expands rather reproducibly at about 400 pounds applied force (6100 psi or 60 MPa). Expansion of the plug forms a positive seal and confines the sample at a known geometry. The sample thickness can be measured, and the density can be calculated. The assembly is then dropped into a preheated metal bath, and the time to explosion is measured as the time to the sound of a reaction. The lowest temperature at which a runaway reaction can be obtained is the T_m . It often requires a large number of tests to determine T_m with confidence, because it is

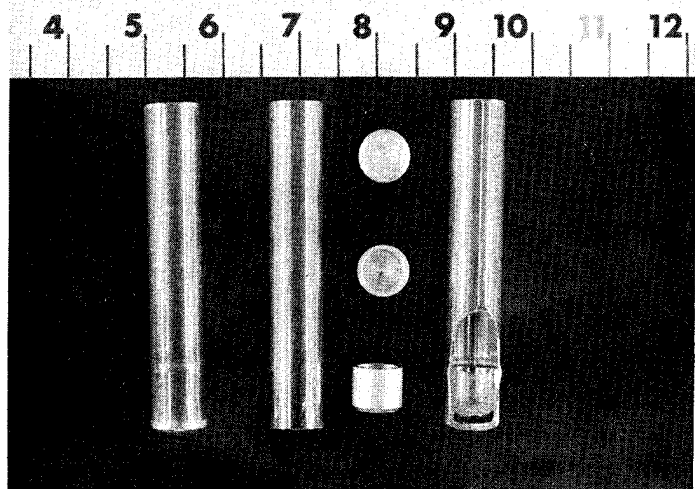


Fig. 1

TIME-TO-EXPLOSION CELLS AND COMPONENT PARTS, LEFT TO RIGHT: 1) LOADED CELL, SHOWING WALL DEFORMATION OVER FLARED PLUG; 2) EMPTY, UNUSED, DU PONT E-83 BLASTING-CAP SHELL; 3) THREE VIEWS OF THE PLUG; AND 4) CUTAWAY VIEW OF LOADED CELL, SAMPLE BLACK FOR VISIBILITY.

necessary to raise and lower the bath temperature across the apparent T_m , make many separate tests, and allow sufficient time for a reaction. No explosion within 1000 seconds is usually a safe criterion for a failure with samples in the specified size range; we have never obtained an explosion at a time greater than 10,000 seconds. Admixture of an incompatible material with an explosive will lower T_m and/or shorten times to explosion compared with the pure explosive.

Incidentally, the time-to-explosion cell provides an excellent system for small-scale surveillance testing. Test materials can easily be encapsulated in the cells, and weight loss can be followed at different temperatures to give data for the calculation of an effective activation energy.

3. GENERAL STUDIES OF INCOMPATIBILITY

Although we believe that we can now predict thermal hazards with some confidence, a lot of work remains to be done with perturbed systems in which the question is one of functional lifetime rather than hazard. It is obvious that small-scale chemical tests will not detect Type I incompatibility problems that are the result of the migration of plasticizers or similar materials into critical components, but small-scale tests can be used to detect and to measure rates of appearance of incompatible volatile decomposition products produced by explosives or propellants.

Detection of incompatible systems. The isothermal DSC method⁽¹⁴⁾ can be used for the detection of incompatible mixtures, and it can also often shed light on the type of incompatibility and specify the degree of incompatibility. Changes in reaction order, increases in rate constants or pre-exponentials, or decreases in activation energies signal incompatibility. Note, however, that the DSC methods measure the rate of disappearance of reactant, that is, the rate of the overall reaction. When a reaction is complex or products are in question, it is useful to obtain information on the rate of appearance of products. Pyrolysis/mass spectrometry can be used, and the method will be discussed in more detail by Loughran. A method that involves a combination of pyrolysis and thin-layer chromatography has been developed for the study of complex mechanisms⁽¹⁶⁾, and it has been applied to the determination of kinetics constants⁽¹⁷⁾. Changes in products or changes in rates of appearance of products can be used for detection of incompatibility and prediction of extent. The same technique can be used, impinging pyrolysis products onto polished

metal sheets as a function of temperature, for the detection of corrosion-promoting decomposition products. Sheets impregnated with spot-test reagents can be used to provide sensitive and selective "thermal spot tests" for decomposition products. Some thermal spot tests that have proved to be useful in the study of explosives and propellants are the following: (1) detection of formaldehyde with chromotropic acid in strong sulfuric acid in porous glass sheets, (2) detection of oxides of nitrogen with diphenylamine, and (3) detection of "oils" on thin layers of silica gel later sprayed with water. Incidentally, a thermal spot test using 5% p,p-dimethylaminobenzaldehyde in 6N HCl or syrupy phosphoric acid provides an excellent method for differentiation between plant and animal materials; it gives a sensitive test for pyrrole, and the ease with which pyrrole is produced by pyrolysis can be a rough indication of the age of bone.

DSC measurements on incompatible systems.

I am currently using DSC methods to study zero-order (interface), solid-state, and higher-order (homogeneous) reactions. The RDX/urea system provides a reasonable model for the demonstration of the DSC method in the study of incompatibility. The decomposition kinetics constants for pure RDX can be measured in the liquid phase⁽¹⁵⁾ ($E = 47.1$ kcal/mole, $Z = 2.02 \times 10^{18}$ sec⁻¹); however, an induction time is observed below the nominal melting point of RDX, and some autocatalysis can be observed in order plots⁽¹⁴⁾ above the melting point. Addition of a small amount of urea (m.p. 132.7°C) to the RDX effectively eliminates the induction time (the time required for the production of a liquid phase), and the early rapid reaction between RDX and urea submerges any autocatalytic reaction that

might have been observed. The reaction with urea is so rapid that all of the urea is destroyed before measurements can be made when low concentrations of urea are used, and the only kinetics constants that can be measured are those for the unperturbed RDX decomposition, liquid and vapor. The change in the order plot early in the process signals incompatibility. When larger amounts of urea are used, 10% or more, it becomes possible to obtain measurements on the RDX/urea reaction. When 30% urea is used, the order plot shows that the first 53% of the reaction is second order: the reaction between RDX and urea is on a 1/3 molar basis. The kinetics constants for the second-order reaction are $E = 22.7$ kcal/mole and $Z = 7.89 \times 10^8$ sec⁻¹, proving marked incompatibility between the components.

Calculation of lifetime. In order to calculate lifetimes from kinetics data, two problems must be faced. There must be some function or safety criterion that specifies what terminates the lifetime of the assembly, and the kinetics measurements must have been made on the same phase or phases that will be present during storage of the assembly. At the present time, homogeneous amorphous, glassy, or liquid systems can be handled with some confidence. Examples of such systems are energy-contributing binder phases and homogeneous propellants. When incompatibility produces a liquid phase at storage temperatures by solvent migration or mixed-melt formation, predictions from kinetics data can be quite good. However, lifetime predictions for solid systems that are based on liquid-phase kinetics measurements will normally be uselessly short.

4. CONCLUSIONS

Small-scale chemical tests can be used to

detect incompatibility resulting from chemical reactions and to provide kinetics constants for prediction of lifetimes. Other tests are required to detect incompatibility resulting from migration of components. Calculation of a lifetime requires specification of a lifetime criterion and care that the phases existing during storage are the same as those existing during kinetics measurements. Considerable work needs to be done on solid systems.

5. REFERENCES

- (1) Rogers, R. N., Ind. & Eng. Chem. Product Research and Development 1, 169 (1962).
- (2) Frank-Kamenetskii, D. A., Acta Physicochem. USSR 10, 365 (1939).
- (3) Chambré, P. L., J. Chem. Phys. 20, 1795 (1952).
- (4) Zinn, J. and Mader, C. L., J. Appl. Phys. 31, 323 (1960).
- (5) Zinn, J. and Rogers, R. N., J. Phys. Chem. 66, 2646 (1962).
- (6) Wenograd, J., Trans. Faraday Soc. 57, 1612 (1961).
- (7) Rogers, R. N. Microchem. J. 5, 91 (1961).
- (8) Kissinger, H. E., Anal. Chem. 29, 1702 (1957).
- (9) Rogers, R. N., Yasuda, S. K. and Zinn, J., Anal. Chem. 32, 672 (1960).
- (10) Rogers, R. N. and Morris, E. D., Anal. Chem. 38, 412 (1966).
- (11) Rogers, R. N. and Smith, L. C., Anal. Chem. 39, 1024 (1967).
- (12) Rogers, R. N. and Smith, L. C., Thermochim Acta 1, 1 (1970).
- (13) Rogers, R. N., Anal. Chem. 44, 1336 (1972).
- (14) Rogers, R. N., Thermochim Acta 3, 437 (1972).
- (15) Rogers, R. N., Thermochim Acta 9, 855 (1974).
- (16) Rogers, R. N., Anal. Chem. 39, 730 (1967).
- (17) Rogers, R. N., J. Chromatog. 48, 268 (1970).
- (18) Rogers, R. N. and Daub, G. W., Anal. Chem. 45, 596 (1973).

PENTAERYTHRITOL TETRANITRATE (PETN) STABILITY AND COMPATIBILITY

D. M. Colman

Monsanto Research Corporation, Mound Laboratory

P. O. Box 32, Miamisburg, Ohio 45342

R. N. Rogers

University of California, Los Alamos Scientific Laboratory

P. O. Box 1663, Los Alamos, New Mexico 87544

ABSTRACT

The decomposition kinetics of pentaerythritol tetranitrate (PETN) alone and in admixture with other materials has been studied using a differential scanning calorimeter. Quantitative rate and reaction order(s), as a function of composition, were obtained.

In order to postulate a reaction mechanism(s), one must be able to identify the reaction products. An attempt to identify reaction products was begun by using a pyrolysis - thin layer chromatographic procedure.

1. INTRODUCTION

Recent observations made at Mound Laboratory in conjunction with a study on the corrosion of gold in contact with pentaerythritol tetranitrate (PETN) have made it important to obtain a complete understanding of the kinetics and mechanism of decomposition of PETN and the effects of materials in contact with PETN.

It was also thought that the PETN system would be excellent to use to check some hypotheses on the quantitative measurement of compatibility, because many materials have been found to be incompatible with PETN.⁽¹⁾ Measurements of rate constants and

reaction order as a function of composition as a second material is added should allow us to observe, measure, and describe the type of compatibility problem encountered.

2. EXPERIMENTAL AND DISCUSSION

In order to observe changes in the decomposition kinetics of PETN, it is necessary to understand the unperturbed reaction rather well. It has generally been recognized that the decomposition of PETN is autocatalytic. Robertson⁽²⁾ noted that there was "---a very nearly constant rate of gas evolution for about the first half of the decomposition, after which this

rate diminished in accordance with the unimolecular equation." He used the "--- slope of the initial straight portion of the curve---" for his calculation of the kinetics constants, obtaining the values $E = 47 \pm 1.5$ kcal/mole and $Z = 6.31 \times 10^{19}$ sec⁻¹. Andreev and Kaidymov⁽³⁾ reported that the absolute rate increased up to about 30% decomposition. They fitted the entire curve to obtain values as follows: $E = 39$ kcal/mole, $Z = 3.98 \times 10^{15}$ sec⁻¹. A DSC rate curve is shown in Figure 1, and the undecomposed fraction (1 - x) is shown in the graph. It can be seen that the rate increases up to 30% decomposition, a feature that can be seen more clearly in lower-temperature runs.

A first-order plot and an order plot for the run shown in Figure 1 are shown in Figure 2. The early part of the decomposition is almost exactly first order, and a very consistent linear first-order plot is obtained for calculation of the rate constant. The entire reaction more closely approaches first order at lower temperatures, as shown in Figure 3.

When the early first-order part of the reaction is used for the calculation of the kinetics constants, the result is as shown in Figure 4. ($E = 46.5$ kcal/mole, $Z = 2.36 \times 10^{19}$ sec⁻¹). This is an excellent check with Robertson's⁽²⁾ results for the same reaction regime. This series of runs was also used to compare results achieved

with the DSC-1B with those from a new DSC-2. It can be seen that there is no significant difference between the two sets of data; however, the noise level in DSC-2 rate curves is extremely low, making those curves easy to measure. Robertson⁽²⁾ had noted that rates did not change over a range of gas pressures from 5 to 76 cm; therefore, we compared DSC runs at two different degrees of confinement: cells perforated with a needle (0.1-mm perforation) and cells perforated with a laser beam (12- to 15- μ m perforation). No significant difference could be seen between the sets of data.

When the late part of the reaction is used for the calculation of the kinetics constants, the results are as shown in Figure 5 ($E = 33.9$ kcal/mole, $Z = 4.68 \times 10^{13}$ sec⁻¹). Again, there is no significant difference observed as a function of instrument used or confinement. A comparison between the early and late data proves that the decomposition is indeed autocatalytic. Robertson⁽²⁾ and Andreev and Kaidymov⁽³⁾ reported that NO₂ was produced early in the reaction and disappeared later; however, the lack of effect of fill-gas pressure and confinement seems to indicate that the main secondary reactant is generated in the liquid phase.

A material that affects the mechanism of the decomposition reaction will cause a change in rate constant of the process at

• any temperature. The change in rate can be the result of a change in activation energy, pre-exponential, or both, and higher-order reactions can appear as a function of mixture composition. Insoluble materials with active surfaces can contribute zero-order processes to an overall decomposition. Examples of all the types of reactions have been observed with the DSC, but there has never been an opportunity to study the systems in detail.

In application, PETN is often used in contact with PBX 9407, a mixture of cyclo-trimethylenetrinitramine (RDX) and Exon 461, a Firestone Plastic Co. polymer containing chlorine; therefore, the first compatibility tests were run with RDX and Exon. Figure 6 shows the Arrhenius plot obtained from mixtures of PETN with 5% RDX, superimposed on the Arrhenius plot of the early PETN data. The RDX degrades the PETN to a barely detectable extent. The order plot of Figure 7 shows that the process is still first order. Studies at other compositions should be made to understand the interaction, but the system certainly is not hazardous.

The Arrhenius plot for the PETN/5% Exon system is shown in Figure 8; there is a definite increase in rate. Figure 9 shows that there is an accompanying increase in reaction order. Other compositions will be studied as time allows.

It is evident that differential scanning

calorimeter (DSC) techniques now exist that could provide useful quantitative compatibility information safely on very small samples. It is hoped that these methods can be developed into practical routine methods in the near future.

The data and conclusions drawn allow the determination of the reaction order and the calculation of the Arrhenius constants E and Z (or A). Although invaluable, this information does not allow the postulation of one or more reaction mechanisms. The reaction products as well must be known in order to elucidate the decomposition reaction mechanisms.

A start in this direction was made using the pyrolysis thin layer chromatographic procedure of Rogers⁽⁴⁾. The experimental parameters were as follows:

- sample weight approximately 50 mg
- nitrogen gas flow 25 ml/min
- linear temperature programming rate 11°/min
- temperature range ambient to 523°K (250°C)

Gelman SA sheets were drawn through a 1.0 wt% aqueous solution of AgNO_3 then hung to dry in a dark hood.

Preliminary experiments had shown that silver precipitated immediately when the impregnated sheet was exposed to formaldehyde. This was not true for other aldehydes. When the impregnated sheet was exposed to Cl^- or Cl_2 , eluted with water in the ascending mode, dried, and finally

exposed to uv light, a gray to black spot formed where the reaction took place.

Pyrolysis of PETN indicated that formaldehyde was forming at approximately 398°K. No attempt was made, at this time, to identify other decomposition products. It is interesting to note that decomposition is taking place below the PETN melting point 414°K. Yates⁽⁵⁾ has identified HCN at temperatures below 414°K. There may be two types of PETN decomposition mechanisms, one that takes place at low temperature (below the melting point), and the other a high temperature decomposition (above the melting point).

Pyrolysis of Exon indicated that Cl is a decomposition product appearing at approximately 433°K. When the mixture of PETN/Exon (95/5) was run, the formaldehyde appeared at 398°K and the Cl appeared at 433°K. One may conclude that the Exon and PETN could be compatible in this mixture and in this temperature range.

It should be noted that both types of experiments were conducted in an inert atmosphere (nitrogen). The question arises as to whether the same results would be obtained if the experiments were made in the presence of oxygen (air).

Though the pyrolysis experiments were done in a dynamic mode, there is no reason that they could not have been done in the isothermal mode. In the isothermal mode, one

may be able to determine the lowest temperature and shortest time at which a particular decomposition product can appear.

Utilizing the information obtained from both types of experiments will no doubt lead to a more complete solution of compatibility studies.

REFERENCES

- (1) R. N. Rogers and E. D. Morris, Jr., Anal. Chem., **38**, 412 (1966).
- (2) A. J. B. Robertson, J. Soc. Chem. Ind. (London), **67**, 221 (1948).
- (3) K. K. Andreev and B. I. Kaidymov, Zh. Fiz. Khim., **35**, 1324 (1961).
- (4) R. N. Rogers, Anal. Chem., **39**, 730 (1967).
- (5) W. G. Yates, Mound Laboratory, private communication.

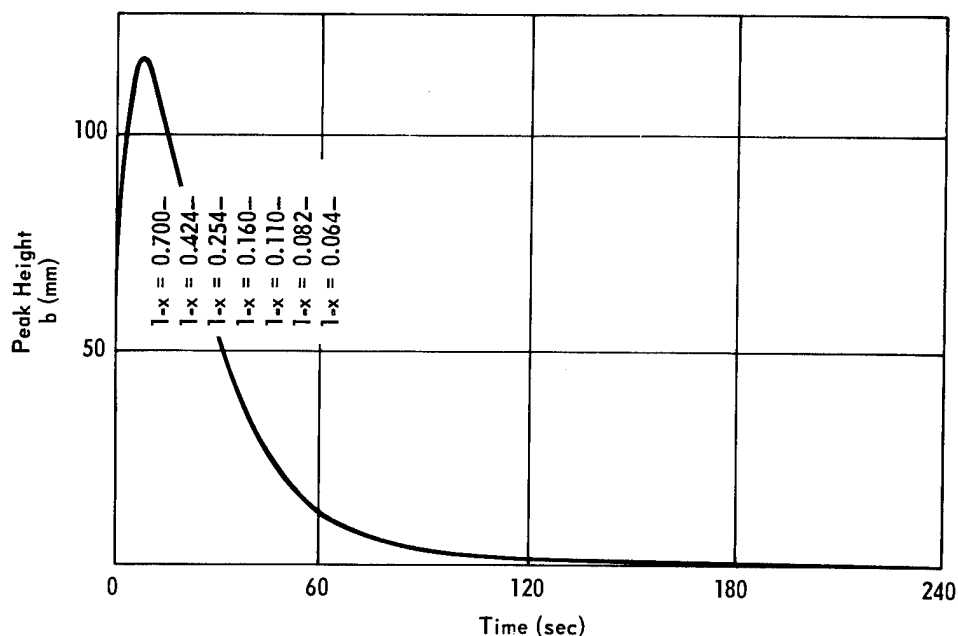


FIGURE 1 - Differential scanning calorimeter (DSC) rate curve from 0.706-mg sample of PETN at 490°K, run in a cell with 0.022-ml capacity and a single 0.1-mm diameter perforation. The residual fraction ($1-x$) is shown at each indicated position.

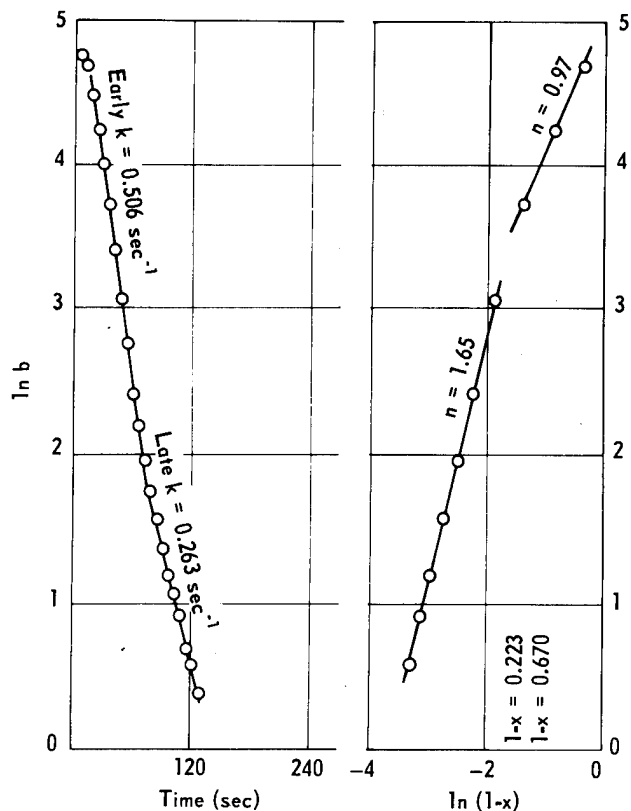


FIGURE 2 - First-order plot (left) and order plot (right) from decomposition curve shown above in Figure 1.

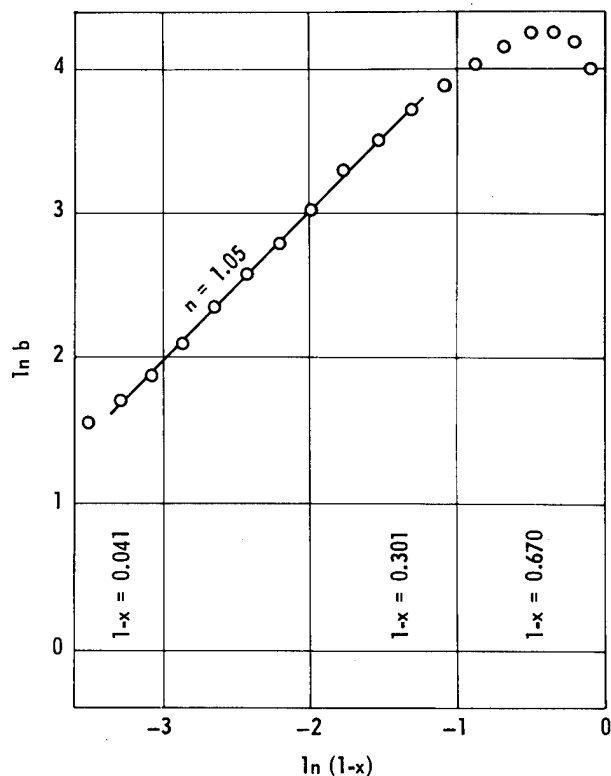


FIGURE 3 - Order plot for 460°K decomposition of PETN.

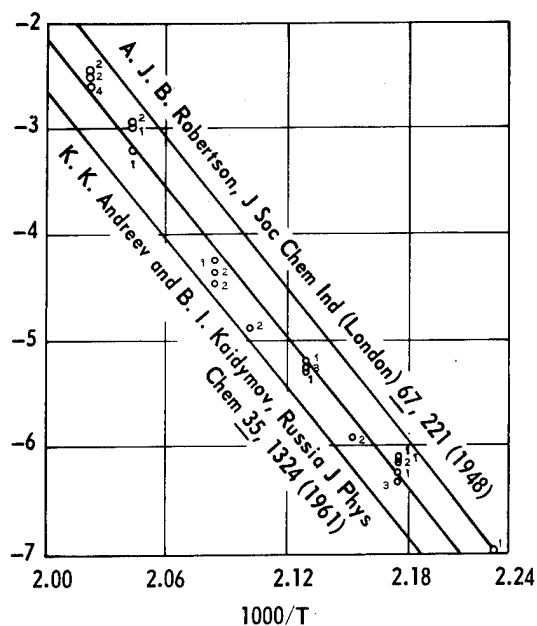


FIGURE 4 - Arrhenius plot of early first-order data (21 points) from PETN decompositions; least-squares results are $E = 46.5$ kcal/mole and $Z = 2.36 \times 10^{10}$ sec $^{-1}$. Robertson⁽²⁾ and Andreev and Kaidymov⁽³⁾ least-squares lines are shown for comparison. Numbered points indicate the following conditions: (1) DSC-2 with 0.1-mm perforation in cell, (2) DSC-1B with 0.1-mm perforation in cell, (3) DSC-2 with 12-15 μ m perforation in cell, and (4) DSC-1B with 12-15 μ m perforation in cell.

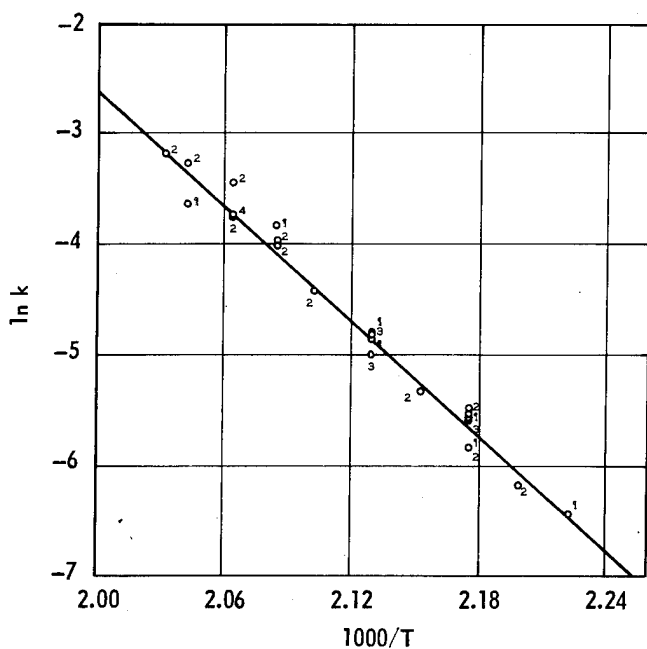


FIGURE 5 - Arrhenius plot of late rate data from PETN decompositions (22 points). Least-squares line indicates $E = 33.9$ kcal/mole and $Z = 4.68 \times 10^{13}$ sec $^{-1}$.

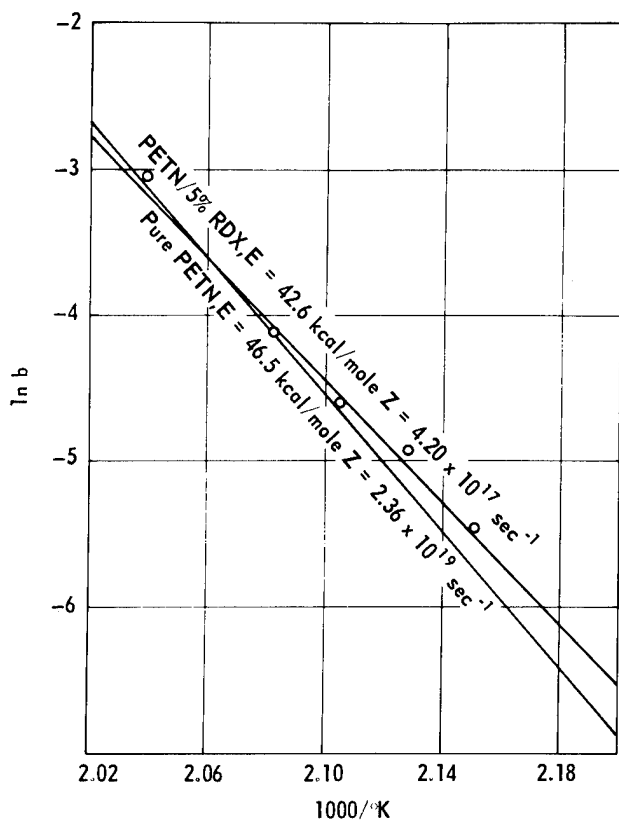


FIGURE 6 - Arrhenius plot of PETN/5% RDX data, superimposed on line for early PETN data.

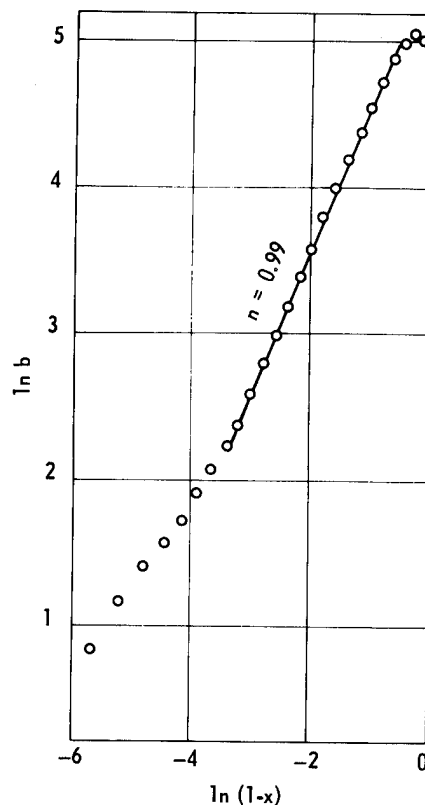


FIGURE 7 - Order plot of 480°K data from a PETN/5% RDX decomposition.

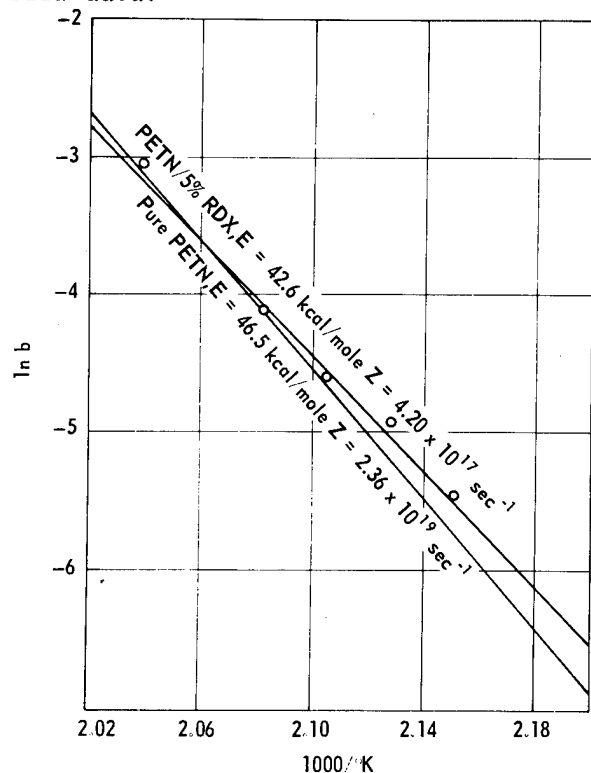


FIGURE 8 - Arrhenius plot of PETN/5% Exon 46l data, superimposed on line for early PETN data.

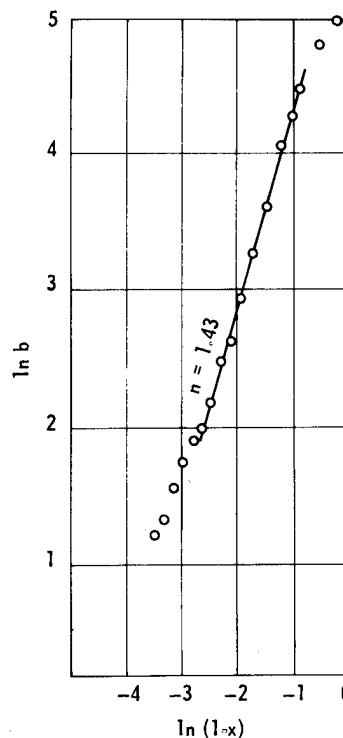


FIGURE 9 - Order plot of 475°K data from a PETN/5% Exon 46l decomposition.

CHEMICAL DEGRADATION OF NITRAMINE EXPLOSIVES

Suryanarayana Bulusu
Chemistry Branch, Explosives Division
Feltman Research Laboratory
Picatinny Arsenal, Dover, NJ 07801

Chemical degradation of two important secondary nitramine explosives, RDX and HMX and a third model compound dimethylnitramine (DMNA) has been studied under a variety of experimental conditions. Thermal and photochemical decompositions will be discussed in some detail and an attempt will be made to review the recent literature on the degradative chemistry of nitramines including the electron impact induced decomposition.

Kinetics of thermal decomposition of HMX below its m.p. shows that the reaction is strongly autocatalytic and that it changes its overall mechanism in different temperature regions even up to 280°. The product analyses show that both HMX and RDX decompose in the solid state yielding as products N_2O and $HCHO$ up to 65% and N_2 , NO , CO , CO_2 and HCN in lesser amounts. In the vapour phase decomposition of RDX, however, NO_2 was also observed. Among the products $HCHO$, NO and the solid residue left after decomposition were each observed to catalyze the reaction.

While photolysis of HMX and RDX gave rise to the same products as thermolysis, photolysis of DMNA gave dimethylnitrosamine as the predominant product. The nitramine group in the latter appears to be more stabilized compared to the cyclic nitramines.

Degradation by electron impact provides a helpful guidance to the understanding of the thermal and photodegradations. These studies indicated a facile loss of NO_2 by most nitramines and formation of several fragments suggestive of likely intermediates in thermal and photodecompositions.

Identification of the primary chemical species and the distribution of ^{15}N in the products of labelled nitramines led to the elucidation of the principal bond breaking steps in each of the above cases. These conclusions are further supported by the results of structural investigations using ^{15}N -NMR and IR spectroscopy. The above findings will be related to the compatibility problem of explosives with special reference to Composition-B, Minol-2 and Tritonal.

EFFECTS OF DIBUTYL TIN DILAURATE ON THE THERMAL DECOMPOSITION OF RDX

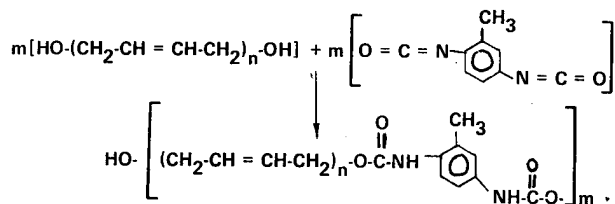
Russell M. Potter, Gaylord J. Knutson, and Martin F. Zimmer
Guns, Rockets, and Explosives Division
Air Force Armament Laboratory
Eglin AFB, Florida

ABSTRACT

This paper presents the results of a study to determine the effects of dibutyl tin dilaurate (DBTD) on the thermal stability of plastic bonded explosive formulations in which it is used. DBTD is a catalyst for the reaction to form the polyurethane binder system for plastic bonded explosives. The two systems studied were RDX/DBTD and an RDX-based plastic bonded explosive in which DBTD was used as the catalyst.

1. INTRODUCTION

The binder system for a number of plastic-bonded explosives is based on hydroxy-terminated polybutadiene crosslinked with toluene diisocyanate to form a urethane:



Dibutyl tin dilaurate (DBTD) has been used to catalyze this process. The purpose of the present study is to determine the effects of this catalyst on the stability of explosive formulations in which it is used.

These formulations are chemically rather complicated and hence are not generally amenable to thorough kinetic analyses. Further, there are a number of plastic-bonded explosives employing DBTD, and to use any one formulation for kinetic analysis would tend to limit applicability of the results. For these reasons, the major portion of the work presented here involved the RDX/DBTD system. Some work has been devoted to the PBX-108 system, however, to give an indication of the applicability of the study to formulations containing a binder system.

2. THEORY

Kinetic data were obtained using the isothermal differential scanning calorimetric method developed by R. N. Rogers^(1,2). The differential scanning calorimeter (DSC) presents data in the form of a deflection from a baseline on a time-base recorder. This deflection, b , is directly proportional to the rate that heat is absorbed or evolved by the sample, dq/dt , and hence, the rate of reaction, dx/dt , where x is the reacted fraction of the

sample. Thus, for a first-order reaction:

$$ab = \beta \frac{dq}{dt} = \frac{dx}{dt} = k(1-x) \quad (1)$$

where a and β are proportionately constants, and k is the rate constant, then:

$$b = \frac{k}{a} (1-x) \quad (2)$$

and

$$\ln b = \ln \frac{k}{a} + \ln(1-x) \quad (3)$$

But, again, for a first order reaction:

$$\ln(1-x) = kt + C \quad (4)$$

where C is an integration constant. Therefore,

$$\ln b = kt + C' \quad (5)$$

Thus, k is obtained as the negative of the slope from a plot of $\ln b$ versus time.

The method developed by Rogers takes advantage of two facts: (1) thermal decomposition of organic explosives is immeasurably slow in the solid phase, and (2) simple decomposition in a homogeneous liquid phase must be first order⁽³⁾. A typical curve obtained by this method is shown in Figure 1. This form of the initial rise is dependent on the decomposition chemistry of the material under study and is caused either by autocatalysis or by melting with decomposition. In the latter case, the trace peak is the point at which the material has reached the homogeneous liquid phase or the greatest extent of its melting. After the initial use, the next part of the event shows the analyzable first-order portion of the decomposition, provided the homogeneous state has been reached. When the liquid decomposition is complete, there is, for RDX, a short,

steeper section of the curve attributable to an analyzable, first-order vapor decomposition. If, on the other hand, the reaction is complex or a homogeneous liquid phase is not obtained, the reaction will generally be neither first order nor analyzable for meaningful kinetic parameters. Thus, it is important to determine an order profile for the reaction, which can be done by production of an order plot as shown in Figure 2.

For a reasonably simple reaction of undetermined order, n ,

$$\frac{dx}{dt} = k (1-x)^n \quad (6)$$

From the DSC theory outlined previously:

$$ab = \frac{dx}{dt} = k (1-x)^n \quad (7)$$

Therefore:

$$\ln b = \ln(1-x)^n + \ln \frac{k}{a} = n \ln(1-x) + C \quad (8)$$

and a plot of $\ln b$ versus $\ln(1-x)$ gives the order as the slope. Thus, the order at any point in the reaction can be determined from a tangent to the curve.

3. EXPERIMENTAL

The RDX used in this study was twice recrystallized from acetone-water that had been dried overnight under vacuum at room temperature and then ground to a fine powder. The RDX/DBTD samples were prepared in the following manner. First, 0.5g RDX was weighed into a 50-ml round bottomed flask. The proper percentage of DBTD was weighed into a 10-ml vial, dissolved in a small volume of chloroform, and washed into the flask with sufficient chloroform to make a total volume of 10 ml in the flask. The mixture was thoroughly stirred, and any clumps of RDX were broken apart. This resulted in a thin slurry of fine particulate RDX in the chloroform solution of DBTD. The chloroform was then removed on a rotary evaporator, and the solid was collected and dried for one hour under vacuum at room temperature.

The PBX-108 formulations were prepared as follows. First, 0.117g vegetable lecithin was dissolved to resin mixture in a 50:50 oil consisting of 16.8g each of Tufflo 100 oil and R-45M hydroxy-terminated polybutadiene. Slight heating was necessary to dissolve the lecithin in the mixture; afterwards, the proper amount of DBTD and 19.9g Class A RDX were added. These ingredients were mixed in a Baker-Perkins remote mixer for 15 minutes at 55°C. Next, 80.1g Class D RDX was added in three increments, with each increment being mixed for 15 minutes. Vacuum was applied after addition of the last increment. The mixture was allowed to

cool to ambient temperature, and 0.680g of toluene diisocyanate was added. Mixing was continued for an additional 15 minutes under vacuum. The mix was poured into 30 ml disposable beakers and cured at 60°C for one week. Small wedges of the formulations were then cut into smaller pieces by hand and prepared for analysis by grinding in a Fisher Scientific mortar grinder for 30 minutes.

The kinetic analysis of all samples employed a Perkin-Elmer Model DSC-1 differential scanning calorimeter according to the following procedure. A sample weighing approximately 1 mg was placed in an aluminum sample pan and was covered with a pan lid; the edges were crimped, and a small hole was punched in the lid to allow for escape of the gases produced in the decomposition. The DSC was set at the desired temperature, allowed to equilibrate, and the differential temperature was checked by the method of Ortiz and Rogers⁽⁴⁾. A reference pan identical to that containing the sample was next placed in the reference support, and the instrument was again allowed to equilibrate. At this point, the desired range was set, and the recorder chart drive was turned on. The enclosed sample was then dropped into its support, and a sharp endotherm occurred due to heat absorption by the cool sample. As the sample temperature was brought under DSC control, the initial exotherm began. The time at which the trace crossed the baseline (extrapolated from the conclusion of the run) was arbitrarily taken as zero time.

The curve was integrated by Simpson's rule to obtain the reacted fractions required for order plots.

4. RESULTS

The results are presented in Figures 3 to 15. The activation energies and pre-exponentials are summarized in Tables I to III. On the tables, subscript L refers to the liquid phase and subscript V, the vapor phase. The PBX-108 systems showed no apparent vapor phase.

5. DISCUSSION

It is obvious from Figure 10 that DBTD causes a destabilization of the thermal decomposition of RDX. The important points here are (1) the significance of this indication in terms of experimental uncertainties, (2) its meaning in terms of the mechanism of the decomposition, and (3) its validity for application to plastic-bonded explosives.

The uncertainties cited for activation energies and pre-exponentials were calculated on the basis of a 75% confidence level and were based on statistical treatment alone. Thus, they would fail to reflect non-random errors arising from sample preparation or from the DSC method. With the RDX/DBTD

systems, sample preparation was comparatively straightforward, and in each case, the sample appeared to be uniform in both chemical nature and particle size. The PBX-108 systems, however, presented greater problems. The grinding process tended to separate the RDX from its binder, leaving a powder of RDX and relatively large flakes of binder. Continued grinding tended to mix the two to some extent, but before complete homogeneity could be reached, a grey coloring of the sample indicated that significant decomposition had taken place. In practice, grinding was discontinued before this level of decomposition occurred; thus, the samples were not necessarily homogeneous in either chemical nature or particle size, nor can it be taken, *a priori*, that the mechanically ground sample is entirely representative of its unground counterpart.

The data analysis has in all cases assumed a simple first-order decomposition. Figure 12, however, indicates that the assumption becomes poorer for the liquid phase as the percentage of DBTD is increased in the RDX/DBTD systems. An analysis based on a second-order reaction was attempted for the low temperature range of the system with 5% DBTD. Only two points were obtainable for an Arrhenus plot, but the activation energy and pre-exponential obtained ($E_a = 39$ kcal/mole, $\ln Z = 15$) seemed to indicate that an appreciable part of the apparent decrease in these parameters with percentage of DBTD was due to the effects of the order change and the reaction complexity on the method of analysis. Nevertheless, the magnitude of these errors is not sufficient to account for the entire decrease in stability. The trends shown by the curves for the liquid phase in Figures 10 and 11 are unquestionably real, although neither the slope nor the change in slope is altogether reliable insofar as magnitude is concerned.

The reaction in the vapor phase was always close to a first-order reaction, and for this reason, true values for activation energies are no doubt within the uncertainties quoted in Table I. This means that the trends for the vapor phase shown in Figures 10 and 11 are real in magnitude as well as direction. Kinetic parameters of the RDX/DBTD systems were based on approximately 30% of the reaction ($K = 0.30$ to 0.60) for the liquid decomposition and on 2% of the reaction ($X = 0.97$ to 0.99) for the vapor. Thus, the kinetic parameters may be considered representative of the reaction as a whole.

As exhibited by the PBX-108 data, introduction of the binder has a profound effect on the reaction. The typical order plots of Figure 2 show that a constant reaction order was not reached (hence, the reaction was not analyzable) until late in the decomposition ($X = 0.90$ to 0.95). This was the case for the three PBX-108 formulations tested. The order

over the range was found to be close to 1.57 for all PBX-108 formulations throughout the temperature range of this study. Nevertheless, as the kinetic parameters were derived from data obtained for only 5% of the reaction, and this 5% late in the reaction, it is questionable how applicable these parameters are to the decomposition as a whole and, more especially, to its most important initial part. Quantitatively, the usefulness is at best severely limited. Qualitatively, the DBTD effect, if sufficiently large, should be observed.

The most immediately apparent effect of DBTD on the decomposition of RDX is the increase in complexity of the liquid reaction. The order of increase shown by Figure 12 has two possible causes: (1) failure to achieve a homogeneous liquid phase due to immiscibility of DBTD in the fused RDX and (2) direct participation of DBTD in the activated complex. No evidence for immiscibility was found in the residue from reactions nor in a sample in an open pan raised to reaction temperature. Because of this lack of evidence and the excellent solvent properties of liquid RDX, DBTD apparently participates directly in the activated complex. This is consistent with the decrease in the values for $\log Z$ observed in Figure 11. Association of DBTD with the RDX activated complex would result in a more highly ordered activated complex and, hence, a lower entropy of activation. The value of $\log Z$ is proportional to the entropy of activation and should show a decrease with the increased percentage of DBTD.

The DBTD effect on the vapor decomposition is somewhat of an anomaly. All of the information from other plots is consistent with a simple, unimolecular decomposition, regardless of the percentage of DBTD, but the effects observed in Figures 10 and 11 are real. The vapor pressure of DBTD at the temperature of RDX decomposition is such that there is an appreciable amount in the vapor state. Thus, the DBTD stabilization may be due to a vapor interaction or a surface effect of the liquid. The activation energies measured are too small for the effect to be one of solution, because decomposition from solution has been shown to be governed by kinetic parameters close to those for liquid decomposition⁽⁵⁾. In any case, the effect is small and in the direction of stabilization, and the simplicity of the vapor reaction is apparently unimpaired.

The ash in the sample pans was examined on completion of the PBX-108 decomposition and showed that the binder phase had remained solid throughout the reaction. This phenomenon was probably primarily responsible for the complexity of the PBX-108 decomposition. The results in Table III show no apparent effect of the percentage of DBTD on this decomposition. The differences are within the uncertainties discussed previously, and there is no trend. The

most likely reason is that the DBTD for the most part is entrained in the binder phase and thus is prevented from contact with RDX during the decomposition. Of course, the effects of DBTD may be masked by those of the binder. The activation energy of the decomposition is lowered sufficiently by the binder for this to be the case. Unfortunately, the complexity of this decomposition is such that little absolute, quantitative information can be reliably obtained.

6. CONCLUSION

Regardless of uncertainties and ambiguities, the effect of DBTD is clearly such that it should cause no problem with either thermal sensitivity or aging of plastic-bonded explosives involving RDX. Although the effect tends to instability, it is small, particularly with small percentages of DBTD, that is, the E_{aL} versus percentage of DBTD curve of Figure 10 is most certainly not concave downward but probably convex. Thus, bearing in mind that DBTD percentages on the order of 10^{-2} or less are generally used in formulating explosives, the effect of the catalyst should be negligible, particularly in conjunction with the binder system.

REFERENCES

1. Rogers, R. N., Anal. Chem., 44(7) (1972) 1336.
2. Rogers, R. N., Thermochim. Acta, 3 (1972) 437.
3. Rogers, R. N. and L. C. Smith, Thermochim. Acta, 1 (1970) 1.
4. Ortiz, L. W. and R. N. Rogers, Thermochim. Acta, 3 (1972) 383.
5. Robertson, A. J. B., Trans. Faraday Soc., 45 (1949) 85.

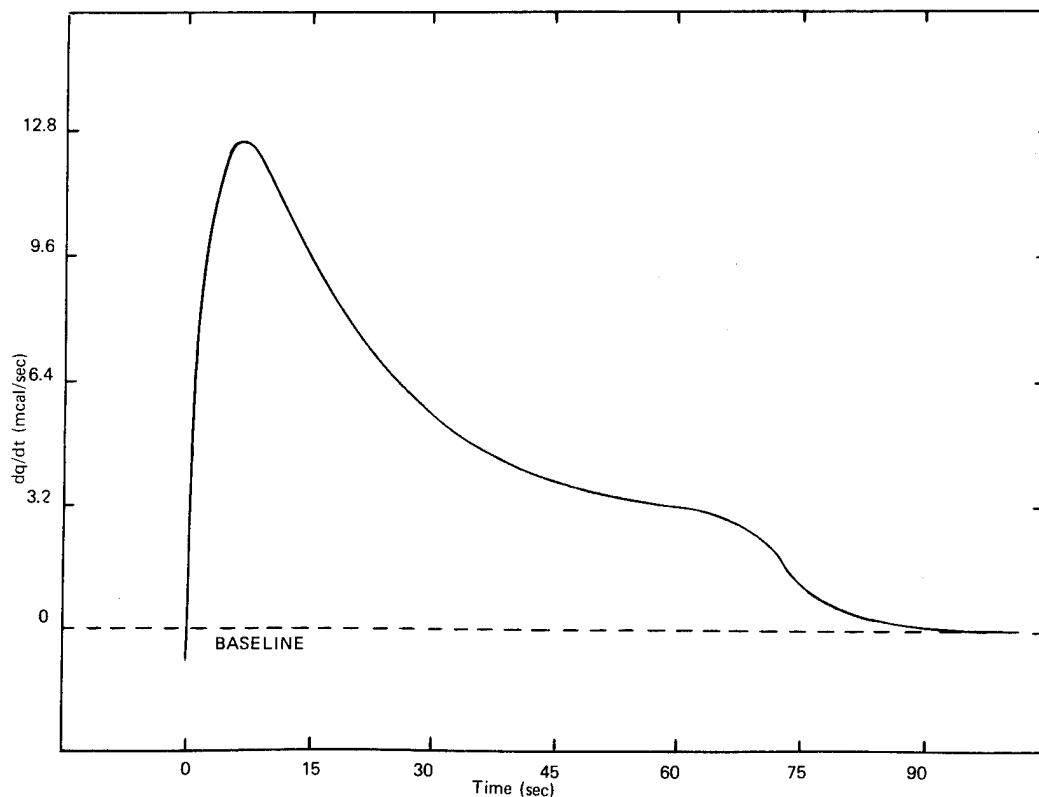


FIGURE 1. TYPICAL DSC CURVE; DECOMPOSITION OF RDX/0% DBTD AT 523.0°K

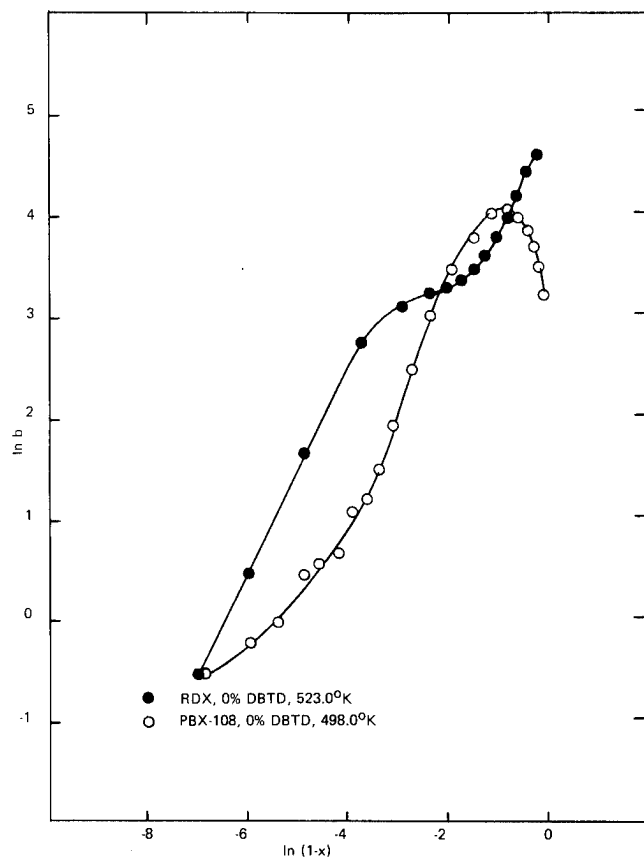


FIGURE 2. ORDER PLOTS FOR THE DECOMPOSITION OF RDX AND PBX-108

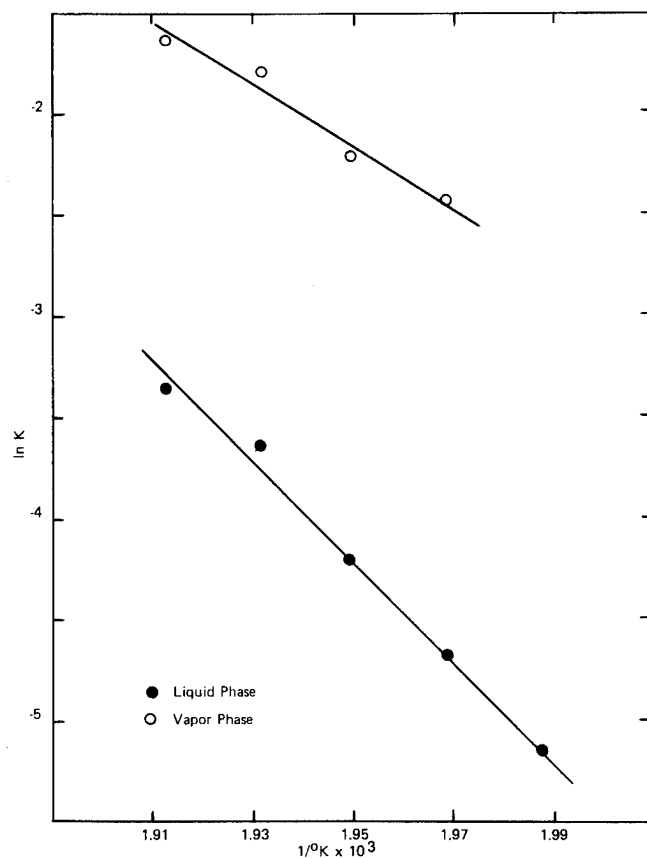


FIGURE 3. ARRHENIUS PLOT FOR DECOMPOSITION OF RDX/0% DBTD

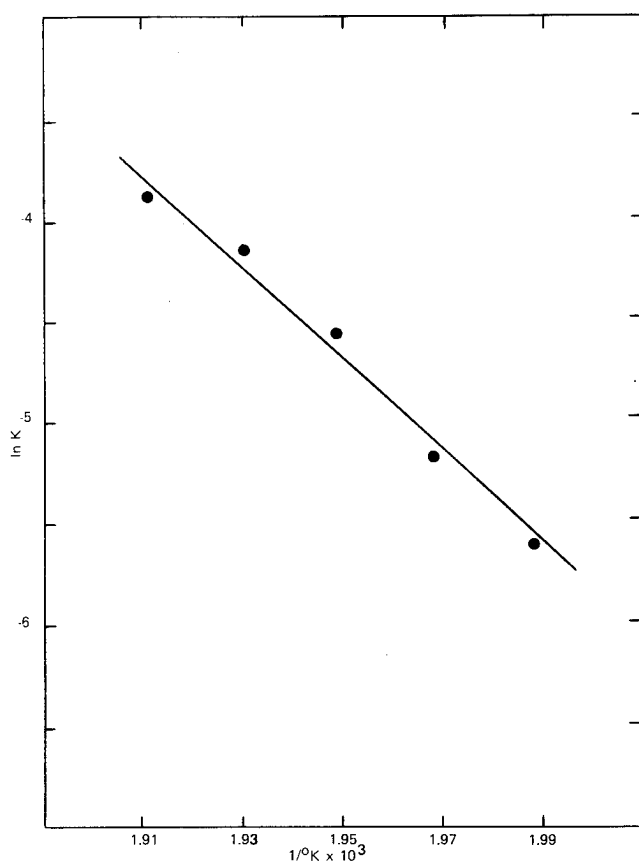


FIGURE 4. ARRHENIUS PLOT FOR DECOMPOSITION OF RDX/1% DBTD, LIQUID PHASE

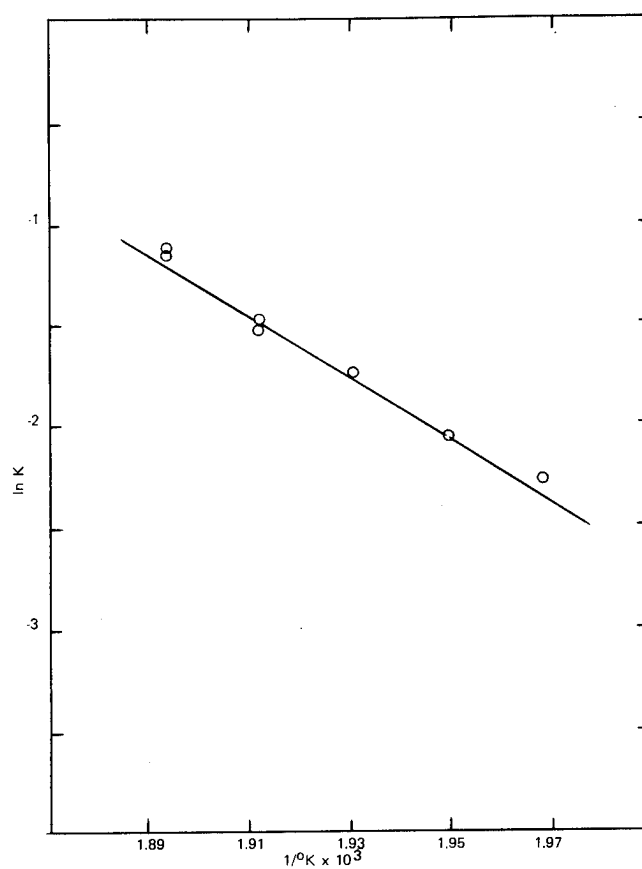


FIGURE 5. ARRHENIUS PLOT FOR DECOMPOSITION OF RDX/1% DBTD, VAPOR PHASE

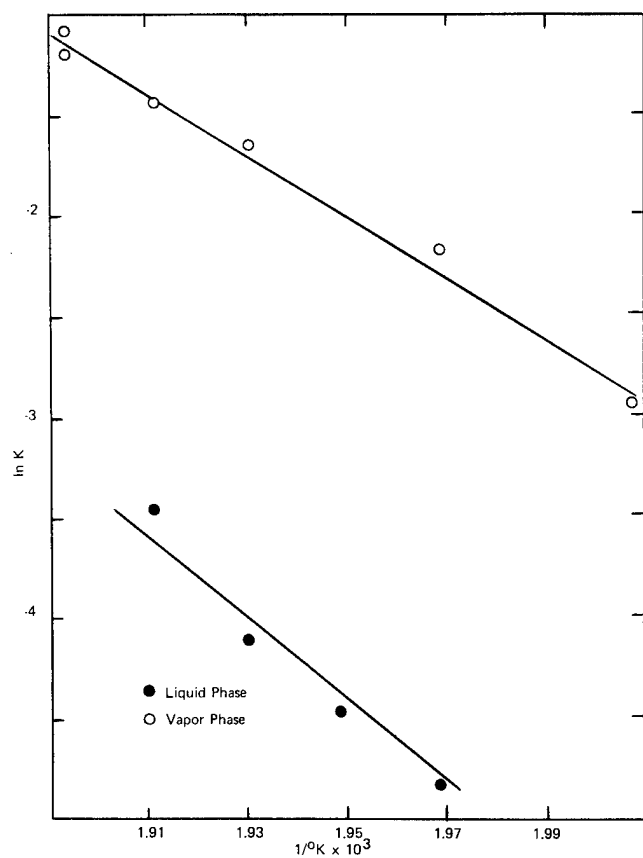


FIGURE 6. ARRHENIUS PLOT FOR DECOMPOSITION OF RDX/2% DBTD

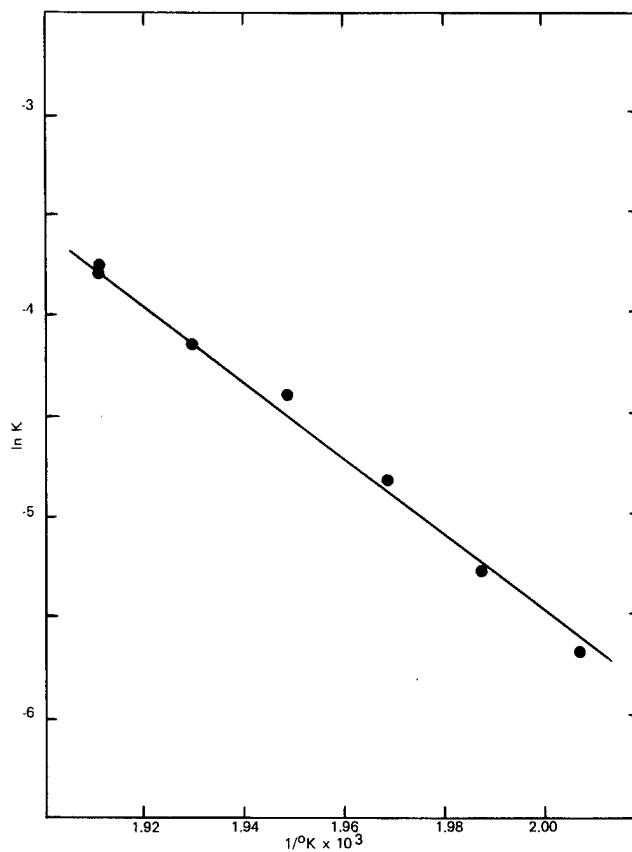


FIGURE 7. ARRHENIUS PLOT FOR DECOMPOSITION OF RDX/3% DBTD, LIQUID PHASE

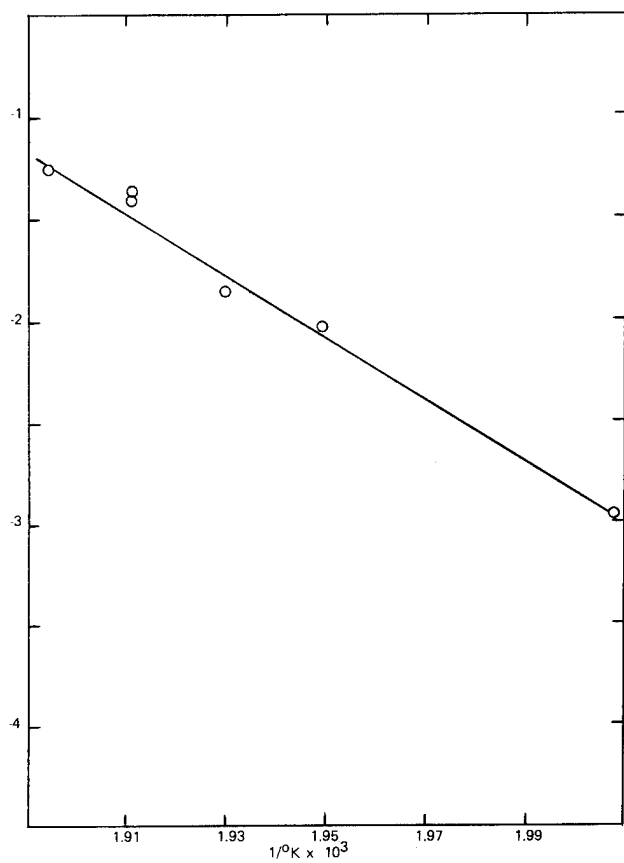


FIGURE 8. ARRHENIUS PLOT FOR DECOMPOSITION OF RDX/3% DBTD, VAPOR PHASE

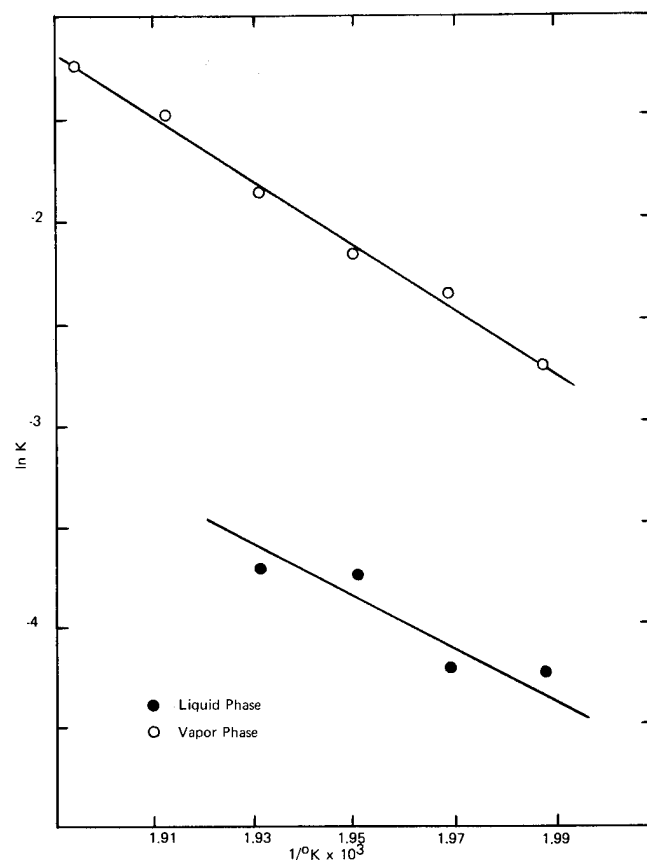


FIGURE 9. ARRHENIUS PLOT FOR DECOMPOSITION OF RDX/5% DBTD

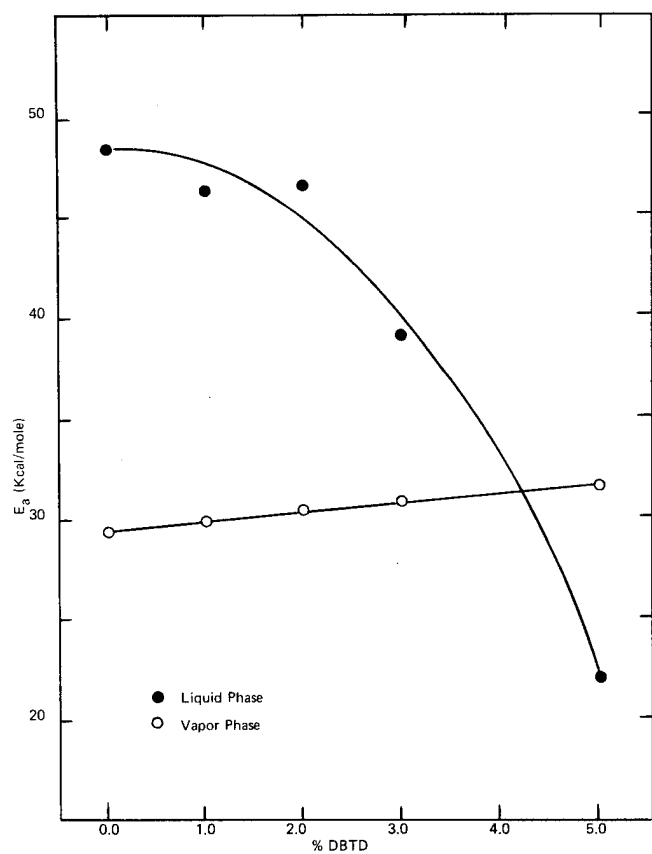


FIGURE 10. ACTIVATION ENERGY VERSUS % DBTD

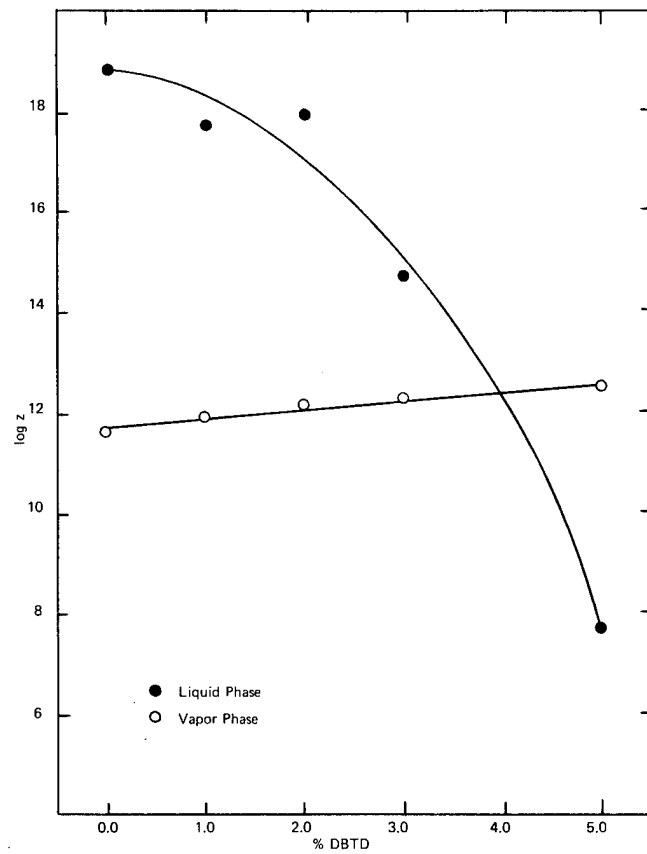


FIGURE 11. LOG PRE-EXponential VERSUS % DBTD

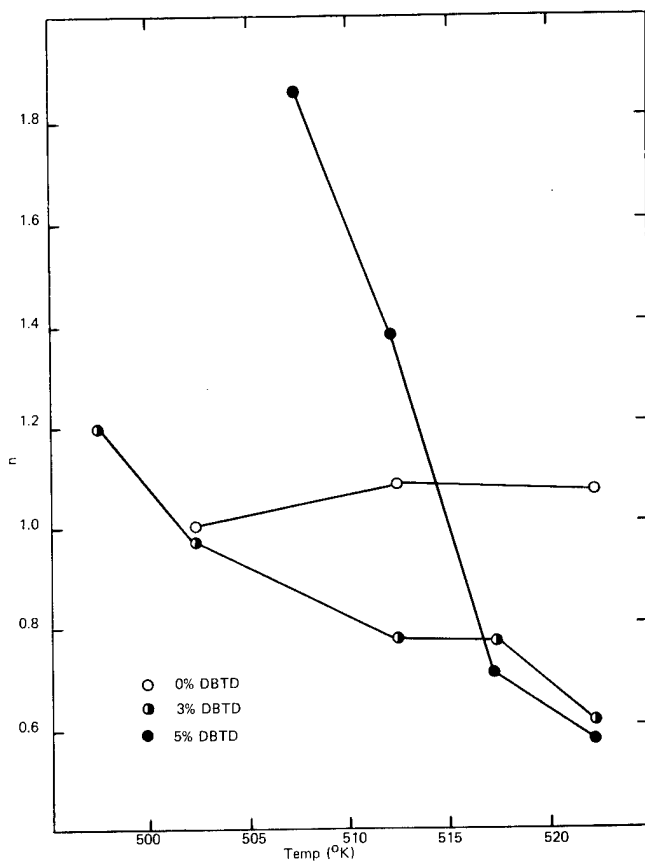


FIGURE 12. REACTION ORDER VERSUS TEMPERATURE LIQUID PHASE

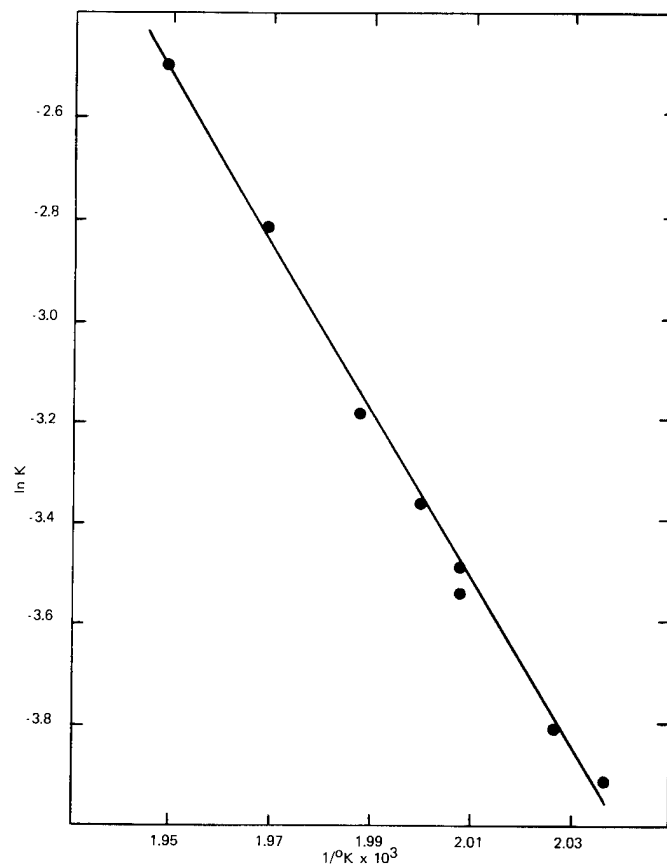


FIGURE 13. ARRHENIUS PLOT FOR DECOMPOSITION OF PBX-108 WITH 0% DBTD

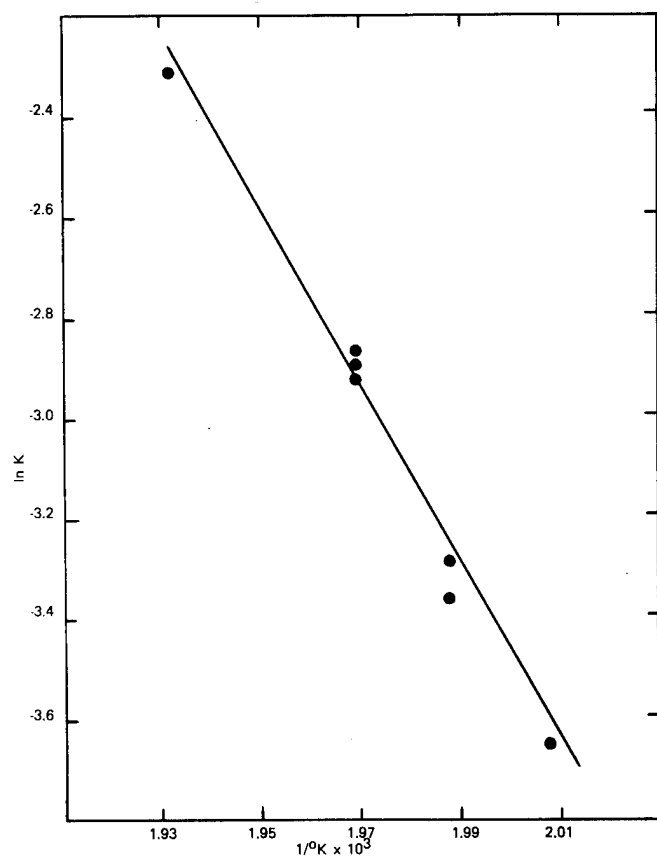


FIGURE 14. ARRHENIUS PLOT FOR DECOMPOSITION OF PBX-108 WITH 5% DBTD

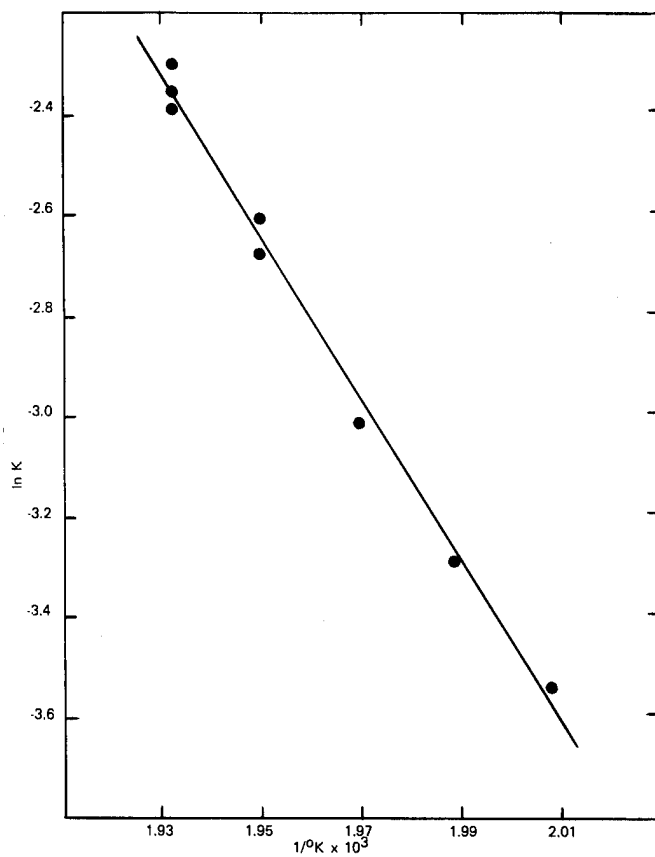


FIGURE 15. ARRHENIUS PLOT FOR DECOMPOSITION OF PBX-108 WITH 10% DBTD

TABLE I. ACTIVATION ENERGIES FOR RDX/DBTD SYSTEMS (See Figure 10)

% DBTD	E_{aL} (kcal/mole)	E_{aV} (kcal/mole)
0	48.78 ± 1.29	29.61 ± 1.85
1	46.60 ± 2.03	30.88 ± 0.86
2	46.79 ± 3.36	30.64 ± 0.88
3	39.28 ± 0.75	30.94 ± 1.12
5	22.10 ± 3.51	31.65 ± 0.67

TABLE II. PRE-EXPONENTIALS FOR RDX/DBTD SYSTEMS (See Figure 11)

% DBTD	Z_L (sec ⁻¹)	Z_V (sec ⁻¹)
0	9.43×10^{18}	4.96×10^{11}
1	6.40×10^{17}	8.86×10^{11}
2	1.01×10^{18}	1.60×10^{12}
3	6.01×10^{14}	1.99×10^{12}
5	5.48×10^7	3.82×10^{12}

TABLE III. ACTIVATION ENERGIES AND PRE-EXPONENTIALS FOR PBX-108

% DBTD	E_a (kcal/mole)	Z (sec ⁻¹)
0	32.81 ± 0.53	7.68×10^{12}
5	35.63 ± 1.30	1.13×10^{14}
10	31.75 ± 0.76	2.41×10^{12}

EXPLOSIVE AND PHYSICAL PROPERTIES OF POLYMER-COATED RDX

Andrew F. Smetana and Thomas C. Castorina
Feltman Research Laboratory
Explosives Division
Picatinny Arsenal
Dover, New Jersey

ABSTRACT

Particulate coating of military grade, Type B, Class A RDX (cyclotrimethylene trinitramine) was achieved by a vapor deposition polymerization technique with Parylene C (poly-chloro-p-xylylene). Optical and scanning electron photomicrographs and ESCA (Electron Spectroscopy for Chemical Analysis) were used to determine the continuity and degree of particulation of coating. The Parylene C coating is shown to be compatible with RDX; has protective action to mechanical and thermal energies; accelerates the dissipation of electrostatic charge; reduces the detonation rate and sensitivity to detonation transfer to RDX. ✓

1. INTRODUCTION

One of the major problems in the formulation of composite castable explosives is manifested by the extensive variations in their flow properties (viscosities) prior to and during pouring operations. The possible parameters affecting viscosity are, particle size and shape, surface impurities, energy of wetting, work involved by the vehicle or host matrix to penetrate between and into agglomerates, and flocculation (dispersion of solid in liquid or liquid in liquid). The cohesive and adhesive forces of the respective constituents in the mixture not only affect interparticulate behavior, but physical and explosive properties as well.

The surfaces of explosives, as contact layers in various chemical environments, can be regarded also as localized regions

on which explosive decomposition may be initiated or catalyzed. Modification of these surfaces can produce not only significant changes in explosive behavior (1-4) but also offer a variety of possibilities for improving the formulation of explosives systems. Attempts to modify interfacial behavior have been by coating the surface of one of the components in the mixture. The conventional method of coating particulate matter involve slurry techniques. The coatings produced by such techniques are non-uniform, physically unstable during formulation, and invariably incorporate agglomerates of uncoated particles. Coating by vapor deposition polymerization (VDP) has been shown (5,6) to produce depositions that are locked-on by virtue of their intimate replication of the surface roughness (on a sub-microscopic scale) with a minimum of agglomeration of the particulate material.

This report describes the coating of polycrystalline RDX powder by VDP, and the effect of particulated encapsulation on the explosive and physical properties of RDX.

2. EXPERIMENTAL

2.1 RDX

Type B, Class A, Lot HOL SR 114-63 was sieved (wet) to remove fines in concentrations of approximately 0.5%. The fractions remaining on a #200 sieve were collected and vacuum dried at ambient temperature for 96 hours. The particle size distribution was determined from photo micrographs; and its surface area by the modified BET method, ⁽⁷⁾ using Kr gas, was found to be 530 cm²/gram.

2.2 DICHLORO-DI-PARAXYLENE (DCDX)

The dimer obtained from Union Carbide Corp., Bound Brook, N.J. was used as received.

2.3 COMPATIBILITY

One gram samples were placed in break-seal ampoules provided with flame seals. The charged ampoules were affixed to a vacuum manifold and outgassed at ambient temperature for 5-7 days to 10⁻⁶ Torr before flame-sealing. The sealed ampoules were heated 40 hours at 90° and 120° ± 1°C, as designated. The gases generated by the heating were fractionated at -78°C and ambient temperatures, and analyzed mass spectrometrically.

2.4 EXPLOSION TEMPERATURE

The explosion temperature determinations were run on the modified PA explosion temperature apparatus described elsewhere ⁽⁸⁾.

2.5 IMPACT SENSITIVITY

Determinations were made of Parylene C-coated RDX on the PA apparatus with a 2kg. weight, according to the procedure given elsewhere ⁽⁹⁾.

2.6 CHARGE RELAXATION TIME

The procedure used for measuring the time of charge relaxation on the Parylene C coatings of RDX is based on Spiller's method ⁽¹⁰⁾, involving the exposure of powder samples to dc charging electrodes. The relaxation time (to zero charge) is obtained by extrapolation from the rate curve of dissipation of the initial electrostatic charge deposited, usually in the range of several microamperes.

2.7 PERCENT PARYLENE C COATING DETERMINATION

A two gram sample of Parylene C-coated RDX was placed in porcelain mortar and ground in acetone. The slurry was transferred to a medium-porosity fritted glass crucible and the RDX extracted with six-25ml portions of acetone under gravity flow (Parylene C is insoluble in acetone). The Parylene C contained in the crucible was air-dried and then placed in a 80°C oven for one hour, cooled and weighed. The extraction procedure was repeated until two consecutive weighings of Parylene C

agreed within 2mg. From the net weight of Parylene C thus obtained, the percent coating on RDX was calculated.

2.8 RDX PERMEABILITY

The procedure used for measuring permeability of RDX through the Parylene C coating is identical to the one used for the percent Parylene C coating determination, except that the coated RDX was not crushed. Incremental determinations per 400ml acetone, as percent RDX permeated through 1.5, 3.0, 4.5, and 6.0% coatings, respectively, were calculated as follows:

$$\% \text{RDX perm.} = \frac{(A - B)100}{A - W} - P$$

where: A = gross weight (coated RDX plus tared crucible)
 B = reduced gross weight (after an incremental permeation of RDX)
 W = tare weight of crucible
 P = percent Parylene C coating

2.9 COATING THICKNESS CALCULATION

Based on the assumed values of 75\AA^2 and 8\AA for the respective area and thickness of the xylylene chloride monomer molecule (XCM), derived from the theoretical values reported (6,11) the following formula was used to calculate the thickness of coating on RDX:

$$N = \frac{\text{mole fraction} \times \text{Avogadro's No.} \times \Sigma_{\text{XCM}}}{\Sigma_{\text{RDX}}}$$

where: Σ = surface area of molecules in subscript

N = no. molecular layers deposited on RDX

then: $T = N \times c$

where: c = thickness of XCM

T = thickness of Parylene C coating on RDX

The corresponding thicknesses of the 1.5, 3.0, 4.5, and 6.0 and 8.0% coatings are, 0.75, 1.50, 2.25, 3.00 and 5.33 microns.

2.10 UNIFORMITY OF COVERAGE

The Electron Spectroscopy for Chemical Analysis (ESCA) investigation of uniformity of Parylene C coverage of polycrystalline RDX powder was carried out with a Varian IEE-5 instrument, using a magnesium anode. This instrument generates x-ray photons with an incident energy of 1.25 kev in a 10 second scan. Approximately 50 scans, over a 10 minute period are required for an analysis. Energy deposition is 0.1 ev total (50 scans) to a half-thickness depth of 30-50Å. The level of x-ray intensity is such that no significant radiolytic perturbation of the sample is produced. The powder samples were mounted uniformly on aluminum cylinders with the aid of a two-sided adhesive Scotch tape and analyzed at room temperature. The 1s and 2p spectra of nitrogen and chlorine, respectively, were monitored to follow the uniformity of coverage with increasing deposition of polymer coating.

2.11 VAPOR DEPOSITION POLYMERIZATION (VDP)

A 4" Parylene coater (Figure 1) was constructed and used in the Laboratory under an experimental license from

Union Carbide Corporation, Bound Brook, New Jersey. The procedure for the VDP technique (detailed elsewhere ⁽¹²⁾) was modified and is described as follows: A measured quantity of DCDX was placed in an aluminum boat, and the boat placed in the distillation zone of the coater apparatus. To maintain particulation during the VDP coating process, the one pint container (for approximately 25g RDX powder) was lined with a 1/4" thick 50-60 durometer silicone rubber sheet, cemented together at the seams with Silastic RTV 731 adhesive, and 100g were added of Parylene-C-coated hemispheroidal solder (tin/lead) wafers. The coater was then evacuated to 10^{-3} Torr using a forepump protected with a -78°C trap. The distillation zone was heated to approximately 150°C and DCDX distilled into the pyrolysis zone set at 600°C . The pyrolysis gas consisting of the activated form of the monomer was then led into the deposition chamber containing the RDX powder. The deposition chamber was held at ambient temperature, and the coating of RDX proceeded by rotation of the sample container in which the hemispheroidal wafers acted as scrapers.

2.12 DETONATION RATES

Uncoated, 1.5% and 8.0% Parylene C-RDX were charged into the test fixture illustrated in Figure 2, under 5-ton pressure. Each charge contained a 1/4" portion of RD 1333 lead azide affixed with an electric bridge wire for initiation. The detonation rates were measured with a streak camera by placing the slit of the camera along the "window" of the test fixture according to the arrangement depicted in Figure 3. Each record is in the form of a still

picture of the streak superimposed on a distance scale and two horizontal lines (perpendicular to the slit) for alignment at the top and bottom.

To reduce the data, the record was aligned in a projection-type film reader such that the time axis (horizontal lines) coincided with the X cross hair. Distance-time points along the streak were then read and automatically punched on IBM cards in film reader units. In the distance direction (Y axis) the calibration scale in the still picture was read to convert film reader units to cm. An accurate scale was then projected on the X-axis and read. This reading combined with the exact writing rate calculated from the measured period was used for the time axis conversion. The calibration constants and data were fed into a linear least squares fitting routine on the computer. The routine solves for m and b in the equation of best fit $y = mx + b$ where y is distance and x is time. For the data reported here, m is the detonation rate but b has no real meaning because the origin was arbitrarily set when reading the film. Along with a printout of the velocity, the program also produced plots of the data with the fitted straight line superimposed. The curve was only fitted for times beyond about 1.5 microseconds because at earlier times the data is generated by the lead azide booster. The theoretical accuracy of this data reduction scheme is much better than 1% but the quality of the streak itself determines the real accuracy. For extremely high quality charges, variations less than 1% have been obtained, but for poorer charges variations of the order of 2.5% are observed.

The variations involved in this study are approximately 2% for any one set of replicate determinations.

2.13 COATED RDX PARTICLE DISTRIBUTION AND TOPOGRAPHY

Both photo-macrography and micrography were used to record pictorially the extent of particulation achieved by the modified VDP technique described above.

The topographical study was done with a MAC model scanning electron microscope under a service contract with Micron, Inc., Wilmington, Delaware.

2.14 THERMAL ANALYSES

Thermal profiles of the Parylene C-coated RDX and the RDX control were obtained with a Differential Scanning Calorimeter (DSC)-1B, Perkin Elmer Corp., Norwalk, Conn., and a Thermogravimetric Analyzer (TGA), E. I. dePont de Nemours & Co., Wilmington, Del. The samples for the DSC determinations were placed in standard aluminum pans and covered loosely with an aluminum lid. The heating rate was programmed at 10°C per minute and the flow of helium gas was controlled at 60 cc per minute. The observed temperature in °K was converted to °C and corrected for Fisher Scientific Chemical Co. thermal standards. The samples for the TGA analysis were weighed directly on the balance pan. The heating and flow rates were the same as those used in the DSC determinations.

2.15 DETONATION TRANSFER TEST

The procedure used in this study is a modified version of the one described

previously (13). All tests were run with a M55 detonator as the donor. The gap between the detonator and lead cup was fixed at 0.095". The lead cup was loaded with the test explosive at 11,000 psi to a density of 1.52 g/cc and a corresponding height of approximately 0.1". The lead cup measured, 0.174" o.d.; 0.134" i.d.; and had an average bottom thickness of 0.006".

3. RESULTS AND DISCUSSION

3.1 PHYSICAL PROPERTIES OF PARYLENE C-COATED RDX

3.1.1 Particulate Coating

One of the major problems associated with the various (including VDP) methods of coating polycrystalline powders is that of agglomeration. By virtue of the cohesive forces between the particles, whether in the dry state or in liquid suspension, coating depositions often-times encompass massive groupings of particles. In suspension media agglomeration may be overcome by using liquids having larger adhesive forces than the inherent inter-particulate cohesive forces. In the dry state, as predicated by the VDP method, the problem of agglomeration may be solved electrostatically or mechanically. Attempts to achieve particulate coating by introducing various forms of electrostatic dissipators resulted in failure. The concept (14) of using scrapers against a soft lining in the sample container proved to be effective in maintaining particulation during the coating process. Metals and metal alloys covering a range of densities were investigated. Aluminum was too light to separate, and lead was

heavy enough to pulverize the polycrystalline particles. The tin/lead alloy of intermediate density was satisfactory as is evidenced by the photomicrographs in Figures 4-6. The polycrystalline powder remains particulate with increasing polymer deposition. The comparative appearance of the RDX powders under higher magnification is shown in Figures 7-9. The 1.5% coating compared to the uncoated RDX shows no apparent difference in the light refracted. Evidentially, a 0.75 micron thick coating is transparent to wavelengths in the visible. However, at 8% coverage opacity becomes discernible.

A more definitive examination of the topography of the coating is shown by the scanning electron micrographs in Figures 10-11. Figures 10a and 11a of RDX with 1.5 and 8% Parylene C coating, respectively, depict encapsulation that is distinctly discrete where the individual crystals appear similar to the uncoated RDX shown in Figure 11d. In the case of excessive coating of 8% Parylene C at 1000 magnification, Figure 11c, the superficial deposition is shown to be spheroidal, whereas underlying depositions appear to be smooth and continuous. That the encapsulation is continuous and replicates intimately the substrate surface is shown in Figure 12. This micrograph was obtained of a section of the coating $1.5 \times 10^4 \text{ \AA}$ thick which had separated from the crystalline substrate.

3.1.2 Continuity of Coating

Examination of the continuity of coverage by the VDP method was done at the sub-microscopic level using ESCA. The level of sensitivity for the detection of nitrogen atoms in their various oxida-

tive states is one part per 10^5 , and only slightly less for chlorine. In addition, the ESCA technique is especially suitable for the analysis of Parylene C coverage of RDX in that the nitrogen and chlorine atoms are not mutually present in both components. The nitrogen and chlorine signals were scanned with increasing coverage and plotted as shown in Figure 13. If complete encapsulation were a requirement then the ESCA technique provides an analysis of the surface layer having a thickness of approximately 100 \AA . Since the chloroxylylene molecule has a thickness of 8 \AA , the effective coverage would be a minimum of twelve molecular layers. However, to establish complete coverage by the ESCA technique twice this minimum value would be required with the proviso that the coating is deposited uniformly. Because this is not the case, the 3% value or $1.5 \times 10^4 \text{ \AA}$ thickness shown in Figure 13 was in fact necessary under the experimental conditions to achieve complete coverage of the RDX polycrystalline powder.

3.1.3 Permeability of Coating

Although the VDP method of coating completely replicates the substrate surface as demonstrated by ESCA analysis, the continuous coating could be considered porous nevertheless because of the fibroidal character of polymers in general. Therefore, it was of noteworthy interest to determine the permeability of RDX through the coating which may be regarded as a permeable membrane. Acetone was selected as the vehicle for such a determination because of the solubility of RDX in it and its ease of evaporation for quantitative measurements. The permeation of RDX as a

function of percent coating of Parylene C is summarized in Figure 14. Even though complete coverage is represented by a 3% coating, the RDX is shown to permeate through the coating rather extensively. As the percent coating increases, the extraction of RDX by acetone is reduced proportionately. Throughout the process of extraction of RDX the coating remains stable, e.g., when all of the RDX was extracted from the 1.5% coating, the Parylene C maintained its capsular shape.

3.1.4 Melting Point

The calorimetric thermogram of uncoated RDX depicted in Figure 15 has a sloping curve on the low temperature side due to HMX impurity and incipient decomposition products of RDX. The double peak is attributed to the non uniformity of sample melting caused by the loosely placed lid on the pan. The endotherm at 186.5°C is equal (within experimental error) to the extrapolated value indicated. The relatively smooth endothermic curves obtained in Figures 16 and 17 for the 1.5% and 8% coated RDX, respectively, are due to the confinement produced by the capsular coating, analogous to a secured lid on the pan enclosing the sample (melting point range Parylene C, $280\text{--}290^{\circ}\text{C}$). Examination of both these thermograms shows that the onset and extrapolated onset temperatures do not coincide (as for the uncoated RDX) and spread from 186.5° to 201°C . This induction period, or delaying action on the melting point of RDX is apparently due to the heat capacity and thermal conductivity of the Parylene C.

3.2 CHEMICAL PROPERTIES OF PARYLENE C-COATED RDX

3.2.1 Compatibility of RDX/Parylene C

The experiments described in Table I were conducted to demonstrate the thermal stability of RDX in contact with Parylene C as an oxidizable substance. Examination of the data shows that the quantities of gases evolved by the control and coated samples of RDX are at trace levels. Therefore, the immediate conclusion to be drawn is that the RDX and Parylene C are compatible under the accelerated conditions of elevated temperatures at which the test was conducted. Any further interpretation is presented only on the basis of the possibility of an incipient trend in the reactivity of RDX with Parylene C under more stringent conditions. This trend is demonstrated by the gases evolved by the uncoated RDX, viz., N_2 , CO_2 and NO which change in quantity only as the temperature is increased from 90° to 120° ; and at 90° , in the presence of Parylene C, the quantity of these gases does not change, but H_2 is shown to be evolved as a function of the percent Parylene C coating. In addition, at 120° the presence of Parylene C increases the quantity of gases attributable to RDX decomposition with increased coating, but the H_2 evolution is the same as at 90° and O_2 starts to be evolved. At 90° or 120° chlorine is not detected in either nascent or combined form. It is possible, therefore, that although Parylene C is not oxidized at these temperatures it may nevertheless induce incipient decomposition of RDX.

3.2.2 Thermal Stability

When RDX is heated to its melting point (190° for the Type used in this study) decomposition starts at approximately 150° and eventually accelerates in the liquid phase as the temperature is increased beyond the melting point. The gravimetric thermogram shown in Figure 18 shows the onset temperature at which weight loss becomes discernible. At 170° this is due primarily to the volatility of RDX. However, at the 4% weight change corresponding to 200° which falls in the induction period, transient species of decomposition could interact with the polymer coating. Examination of the thermograms of 1.5% and 8% coated RDX in Figures 19 and 20, shows a retarding effect on the volatilization and subsequent decomposition rate of RDX, the onset temperatures (175° and 190°), and the 4% weight loss temperatures (203° and 208°), respectively. The retardation of the weight loss rate may be attributed to the diffusion process of gaseous products through the permeable membrane-type coating. The discontinuity at the 62% weight loss in Figure 20 could be explained on the basis of this model where the rate of formation of products of decomposition is much faster than the rate at which the products can diffuse through the encapsulant. The resultant build-up of products causes a momentary cessation of weight loss until pressures (known to be constrained up to several atmospheres within membranes that are permeable) increase to the point of rupturing the coating and thereby effect a resumption in the release of products of decomposition as indicated. Such an interpretation is considered consistent with

the permeability and compatibility data presented above.

3.2.3 Thermal Initiation

The explosion temperature determinations of the various percent coated RDX, plotted in Figure 21 were conducted isothermally at 300° . Any contribution made by the Parylene C to the thermal initiation of RDX could be in the form of some interaction with the substrate, RDX. As had been demonstrated by the gravimetric thermograms and the compatibility data cited previously, there is an apparent absence of such interaction, even at temperatures of explosive decomposition of RDX; and the delays in time to explosion to the percent coatings up to 3%. Although Parylene C melts at approximately 300° , it appears to remain intact as an encapsulant for the seconds-long period involved in the initiation of RDX and serves to momentarily retard the transfer of heat to the RDX substrate. However, the leveling-off of the protective action demonstrated by the 8% coating may be due to the confining action of the encapsulant. As indicated in the gravimetric thermogram, (Fig. 17) confinement of gaseous products of decomposition could conceivably accelerate decomposition of the explosive substrate after a given interval, thereby off-setting the initially-induced retardation of time to explosion to the extent shown in Figure 21.

3.2.4 Impact Sensitivity and Electrostatic Charge Relaxation

The impact sensitivity data shown in Table II demonstrates, once again, the protective role played by the encapsulant, Parylene C on RDX. The reduction

in sensitivity to mechanical energy relative to the uncoated RDX is observed to be one third by the 3% and 8% coatings. This leveling-off effect of the coatings by the 3-8% values was observed also in the explosion temperature test (Fig. 21). In that case, the otherwise expected increase in protection with increased coating thickness, presumably is offset by a corresponding enhancement of sensitivity with increasing confinement of gaseous products of decomposition. Whereas, in the impact sensitivity test the same departure from the inverse relationship of thickness of coating to sensitivity could be attributed instead to a correspondingly enhanced adiabatic compression of air entrapped by the encapsulation ⁽¹⁵⁾.

The decrease in the time to electrostatic charge relaxation is shown in Table II to be a function of the Parylene C coating, and is inversely related to the thickness of the coating. The approximately 50% reduction may be interpreted in terms of the comparative electrophilicity of RDX and Parylene C derived from their respective surface interactions with water. The extent of hydrophilicity of the RDX surface ⁽³⁾ was calculated by Zettlemoyer's method ⁽¹⁶⁾ to be 100%; whereas, the surface of Parylene C is virtually hydrophobic ⁽⁴⁾. Water, being amphoteric, interacts with either negatively or positively charge-deficient surfaces, and adsorption on the RDX surface is at electron-deficient sites. Therefore, if one considers electrons as nucleophiles, their residence time on the RDX surface are expected to be longer than on the Parylene C coating as indeed has been observed.

3.2.5 Detonation Transfer

According to the data listed in Table III the presence of Parylene C increases the transit time though the lead, presumably by affecting the time to and plane of initiation of detonation (run-up). However, no significant difference is found between 1.5% and 8% Parylene C samples perhaps due to the variance of the experiment. Therefore, the role of alteration of detonation velocity and run-up to initiation can not be differentiated by this data.

3.2.6 Detonation Rates

The velocities of detonation were derived from the slopes of the straight lines fitted through the data points shown in Figures 22 to 24. The observed slight deviations from the straight lines are attributed to minor discontinuities in density produced by the incremental pressing of the samples into the fixtures. The results are summarized in Table IV. The detonation rates are the average of the multiple determinations with their associated experimental deviations. Also shown are the normalized detonation rates based on the variation in densities listed in column three. The rates were normalized by using the factor: 300 m/sec. for every 0.1 difference in density relative to the density of the uncoated RDX.

According to Urizar ⁽¹⁷⁾, the detonation velocities of composite explosives can be estimated empirically by the relationship:

$$\text{Det. Vel. } \{A,B\} = \{ \text{Vol.\%A} \} (\text{Urizar Const. A}) + \{ \text{Vol.\%B} \} (\text{Urizar Const. B})$$

where the assumption is made that the product of the volume percent and the

Urizar constant (in cm./microsecond) of each component in the composite explosive {A,B} contributes to the detonation velocity of that mixture. This relationship was used to determine whether the Parylene C behaved as an inert diluent.

The volume percents were calculated using the densities, 1.289 and 1.804 g/cc for Parylene C and RDX respectively, and are shown in column two of Table IV. The Urizar constant for Parylene C at the 10.8 Vol.% concentration in RDX was calculated to be 0.1120 cm/microsecond. Based on this value for Parylene C, the detonation velocity for a mixture of 18 Vol.% Parylene C was calculated as 0.6640 cm./microsec. The extrapolated value of the detonation velocities from the experimental values plotted in Figure 25 at the 18 Vol.% Parylene C is shown to be 0.6650 cm./microsec. which is in good agreement with the calculated value, 0.6640. What has been thus demonstrated once again is that Parylene C does not interact with RDX even under the most stringent of conditions.

4. CONCLUSIONS

Significant changes in the physical and explosive properties of polycrystalline RDX powder have been established by particulate encapsulation with an inert polymer coating. Such changes are attributed not only to the chemical properties of the protective polymer coating, Parylene C, but also the virtual absence of encapsulated agglomerates of RDX crystals. Because the polymer coating on RDX retains its integrity as an encapsulant at temperatures approaching 300°C, RDX would be rendered insoluble

in composite matrices which do not include a solvent for RDX, its particle size distribution optimized and maintained during casting operations, and the rheology of such castings improved, making possible higher solids loading compositions. If indeed, the interparticulate behavior of polycrystalline powders of explosives can be altered favorably and warrants the associated effort, emphasis should be placed on developing coating techniques which achieve particulate encapsulation at a cost effective level.

Acknowledgement

The authors are indebted to the following who have contributed their services and talents in furnishing some of the data included in the report: Drs. J. Sharma, C. Feng and B. Pollock, Messrs. L. Hayes, H. Jackson, R. J. Graybush, E. Dalrymple, and M. Kirshenbaum; and are especially appreciative of the helpful consultations with J. Hershkowitz.

References

1. Castorina, T.C., Haberman, J., and Smetana, A.F., "Int. J. Applied Radiation and Isotopes", 19, 495 (1969).
2. Haberman, J. and Castorina, T.C., "Thermo chimica Acta", 5, 153 (1972).
3. Castorina, T.C., Haberman, J., Avrami, L., and Dalrymple, E.W., "Reactivity of Solids, Proceedings of the 6th International Symposium, Schenectady, N.Y.", August 25, 1968, pp. 299-309.
4. Castorina, T.C., and Smetana, A.F., "J. of App'd Polymer Sci.", 18, 1373-1383 (1974).

5. Spivack, M.A. "Corrosion" 26, No. 9, 371-376 (1970).

6. Gorham, W., and Niegisch, W.D., "Ency. Polymer Sci. and Tech." 15, 98-124 (1971).

7. Zettlemoyer, A.C., Young, G.J., Chessick, J.J. and Healing, F.H., "J. Phys. Chem." 57, 649 (1953).

8. Castorina, T.C., Haberman, J., Dalrymple, E.W., and Smetana, A.F., "PATR 3690", April 1968.

9. Clear, A.J., "Tech. Re. FRL-TR-25", January 1961.

10. Spiller, L.L., "J. Paint Tech." 19, 98 (1972).

11. White, C.E., Union Carbide Corporation, Bound Brook, N.J., "Private communication".

12. Shechter, L., "U.S. Pat. 3,556,881 (1971).

13. Smacker, W.G., Voreck, W.E., and Dalrymple, E.W., "PATR 4659", February 1974.

14. Fleming, P., Univ. Calif., Livermore, "Private communication".

15. Bowden, F.P., and Yoffee, A.D., "Fast Reactions in Solids", Butterworth, London, 1958.

16. Chessick, J.J., Healing, F.H., and Zettlemoyer, A.C., "J. Phys. Chem." 60, 1345 (1956).

17. Mader, C.L., Defense Standards Laboratories, Maribyrnong, Victoria, Australia, "Tech. Memo.", 29 August 1969.

Biographies

Andrew F. Smetana received a B.S. in Chemistry from Seton Hall University in 1954, and has done graduate work there and at Stevens Institute of Technology. He was employed by Picatinny Arsenal in 1955 as a chemist in the Propellants Analytical Section of the General Laboratories. From 1956 to 1958 Mr. Smetana was a member of the U.S. Army serving as a Petroleum Products Quality Control Specialist in Leghorn, Italy. He returned to the Arsenal in 1959 and from 1960 to the present he has been a member of the Explosives Division of the Feltman Research Laboratory. His specialties include gas chromatography and mass spectrometry.

Thomas C. Castorina is Chief of the Surface and Analytical Chemistry Section which is engaged in the characterization of energetic materials, including the detection and identification of explosives and explosive residues by their elemental, molecular impurity profiles, and vapor-substrate interactions. He received a B.S. in chemistry from Brooklyn College and an M.S. in chemistry from Stevens Institute of Technology, followed by 60 credit hours of postgraduate studies. He has been involved in the field of explosives technology for the past 25 years at Picatinny Arsenal with experience in organic radio tracer methodology, radiation and surface chemistry and modern instrumental methods of analyses.

Table I
Compatibility of RDX with Parylene-C Coating

Percent PC Coating	cm ³ Gas x 10 ³ STP/g Coated RDX											
	90°C						120°C					
	N ₂	O ₂	CO ₂	H ₂	NO	Total	N ₂	O ₂	CO ₂	H ₂	NO	Total
Uncoated	3		4		1	8	12		1		3	16
1.5	3		3	2	1	10	24	1	1	1	4	31
8.0	2		1	8	1	12	36	1	1	9	8	55

Table II
Effect of Parylene-C Coating on RDX Response
to Mechanical Energy and Electrostatic Charge Relaxation

Test	Uncoated RDX	Percent PC Coating on RDX	
		3	8
Minutes to Electrostatic Charge Relaxation	33	20	16
Impact Sensitivity 2 kg. wt., inches	11	15	14

Table III
Detonation Transfer Initiation of
Parylene C Coated RDX

Sample	Lead Time ⁽¹⁾ (micro seconds)
Control Lead (uncoated RDX, Type B)	0.91 ± .05
Standard Lead (RDX + 0.5% graphite)	0.91 ± .02
1.5% Coated RDX	1.07 ± .07
8.0% Coated RDX	1.07 ± .05

(1) average of five determinations

Table IV

Detonation Rates of Parylene-C Coated RDX

Wt. Percent Coating	Vol. Percent Coating	5-Ton Press Loading Density	Detonation Rate cm/microsec \pm av. dev.	Normalized Detonation Rate cm/microsec \pm av. dev.
0	0	1.671	0.7846	0.0119
1.5	2.0	1.695	0.7766	0.0102
8.0	10.8	1.725	0.7288	0.0017

d Coating = 1.267
RDX = 1.604

Figure 1. Vapor Deposition Polymerization Apparatus

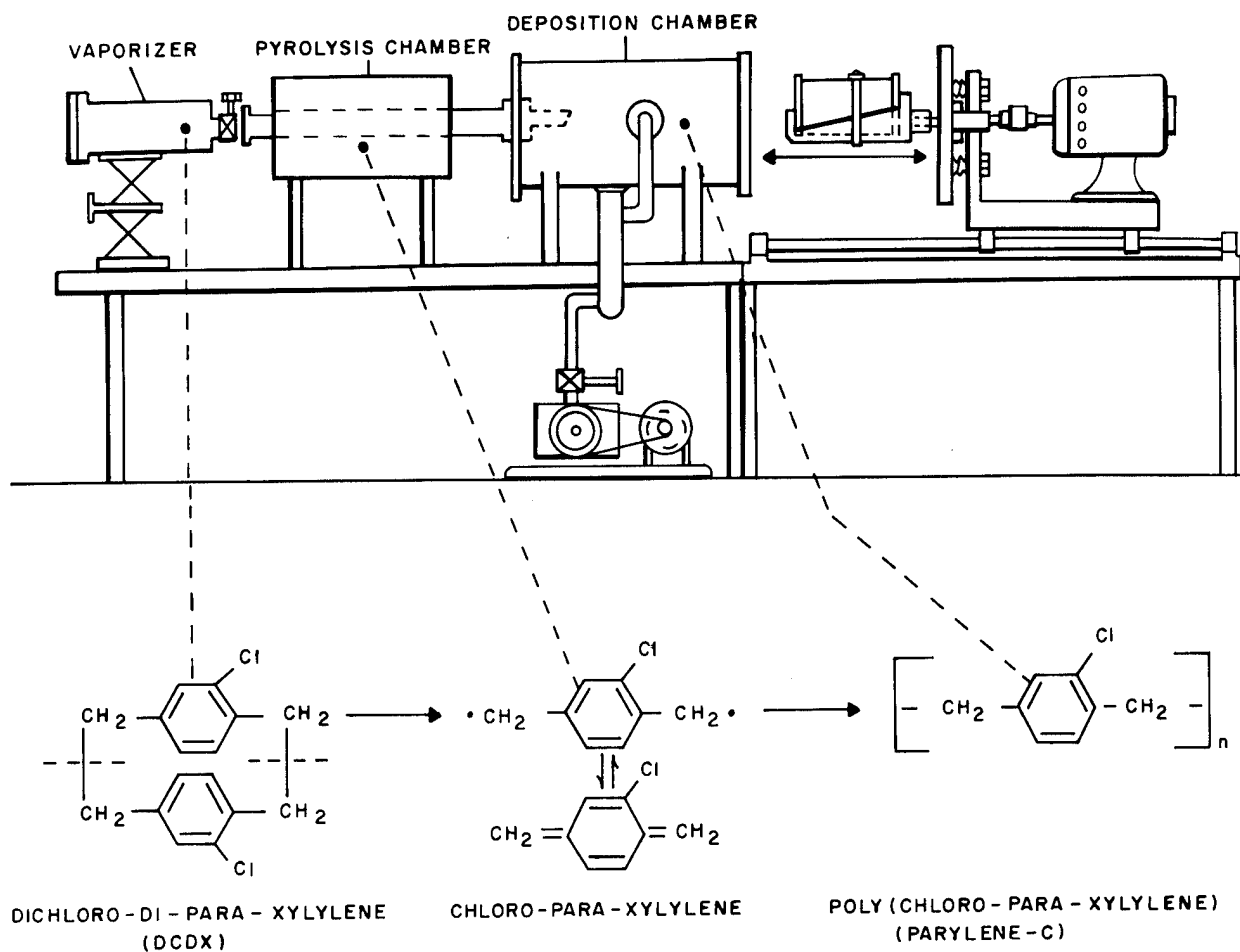
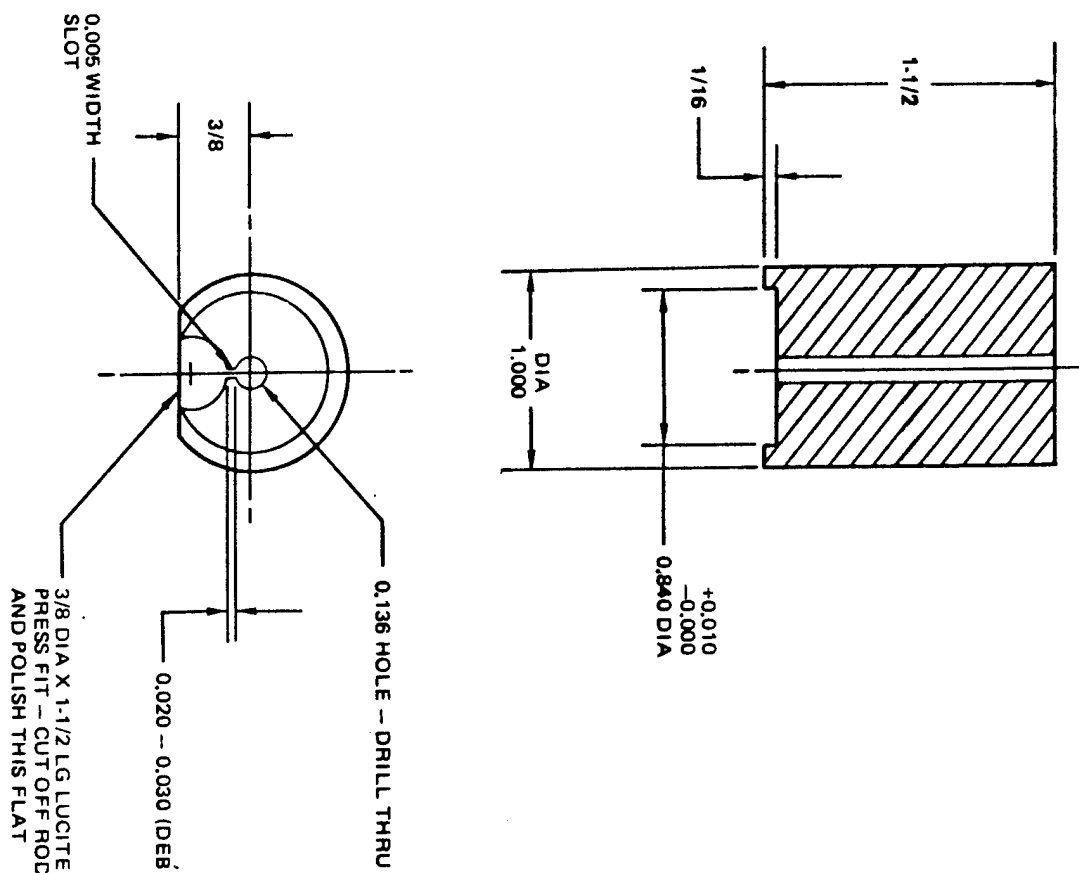


Figure 2. Detonation Velocity Fixture



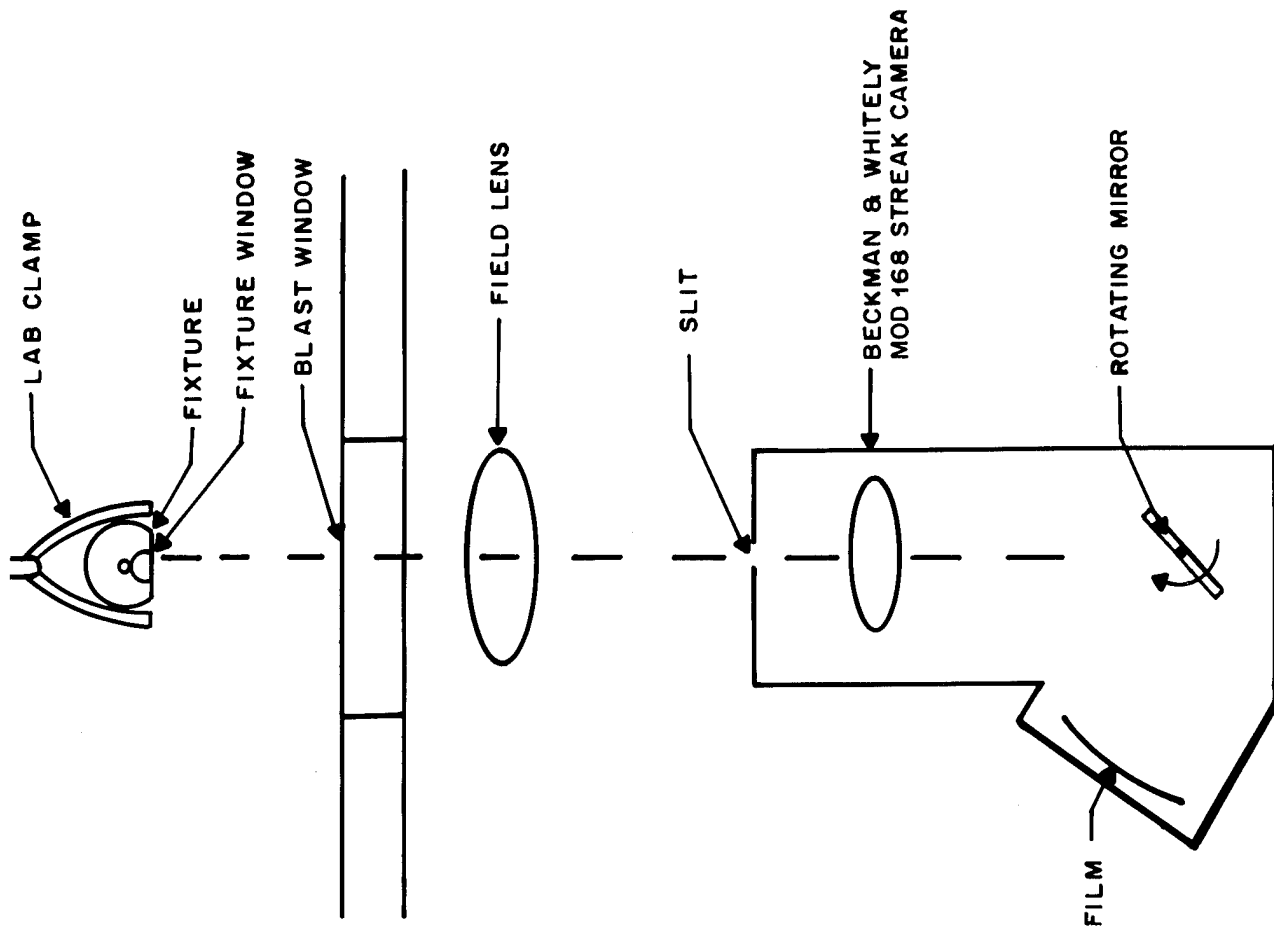


Figure 3. Top View of Experimental Arrangement of Detonation Rate Determination

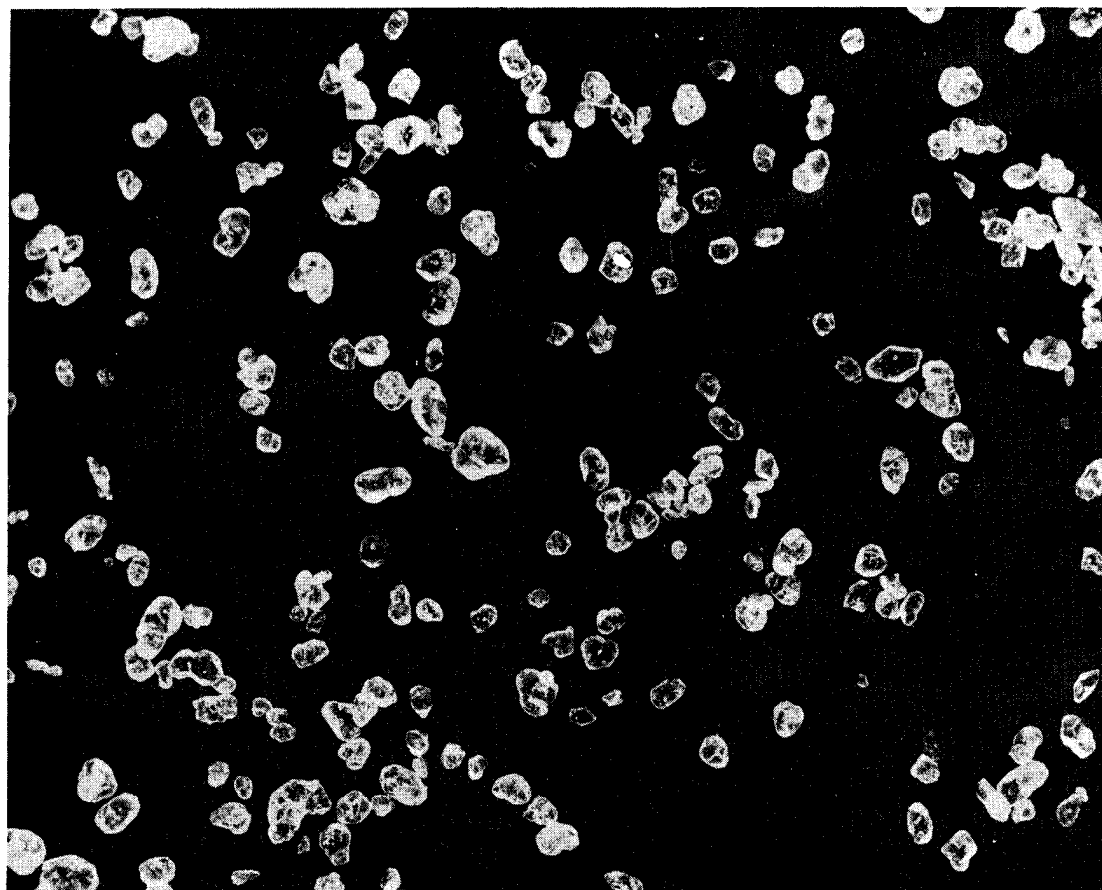


Figure 4. Photomicrograph (x20) RDX, Type B, Class A >#200 Mesh

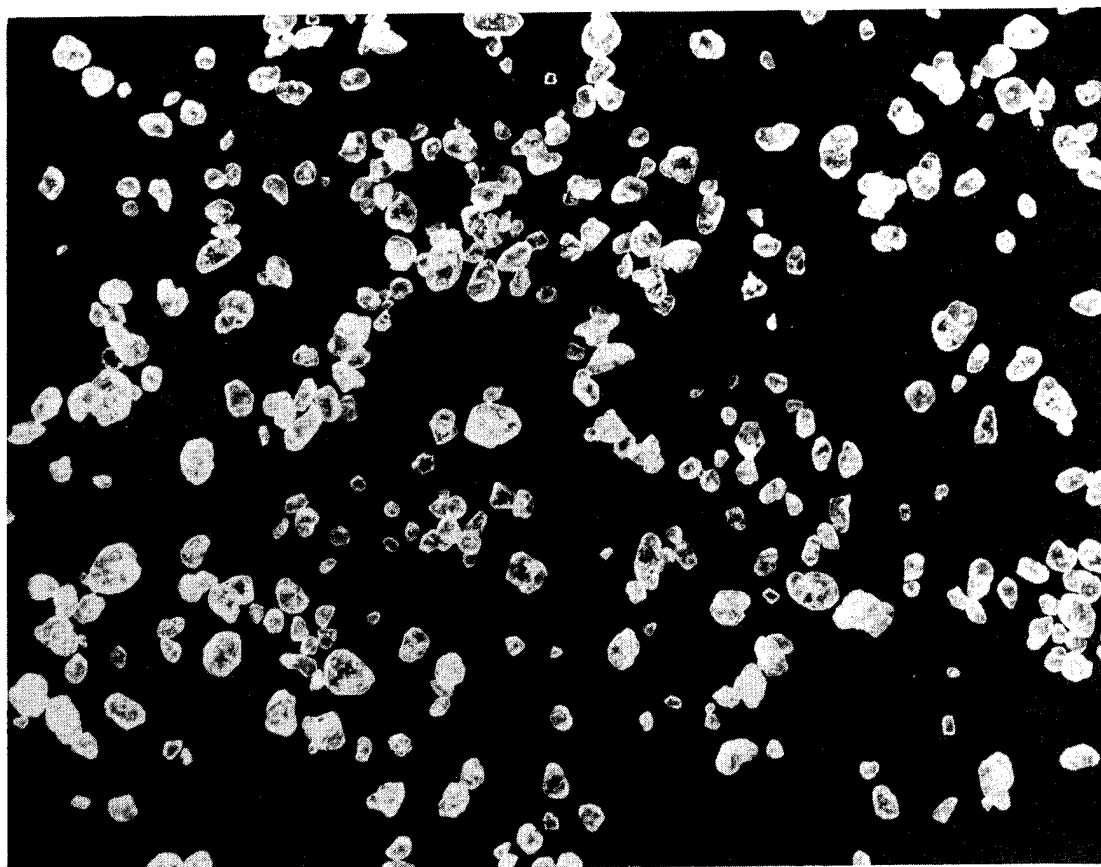


Figure 5. Photomicrograph (x20) RDX Coated with 1.5% Parylene C

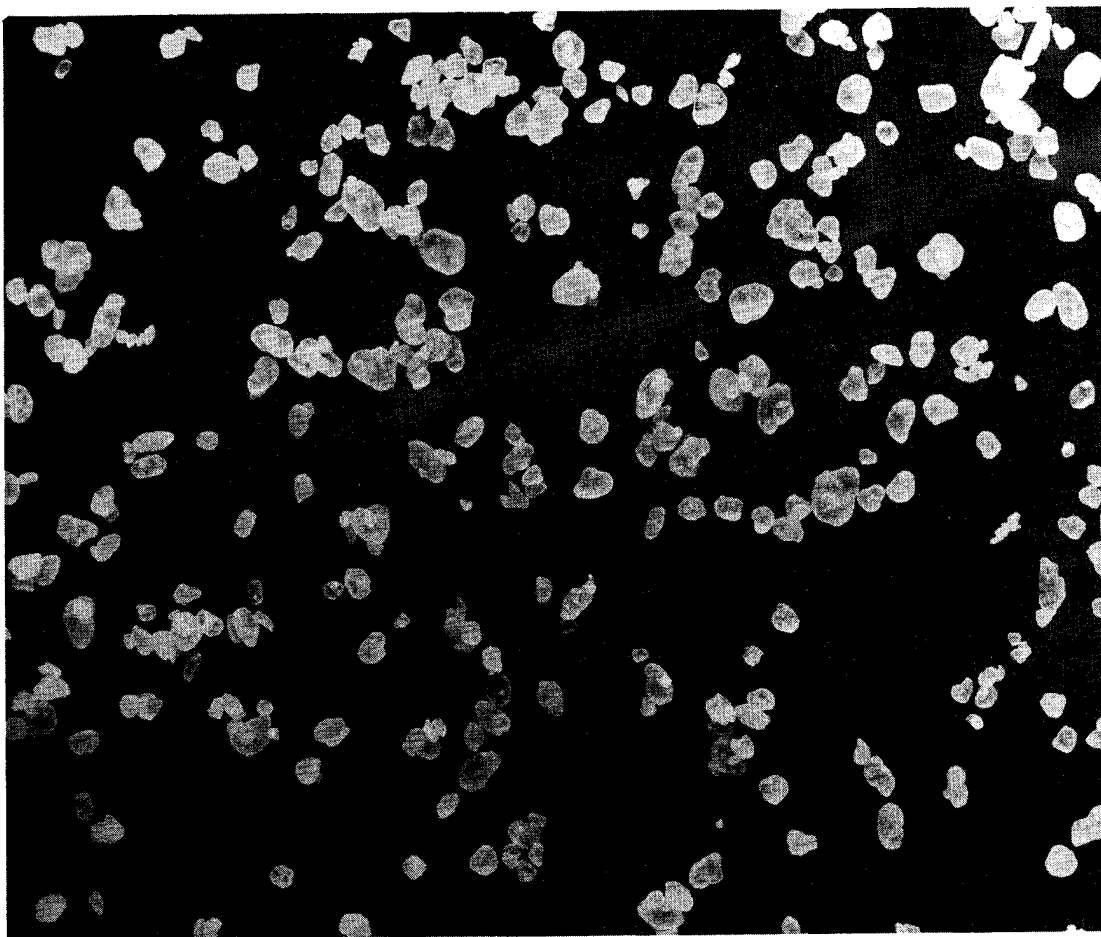


Figure 6. Photomicrograph (x20) RDX Coated with 8% Parylene C



Figure 7. Photomicrograph (x90) RDX, Type B,
Class A >#200 Mesh

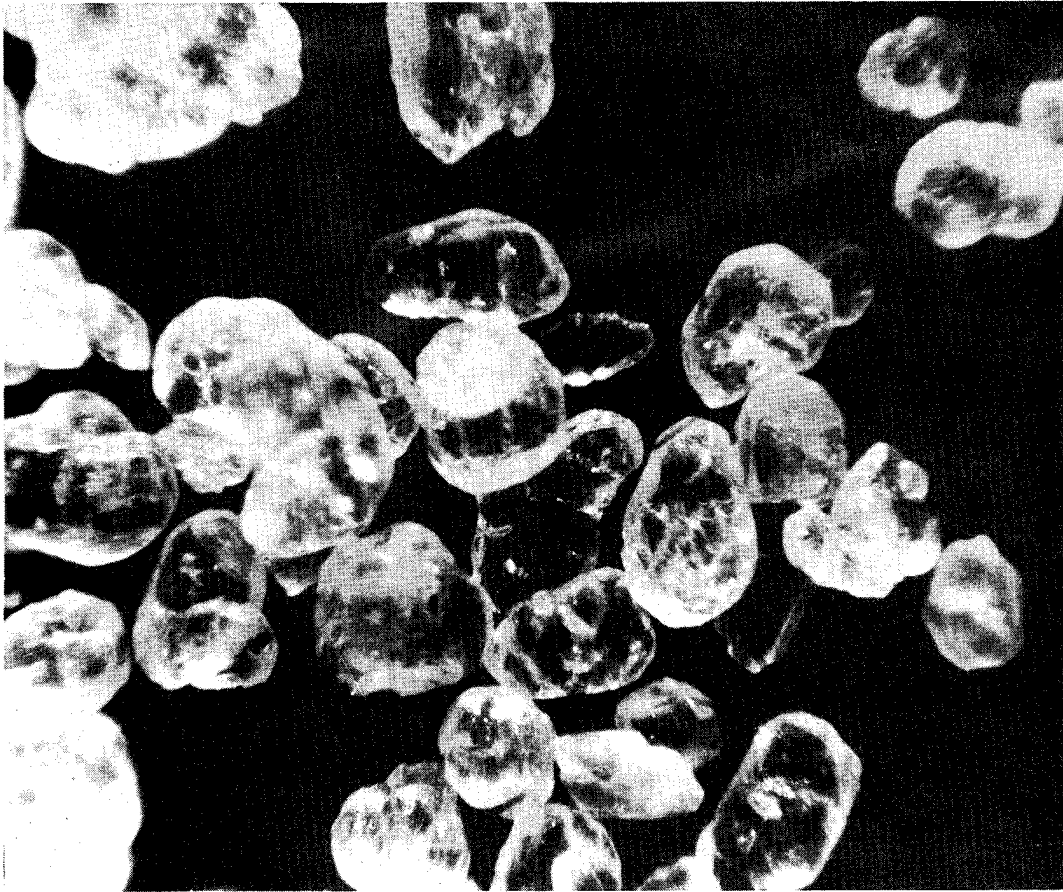


Figure 8. Photomicrograph (x90) RDX coated with
1.5% Parylene C

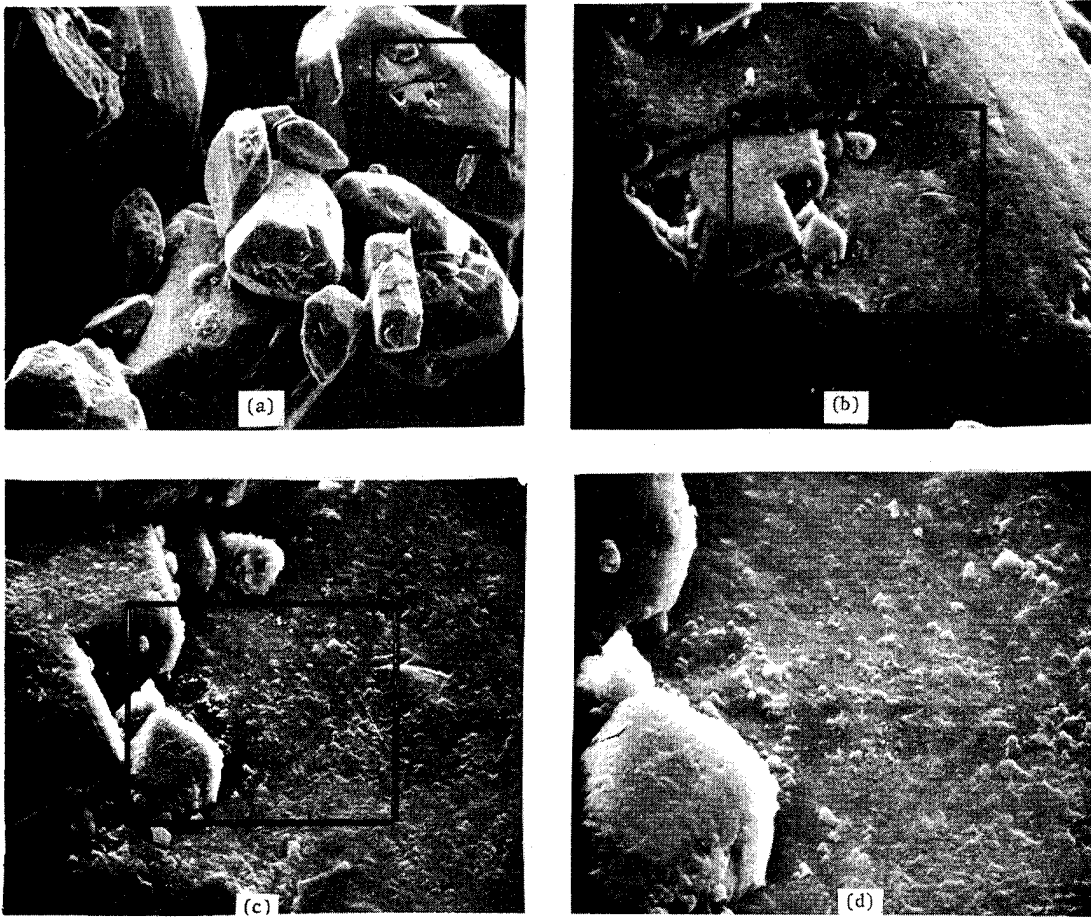


Figure 10. Scanning Electron Micrographs, (a) x100;
(b) x500; (c) x1000; (d) x2000, RDX
Coated with 1.5% Parylene C

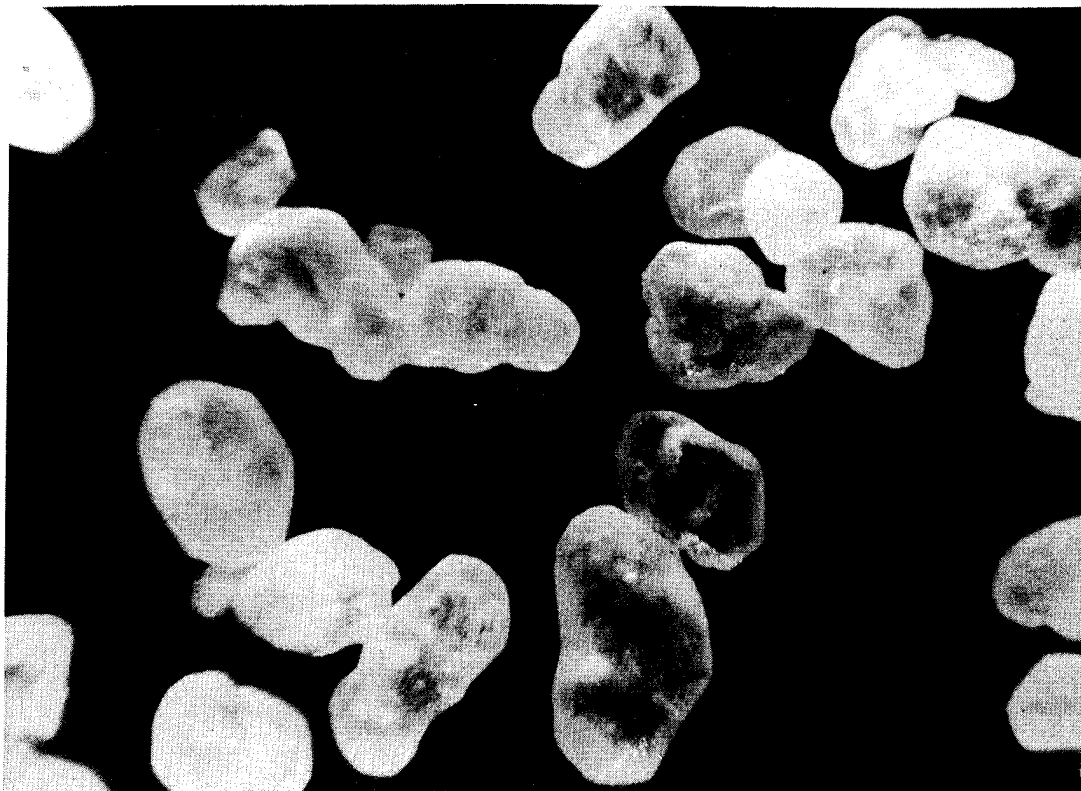


Figure 9. Photomicrograph (x90) RDX Coated with
8% Parylene C

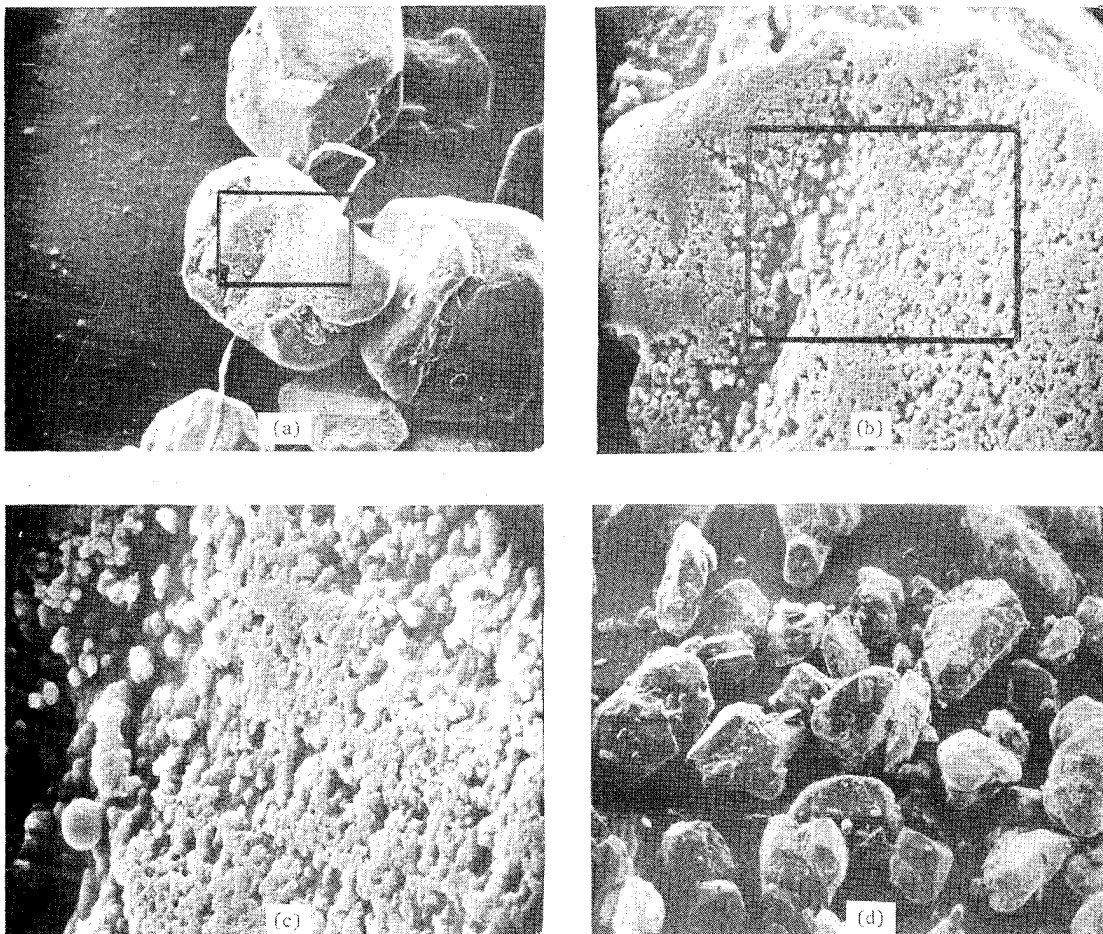


Figure 11. Scanning Electron Micrographs, (a) x100;
(b) x500; (c) x1000, RDX Coated with
8% Parylene C; (d) x50, RDX Uncoated

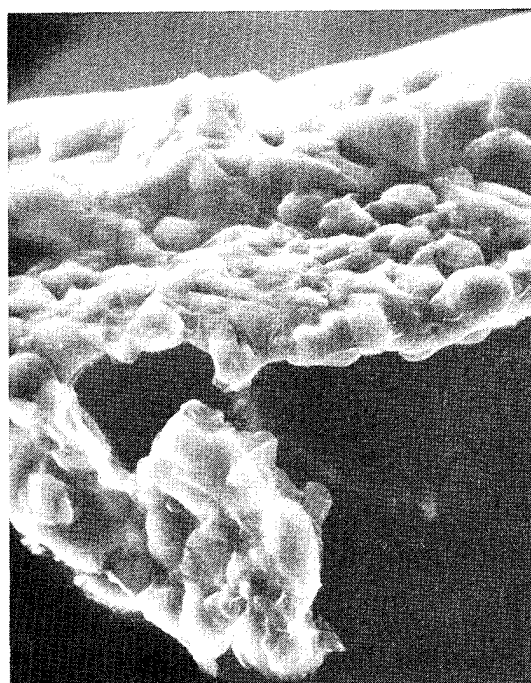


Figure 12. Scanning Electron Micrograph, x1000,
Parylene C Capsular Structure

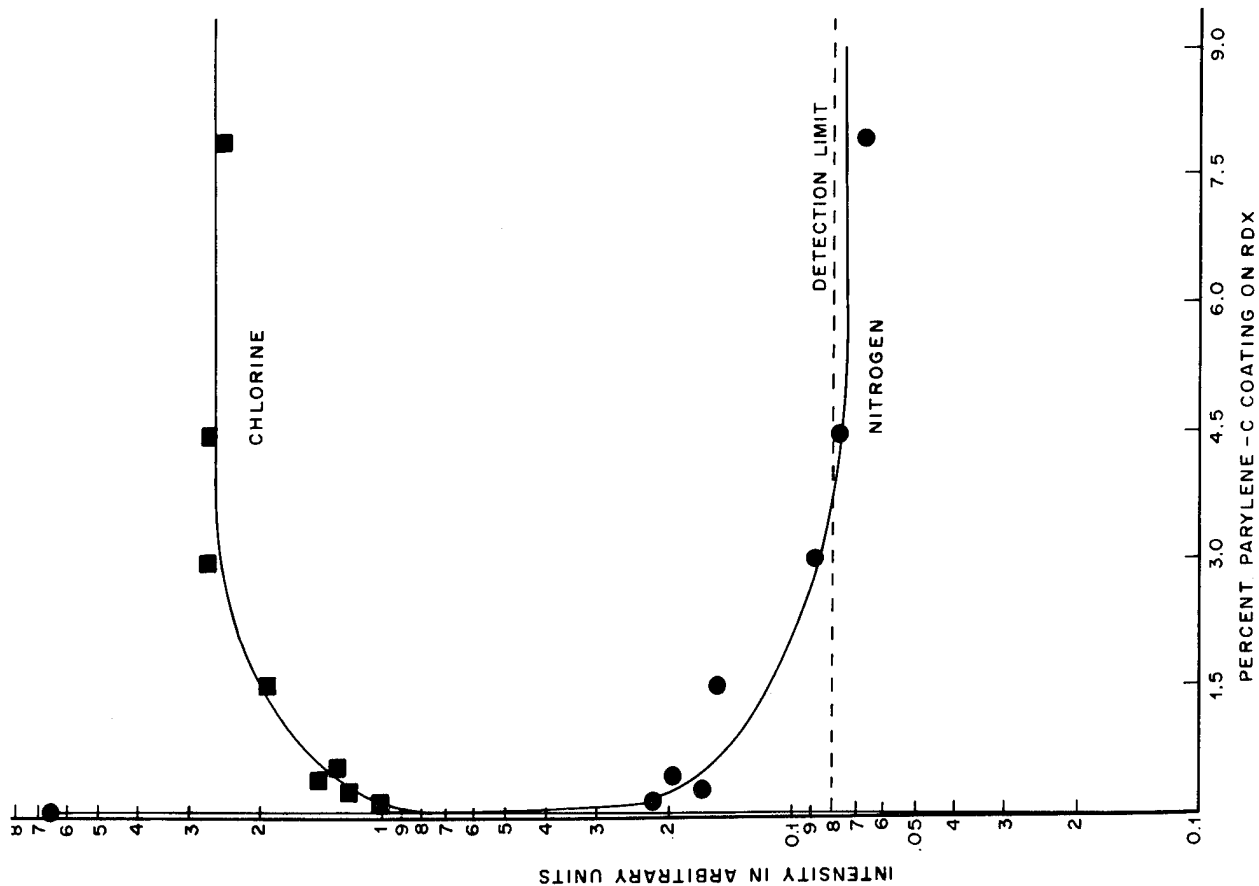


Figure 13. ESCA Signal for Nitrogen and Chlorine as Function of Percent Parylene C Coating on RDX

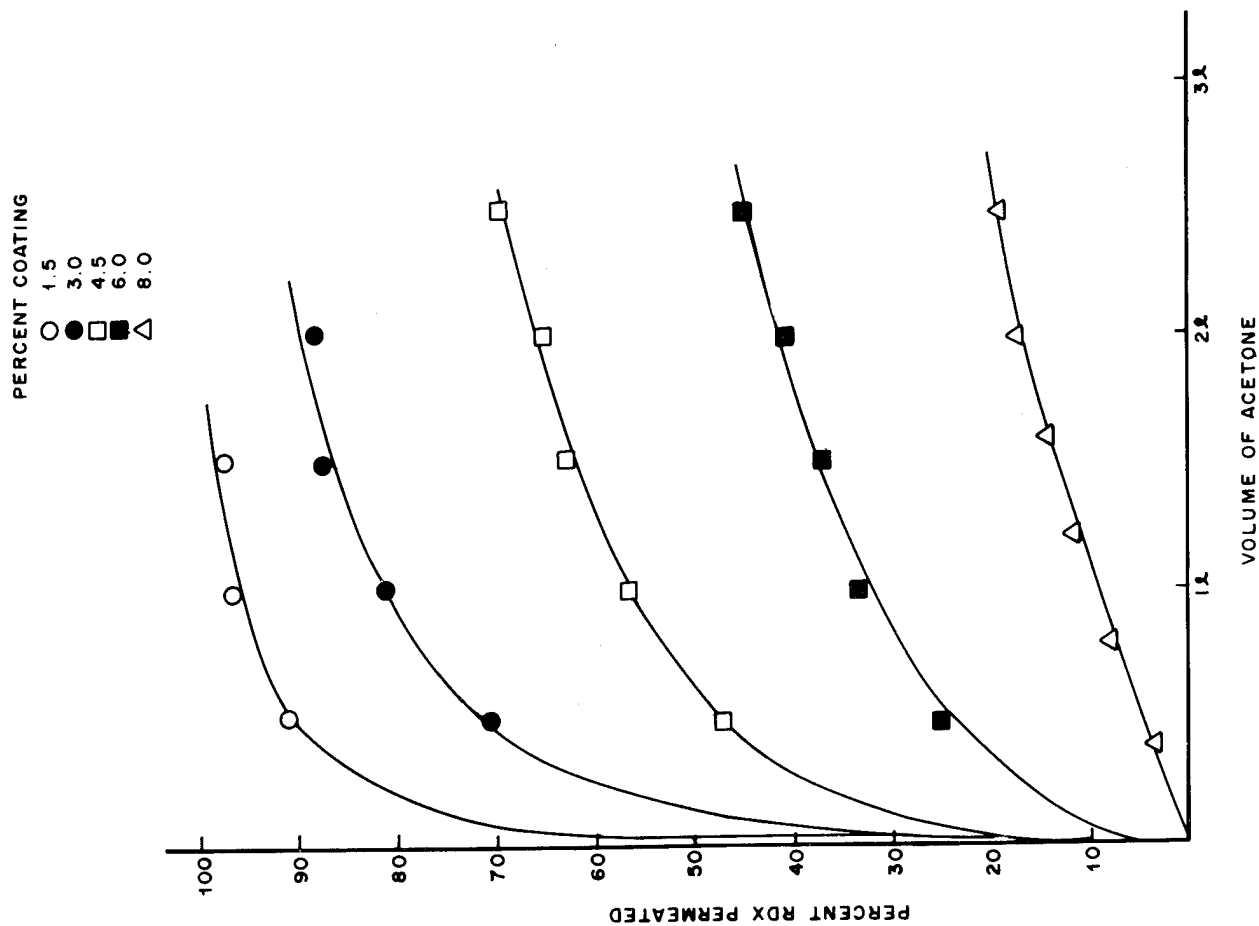


Figure 14. RDX Permeability as Function of Percent Parylene C Coating

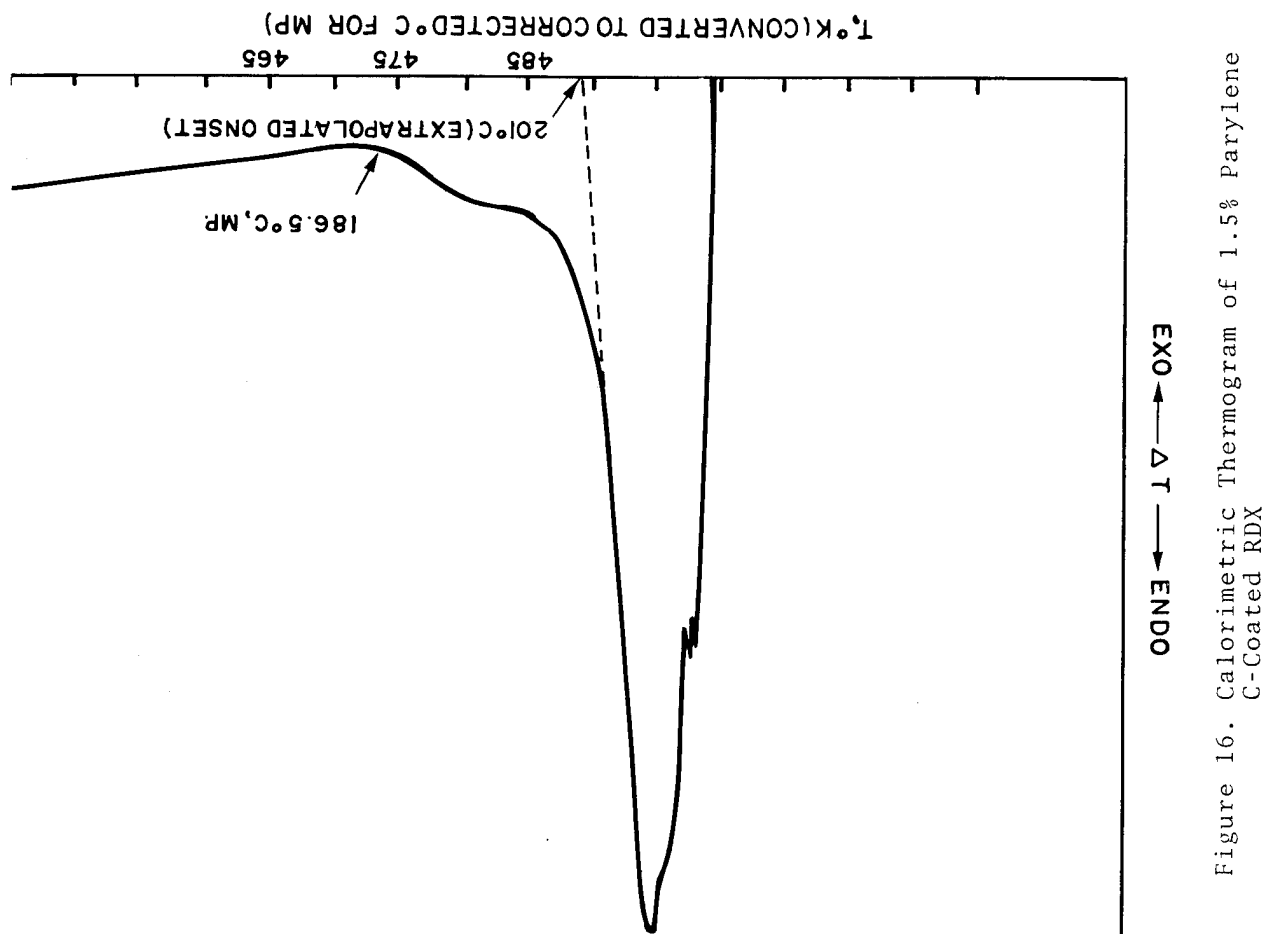


Figure 15. Calorimetric Thermogram of Uncoated RDX

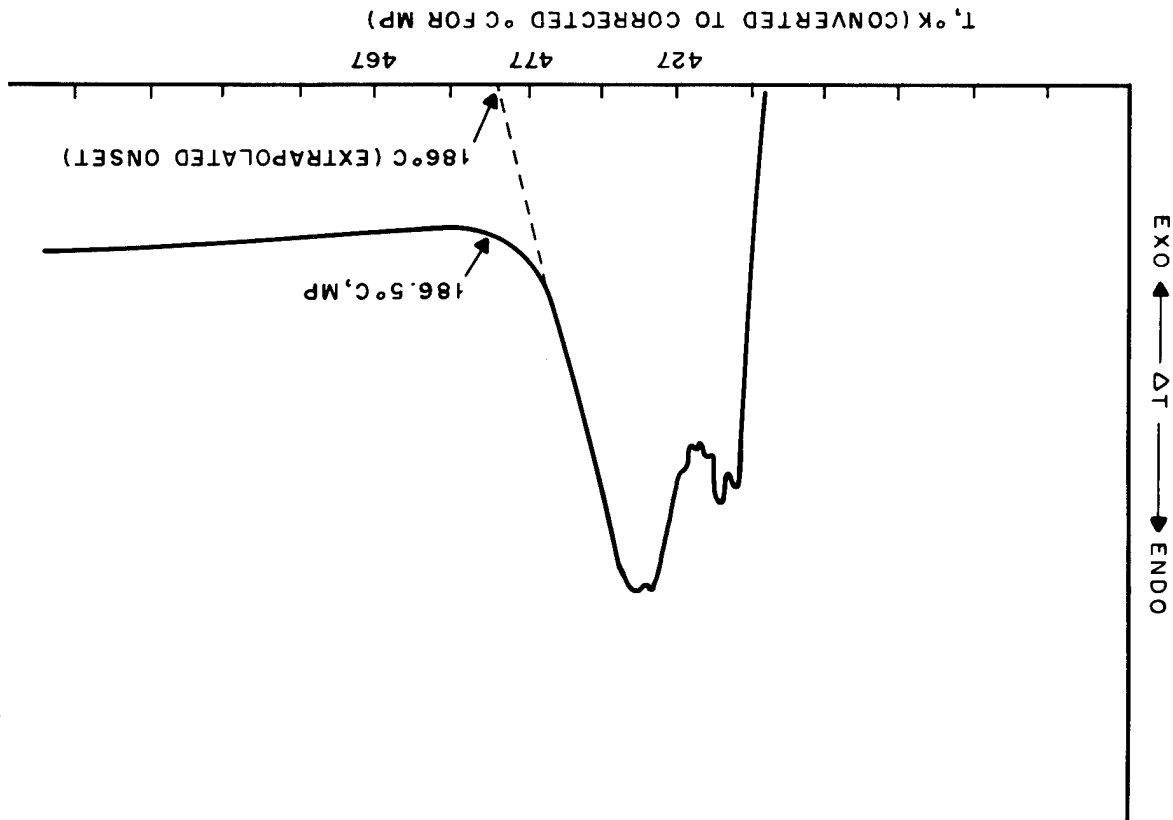


Figure 16. Calorimetric Thermogram of 1.5% Parylene C-Coated RDX

Figure 17. Calorimetric Thermogram of 8% Parylene C-Coated RDX

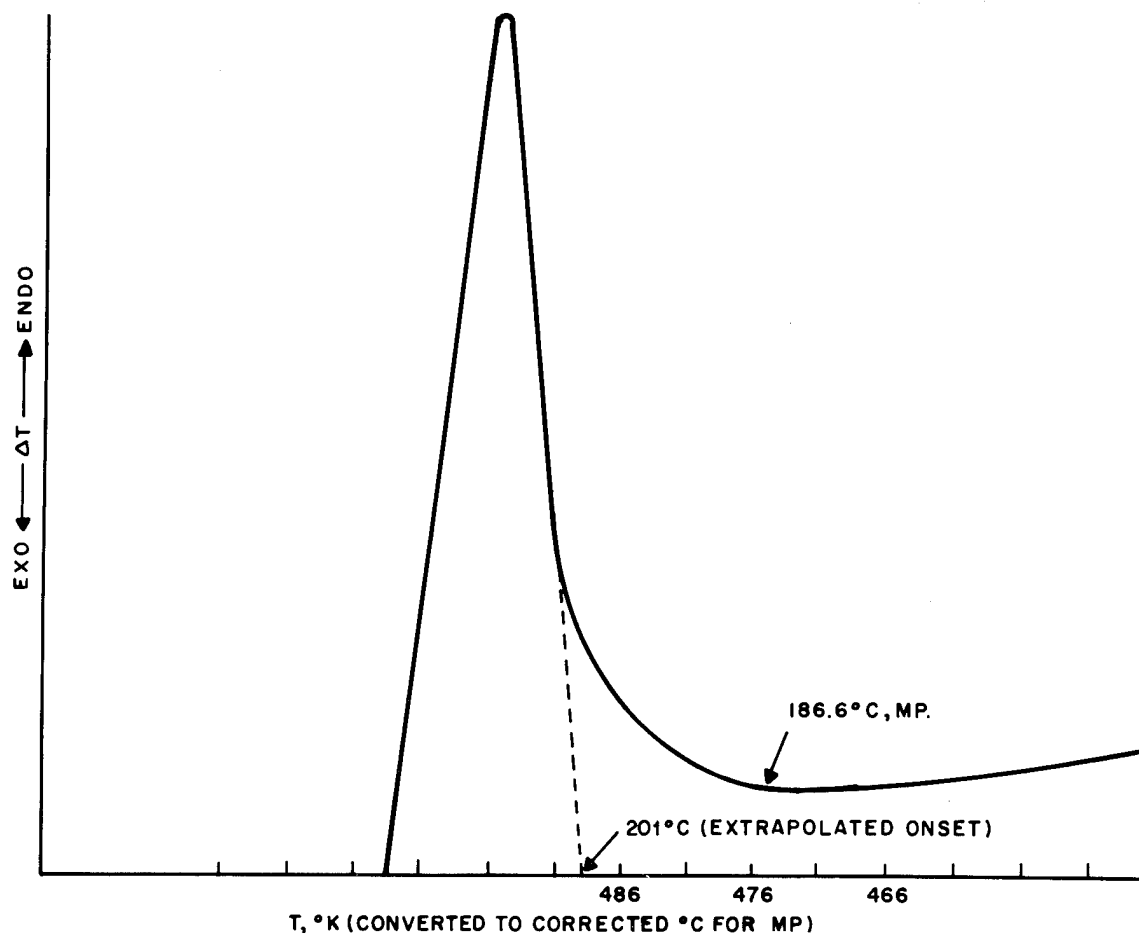
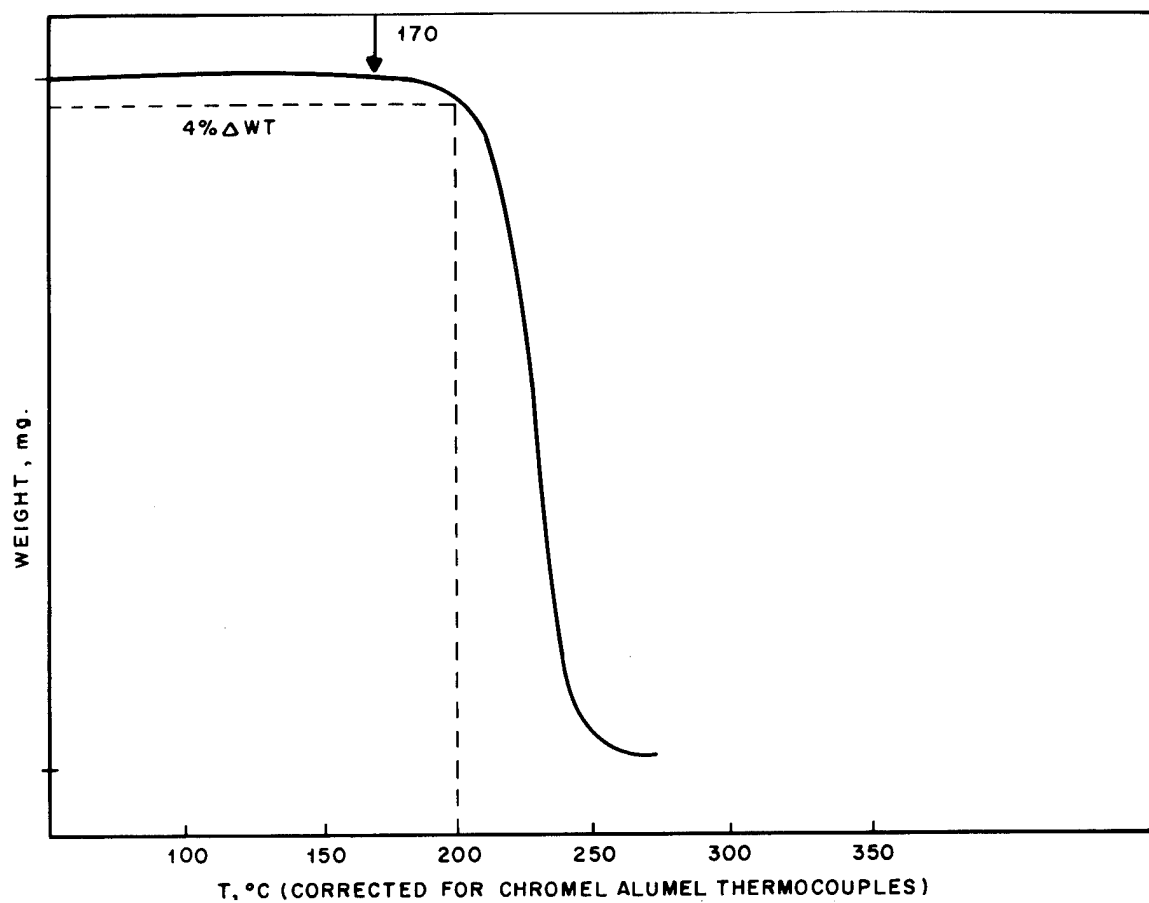


Figure 18. Gravimetric Thermogram of Uncoated RDX



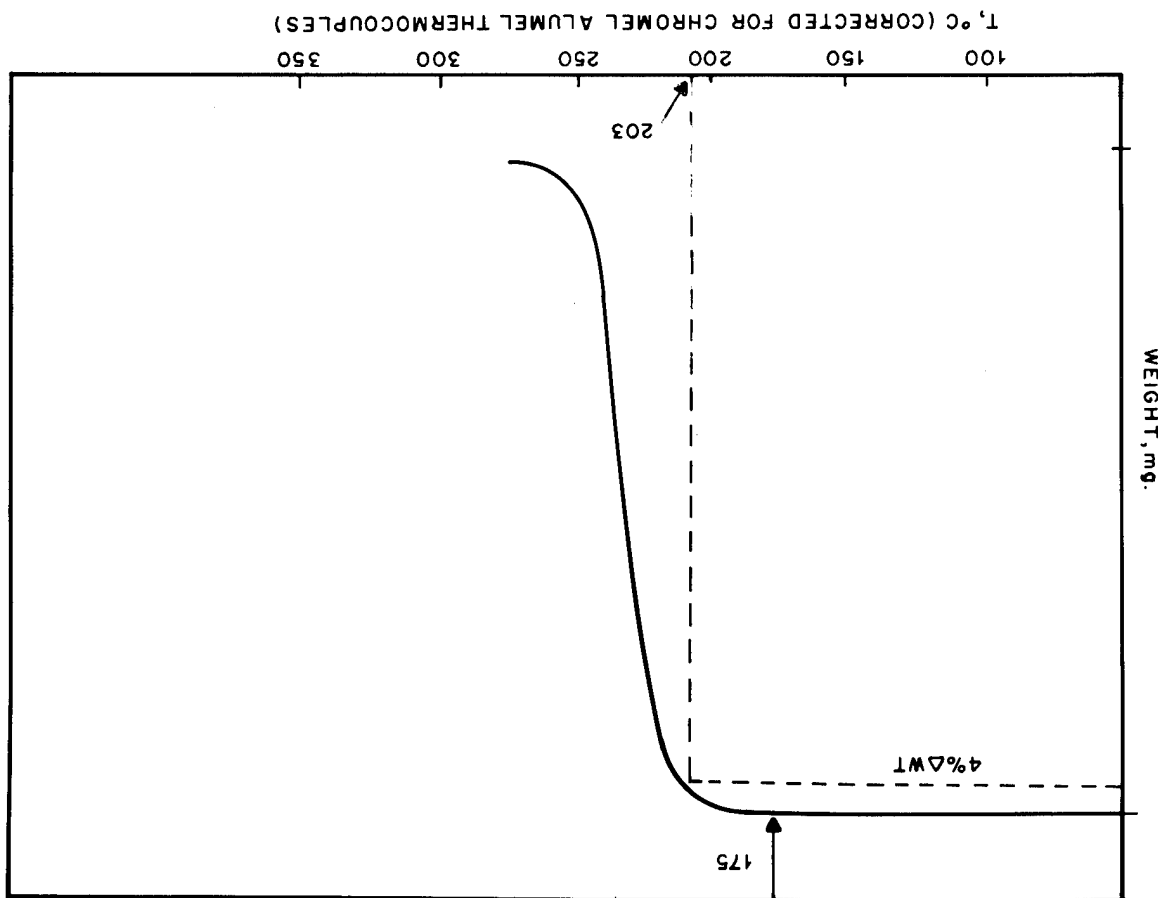


Figure 19. Gravimetric Thermogram of 1.5% Parylene C-Coated RDX

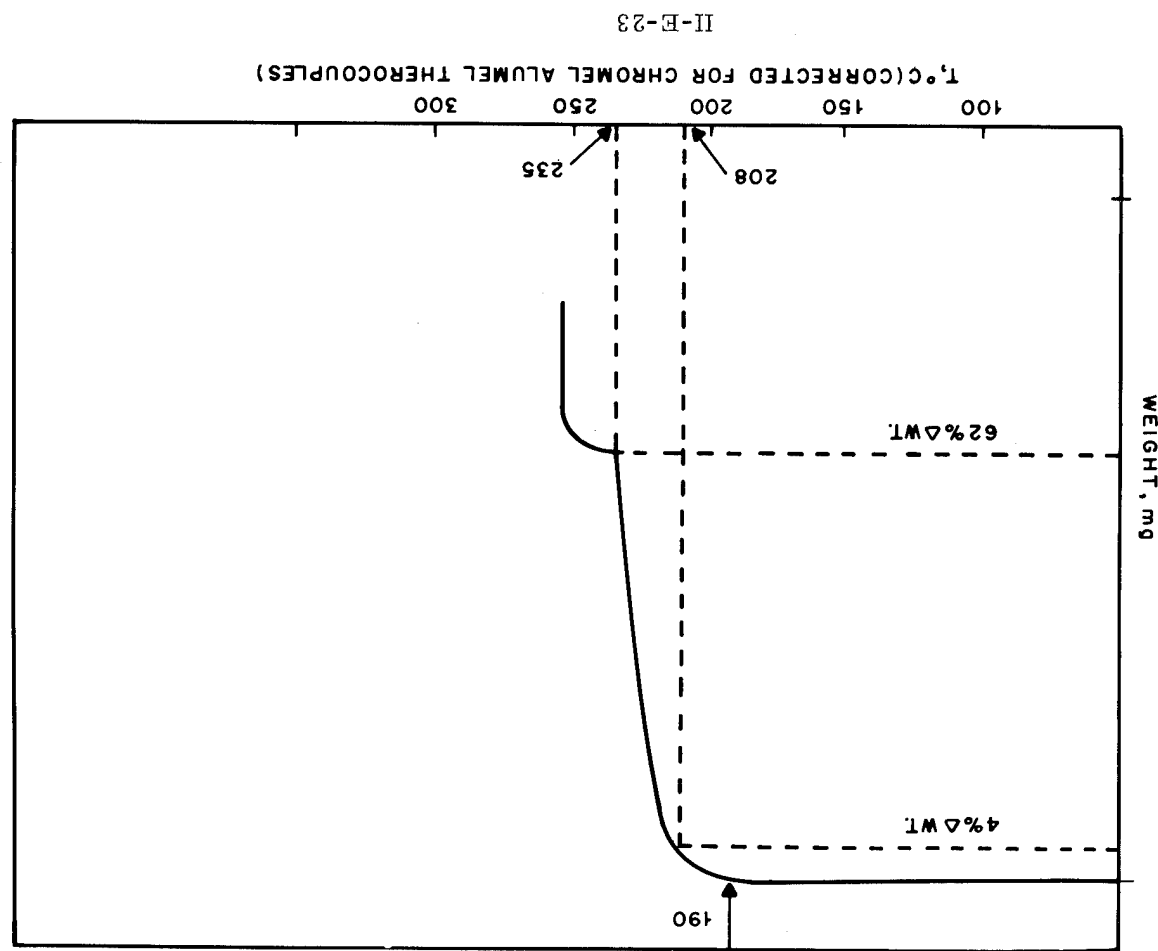


Figure 20. Gravimetric Thermogram of 8% Parylene C-Coated RDX

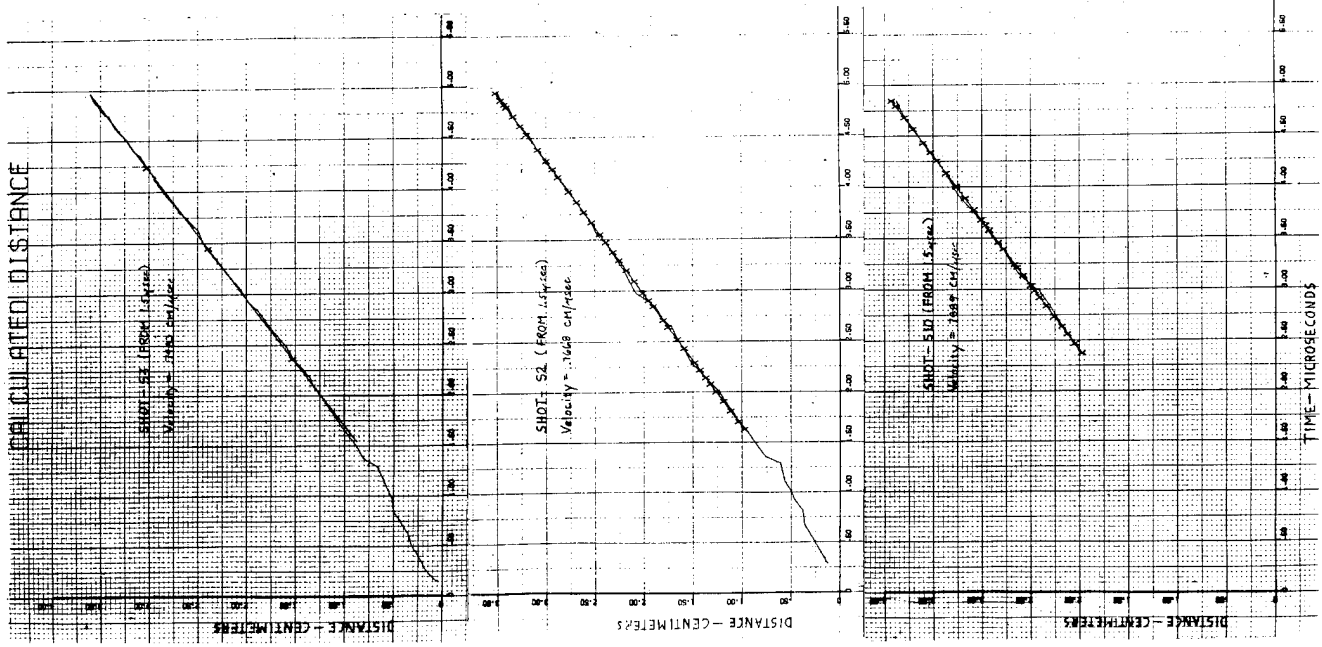


Figure 22. Plots of Streak Traces of Uncoated RDX

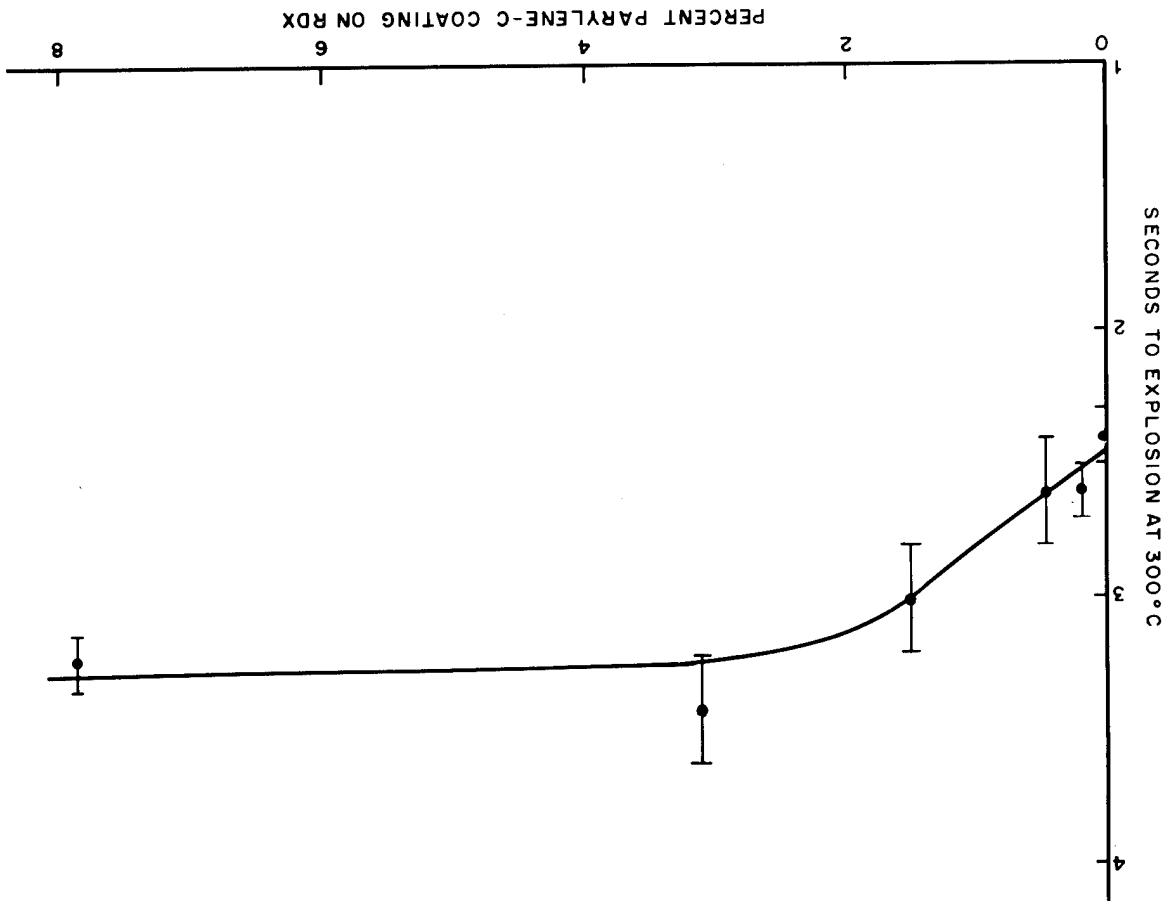


Figure 21. Thermal Initiation to Explosion of Parlyene C-Coated RDX

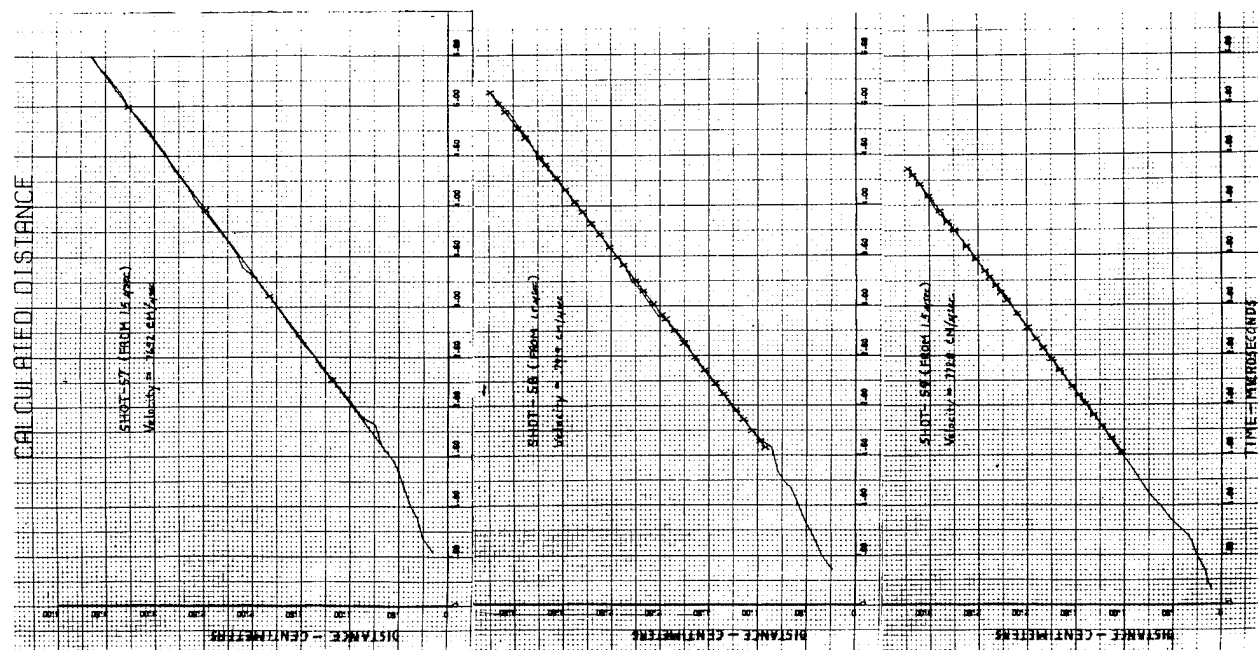


Figure 23. Plots of Streak Traces of 1.5% Parylene C-Coated RDX

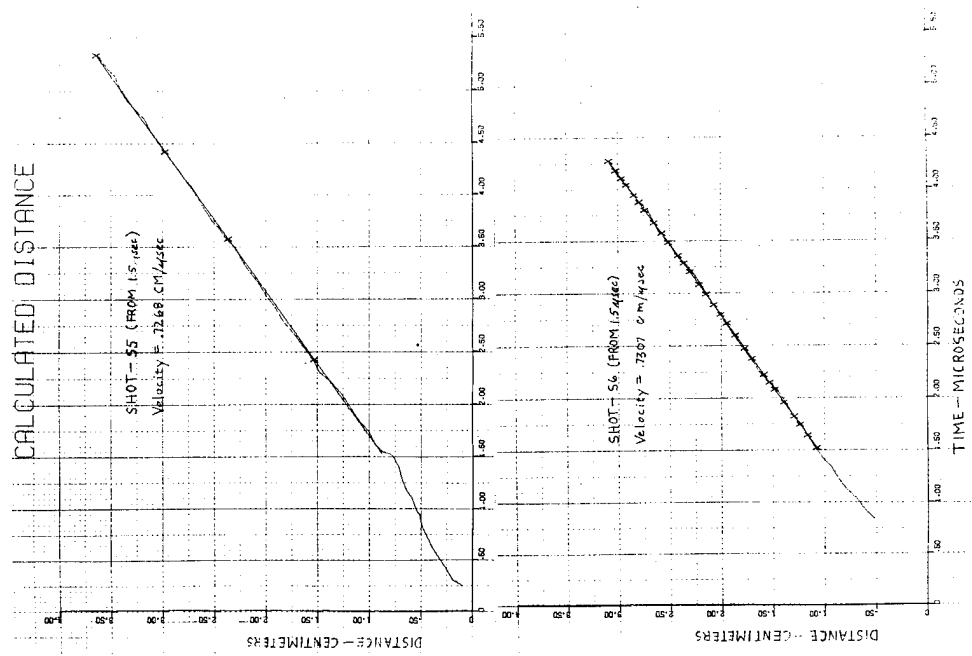


Figure 24. Plots of Streak Traces of 8% Parylene C-Coated RDX

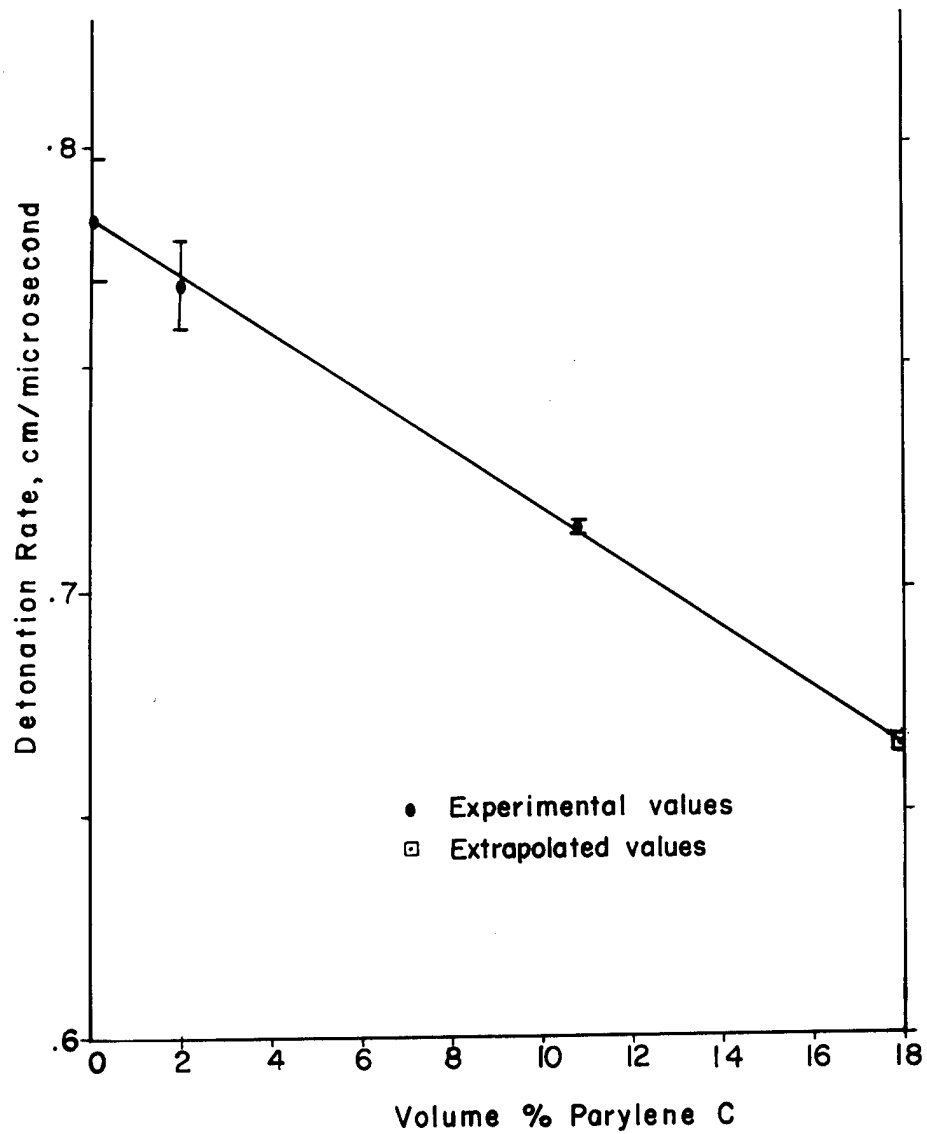


Figure 25. Detonation Rate of RDX as Function of Volume Percent of Parylene C

ELASTOMERIC FLUID CONTAINMENT MATERIALS
FOR ENERGETIC LIQUID ROCKET PROPELLANTS

Jerry K. Sieron
Air Force Materials Laboratory
Air Force Systems Command
Wright-Patterson Air Force Base, Ohio

Abstract

This paper presents recent significant progress made under the Air Force Materials Laboratory (AFML) program for development of elastomeric materials/components for the containment/transfer of liquid propellants on Air Force missile and satellite systems. The development and rapid translation into qualified hardware of seals, valve seats, and positive expulsion devices for monopropellant hydrazine propulsion systems is emphasized because critical management of propellant supply is essential for extended duration performance of Air Force and other major U.S. satellite systems. Current and projected efforts to develop similar elastomeric materials/components for management of nitrogen tetroxide or other high energy oxidizers for use in high thrust, hypergolic bipropellant systems are also summarized.

1. INTRODUCTION

Elastomeric components such as seals, valve seats, and positive expulsion bladders play a critical role in the operational performance of liquid rocket propulsion systems. These components are responsible for not only containment of the propellants, but also in many cases for transfer of the propellants to the rocket engine. In addition to possessing normal elastomeric properties such as flexibility and compliance, these components must have exceptional chemical resistance and maintain mechanical stability under rigorous operational conditions. In response to requirements outlined by the Air Force's Space and Missile Systems Organization (SAMSO) and liaison with the Air Force Rocket Propulsion Laboratory, AFML has for several years placed emphasis on programs to develop elastomeric

materials and components for monopropellant hydrazine (N_2H_4) propulsion systems for long life satellite systems. This paper describes the development, evaluation, and translation into qualified hardware of a novel series of elastomer compounds for use as seals, valve seats, and positive expulsion bladders/diaphragms for N_2H_4 systems. It also reviews progress on development of compatible elastomeric materials for high thrust bipropellant systems using nitrogen tetroxide (N_2O_4) oxidizer and, in addition, summarizes projected development of materials resistant to very energetic fluorinated oxidizers.

2. BACKGROUND

The long term reliable performance of functional satellites such as communications or surveillance types is dependent on accurate and continuous deployment of the satellites

in precise orbits and attitudes. Maintenance of such satellites in precise orbits and positions is normally accomplished by small onboard hydrazine monopropellant rocket engines or thrusters. For many satellite systems the thrusters must be actuated thousands of times over a period of several years for station-keeping purposes. Since the thrusters operate in a zero gravity environment, hydrazine propellant has to be forced to the engine. Positive expulsion systems based on propellant filled ethylene propylene terpolymer (EPT) elastomeric (rubber) bladders encased in metal tankage and driven by gas pressure between the bladder exterior and the metal tank were developed for early satellite propellant management systems. This expulsion system works similar to a toothpaste tube -- required amounts of propellant are squeezed to the thruster by gas pressure on the bladder exterior when flow control valves are actuated. For short term missions the earlier EPT bladders performed satisfactorily for several SAMSO and NASA space systems. However, as missions became more complex and time requirements were extended for up to seven years, operational problems occurred and satellite lifetimes were occasionally decreased because of thruster problems. Some of the problems were eventually traced to the EPT positive expulsion bladders. It was determined that the bladder material promoted excessive decomposition of hydrazine propellant, thus increasing total pressure within the bladder which subsequently caused erratic thruster response. This situation necessarily required additional corrective firings and hence propellant waste. It was also determined that hydrazine extracted particulates from the bladders over long time periods. The particulates eventually found their way to flow control valves and occasionally would

cause the valves to operate erratically, again causing propellant waste because corrective thruster firing was required for proper satellite orbital adjustment. In early systems, valve problems also were traced to permanent deformation of tiny (dime size) elastomeric valve seat material. Excessive swelling of the seat caused by propellant and/or changes in surface topography due to high thruster soak back temperatures in conjunction with several thousand duty cycles resulted in changes in the "Effective Orifice Area" (EOA) of the valve. The net result was inaccurate thruster response with attendant propellant waste and therefore decreased satellite lifetime.

In response to these operational problems, AFML initiated programs for development and functional evaluation of valve seats, seals, and positive expulsion bladders/diaphragms for monopropellant N_2H_4 systems with a goal of developing components which would perform reliably for at least five years under operational conditions.

Development of elastomeric materials for N_2O_4 components was included in the programs because it was recognized that alternative materials or devices for containment or transfer of N_2O_4 such as Teflon seals or bladders, metal bellows, surface tension devices, pumps, and non-optimized elastomers had one or more characteristic weakness such as low expulsion cycle lifetime, excessive weight, inoperability in G-fields even below 1.0 G, incompatibility with propellants, or excessive permeability to either propellants or pressurant gases. In essence it was firmly believed that designers would have higher confidence in elastomeric seals, valve seats, and expulsion devices for N_2O_4 and that availability of such components would significantly

increase the Air Force's capabilities in areas requiring either high ΔV propulsion systems or long life hypergolic thrusters.

3. DEVELOPMENT OF MATERIALS FOR HYDRAZINE MONOPROPELLANT SYSTEMS

3.1 VALVE SEAT AND SEAL MATERIALS

3.1.1 Functional Requirements

As mentioned previously, hydrazine monopropellant thrusters (Figure 1) are used to maintain precise orbital and attitude control of satellites over a period of five years or more. The flow control valves that microfeed hydrazine to the thrust chamber must function perfectly for hundreds of thousands of cycles in order for the satellite program to succeed. To maintain this kind of track record, systems experience dictated that the tiny (<1 gram) elastomeric valve seat must have the following properties:

- (1) Compatibility with hydrazine
- (2) Excellent sealing properties

- (3) Negligible volume change after N_2H_4 exposure at 160°F under severe mechanical conditions
- (4) No change in shape of seating surface

3.1.2 Valve Seat Materials Development/ Evaluation

To achieve the above properties, AFML initiated a program in 1969 with TRW Systems to develop and functionally evaluate elastomer compounds specifically for valve seat applications. (1) Based on comprehensive N_2H_4 compatibility evaluations and competitive in-valve testing against a state-of-the-art valve seat compound, an elastomer compound based on ethylene propylene diene rubber (EPT) and a 1,2-polybutadiene resin (HYSTL) and identified as AF-E-102 was selected as an optimum material for flow control valves. The final selection of AF-E-102 was based on initial and final performance of the material in an Intelstat type valve over a period of 79 days over which the valve was

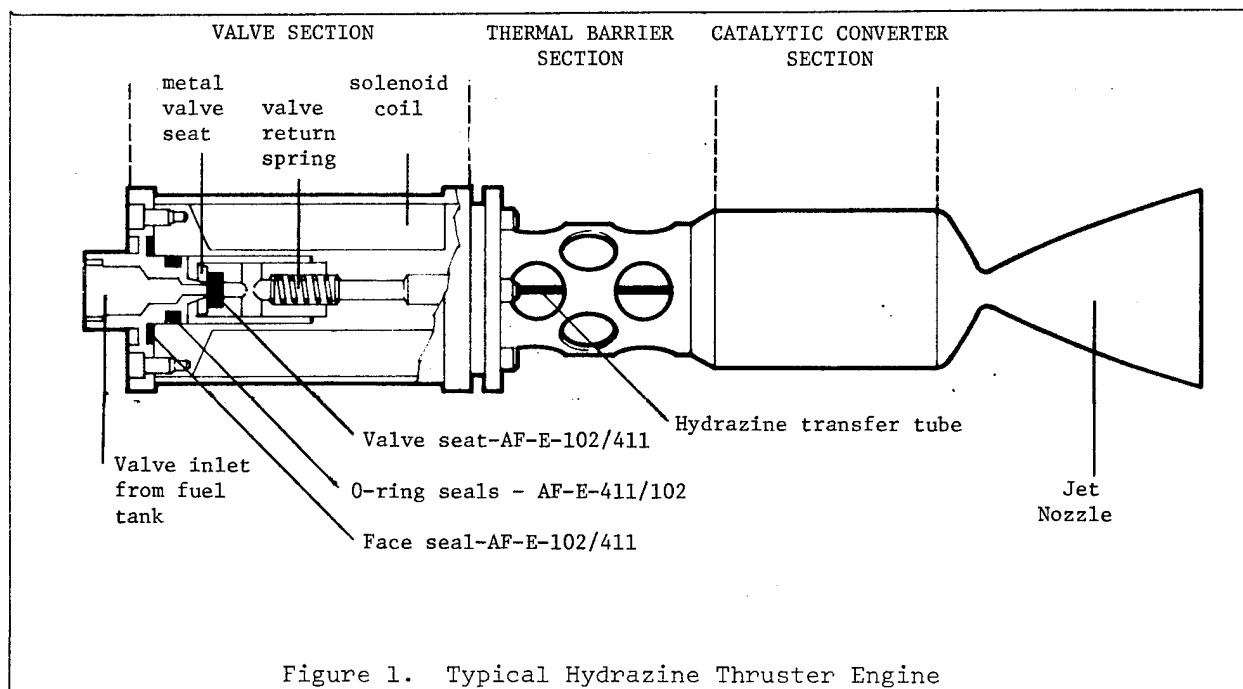


Figure 1. Typical Hydrazine Thruster Engine

pulsed to simulate accelerated satellite stationkeeping thruster service. Post-test examination of the control seat and the AF-E-102 seat clearly indicated the reasons for the latter's superior performance. Due to excessive swelling and surface marring of the control seat, the effective orifice area (EOA) of the control valve was reduced by approximately 80% of the original value. The AF-E-102 seat was essentially unchanged and the original EOA was correspondingly unchanged.

3.1.3 Translation of Technology Into Hardware

In order to expedite the translation of the new valve seat material into hardware, technical information and/or samples were furnished to numerous hydrazine valve manufacturers and organizations such as the Jet Propulsion Laboratory (JPL), Naval Research Laboratory (NRL), Air Force Rocket Propulsion Laboratory (AFRPL), and Goddard Space Flight Center. The Aerospace community responded favorably to AF-E-102 and the material was qualified and launched in 1971 by NRL on the Solrad X scientific satellite. The flow control valve on this satellite has had no problems and this experience unquestionably hastened acceptance of the material into many subsequent Air Force, NASA, and commercial satellite systems.

3.1.4 O-Ring Materials Development

For certain high performance applications O-ring seals with higher tear strength and elongation than AF-E-102 were desired. To address this requirement a high tear strength modification of AF-E-102 identified as AF-E-411 was developed and thoroughly evaluated as an optimized O-ring material for hydrazine.⁽²⁾ The

properties of the seal/valve seat materials are listed in Figure 2.

PROPERTY	AF-E-102	AF-E-411
TENSILE STRENGTH, PSI	1600	2100
ELONGATION AT BREAK, %	100	170
SHORE A HARDNESS	90	88
COMPRESSION SET, %	17	17
TEAR STRENGTH, PLI	80	200
PRESSURE RISE (IN N_2H_4), PSID	NIL	NIL

Figure 2. Properties of Valve Seat and O-Ring Compounds.

As was the case with AF-E-102, AF-E-411 was quickly evaluated and accepted by valve/tankage suppliers and the aerospace industry for hydrazine valves and plumbing. Both AF-E-102 and AF-E-411 have been qualified as seals and valve seats for several satellite systems.

3.1.5 Systems Implications

Development and qualification of AF-E-102 and 411 valve seats and seals provide the following advantages for spacecraft hardware:

- (1) Valve design is considerably simplified since volume swell and change in shape of the valve seat are no longer of primary concern.
- (2) Short stroke valves may be used reliably, thus reducing spacecraft on-board power requirements (and weight).
- (3) Soft-seat valves, with the increase in reliability afforded by the new materials, may be used in place of hard-seat valves with the attendant relief from leakage caused by particulate contamination.
- (4) In Positioning and Orientation Propulsion Systems (POPS), impulse

predictability is improved, repeatability is assured, multi-thruster firing calibration is simplified, and the need for multiple engine firings to achieve precise orbit or attitude is reduced.

- (5) The operational life of satellite systems is increased due to maximum utilization of propellant.

3.2 POSITIVE EXPULSION BLADDERS/ DIAPHRAGMS FOR HYDRAZINE

3.2.1 Advantages of Bladders

High strength elastomeric materials which stretch without tearing or other damage are very desirable for positive expulsion systems. For example, elastomers can be used in symmetrical or nonsymmetrical volumes and can operate effectively in both random or controlled folding modes. Elastomeric bladders can generally be designed after the tank; the successful use of non-elastomers almost always requires the tank and bladder to be designed as a unit.

Positive expulsion bladders are desirable for liquid rocket systems because they provide the following functional advantages:

- (1) Expulsion of the propellant at any attitude relative to the acceleration field
- (2) Prevention of chemical reaction between the pressurant and propellant
- (3) Prevention of the pressurant gas mixing with the propellant
- (4) Retention of all of the propellant so that it is available to the engine

- (5) Reduction in the rate of heat transfer between the pressurant and the propellant
- (6) Reduction in the surface area of the tank wetted by propellant which could reduce corrosion
- (7) Minimization of propellant sloshing
- (8) Reliable multi-cycle performance

3.2.2 Functional Requirements

To attain these functional advantages, AFML initiated a comprehensive effort in 1970 ^(2,3) with TRW Systems which emphasized development of advanced bladder materials for hydrazine with the following characteristics:

- (1) Excellent chemical compatibility with and non-reactive to N_2H_4
- (2) Low propellant and pressurant gas permeability
- (3) Easy processibility

Development of elastomeric materials with low permeability to propellant is necessary to minimize the loss of propellant into the ullage where it is unavailable to the engine and from where it may corrode the pressurization system, particularly during long storage. Low permeability to the pressurant is necessary to minimize bubbles of gas in the propellant which can cause variations in propellant flow rate to the engine that results in rough burning.

Because propellants are intrinsically reactive substances, it is difficult to find materials with the required mechanical properties which also are inert to the propellants. If the propellant attacks the bladder, deterioration of the bladder wall takes place by softening, blistering, or formation of hard, brittle substances. Obviously, deterioration of the bladder

is to be avoided because of the chance of an expulsion malfunction. Similarly, it is important that the bladder materials not degrade the propellant. Propellant decomposition or reaction is likely to cause the generation of gas inside the bladder, thus defeating one function of the bladder (i.e., separation of the liquid and gas phases to assure smooth engine operation). A further hazard is that reaction products or particles from a disintegrating bladder may flow out of the tank and into critical components whose function may be impaired, such as clogging of filters and injector orifices, jamming of valves, etc.

3.2.3 Bladder Materials Development/ Evaluation

The basic program approach was to modify the already successful EPT/HYSTL technology developed for hydrazine valve seat and seal applications. Elastomer compounding methodology was used to develop lower modulus varieties of AF-E-102 with greatly increased tear strength and flex life. Following this intensive materials development and evaluation effort which is detailed in References 2 and 3, an EPT/HYSTL compound identified as AF-E-332 was selected for more detailed functional testing in the form of positive expulsion bladders and diaphragms.

Comprehensive hydrazine compatibility evaluations indicated that AF-E-332 was unaffected by hydrazine and did not catalyze propellant decomposition. The following accelerated test procedure was used to establish the latter point. A 5 gram sample of AF-E-332 was placed in 50 ml of MIL-P-26536C hydrazine with an ullage volume of 30 ml. After one day at ambient temperature, no pressure rise above the

control (no rubber) was observed. The propellant was then heated to 160°F and after seven days no pressure rise above the control occurred. Again, after heating for an additional seven days at 212°F for one week, the following pressure readings confirming non-reactivity of the bladder were observed:

- (1) Control - 14.5 psia
- (2) AF-E-332 + Control - 12.0 psia

Next, data tabulated in Figure 3 indicate that AF-E-332 was unaffected by N_2H_4 after 12 months exposure to the propellant at 160°F.

Property	Original Controls	3-Month Exposure	5 1/2-Month Exposure	12-Month Exposure
M_{100} , psi	1150	1200	1250	1175
T_B , psi	2000	2075	2075	2000
E_B , %	350	310	320	310
Set, %	16	19	19	18
Shore A	90	90	92	91
Tear, pli	515	475	475	475
Δ Weight, %	--	+0.3	+2.8	+2.6
Δ Volume, %	--	Nil	Nil	Nil

FIGURE 3. Properties of AF-E-332 after Storage in N_2H_4 at 160°F (2)

Many other functional tests were conducted including flex testing in N_2H_4 , multiple propellant expulsion cycles, and permeability to N_2H_4 and pressurant gases. Pertinent information is given in Figure 4:

Expulsion Efficiency --	99+%
Permeability to N_2H_4 at 75°F --	0.0034 mg/cm ² - hr
Permeability to N_2 (ΔP 315 psi, 70°F) --	0.013 Scc/cm ² - hr
Permeability to He (ΔP 315 psi, 70°F) --	0.31 Scc/cm ² - hr

Figure 4. Functional Testing of AF-E-332

3.2.4 Prototype Development

To further explore the systems potential of AF-E-332, a process using an inflatable reusable mandrel was successfully developed and 10.5 inch diameter bladders were successfully molded to a "Mariner 69" configuration and evaluated. Three bladders were furnished to AFRPL for long term N_2H_4 storage tests which have now been under way for more than two years with no apparent problems.⁽²⁾

3.2.5 Translation of Expulsion Bladder/Diaphragm Technology into Systems

Other systems applications quickly developed. For example, at SAMSO's request, AFML cooperated with AFRPL to develop and qualify large AF-E-332 diaphragms for a current satellite program which had experienced some problems with earlier rubber bladders. Further, 28 inch diameter diaphragms were easily molded using matched metal tooling and supplied to Martin Co. for evaluation in a launch vehicle upper stage attitude control system. Additionally, 9.5 inch diameter bladders were molded using the inflatable mandrel and subsequently qualified for a high priority Air Force program. Finally, the 22 inch diameter diaphragm shown in Figure 5 has been qualified in the propulsion system for the FLTSATCOM program. The FLTSATCOM program particularly emphasizes the importance of the AFML developed elastomeric components for hydrazine. The satellite which is illustrated in Figure 6 will have AF-E-411 valve seats/seals and AF-E-332 expulsion diaphragms for its hydrazine monopropellant propulsion system with a design life of five years. This joint Navy/Air Force satellite system will provide world-wide high priority UHF communications between naval

aircraft, ships, submarines, ground stations, SAC, and the presidential command network.

4. ELASTOMERIC MATERIALS FOR NITROGEN TETROXIDE APPLICATIONS

4.1 CARBOXY NITROSO RUBBER

The development of elastomeric materials/components which are compatible with N_2O_4 oxidizer represents a very challenging problem for materials engineers. Commonly used elastomers such as neoprene, nitrile, and natural rubber are severely degraded or dissolved by N_2O_4 . Others such as resin-cured butyl and EPDM resist the oxidizer for only a few days before they are severely oxidized and lose mechanical properties. Some years ago, AFML developed a new perfluorinated material known as carboxy nitroso rubber (CNR) which did have excellent resistance to N_2O_4 for periods up to one year. CNR, however, had very high permeability to N_2O_4 and pressurant gases and, in addition, suffered from high compression set which limited its usefulness to a few specialized seal applications. It should be mentioned, however, that CNR seals were used successfully as N_2O_4 seals on the Lunar Module Descent Engine and the Apollo RCS system.⁽⁴⁾

4.2 AF-E-124D ELASTOMER DEVELOPMENT

Recognizing that CNR would not satisfy future Air Force requirements for N_2O_4 compatible components, AFML maintained a continuous cooperative program with the elastomer industry to evaluate and identify potential polymer systems which might have adequate mechanical and chemical resistance for long life hypergolic rocket systems seals and bladders. Over a period of several years and following comprehensive

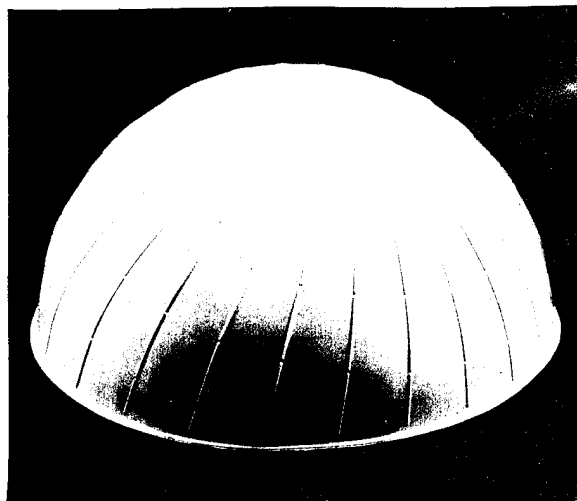


FIGURE 5. AF-E-332 POSITIVE EXPULSION
DIAPHRAGM FOR FLTSATCOM

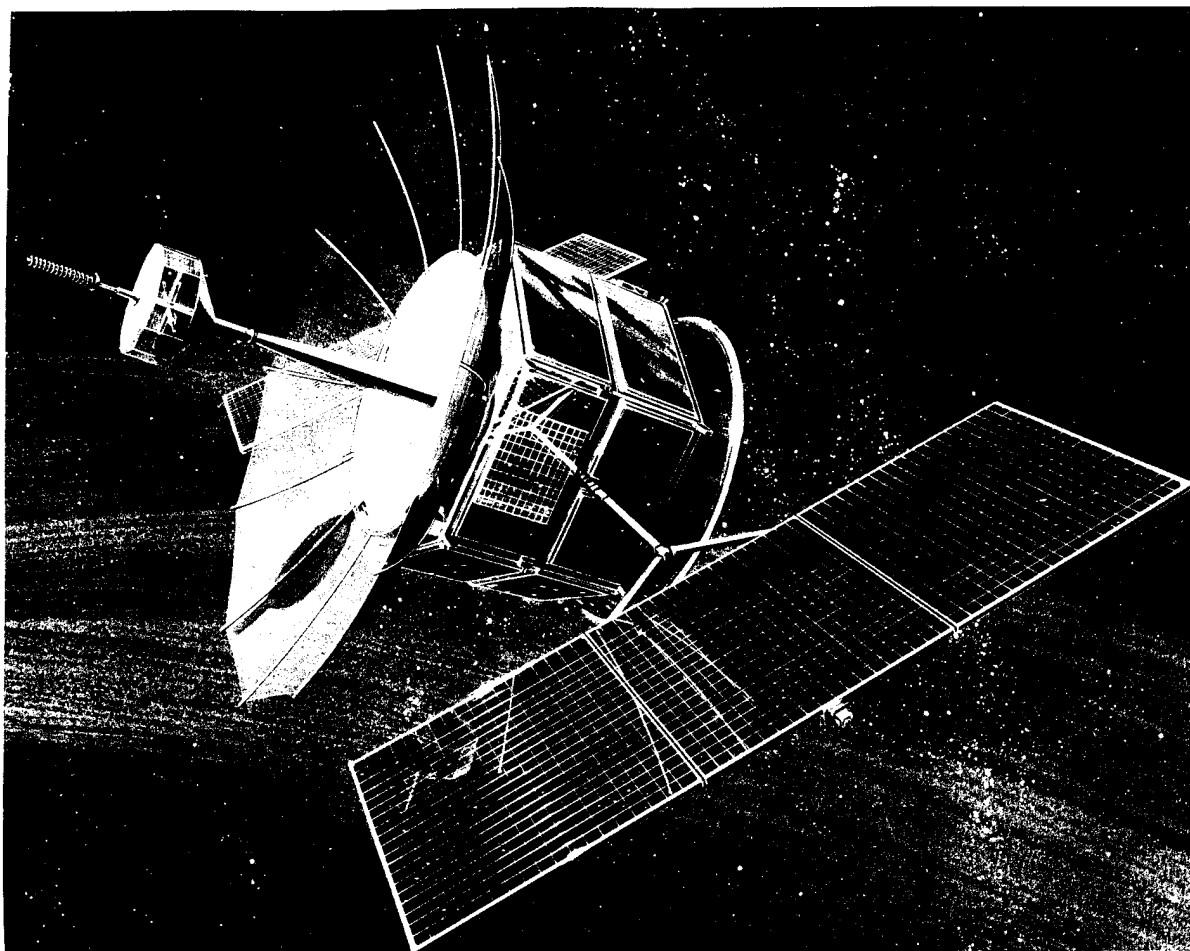


FIGURE 6. FLEET SATELLITE COMMUNICATIONS SYSTEM SPACECRAFT

propellant testing, a new elastomer identified as AF-E-124D appeared to be a promising contender as a seal, valve seat, and bladder material for N_2O_4 . Under an existing program, comprehensive processing and compounding studies are being conducted and we are optimistic that the above N_2O_4 components will be developed and qualified within two years. The following data in Figures 7 and 8 illustrate the promising properties and compatibility of AF-E-124D with N_2O_4 :

Parameter	Test Temperature	Value
T_B , psi	-100°F	3100
E_B , %		25
Tear, pli		70
M_{100} , psi	+75°F	925
T_B , psi		2150
E_B , %		205
Tear, pli		180
Shore A		86
M_{100} , psi	+160°F	275
T_B , psi		900
E_B , %		155
Tear, pli		100

FIGURE 7. Mechanical Properties of AF-E-124D in Air at Various Temperatures. (2)

Storage Temperature	Tensile Retained	Elongation Retained	Shore A
75°F	96%	100%	±0
120°F	95%	95%	-1
160°F	92%	96%	-3
200°F	51%	180%	-18

FIGURE 8. Retention of AF-E-124D Mechanical Properties after 8 Days in N_2O_4 (2)

In addition to working out processing problems, the current program at TRW Systems includes development of materials with reduced permeability to helium and N_2O_4 .⁽⁵⁾ At the present stage of development, the permeability to He is about 1/2

that of Teflon and to N_2O_4 it is about 1/5 that of Teflon. It also should be mentioned that AF-E-124D is compatible with N_2H_4 and has already found a use as O-ring seals on a system where compatibility with fuel and oxidizer was desired. (2)

5. ELASTOMERIC MATERIALS FOR CONTAINMENT OF FLUORINATED OXIDIZERS

The development of elastomeric seals and valve seats appears to be a limiting technology for long range very high thrust propulsion systems which require the use of very energetic fluorinated oxidizers. AFML has conducted a continuous, but limited effort, to develop the necessary technology which ultimately will lead to development of seals, valve seats, and bladders for fluorinated oxidizers. (5,6) Our approach has been two-fold: (1) Synthesis of perfluorinated elastomers and cross-linking materials, and (2) development and modification of existing materials such as AF-E-124D. Notable progress has been made as indicated by the data in Figure 9. This effort is continuing and it is believed that sufficient technology base is being generated to develop fluorinated oxidizer compatible components on an accelerated basis if high priority systems requiring this capability are identified at a future date.

6. CONCLUSIONS

6.1 Fluid containment and transfer materials/components for hydrazine monopropellant propulsion systems identified as AF-E-102 valve seat material, AF-E-411 valve seat or seal material, and AF-E-332 positive expulsion bladder/diaphragm material have been developed, qualified, and rapidly translated to existing Air Force, Navy, NASA, and commercial satellites.

PROPERTY	Original	After 100 Hrs. in ClF ₃ at RT
100% Modulus, psi	575	475
Ultimate Tensile Strength, psi	1300	1100
Elongation at Break, %	180	170
Tensile Set, %	2	2
Hardness, Shore A	76	75

FIGURE 9. Compatibility of AF-E-124D with Chlorine Trifluoride (ClF₃)

6.2 Materials development and preliminary component development of seals, valve seats, and expulsion devices based on AF-E-124D for hypergolic propulsion systems using N₂O₄ oxidizer are proceeding smoothly. The program is expected to be completed within two years.

6.3 Technology base effort to develop elastomeric components for use with very energetic fluorinated oxidizers has made notable progress. Variations of AF-E-124D appear to be viable candidates for sealing oxidizers such as ClF₃. Synthesis of perfluorinated elastomers and crosslinking systems appears to be necessary to solve long term compatibility problems.

7. REFERENCES

1. Martin, J. W. and J. F. Jones, "Elastomeric Valve Seat Materials for Hydrazine Propulsion Systems," Technical Report AFML-TR-70-200, December 1970.
2. Martin, J. W. and H. E. Green, "Elastomers for Liquid Rocket Propellant Containment," Technical Report AFML-TR-71-59, Part II, October 1973.
3. Martin, J. W., J. F. Jones, and R. A. Meyers, "Elastomers for Liquid Rocket Propellant Containment," Technical Report AFML-TR-71-59, Part I, June 1971.
4. Levine, N. B., "Carboxy Nitroso Rubbers," RUBBER AGE 101, Number 5, (1969).
5. Contract F33615-74-C-5099, Air Force Materials Laboratory.
6. Jones, R. J., P. Tarrant, C.D. Bertino, H. E. Green, and J. W. Martin, "Development of Elastomeric and Compliant Materials Resistant to Liquid Rocket Propellants," Technical Report AFML-TR-72-242, Nov. 1972.

8. BIOGRAPHY OF AUTHOR

Jerry K. Sieron is a Senior Materials Engineer in the Elastomers and Coatings Branch, Air Force Materials Laboratory. As Project Engineer, his primary responsibilities involve initiation and direction of contractual and inhouse programs in the areas of liquid propellant compatible elastomers, aircraft tire materials, hydraulic system seals, and elastomer reinforcement technology. He also is a consultant to other Air Force organizations on system problems involving elastomeric components. He is a former member of the AIAA Liquid Rocket Technical Committee and presently is a member of the AIAA Propellant Expulsion Working Group. His B.S. in Chemistry is from Indiana University.

THE EFFECT OF EXPLOSIVES AND PROPELLANTS ON THE TENSILE PROPERTIES OF POLYMERS

D Sims and A L Stokoe
Explosives Research and Development Establishment
Waltham Abbey
England

ABSTRACT

The paper presents the collected results of studies to determine the effects of a range of explosives and propellants on common plastics and rubbers. Some more detailed work on four rubbers is also reported.

1 INTRODUCTION

Plastics and rubbers are being used increasingly in modern weapons, and a specialized knowledge of their use in this field is essential. In addition to the stringent mechanical property requirements demanded of the polymers in any weapon system, there is often contact or close proximity to explosives or propellant compositions. The polymers must be able to withstand these explosives and any vapours from them without showing significant deterioration in physical properties. Although military specifications often require satisfactory performance of plastics components from -40 to $+70^{\circ}\text{C}$ it is in general only at the higher temperature that compatibility problems arise. For this reason it has become practice at ERDE to test materials under prolonged storage conditions at one temperature only, namely 60°C for periods of up to 2 years (1-4). Exposure has normally been restricted to CE (tetryl, trinitrophenylmethylnitramine), RDX (1:3:5 trinitro 1:3:5: triazacyclohexane), TNT (trinitro-toluene) together with single and double base propellants. Other materials such as PE (plastic explosive) and amatol are likely to be similar in action to their base constituents and HMX is likely to be similar to RDX. Over the years it has become apparent that TNT and nitroglycerine

containing compositions have the most severe effects on polymeric materials and therefore most recently these have been the only materials examined.

Materials have been classified according to the effects observed, i.e. none or slight effect less than 10% change; moderate greater than 10 but less than 50%; severe greater than 50% change in tensile properties. Changes in tensile properties can occur due to degradation or absorption of various components of the explosive or propellant. Changes in properties have to be considered in the light of the role of the component. It may not matter if an O-ring swells considerably and loses more than 50% of its strength provided it remains sealed and the seal is not required to be broken for inspection. Similarly cellulose acetate is often used for inhibition of low NG containing cordite but it rapidly absorbs NG and loses strength by plasticisation. This may not matter in practice. Often the greater problem is the change of burning rate of the composition due to the loss of nitroglycerine.

Other materials may not lose significant strength but they become slightly sticky and thus fail for

this reason, still others do not change in strength but become brittle.

The results presented should therefore be used as a guide by the designer when considering the functioning of the weapon as a whole.

Four of the rubbers considered have been examined in a little more detail to attempt to find out exactly what the effects of TNT and NG are on hot storage.

Rubbers were exposed as unvulcanised gumstocks, unfilled crosslinked elastomers and black elastomers. Molecular weights of the unvulcanised gums were measured by osmometry where possible. Changes in the unfilled crosslinked elastomers and normal black elastomers were measured by swelling in benzene and molecular weights between crosslinks calculated. NG, TNT and bound nitrogen estimations were made to give an insight into how the rubbers change on exposure.

2 EXPERIMENTAL

Rubbers and plastics used were normal commercial general purpose grades. The rubbers were compounded and cured into ASTM standard sheets and small E type dumb-bells (described in BS 903) cut for exposure. Plastics were injection moulded into miniature dumb-bells using manufacturers' recommended conditions.

Explosives and propellants used

- (1) CE (TETRYL) TRINITROPHENYLMETHYLNITRAMINE TO CS 1004
- (2) RDX/TNT 60/40 BY WT TO CS 5446
- (3) TNT TRINITROTOLUENE TO CS 5023
- (4) SINGLE BASE PROPELLANT NH CONTAINING ABOUT 85% NC
- (5) CORDITE NQ DOUBLE BASE PROPELLANT CONTAINING ABOUT 20% NG

- (6) HUK DOUBLE BASE PROPELLANT CONTAINING ABOUT 45% NG
- (7) CASTING LIQUID CONTAINING ABOUT 40% NG IN TRIACETIN

Samples of materials were placed in aluminium trays approximately 300 x 100 x 40 mm, the trays being separated by weirs into 4 compartments. With TNT or RDX/TNT small foil trays were made to lay in the bottom of the larger tray. Molten explosive was poured into the foil trays and the polymer samples laid in the molten explosive. After cooling more molten explosive was poured in so as to completely cover the specimens. Slide 1 shows the general arrangement. Tetryl and the cordites were supplied as fine powders which were liberally spread over and around the polymer samples. With casting liquid foil inner containers were not used. The samples were grouped in fives separated by the weirs. Just sufficient liquid was used to cover the specimens (approx 60 ml). The whole tray in this case was then covered with a heat sealed polythene bag. Each large tray therefore contained sufficient specimens (4 x 4 or 4 x 5) to provide for four withdrawals. Trays were covered with a loose polythene lid, wrapped in foil to prevent evaporation and stored in explosives ovens at 60°C. Control samples with no additive were exposed under identical conditions. Additional controls immersed in triacetin were provided for studies on selected rubbers. Withdrawals were usually made at 3, 6, 9 and 12 months. At these times the large container was unsealed, one foil container removed completely. In the case of Tetryl and the cordite propellants the polymer samples were freed from adhering powder as far as possible. With TNT and RDX the explosive was carefully broken away by hand using polythene gloves.

Casting liquid presented some extra problems. At the end of the exposure period the trays were removed and allowed to cool in a fume cupboard. The seals were removed and samples were removed using plastic spatulas. Trays were then resealed

in fresh bags and replaced in the ovens. Excess liquid was carefully wiped off the specimens with soft tissue, protective clothing was used to prevent the contact of casting liquid with skin.

Specimens were weighed in batches of four or five to determine weight changes and then normally conditioned overnight before tensile measurements were made. Exceptions were those immersed in casting liquid or triacetin; these were tested as soon as possible after withdrawal from exposure to minimise evaporation.

Chemical and physical examination of samples

Miniature plastic dumb-bells were tested at 2.5 mm/min whereas rubbers were tested at the standard crosshead rate of 500 mm/min. The ultimate tensile strengths and elongations to break were recorded.

The four selected rubbers for more detailed examination were treated as follows. Broken portions of dumb-bells which had been tested were extracted in a Soxhlet extractor using acetone or methanol for TNT and casting liquid respectively for 24 hours. TNT and nitroglycerine contents of the extract were determined colorimetrically using standard methods (Table 6).

Extracted samples were returned for combined nitrogen and swelling measurements.

Combined nitrogen was determined by combustion but results obtained are not very accurate at the levels found. Swelling was determined as follows. Returned samples were dried to constant weight, immersed in benzene in a flask in a thermostat for 3-4 days. Samples were removed, quickly dried and weighed; they were then redried to constant weight. Swell was calculated making the assumption that the volume of swollen rubber = v_0 + volume of benzene absorbed and a simple correction could be applied for the non rubber

constituents. Molecular weights between cross-links were calculated from these figures.

The unfilled uncrosslinked rubbers exposed were freed from TNT or dried of superficial liquid as appropriate. Small weighed pieces were placed in toluene for 48 hours. After this time the solution was filtered to remove gel and made up to a known volume. An aliquot was taken to determine polymer concentration and calculate the gel content. The molecular weight of the rubber in solution was determined by osmometry.

The tabulated results of the effects of explosives and propellants on common polymers are given in Tables 1-4. Detailed figures are not given; as mentioned in the introduction materials are classified according to the effect of the environment. Slight indicates changes of less than 10%, moderate less than 50% and severe greater than 50%. In addition the amount of nitroglycerine absorbed from cordite NQ and the change in appearance of the specimens is given in the last column.

3 RESULTS

Results show that the severity of attack of the explosives and propellants is in the approximate order CE, PE, NH, RDX/TNT, TNT, NQ, HUK respectively. For this reason some of the later materials examined have only been exposed to TNT and NQ.

CE, PE and NH rarely cause any severe problems in contact with plastics or rubbers. Exceptions are where the wax in PE produces softening in EVA. RDX/TNT is obviously less severe than TNT alone and in the later work none of these materials have been used as an exposure medium. TNT and particularly NQ and HUK provide severe environments for many materials.

With all materials the saturated chain polymers such as polyethylene, polypropylene, EPDM and butyl are least affected. More polar materials such as acetal, polycarbonate, polysulphone,

nitrile, neoprene and urethane rubbers and also materials containing unsaturation such as ABS, natural rubber, polybutadienes and block SBR thermoelastomers are badly affected by TNT and NG.

Crystallinity in materials provides resistance. This is shown by the different results for low density polythene and polypropylene and by the resistance of nylon 66 and polyethylene terephthalate. High cross link density also helps to provide resistance; this is shown by the outstanding resistance of the Daltocast polyurethanes to almost pure NG and the resistance of thermosetting resins in general. Exceptions to the general rules are shown by Trogamid, a transparent apparently amorphous nylon, which has excellent resistance to TNT and NG and Viton, a fluoroelastomer which is also highly resistant. Silicone rubbers are similarly resistant but fluorosilicone is affected by nitroglycerine containing propellants.

Highly loaded rubbers also appear to have better resistance from the limited information we have. For instance, highly filled SBR and hypalon materials used in contact with cordite as rocket motor insulants show moderate resistance. Here of course the rubbers are very hard and stiff and require only limited minimum mechanical performance in most designs.

The results highlight the shortage of transparent plastic materials which are compatible with cordites. Common transparent materials PMMA, MBS, SAN, PC, polysulphone and CA are all badly affected. Trogamid is an exception and since its chemical and ageing resistance are quite good it should find use in military stores. We already use it in the UK for small ammunition box lids where visual identification of charges is required. Penton could be equally useful but I believe the material is now out of production.

The extra tests on four rubbers namely polyisoprene (IR), polybutadiene (BR), EPDM and Butyl

(IIR) are reported in Tables 4-6. The results are not very informative. The changes in tensile strength observed are as expected but the changes in crosslink density (M_c values) do not necessarily mirror these changes.

The unvulcanised gumstocks are degraded rapidly by contact with both casting liquid and TNT; TNT however does promote crosslinking with both polyisoprene and polybutadiene since these samples were almost 100% gel after 4 weeks' exposure (Table 4). Tensile strengths and M_c values are given in Table 5.

Polyisoprene rubber unfilled and black shows a rapid fall in tensile strength on exposure even with the control samples; corresponding measurements of molecular weights between crosslinks show only small changes. Only in contact with casting liquid does the M_c value change by a significant amount indicating formation of further crosslinks. The fall in tensile (and elongation at break) is therefore likely to be partly due to oxidative surface attack, especially in the case of TNT and controls and partly due to swelling in the case of casting liquid. Butadiene rubber shows a significant fall in M_c value in contact with both TNT and casting liquid but fails to show any great change in tensile strength. Elongation at break measurements fall quickly thus indicating embrittlement setting in. This is in accord with the changes in M_c . Butyl rubber has a higher initial crosslink density when unfilled than when black. Exposure to casting liquid produces an increase in molecular weight between crosslinks, i.e. reversion, but little change in strength is apparent.

EPDM shows undercure and the M_c value decreases in all environments in the first two weeks but shows little subsequent change.

Taken in their own groups the results are self consistent but regrettably they are not very informative.

TNT and NG contents determined by extraction show that absorption in all the rubbers is initially a rapid process followed by a further slow build up. The two unsaturated rubbers polyisoprene and polybutadiene have about ten times the absorption of the saturated butyl and EPDM rubbers. Bound nitrogen determinations given in the table as (actual amount minus control determination) show that in all rubbers a small but significant amount of nitrogen becomes bound to the polymer chain.

Regretfully in conclusion this part of the work has not thrown much light on the way the four rubbers change on exposure. No immediate further work on this is proposed.

4 CONCLUSIONS

A tabular presentation of the effects of certain explosives and propellants has been produced as a guide for weapons designers to consider with the system as a whole. Results show that TNT and high NG containing cordites are the most severe environments.

Structural considerations conferring high resistance to polymers are:

- (1) SATURATED CHAINS
- (2) LOW POLARITY
- (3) HIGH CRYSTALLINITY
- (4) HIGH CROSSLINK DENSITY

5 REFERENCES

- (1) Ledbury K and Stokoe A L, Degradation of Materials in Contact with Explosives, ERDE Memo 7/M/65
- (2) Hollingsworth B L, Ledbury K and Stokoe A L, Effect of Explosives and Propellants on Plastics and Rubbers (Review of Work from 1957), ERDE 11/R/68

- (3) Sims D, et al, Part 2, ERDE Tech Report 5 (1969)

- (4) Sims D, et al, Part 3, ERDE Tech Report 29 (1970)

BIOGRAPHIES

Dr D Sims obtained a BSc Honours degree in Chemistry in 1958 and obtained a PhD on the Physical Properties of Polymers at Manchester University in 1961. Since that time he has been working for the Ministry of Defence at Explosives Research and Development Establishment. He has published papers on a wide range of subjects including the measurement of physical properties of polymers, kinetics of polymerisation and the processing of rubbers and plastics. He is at present Section Leader, Polymer Development and Applications.

A L Stokoe studied at Glasgow University and obtained a BSc degree in Applied Chemistry in 1938 followed by the Associateship of the Institution of the Rubber Industry in 1950. He joined the Chemical Inspectorate Division of the Ministry of Supply in 1939 and has been in the Polymer Development and Applications Section of the Explosives Research and Development Establishment, Ministry of Defence since 1953.

Table 1 GENERAL PURPOSE PLASTICS - Effect of exposure

	Slight	Moderate	Severe	NQ absorption and effect
ABS	NH	RDX/TNT, TNT	NQ	30% Different grades soften or embrittle
Polythene LDPE	TNT, NQ	PE, HUK		3% Softens
Polybutylene		TNT	NQ	7% Brown, brittle
Polythene HDPE	TNT, NQ, HUK	PE		0.2% No change
Polypropylene	RDX/TNT, TNT, NH	NQ		0.2% Yellow
EVA	CE	TNT	NQ	11.0% Softens
Polystyrene	RDX/TNT, TNT, NQ, HUK			Nil No change
Toughened PS	RDX/TNT	TNT, NQ, HUK		0.2% Yellows
SAN	NH	RDX/TNT, TNT	NQ	Softens and disintegrates
MBS	CE, TNT		NQ	Sticky, encrusted and brown
PVC flexible		RDX/TNT, TNT, HUK		5% No change
PVC rigid	RDX/TNT, TNT, NH, NQ			4% No change
*Polyester/glass laminates	RDX/TNT, TNT, NH	NQ		-
Epoxy/glass laminates	RDX/TNT, TNT, NH, HUK			-
PF resins	PE, RDX/TNT, TNT, NH, HUK			
PMMA			TNT, NQ, HUK	Sticky, brown and encrusted
CA	NH	NQ	HUK	60% Softens
EC		NQ, HUK		12% Little change
Dough moulding compound	TNT, NQ			Little effect

*Depends on composition

Table 2 ENGINEERING AND SPECIALITY POLYMERS - Effect of exposure

	Slight	Moderate	Severe	NQ absorption and effect
Acetal		RDX, TNT	TNT, NQ	6% Yellow, crazed
Nylon 11			TNT, NQ	Brown, brittle
Nylon 6	PE	TNT	NQ	0.5% Orange, embrittles
Nylon 66	CE, TNT	NQ		0.1% Orange, embrittles
GF Nylon 66	NQ			
Polysulphone	CE	TNT, NQ		Sticky and encrusted
Polycarbonate	RDX/TNT, NH	TNT, NQ		10% Sticky and encrusted
Polyphenylene oxide (Noryl)	TNT, NQ			0.2% No effect
Chlorinated polyether (Penton)	RDX/TNT, TNT, NH, NQ			1% No change
Phenoxy		CE, TNT, NQ		5% Embrittles slowly
Thermoplastic polyester (mouldings) + film	TNT, NQ			3% No change
Surlyn A	CE, TNT, NQ			6% Softens, goes black
Trogamid	TNT, NQ			Nil No effect
Arylon			TNT, NQ	Severe cracking
TPX	CE, TNT	NQ		0.5% Turns translucent
Daltocast rigid PU	TNT, NQ, 98% NG			No effect

Table 3 RUBBERS - Effect of exposure

	Slight	Moderate	Severe	NQ absorption and effect
Natural		NH	TNT, NQ	28% Embrittles
Nitrile	PE	CE	TNT, NH, NQ, HUK	25% Embrittles
Neoprene	PE, CE	NH	TNT, NQ, HUK	15% Embrittles slowly
SBR		TNT	NQ	16% Embrittles slowly
Butyl	NH, TNT	NQ, HUK		10% No change
Chlorobutyl		TNT	NQ	5% No change
Polybutadiene		TNT	NQ	24% Embrittles
Viton	CE, TNT, NQ			8% Surface colour
Silicones	CE, TNT, NQ			2% No change
Fluorosilicone	CE, TNT	NQ		8% Softens
Polyester urethane			CE, TNT, NQ	Disintegrates
Polyether urethane		TNT	NQ	Disintegrates
Adiprene CM Sulphur cured			TNT, NQ	Softens badly
Polysulphide			TNT, NQ	Too sticky to test
Thermoelastomers polyester urethane			TNT, NQ	> 50% Softens
Thermoelastomers polyether urethane			TNT, NQ	Disintegrates
Thermoelastomers SBR type			TNT, NQ	Disintegrates
Thermoelastomers Hytrel		TNT, NQ		-
Acrylate copolymer	TNT	NQ		36%
Acrylate homopolymer		TNT	NQ	40%
Epichlorhydrin copolymer and homopolymer			TNT, NQ	Too weak to test
Polypropylene oxide rubber			TNT, NQ	Too weak to test
Hypalon	TNT	NQ		10% softens
EPDM	TNT	NQ		4% no change

Table 4a TENSILE STRENGTHS OF SELECTED RUBBERS MPa EXPOSED AT 60°C

Controls	unfilled rubbers				black rubbers (50 pph)			
	IR	BR	IIR	EPDM	IR	BR	IIR	EPDM
0	6.0	0.5	1.8	0.6	25	6.8	15	17
4 weeks	6.0	0.6	1.8	1.0	18	6.3	15	16
12 "	-	0.6	1.5	-	12	5.8	14	16
24 "	1.0	0.6	1.5	1.0	8	5.5	15	16
TNT exposure								
4 weeks	5.5	0.6	1.8	1.0	18	5.8	15	17
12 "	7.6	0.5	1.6	-	10	6.1	14	17
24 "	2.2	0.8	1.4	1.0	6	5.9	13	16
Casting liquid exposure								
4 weeks	5.6	0.5		0.9	8	4.5	14	18
8 "	0.4	0.5	1.5	1.0	5	5.2	13	18
12 "	0.2	0.6	1.5	1.0	4	4.5	14	17
Triacetin exposure								
4 weeks	5.1	0.5	1.5	0.8	17	4.6	15	15
8 "	4.7	0.5	1.6	0.9	11	5.6	15	15
12 "	1.5	0.5	1.7	1.0	8	4.1	15	17

Table 4b MOLECULAR WEIGHTS BETWEEN CROSSLINKS M_c

(calculated from swelling values using the Flory Rehner relationship $\frac{1}{M_c} = \frac{\mu v_r^2 + \ln(1-v_r) + v_r}{\rho v_o v_r^{1/3}}$)

Controls	IR	BR	IIR	EPDM	IR	BR	IIR	EPDM
0	6.2×10^3	2.6×10^3	3.5×10^3	2.2×10^3	6.5×10^3	1.5×10^3	7.7×10^3	4.8×10^3
2 weeks	6.0	2.4	4.5	2.1	7.0	2.5	9.7	3.0
4 "	5.6	2.3	4.1	1.9	6.8	2.3	8.6	2.7
24 "		2.4	4.3	1.6	5.9	1.8	8.4	2.5
TNT exposure								
2 weeks	6.4	2.6	4.9	2.0	6.5	2.5	9.8	3.8
4 "	6.0	2.5	4.0	1.8	6.6	2.3	10	2.9
12 "	6.6	2.4	4.8	1.8	7.8	2.0	9.4	2.9
24 "	7.4	1.9	4.5	1.7	7.0	1.5	-	3.1
Casting liquid exposure								
2 weeks	7.2	2.5	4.8	1.9	7.5	2.2	11	3.2
4 "	7.8	2.5	5.2	2.0	7.8	2.0	13	3.1
8 "	11	2.2	5.0	1.8	6.5	1.8	17	2.9
12 "	8.6	1.8	5.5	1.5	4.0	1.5	17	2.7
Triacetin exposure								
2 weeks	6.0	2.6	5.2	2.0	6.6	2.5	10	3.0
4 "	5.7	2.5	4.4	1.9	6.8	2.4	10	2.4
8 "	6.1	2.5	4.7	1.9	7.8	2.1	11	3.1
12 "	7.3	2.6	4.5	2.0	8.5	2.1	8.7	2.8

Table 5 MOLECULAR WEIGHTS AND GEL CONTENTS OF GUM RUBBERS

<u>Material</u>	<u>Mol wt</u>	<u>Gel</u>	<u>2 weeks</u>	100% gel content
IR	55,000	< 0.1		
BR	84,000	< 0.1		
IIR	127,000	< 0.1		
EPDM	84,000	< 0.1		
2 weeks in casting liquid			<u>4 weeks</u>	too soft to remove
IR	32,500	3		
BR	9,900	5		
IIR	36,000	2		
EPDM	15,000	2		
4 weeks in TNT			<u>12 weeks</u>	unable to separate from TNT
IR	-	100		
BR	4,500	78		
IIR	13,200			
EPDM	8,500	3		

Table 6

Material weeks	TNT content by extraction				NG by extraction				N content %	
	2	4	12	26	2	4	8	12	2	4
BR gum	1.9	2.9								
IIR "	1.0	1.0								
EPDM "	0.9	1.1								
IR white	1.8	1.4	1.6	1.8	1.1	1.9	2.0	2.6	0.3 \pm 0.1	0.3 \pm 0.1
IR black	1.7	1.5	1.9	3.1	0.8	2.0	2.0	2.5	0.5	0.5
BR white	2.0	1.6	1.9	3.4	0.7	1.0	1.3	2.1	0.4	0.2
BR black	1.5	1.3	1.4	2.3	0.4	0.9	1.0	1.5	0.4	0.2
IIR white	0.3	0.1	0.5	0.7	0.1	0.2	0.2	0.2	0.2	0.1
IIR black	0.4	0.5	0.8	1.0	0.1	0.2	0.3	0.4	0.2	0.2
EPDM white	0.2	0.1	0.3	0.6	0.3	0.3	0.3	0.3	0.2	0.1
EPDM black	0.3	0.6	1.1	1.4	0.3	0.4	0.6	0.6	0.2	0.4

THE DETERMINATION OF BINDER DEGRADATION IN PLASTIC-BONDED EXPLOSIVES

E. M. Wewerka, E. D. Loughran and J. M. Williams
University of California, Los Alamos Scientific Laboratory
Los Alamos, New Mexico 87544

ABSTRACT

In this paper we describe how molecular-size-distribution measurements made by gel-permeation chromatography can be used to detect degradation in the binder systems of plastic-bonded explosives. The procedures for sample preparation and chromatographic analysis are outlined. Several examples are given to illustrate the usefulness of this method for studying the stabilities of a variety of explosives systems.

1. INTRODUCTION

The binder systems in many plastic-bonded explosives (PBX's) are plasticized with highly mobile, low-molecular-weight compounds of limited stabilities, and frequently the polymers in these systems contain bonds that are readily susceptible to attack. Consequently, there is considerable uncertainty about how well the binder components of PBX's can withstand long exposures to elevated temperatures. Main-charge explosives like HMX or RDX, on the other hand, are thought to be sufficiently stable to meet current requirements.

In the past, we have utilized many methods to detect degradation or changes in PBX systems. These techniques, including evolved-gas analyses, weight and density measurements, DTA, DSC, TGA and vacuum-stability tests, measure properties or behavior of the system as a whole; they do not directly examine the area that we now feel is the main source of trouble, structural degradation in the binder. Only

recently have we directed much attention to methods for detecting and analyzing binder degradation.

We have been able to demonstrate that binder degradation can be characterized by measuring the changes that occur in the molecular sizes of the binder components with gel-permeation chromatography (GPC). With this method, we can detect changes in binder structure as distinct from those in the explosive or other components. In the following sections of this paper, we describe the analytical details of this method and offer a few examples to illustrate its utility.

2. EXPERIMENTAL PROCEDURES

The binders were separated from the explosives systems by solvent extraction. (The preferred solvent for this work is 1,2-dichloroethane because of the low solubility of HMX.) A 0.5-g sample of crushed PBX, 5 ml of solvent and four 4 mm glass beads were placed in a 10-ml volumetric

flask. The flask was shaken for a 24-hr period to ensure dissolution of the binder components, then the liquid phase was separated from the residual solid materials by centrifugation. The extract was diluted to 40 vol% with tetrahydrofuran (THF). A 1-ml aliquot of this solution was subjected to GPC analysis.

GPC analyses were done with a Waters Model 200 gel-permeation chromatograph. The chromatograph was equipped with two column sets that could be used alternately. For high-molecular-weight materials, we used the large-pore column set, consisting of five 1.2 m polystyrene columns connected in series and having porosities of 10^6 , 10^5 , 3×10^4 , 10^4 and 900 Å. Low-molecular-weight compounds were analyzed with a similar arrangement of columns; however, column porosities were 3×10^3 , 500, 250, 250 and 60 Å. THF, flowing at 1 ml/min, was used as the chromatographic solvent. Sample injection times varied between 10 and 90 s, depending on the sensitivity of the detector for the materials being analyzed. Results were recorded as the change in refractive index as the chromatographed sample passed through the detector. The relative concentration in any given elution volume is directly proportional to the change in refractive index.

3. RESULTS AND DISCUSSION

An excellent example of the usefulness of GPC for detecting binder degradation was provided by a recent study of the long-term stability of PBX X-0242.* A series of X-0242 samples had been stored in sealed glass ampoules in Ar at 75°C for various periods of time. After 64 weeks of

storage, a total of only 0.6 cm³ of gas had evolved per g of sample. There were no appreciable weight losses or density changes in any of the samples. Gas chromatography revealed that a small loss of nitroplasticizer had occurred during storage, but an infrared spectrum of the polyurethane failed to detect any substantial structural changes. However, we found that the compressive strengths of these samples had progressively decreased as a function of storage time. After 64 weeks, the X-0242 test samples retained only about one-third of their original strengths. The reason for this degradation was provided by GPC analyses of the molecular-size distributions of the binders in the surveillance samples.

In Figure 1, we have reproduced the GPC curves for the binder systems of several X-0242 samples. The continuous curve was obtained from a reference sample composed of equal amounts of Estane and nitroplasticizer. Estane, which has a peak molecular weight of about 50,000, is seen to have a broad molecular-size distribution. The nitroplasticizer peak, on the left side of the GPC curve, is clearly separated from the Estane region. The GPC curves for the 32- and 64-week samples show beyond a doubt that severe Estane degradation has occurred as a result of the storage conditions. The average molecular weight of the Estane in the 64-week sample is down to approximately 2,000. This degradation in the polymeric binder component is the cause for the loss of sample compressive strength. Interestingly, as Fig 1 also illustrates, the Estane in a newly prepared sample (X-0242 control) was found to be partially degraded. This shows

* PBX X-0242 is composed of 95 wt% HMX, 2.5 wt% polyurethane (Estane) and 2.5 wt% nitroplasticizer [a 50/50 mixture of bis(2,2-dinitropropyl)formal and bis(2,2-dinitropropyl)acetal].

that the first bond cleavages in the polymer take place during the preparation or fabrication of the explosives system.

The results obtained for the X-0242 system amply illustrate the pitfalls of attempting to evaluate PBX stabilities or compatibilities without sufficient information about what is happening to the individual components. Without recourse to the molecular-size analyses, grossly erroneous conclusions about the stability of the PBX could have been made.

Another explosives system of interest to many is PBX 9404.* A GPC curve of the binder from a reference sample of this PBX is given in Fig 2. The nitrocellulose peak appears on the right side of the trace, and the CEF is seen as a shoulder on the lower-molecular-weight side of the larger HMX peak. HMX appears in this GPC curve because ethyl acetate, rather than dichloroethane, was used in the initial extraction.

GPC was used to examine binder samples from both the center and the surface of a block of PBX 9404. This material had been stored in a sealed container with several other plastic and metal components for approximately 1.5 years at 49°C. Although a relatively large amount of plasticizer appeared to be present, we found the binder from the center of the surveillance sample to be in good condition, as shown by the GPC trace in Fig 3. However, the nitrocellulose is seen to be absent altogether from the GPC curve of the binder

removed from the surface (Fig 4). These observations indicate that the nitrocellulose was depleted at the surface either by migration or reaction during storage; however, it is possible that it crosslinked and was no longer soluble in the extraction solvent.

A final example of the use of GPC for analyzing binder degradation in explosives system is provided by our experience with a surveillance sample of PBX X-0234.** A GPC curve of a X-0234 reference sample is shown as the continuous trace in Fig 5. The acrylate polymer in this explosive has been poorly polymerized, shown by the low-molecular-weight tail extending all the way to the CEF peak. The dashed curve was obtained from the binder in an X-0234 sample that had been stored for just 4 weeks at 75°C. Here, as in the 9404 case just discussed, the polymeric component was found to be largely absent from the GPC curve; however, prior experience with another explosive similar to X-0234 suggests that the acrylate polymer in the surveillance sample was crosslinked during storage, rendering it insoluble.⁽¹⁾

The foregoing examples have demonstrated that binder degradation in a variety of explosives systems can be detected by measuring changes in the molecular-size distributions of the binder components with gel-permeation chromatography.

4. REFERENCES

- (1) Private Communication with D. Seaton, LLL.

*The composition of PBX 9404 is: 94 wt% HMX, 2.9 wt% nitrocellulose, 2.9 wt% tris(chloroethyl)phosphate (CEF) and 0.2 wt% diphenylamine.

**PBX X-0234 is composed of 94 wt% HMX, 3.6 wt% dinitropropyl acrylate polymer and 2.4 wt% CEF.

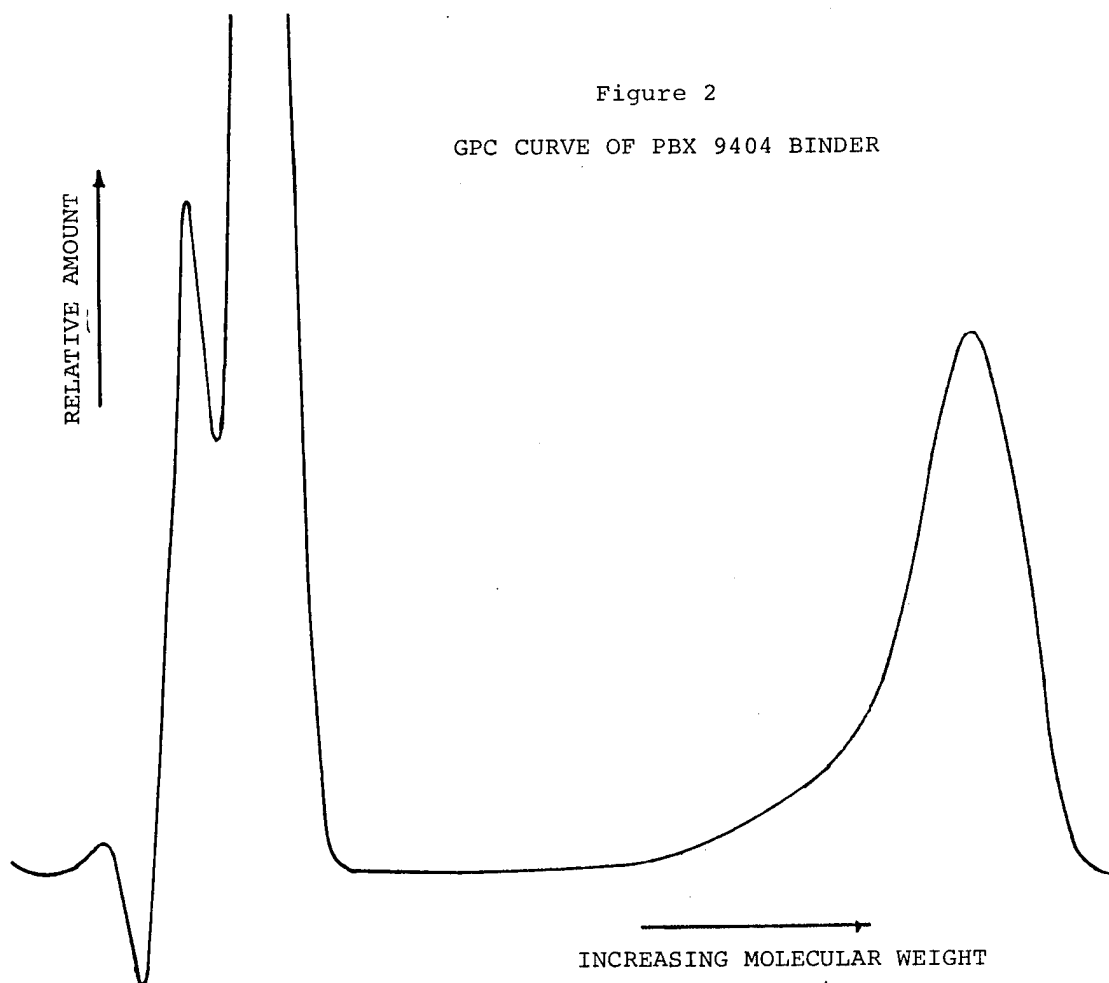
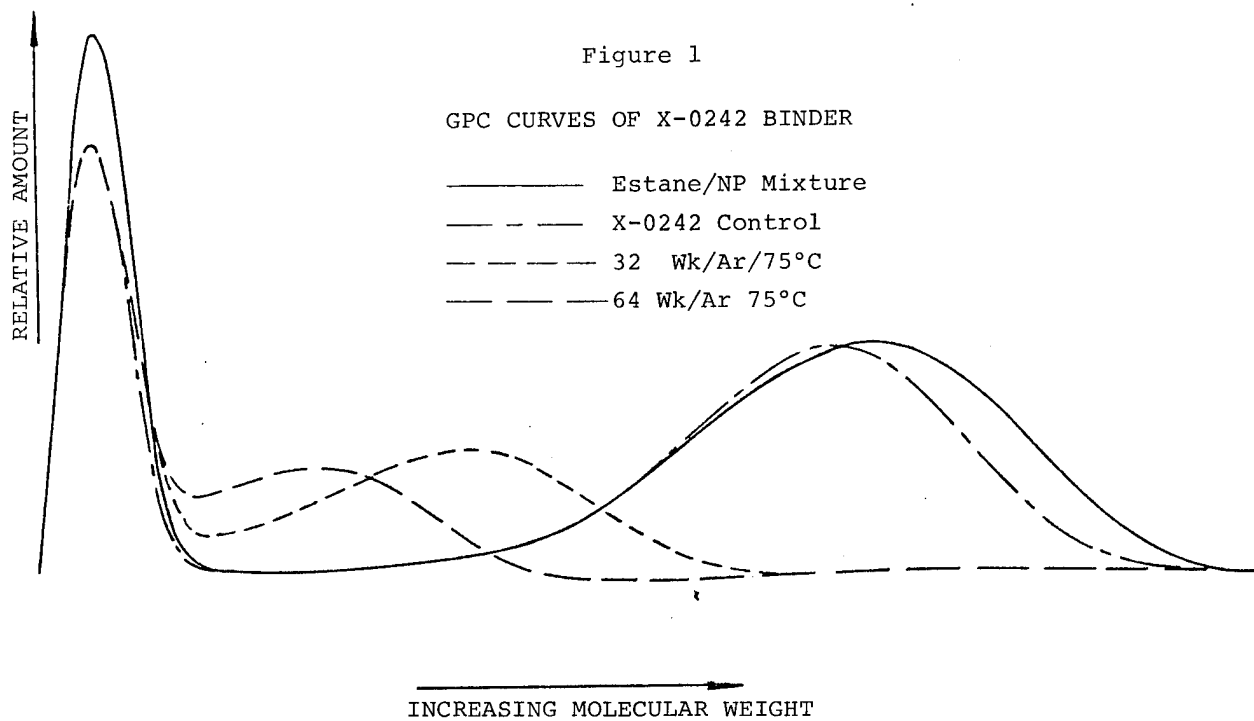
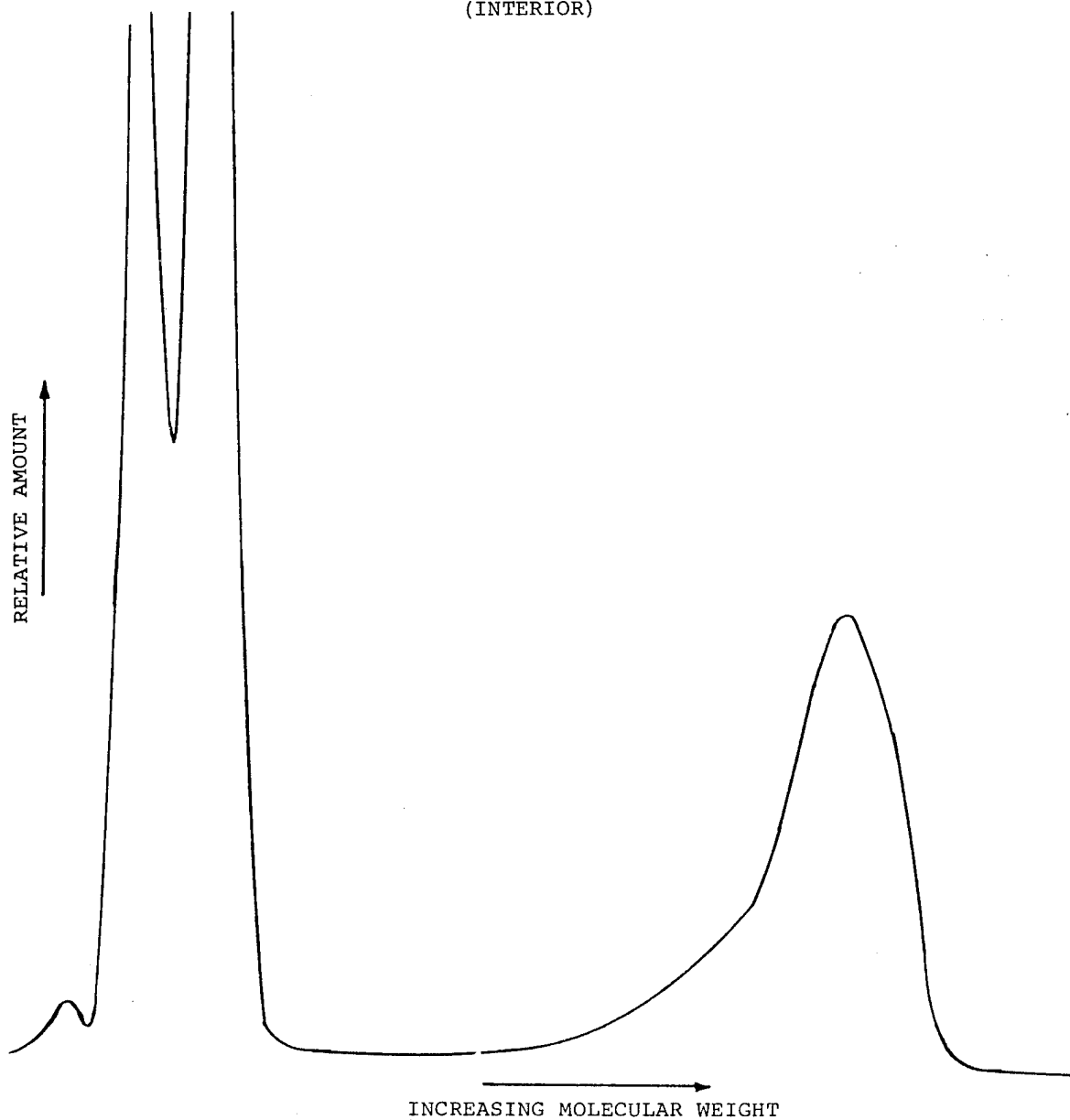
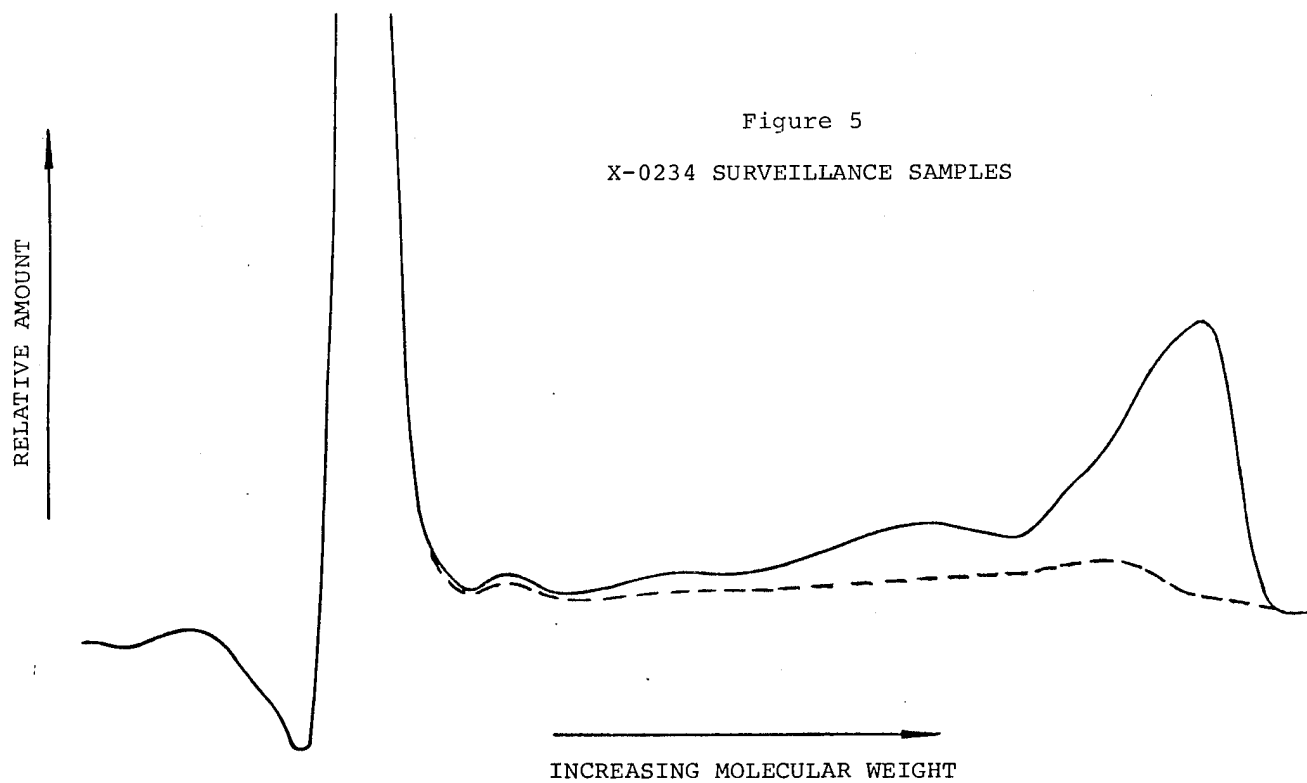
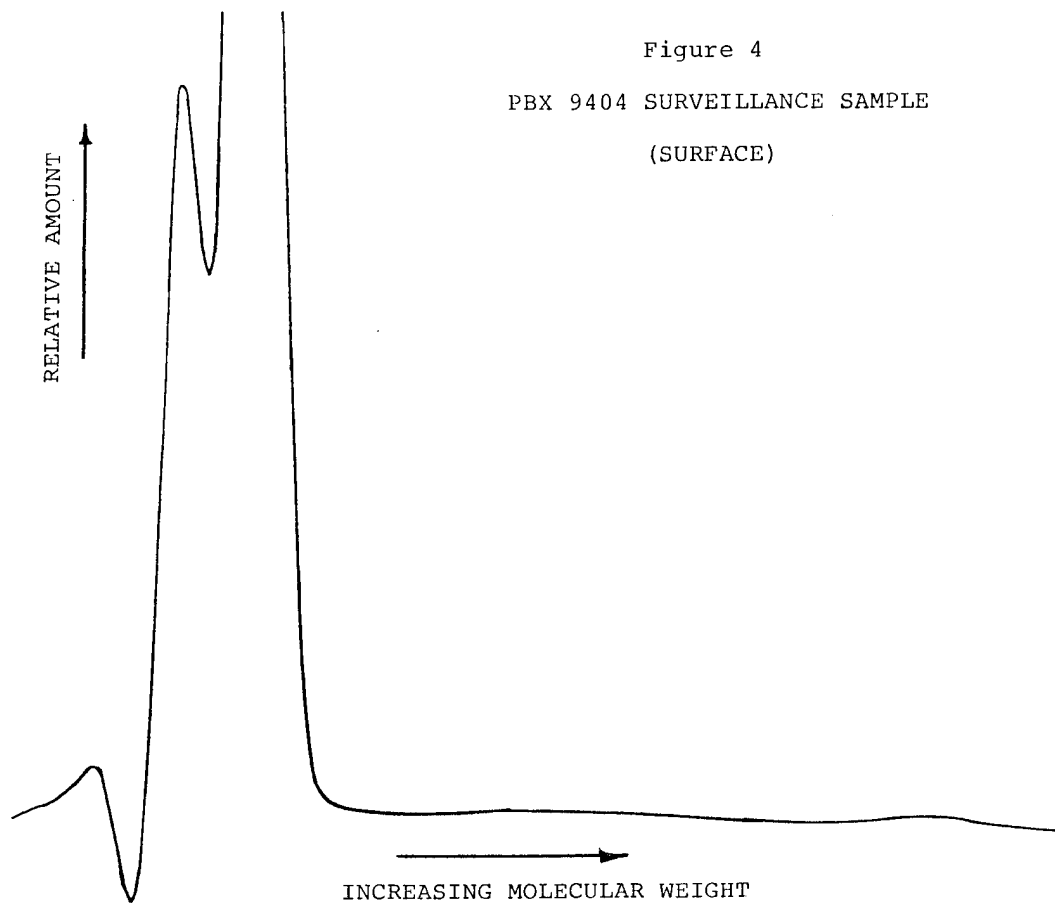


Figure 3

PBX 9404 SURVEILLANCE SAMPLE

(INTERIOR)





THE HE COMPATIBILITY OF SOME RIGID POLYURETHANE FOAMS

C R Thomas

Chemical Technology Division, Ministry of Defence (PE)
Atomic Weapons Research Establishment
Aldermaston, Reading RG7 4PR, England

ABSTRACT

Low density rigid polyurethane foams were less compatible than high density foams prepared from the same polyester/isocyanate system when tested by the vacuum stability method. The reasons for this behaviour were investigated by the use of model compounds representing the different chemical groups in the foam and also by examination of the individual constituents of the foam formulation. Results from these two approaches showed that the major source of incompatibility in low density foams was the blowing reaction in which water reacts with isocyanate to produce carbon dioxide and an incompatible primary amine.

1. INTRODUCTION

Rigid polyurethane foams are versatile materials which find many applications such as thermal insulation, shock absorption, low density structural materials and as a packaging medium. Where such materials are in proximity to high explosives their compatibility is of considerable importance.

Early tests in which the vacuum stability method was used to assess compatibility gave inconsistent results which appeared to vary considerably with the type of polyurethane under test. Further investigation indicated a trend in which low density foams prepared from a specific polyester/isocyanate system appeared to give higher gas evolution (ie were less compatible) than high density foams prepared from the same starting materials.

The work described in the paper was undertaken to determine whether there was a correlation between

density and gas evolution and if this was so to determine the cause of incompatibility in low density foams and if possible to remedy it.

The problem was approached in two ways. First a large number of compatibility tests were carried out in order to establish a statistically sound basis for comparison of the high and low density foams. This was followed by an examination of the individual components of the foam formulation and their relative quantities. Secondly a series of model compounds was prepared in which the chemical groupings present in the foam were isolated and examined separately.

2. DENSITY-COMPATIBILITY RELATIONSHIPS

2.1 MATERIALS TESTED

The polyurethane foam used in this investigation was prepared from a polyester resin (designated 422) and tolylene diisocyanate (TDI). The polyester

contained trimethylol propane, adipic acid, phthalic anhydride and ricinoleic acid. It had a hydroxyl value of 460-480 mg KOH/g, an acid value less than 2 mg KOH/g, a water content less than 0.2 % and a viscosity of 140-200 poise at 25°C. The TDI was an 80/20 mixture of the 2.4 and 2.6 isomers. Water was used to generate carbon dioxide as the blowing agent to produce low density foams with densities of 9.75 and 11.25 and high density foams in the range 40-65 lb/ft³.

The explosive used was Composition B₃, a blend of RDX and TNT. Some tests on high density foam were also carried out with an HMX/TNT composition with similar results.

2.2 TEST RESULTS

A total of 102 test results were obtained for the 9.75 lb/ft³ foam, 161 for the 11.25 lb/ft³ foam and 114 for the 40-65 lb/ft³ foam. Gas evolution results from the vacuum stability tests ranged from 1.8-6.6 cm³ for the low density foams and from 0.2-3.5 cm³ for the high density foams. Arithmetic means and standard deviations were calculated and these are given in Table 1.

The results were plotted in histogram form and the curves for normal distribution calculated from the data in Table 1 were superimposed. Figures 1 and 2 show these curves for the low density foams and Figure 3 shows the curve for high density foams.

It will be seen that the distribution of test results may be considered normal. As further confirmation of normal distribution the probability of gas evolution exceeding the compatibility limit of 5 cm³ was calculated and compared with the actual number of specimens which exceeded this limit. These results are shown in Table 2.

From these results it was concluded that there is a highly significant difference in the gas evolution figures for low (9.75 or 11.25 lb/ft³) density and high (40-65 lb/ft³) polyurethane foams prepared from the same basic raw materials.

3. THE USE OF MODEL COMPOUNDS

3.1 POLYURETHANE CHEMISTRY

Polyurethane foams are prepared by the simultaneous occurrence of two important chemical reactions,

TABLE 1
MEANS AND STANDARD DEVIATIONS OF GAS EVOLUTION RESULTS

Foam density (lb/ft ³)	9.75	11.25	40-65
Number of Results	102	161	114
Mean gas evolution (cm ³)	4.64	4.22	1.47
Standard deviation	0.67	0.83	0.65

TABLE 2
CALCULATED PROBABILITY AND OBSERVED INCOMPATIBILITY

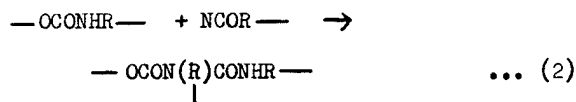
Foam Density (lb/ft ³)	9.75	11.25	40-65
Calculated probability of gas evolution exceeding 5 cm ³	0.29	0.17	<0.001
Observed fraction of results exceeding 5 cm ³	0.30	0.14	0

both of which involve reaction of the isocyanate with active hydrogen.

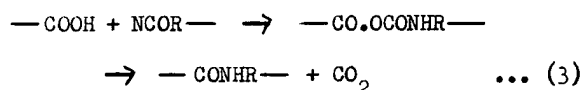
In the first important reaction the isocyanate reacts with hydroxyl groups in the polyester to produce a polymer linked by urethane groups (Equation 1).



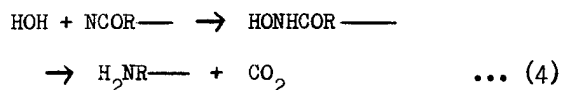
Excess isocyanate can react further with the urethane group to form an allophanate (Equation 2).



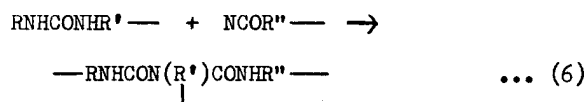
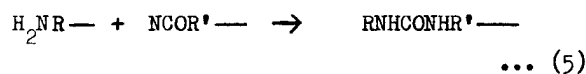
An analogous reaction also occurs between isocyanate and acid groups in the polyester (Equation 3) leading to a substituted amide and carbon dioxide.



The second important reaction is between isocyanate and water, forming an unstable intermediate which breaks down to give a primary amine and carbon dioxide which blows the foam. (Equation 4)



The primary amine can then react with further isocyanate to produce substituted urea (Equation 5) and biuret (Equation 6) groups.



3.2 CHOICE OF MODEL COMPOUNDS

In the polyester 422/TDI system the urethane groups may be of two types, primary urethanes from the primary hydroxyl groups of the trimethylol

propane and secondary urethanes from the secondary hydroxyl groups in the ricinoleic acid. The contribution from the isocyanate will always be aromatic. Hence model urethanes chosen were those prepared from phenyl isocyanate and normal isopropyl alcohols. Allophanate groups were represented by ethyl- α - γ -diphenyl allophanate prepared from ethanol and excess phenyl isocyanate.

Carboxylic acid derivatives may also be of two types; aliphatic, arising from the adipic and ricinoleic acid residues, and aromatic from the phthalic anhydride residues in the polyester. Accordingly butyranilide and benzanilide were chosen to represent the two types of substituted amide which are likely to be present.

The initial reaction product of TDI and water is a primary amine which was represented by m-phenylenediamine. Urea structures from further reaction of amine with isocyanate will always be of the NN' disubstituted type for which NN' diphenyl urea was chosen as a model. Similarly a triphenyl substituted biuret would have been a suitable model but, as this was unavailable, ordinary biuret was used and was compared with ordinary urea and NN' diphenyl urea to estimate the contribution from the phenyl groups.

All the model compounds were either purchased or were prepared by standard literature methods and characterised by melting point and chemical analysis.

3.3 TEST RESULTS

Table 3 shows the results of vacuum stability tests carried out with Composition B3 and the model compounds described above.

TABLE 3

GAS EVOLUTION RESULTS WITH MODEL COMPOUNDS

COMPOUND	ORIGIN	GAS EVOLUTION (cm ³)	COMPATIBILITY
n-propyl phenyl urethane) Isocyanate + Hydroxyl	0.7	Admixture
i-propyl phenyl urethane		0.7	Admixture
Ethyl α - γ -diphenyl allophanate		2.3	Contact
Butyranilide) Isocyanate +) Carboxylic acid	0.4	Admixture
Benzalinide		1.7	Contact
m Phenylene diamine) Isocyanate + Water	> 20	Incompatible
NN' Diphenyl urea		2.1	Contact
Urea		> 20	Incompatible
Biuret		6.3	Incompatible

These results show that the urethane and allophanate groups are compatible. Thus a polyurethane formed simply from a compatible polyhydroxyl compound and an isocyanate (eg a polyurethane adhesive, solid casting or coating) should be compatible. Substituted amide groups are also compatible so that the carboxylic acid/isocyanate reaction could also be used to prepare compatible polyurethane foams.

However, the conventional foaming method, using water and isocyanate, can give rise to incompatible amine, urea and biuret groups. Amines are well known to be incompatible with explosive compositions. Of the other groups the substituted urea is contact compatible and, by analogy, a substituted biuret would probably be compatible also. Hence the use of model compounds indicates that primary amines from the water/isocyanate reaction are the major source of incompatibility.

4. EXAMINATION OF POLYURETHANE FOAM FORMULATIONS

4.1 COMPONENT MATERIALS

In order to apply the results from the model compound study to the foams it was necessary to establish the compatibility of the actual components of the foam formulation with Composition B3. Results of these tests are shown in Table 4 together with the proportions of each material used in the high and low density foams. It is evident that the major components ie polyester and isocyanate are themselves compatible but that some of the minor constituents (particularly the catalyst) are not. However, the small concentrations of catalyst and the fact that it is present in equal proportions in the high and the low density foams makes it unlikely that it is the source of the low density foam incompatibility.

TABLE 4
FORMULATION AND COMPATIBILITY OF FOAM COMPONENTS

Material	Chemical Type	Gas Evolution (cm ³)	Foam Formulation (pbw)	
			Low Density	High Density
Resin 422	Polyester	2.0	100	100
TDI	Isocyanate	3.6	78	76.5
Catalyst	Tertiary amine	> 20	0.04	0.04
Wetting agent	Non-ionic detergent	7.1	0.45	0.06
Blowing agent	Water	-	2.25	0.21
Cell modifier	Silicone	0.8	2.0	

The gas evolution results were unchanged from normal low density foams when foams were tested in which the incompatible catalyst and wetting agent were omitted from the formulation.

The results in Table 4 taken in conjunction with the evidence from the model compounds strongly suggest that amines arising from the larger quantity of water used to blow the low density foams are the major source of incompatibility.

4.2 FORMULATION EFFECTS

A series of foams was prepared in which the water concentration was varied whilst all other components were held constant, and these were tested for compatibility with Composition B3. The results of these tests are shown in Figure 4 and indicate a strongly dependent relationship between water content and compatibility. This figure also shows that compatible low density foams were obtained when an inert fluorocarbon blowing agent (trichlorofluoromethane) was used in place of the carbon dioxide from the water/isocyanate reaction. It is noteworthy that the very low density fluorocarbon blown foams contained a five-fold excess of amine catalyst (to prevent cell collapse) without any adverse effect on its compatibility as shown by the vacuum stability test.

5. CONCLUSIONS

There is a significant difference between the HE compatibility of high density and low density polyurethane foams made from the same starting materials and blown by the water/isocyanate reaction.

The difference is attributable to the amines and ureas which are produced by the water/isocyanate reaction and which are present in greater quantity in the low density foams. Compatible low density polyurethane foams are obtainable by the use of an inert volatile blowing agent in place of water.

ACKNOWLEDGEMENTS

The author wishes to thank Messrs H Briscall and D N B Mallen for experimental assistance and the Director, AWRE, for permission to publish this work. Crown copyright reserved.

BIOGRAPHY

Dr C R Thomas was born and educated in Cardiff where he gained BSc and MSc degrees in Chemistry at the University of Wales. He was awarded the PhD from Birmingham University for research into organic fluorine chemistry. He has worked at

AWRE, Aldermaston since 1956, initially in the Explosives Division but now in the Chemical Technology Division where he is a section leader with interests in cellular materials and carbon fibre composites.

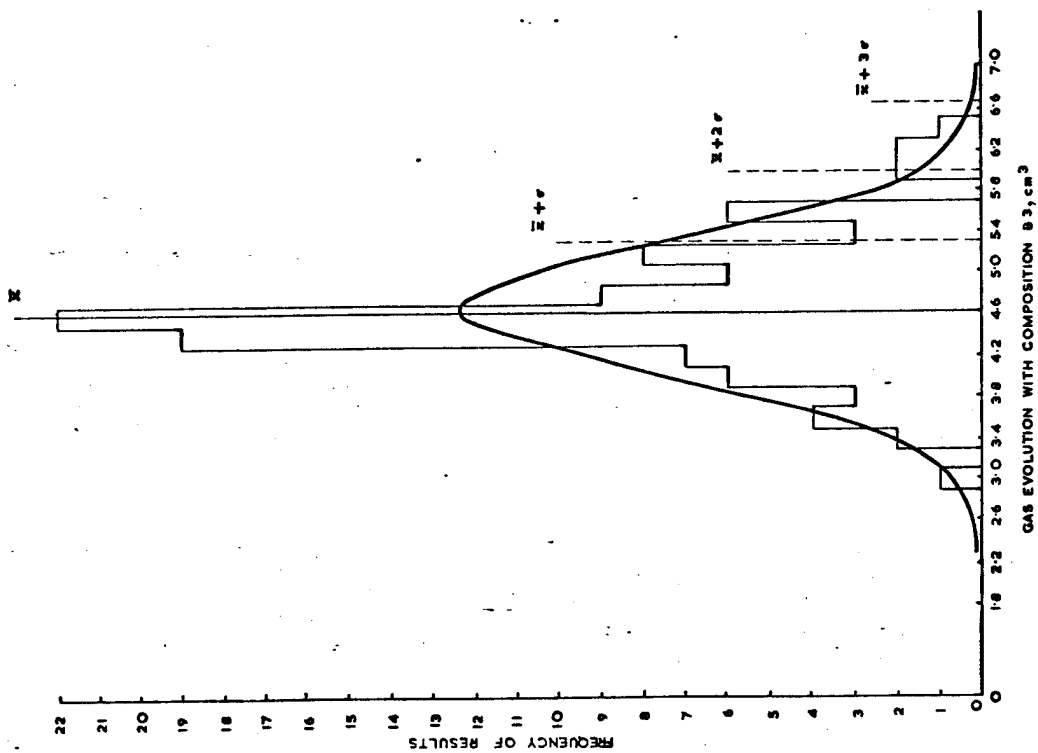


FIGURE 1. H.E. COMPATIBILITY
RESULTS FOR 9.75 lb/ft³ FOAM

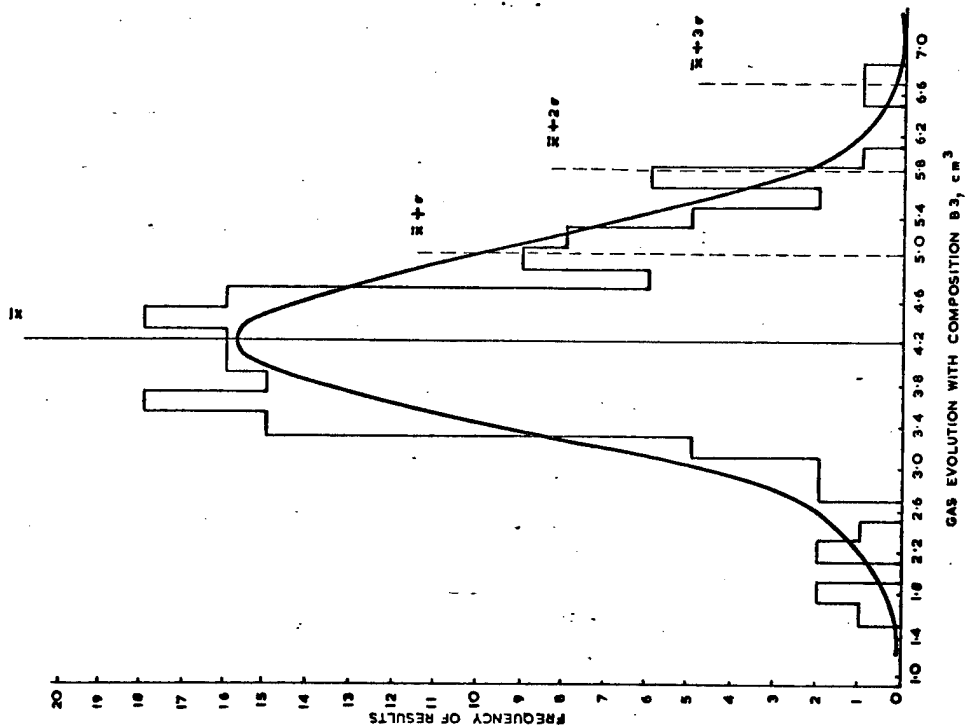


FIGURE 2. H.E. COMPATIBILITY
RESULTS FOR 11.25 lb/ft³ FOAM

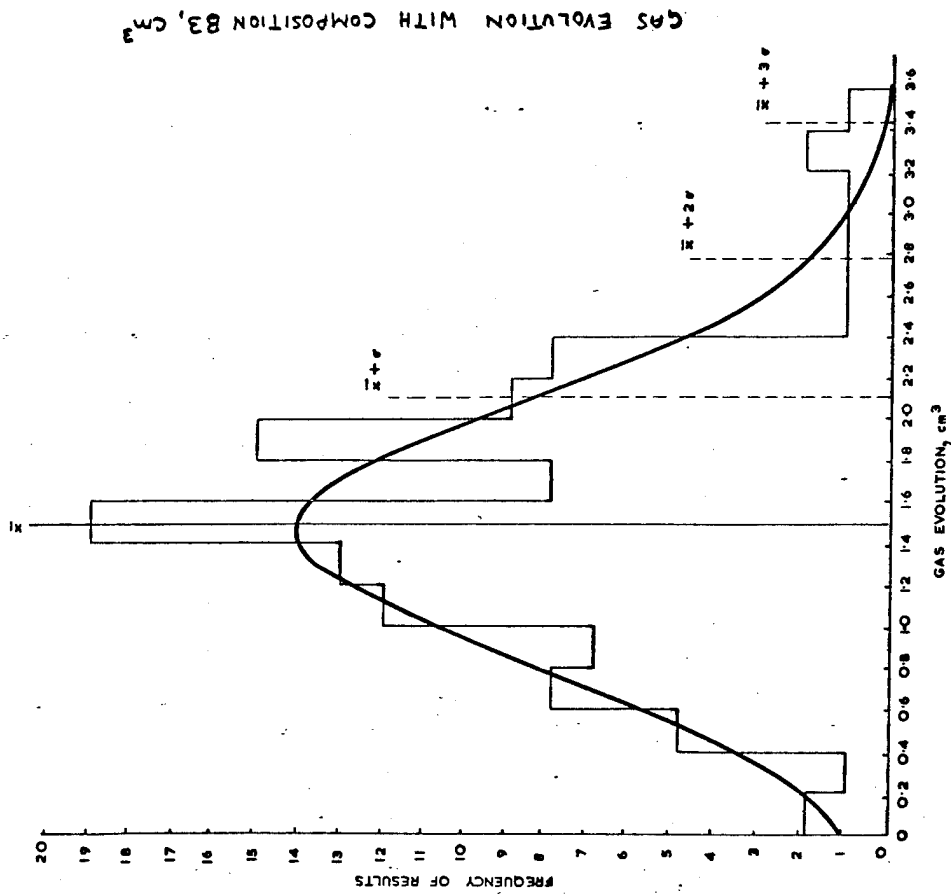


FIGURE 3. H.E. COMPATIBILITY RESULTS FOR HIGH DENSITY FOAM

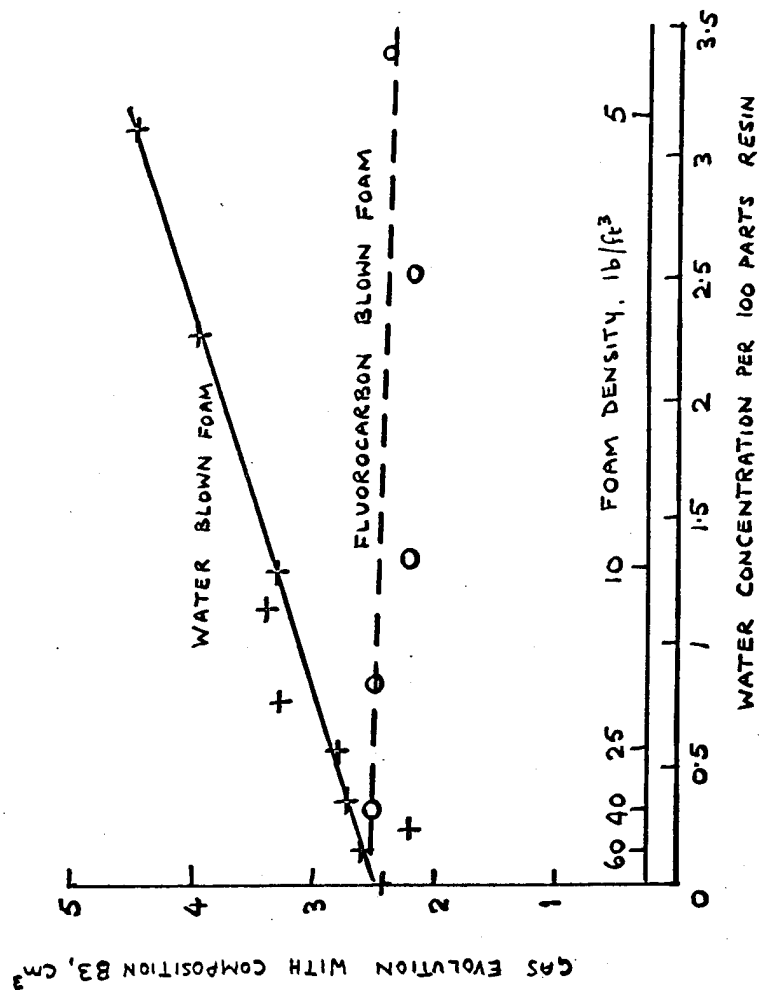


FIGURE 4. FOAM DENSITY AND COMPATIBILITY

RESPONSE OF SOME POLYURETHANES TO HUMID ENVIRONMENT

L. B. Jensen and H. P. Marshall
Lockheed Palo Alto Research Laboratory
3251 Hanover Street
Palo Alto, California 94304

ABSTRACT

The hydrolytic degradation of polyester-urethanes (PUR) has been followed by crosslink density measurements of elastomer exposed to moisture for various times at fixed temperatures. Reaction rate constants of the hydrolysis reaction were derived from the measured changes in crosslink density of the elastomer. Studies of hydrolytic degradation of PUR in a propellant formulation containing aluminum were complicated by the reaction of water with aluminum followed by interaction with the PUR.

1. INTRODUCTION

This paper deals with two polyurethanes used in the Polaris system. The first polyurethane is used as a potting compound (PC) to fill a gap between the shrinkage liner and the insulator in second-stage motors. The potting compound prevents flame or hot gases from getting into the area next to the liner. Figure 1 shows schematically the area of interest. Degradation of the potting became so severe that liquefaction of the potting occurred. The dripping of the degraded potting compound onto the propellant resulted in an undesirable situation. The purpose of this study was to determine the cause of potting compound degradation and, if possible, to establish rates of degradation for use in assessing impact on fleet motors.

The second polyurethane material discussed in this paper serves as the binder for Polaris first-stage (F/S) motors. Some motors showed that separation had occurred between the propellant and insulator. Other studies showed that the presence of water in the insulator at the time of casting contributed significantly to the separation. It appeared advisable to

assess the degradation rates of the binder in the propellant for use in assessing motor life.

2. BACKGROUND

Much work has been performed in the study of the response of polyurethanes to humid environment. Since it is obviously impossible to list all of the published papers and documents pertinent to this general topic, only a few papers have been selected for review in this section. We recognize that many good publications in this general area may inadvertently have been overlooked.

Hydrolytic degradation has been studied by Cohen and Van Aartsen. ⁽¹⁾ They investigated the hydrolytic degradation by following the viscosity changes in the solutions of the elastomer exposed to moisture. Other workers ^(2,3,4) have used tensile properties and/or hardness to follow the hydrolytic degradation process. References 5 through 12 are additional publications that provide information on this general subject.

3. EXPERIMENTAL

3.1 MATERIALS

3.1.1 Potting Compound Series

Potting compound (PC). The potting compound was a polyurethane elastomer formulated as given in Table 1. The Multron [®] R-18 (Mobay Chemical Company), a polyethyleneglycol adipate, contains some triol that results in an elastomer with a network structure. The material was prepared by Hercules, Inc.

Table 1
POTTING COMPOUND (PC) COMPOSITION

Component	Weight Percent
Multron R-18 (Polyethyleneglycol adipate)	68.73
L-26 (catalyst) (Lead-2-ethyl hexoate)	0.03
TD-80(a) (Tolylene Diisocyanate)	6.24
DMS (plasticizer) (Dimethyl Sebacate)	25.00

(a) Mixture, by weight, of 80% 807.2, 4-tolylene diisocyanate and 20% 2, 6-tolylene diisocyanate.

Extracted potting compound (PC-X). Extracted potting is cured potting compound (PC) with the dimethyl sebacate plasticizer extracted. The cured potting compound was cut into about 1 g pieces and extracted for 24 hours with solvent grade methyl ethyl ketone in a Soxhlet extractor. The extracted material was dried in a vacuum oven at 50°C and 25 mm Hg for 64 hours. The samples were then placed in a vacuum desiccator at 10^{-3} mm Hg for 24 hours. The weight loss was about 28%.

Capped Multron R-18 resin (R-18C). As part of the model compound study, the hydroxyl groups of the Multron R-18 resin were reacted (capped) with phenyl isocyanate. The capped resin was prepared by reacting Multron R-18 resin with a slight excess of phenyl isocyanate employing lead-2-ethyl-hexoate as a

catalyst in an argon atmosphere. Infrared spectra of the product indicated the absence of free hydroxyl groups. ⁽¹³⁾

3.2 PROPELLANT MATERIAL SERIES

Bulk propellant, ANP 2969-1, was supplied by Aerojet Solid Propulsion Company (ASPC). Neat propellant binders, whose composition was the same as that used in preparing propellant, was prepared by ASPC. Additional binders, prepared with added water, resulted in elastomers with various initial crosslink densities. The main components employed in forming the propellant binder are given in Table 2. Ferric acetyl acetate is used as the catalyst to promote the methane reaction. The propellant differs from the binder primarily in that it contains ammonium perchlorate, powdered aluminum, and a higher concentration of plasticizer.

Table 2
COMPONENTS OF NEAT
PROPELLANT BINDER

Component
3-nitro-1, 5-pentane diisocyanate
neo-pentyl glycolazolate (NPGA)
1,1,1, tris (hydroxy- methyl) propane (TMP)
poly 1, 4 (butylene) glycol (LD-124) or "PBG")
bis (2,2-dinitropropyl) acetal/formal (50:50) (BDNPA/BDNPF)(a)

(a) The BDNPA/BDNPF is the plasticizer used in the binder.

3.3 SOLVENTS AND REAGENTS

Acetone commercial grade was employed as the swelling solvent. Other solvents were either purified by the method of Wiberg⁽¹⁴⁾ or were analytical reagent grade.

Aqueous standard acid and base were made with Acculate[®] concentrates and were standardized with primary standard potassium acid phthalate. Ethanolic acid and base were prepared from reagent grade materials and standardized by the same method.

Perchloric acid in glacial acetic acid was prepared by standard techniques and standardized with primary potassium acid phthalate in glacial acetic acid using a Beckman pH meter for endpoint determination. Electrodes (glass-calomel) used for these titrations were first equilibrated in glacial acetic acid for several days before use in order to minimize drift.

Stabilized Karl Fisher reagent, standardized by accepted method,⁽¹⁵⁾ was used in determining the water content of various materials.

3.4 SAMPLE PREPARATION AND EXPOSURE FOR HYDROLYSIS

Propellant samples were cut into cylinders 9.5-mm diameter by about 16 mm long. All other samples were cut in cubes about 1 cm³. Most samples were weighed and then placed in small labeled polypropylene cups. Samples exposed at 100°C, or higher, were contained in sealed test tubes. Desired humidities were obtained from use of saturated salt solutions.⁽¹⁵⁾

3.5 DETERMINATION OF CROSSLINK DENSITIES^(17,18,19,20)

Crosslink densities were derived from: (1) stress-strain response in compression of swollen samples, (2) volume fraction of elastomer in swollen gel, or (3) stress-strain response of unswollen samples.

Propellant samples required at least 20 days to reach equilibrium with the swelling solvent; the long time was

required to remove the ammonium perchlorate. Non-filled samples generally were equilibrated with solvent in less than a week. Imbibed solvent was removed by air drying overnight followed by an additional 16 hours of drying at 50°C in vacuo.

The solvent-polymer interaction coefficient,^(19,21) required for calculating the crosslink density from swelling data, was assumed to have a value of 0.43 for the potting compound. This coefficient was determined by two methods for the Polaris propellant (ANP 2969-1):

- (1) Equating the crosslink density of the binder from the propellant sample determined from stress-strain data on swollen samples with the swollen characteristics of the binder as described by the Flory equation⁽¹⁹⁾
- (2) Examining the solution properties⁽²¹⁾ of the binder of the propellant. The vapor pressure of the swelling solvent is monitored as the volume fraction of polymer is changed.

A value of 0.453 ± 0.012 was obtained for the interaction coefficient of acetone-binder from ANP 2969-1 propellant by the first method. The value of the coefficient as determined from the solution properties was consistent with a value of 0.45, but showed a larger standard deviation.

3.6 HYDROCHLORIC ACID TREATMENT

Propellant specimens were swollen in acetone to their equilibrium value and placed for 60 minutes at room temperature in freshly prepared HCl-acetone solution (5 cc conc. HCl + 100 cc acetone), and were then immersed in clean acetone containing some CaCO₃.

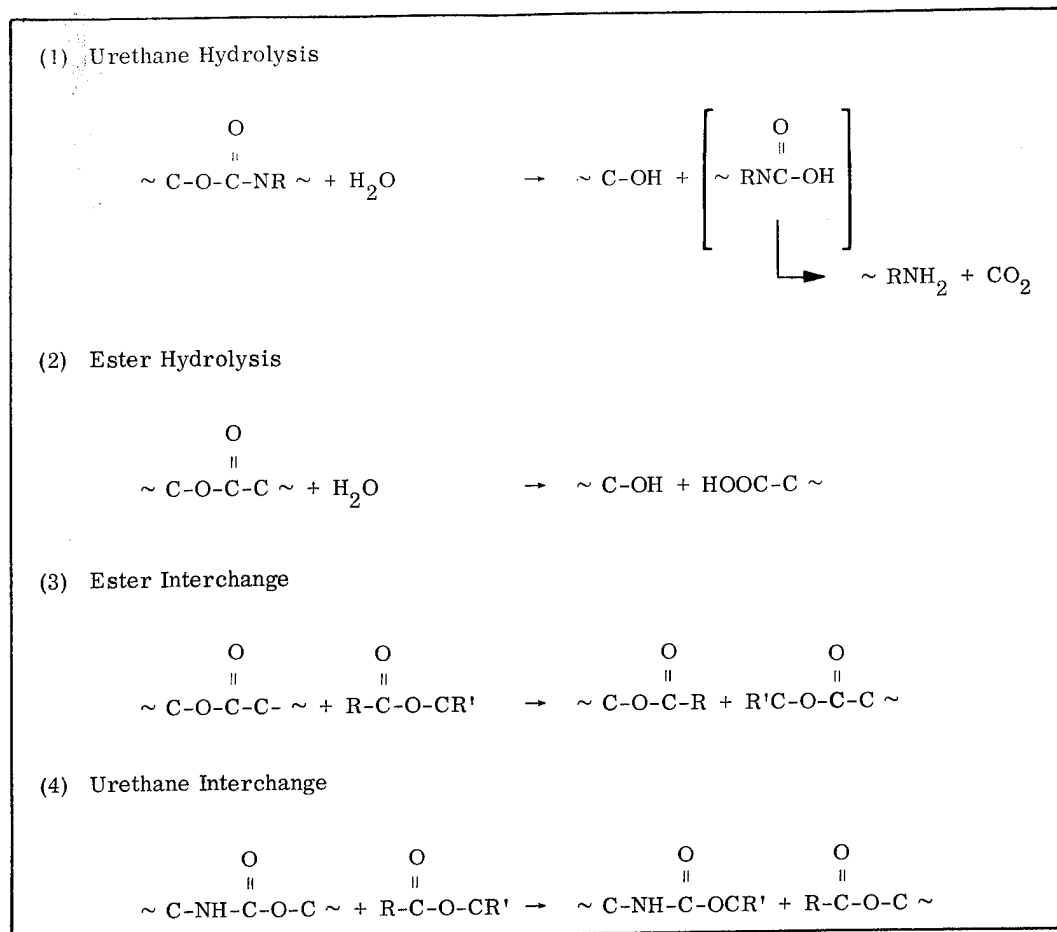
4. RESULTS AND DISCUSSION

4.1 GENERAL

Although studied by many investigators, the chemistry of polyurethanes has been directed mainly toward the reaction of its formation.^(20,22-26) Some information relating to the degradation process has been touched on in a previous section.

Table 3 lists the most probable reactions that may occur upon exposure of the polyester-urethane elastomer to moisture.

Table 3
POSSIBLE REACTIONS RESULTING IN DEGRADATION OF POLYESTER URETHANES



We hope to cover each of these reactions and to show their contribution to the hydrolytic degradation process. Other functional groups may be present in the elastomer, such as ureas, allophanates, and biurets, but would be expected to be in low concentration and as such are not considered to contribute to the chemistry of hydrolytic degradation. Consequently, they will not be considered in this paper.

4.2 KINETICS OF DEGRADATION

4.2.1 Potting Compound Degradation

Table 4 lists the specific first-order rate constants derived from changes in crosslink density as a function

of exposure time at various temperatures for the potting compounds. Relative humidity in these tests was 100%.

A typical set of data are shown graphically in Figure 2. In the figure it can be seen that the reaction shows good first-order kinetics over an order-of-magnitude change in the crosslink density.

The calculated activation energy for the hydrolytic degradation process was about 20 kcal/mol in good agreement with previously reported values in the literature.

Thermal degradation rates for the potting compound and the extracted potting compound were also determined.

Table 4
FIRST-ORDER RATE CONSTANTS AND ACTIVATION ENERGIES FOR POTTING
COMPOUND DEGRADATION^(a)

System	Rate Constant, k ^(b) (sec ⁻¹)		Activation Energy, ΔE^\ddagger (kcal/mol)
	100°C	125°C	
PC + Benzene	8.7×10^{-7}	3.9×10^{-5}	44.8
PC-X + Benzene	8.6×10^{-7}	3.8×10^{-5}	39.6
PC + Water	1.4×10^{-6}	3.9×10^{-5}	19.3
PC-X + Water	1.8×10^{-5}	9.2×10^{-5}	21.5

(a) From crosslink density versus time plots.

(b) Rates are based on the initial part of the reaction.

The PC and PC-X were placed in a nonreactive solvent (benzene) and exposed to elevated temperatures. The first-order rates were derived from the observed changes in crosslink density. The rate of degradation was appreciably slower at 100°C. At 125°C, the rate difference was only about 2.5. A plot of the PC-benzene data is also included in Figure 2. The activation energy for the thermal process was calculated as 44.8 kcal/mol.

To assess the importance of the ester interchange reaction between dimethyl sebacate (DMS) and potting compound, the potting compound was heated at elevated temperature in an excess of DMS. The degradation rates were found to be essentially the same as for the thermal process with a similar value for the activation energy. It is quite possible that the two processes, thermal and ester interchange, are the same.

In addition, the appearance of the carboxylic acid group (RCOOH) from cleavage of the ester group and the formation of amine (RNH₂) functional group was monitored as a function of time under hydrolytic degradation conditions. The fractions of ester groups and methane groups cleaved as a function of time at 125°C are plotted, respectively, in Figures 3 and 4. In Figure 3, the total amount of ester groups formed was monitored not only in the gel portion. Formation of RCOOH was followed by titration of acetone swollen samples with an ethanolic base. The fraction of ester groups formed is identical to that for the potting compound, the extracted potting compound, and the capped R-18.

The latter compound is the base resin Multron R-18[®] with the hydroxyl groups capped. Similar results were obtained at 75° and 100°C. The activation energy for the hydrolytic process was 17 kcal/mol based on the formation of RCOOH at a degree of reaction of 10%. The activation energy was calculated from a plot of logarithm of reciprocal times to reach 10% reaction versus the reciprocal temperature.

The formation of amine in the potting compound, the extracted potting compound, and the capped base resin was followed by titration of the sample with perchloric acid in acetic acid after swelling in acetone. PC and PC-X exhibit a degree of hydrolysis of about 5 to 6% in 50 to 60 hours of exposure to 100% relative humidity and are then leveled off. The R-18C shows only 2% degradation. In the calculations, it was assumed that the isocyanate formed only urethane groups. Close inspection of Figure 4 shows that there appears to be a very rapid generation of the RNH₂ at short exposure times followed by a slow rate of RNH₂ generation. The slow generation of RNH₂ is probably due to hydrolytic cleavage of the urethane group.⁽²⁶⁾ The reason for the rapid formation of RNH₂ is not clear from the present work. Similar observation, i.e., the rapid formation of RNH₂ at short times followed by slow formation of RNH₂, was also observed at 75° and 100°C.

At 125°C, the calculated half-life for the hydrolytic degradation of the polyurethane, as determined from changes in the crosslink density, is only 2.1 hours. In this time interval, however, only a very small fraction

of the ester or urethane groups is hydrolyzed. In other words, a small degree of hydrolysis can lead to gross changes in the properties of the elastomer.

4.2.2 Polaris ANP 2969-1 Propellant Degradation

Neat propellant binder. Propellant binder having the same composition as that used in formulating the binder for propellant was exposed to 100% relative humidity and the crosslink density determined as a function of exposure time. Table 5 gives the derived hydrolysis rate constants.

The hydrolysis rate constants and the activation energy were found to be independent of the initial crosslink density. The initial crosslink density was controlled by addition of water and/or variation of the NCO/OH ratio.

Propellant ANP 2969-1 degradation. Samples of propellant were exposed to temperature in the range 40° to 80°C and relative humidities of 30 to 75%. Table 6 shows a set of typical results. Two things are apparent:

Table 5
HYDROLYSIS RATE CONSTANTS FOR NEAT POLYURETHANE BINDER EXPOSED TO
100% RELATIVE HUMIDITY

Formulation No.	Initial Crosslinking Density (moles/cm ³ × 10 ⁵) (a)	25°C (b) (sec ⁻¹ × 10 ⁹)	Specific Rate Constants			Activation Energy, ΔE [‡] (c) (kcal/mol)
			75°C (sec ⁻¹ × 10 ⁷)	100°C (sec ⁻¹ × 10 ⁶)	125°C (sec ⁻¹ × 10 ⁶)	
A-3	45.0	5.3 (d)	—	2.33	11.4	18.7
B-3	34.5	4.0 (e)	—	2.50	11.3	17.8
A-2	22.0	—	—	2.08	9.14	17.5
C-3	16.0	—	—	2.49	11.2	17.7
B-2	14.0	—	16.4	2.33	9.50	16.7
D-3	7.8	—	—	2.56	9.92	16.0
B-1	2.22	—	2.83	1.81	13.8	23.9

(a) Values derived at $t = 0$ from extrapolation of kinetic data.

(b) Specific rate constant at 25°C calculated to be $6.0 \times 10^{-9} \text{ sec}^{-1}$ from an average of first five values and a E^{\ddagger} of 17.6 kcal/mol.

(c) Activation energies calculated based on elevated temperature data.

(d) Samples stored for 1-1/2 yrs at 53% RH, corrected to 100% RH by multiplying observed value by 100/53.

(e) Sample stored for 1-1/2 yrs at 90% RH, corrected to 100% RH by multiplying by 100/90.

The activation energy for most of the runs is about 18 kcal/mol, in good agreement with data on the potting compound. It is instructive to note that rate constants for the hydrolysis of the binder were also obtained at 25°C for two of the samples.

Since the rate constants measured at 25°C were for samples exposed to lower humidities, the rates were corrected to 100% relative humidity. An Arrhenius plot of the data is shown in Figure 5. One of the reported rate constants appears to be unduly high; in addition, this run gave an activation energy which was also slightly higher than the other observed activation energies.

- (1) The value of the calculated rate constant gyrates up and down.
- (2) The gel content for the binder gives value greater than 1.0.

In extracting the propellant samples, everything is removed except the binder gel and the aluminum. It thus appeared that the aluminum was reacting with moisture and that its subsequent reaction with binder gel gives the observed results. That the aluminum was interacting with the gel was demonstrated when efforts were made to reswell samples of propellant and neat binder. Samples of propellant and neat binder, which had not been exposed to temperature and relative humidity,

Table 6
KINETIC DATA FOR REACTION OF
PROPELLANT AT 80°C AND 75%
RELATIVE HUMIDITY

Sample No.	Exposure Time (days)	Gel Fraction, g	Crosslink Density $v_e/v \times 10^6$ (moles/cm ³)
A	0	0.790	15.2
41	13	0.951	26.0
197N	14	0.668	46.7
42	23	1.051	32.1
196N	24	0.565	50.7
195N	70	0.874	63.1
43	71	0.880	18.7
44	100	1.821	77.3
194N	100	0.527	55.7
45	122	2.191	103.6
193N	122	0.807	62.1
46	140	2.472	104.7
47	160	1.999	85.9
70	179	0.933	19.4
48	199	0.249	100.2

were swelled, dried, and then reswelled. In all cases, as shown in Table 7, the propellant showed an increased crosslink density as calculated from the swelling data (up to three times as large), whereas the crosslink density for the neat binders was invariant with this treatment.

Thus, the increased gel and gyrating crosslink data for the hydrolysis runs appeared to be due to an interaction between the aluminum and the propellant binder. Qualitative experiments showed that HCl treatment would cause reversion of the aluminum-binder interaction. The procedures were therefore quantitized.

Propellant samples that had been dried were reswollen in acetone and then treated with HCl for various times up to 90 minutes. The crosslink density was then determined. As Table 7 shows, treatment with HCl resulted in reversion of the material to one with a crosslink density close to that measured initially.

Table 7
CHANGE IN CROSSLINK DENSITY OF DRIED
PROPELLANT SAMPLES EXPOSED TO
HCl TREATMENT

Sample	HCl Treatment Time (min)	Gel Fraction, g			Crosslink Density $v_e/v \times 10^6$ (moles/cm ³)		
		Initial	After Drying	After HCl Treatment (a)	Initial	After Drying	After HCl Treatment
A	30	0.756	0.716	(0.716)	13.2	28.3	17.1
AA	50	0.778	0.713	(0.713)	15.3	23.6	15.1
B	60	0.799	0.702	(0.702)	15.1	21.5	15.2
BB	70	0.771	0.645	(0.645)	15.0	16.7	12.0
C	90	0.788	0.706	(0.706)	14.8	21.5	16.8

(a) Assumed the same as after drying.

Several other tests were applied to ensure, if possible, applicability of the HCl treatment to propellant samples exposed to moisture at elevated temperatures.

Hydrolysis of the neat propellant binder was fairly rapid, giving a first-order plot of crosslink density as a function of time. The rate constant was $1.64 \times 10^{-2} \text{ min}^{-1}$, which corresponds to a half-life of 42 minutes. A typical graph of the data is given in Figure 6. Propellant samples were treated with HCl for up to 150 minutes, and the crosslink densities were determined as a function of HCl treatment time. The results are given in Table 8. As the table indicates, at times up to 60 minutes, the propellant samples do not show appreciable change in the crosslink density. This treatment was applied to a limited number of the hydrolysis propellant runs.

Figure 7 gives the result for a propellant exposed to moisture at elevated temperature followed by the HCl treatment. The decimal rate constants are given in Table 9. An activation energy of 19 kcal/mol is obtained in good agreement with the activation energy observed for the neat binder. The data were extrapolated to 25°C and 75% relative humidity using an activation energy of 17.6 kcal/mol for both neat binder and propellant hydrolysis reaction. To obtain the 75% relative humidity rate for the neat binder, the 100% relative

Table 8
CHANGE IN CROSSLINK DENSITY OF NONDRIED
PROPELLANT SAMPLES EXPOSED TO
HCl TREATMENT

Sample	HCl Treatment Time (min)	Gel Fraction, g After HCl Treatment	Crosslink Density $v_e/v \times 10^6$ After HCl Treatment (moles/cm ³)
(a)	0	0.782 ± 0.010	14.7
J	20	0.767	16.5
K	20	0.779	17.2
L	30	0.767	15.0
R	40	0.742	13.4
S	40	0.751	15.3
T	50	0.726	14.3
U	60	0.682	12.7
V	70	0.667	10.7
W	70	0.683	10.5
X	90	0.715	10.6
Y	120	0.587	7.6

(a) Average of all samples listed here, before HCl treatment.

humidity value of 25°C was multiplied by 75/100. The rate constants for the neat binder and the propellant are nearly the same with a calculated half-life of about 5.0 years.

Table 9
HYDROLYSIS RATE CONSTANTS FOR
PROPELLANT AND PROPELLANT BINDER

Material	Rate Constant 25°C/75% RH (sec ⁻¹)	Activation Energy, E [‡] (kcal/mol)
Binder	4.5×10^{-9}	17.6
Propellant	9.1×10^{-9}	(19.0)

Whether this technique can be further refined to overcome the difficulties encountered in this study is not known, but certainly the results on the control samples were convincing. It appears that other phenomena, or reactions, occurring in the samples under these exposure conditions must be characterized in greater detail

before a successful method can be developed for following crosslink density changes in elastomeric network structures in propellant samples, particularly those containing solids sensitive to moistures.

5. FIELD SERVICE LIFE PREDICTIONS

It must be remembered that simulating field behavior in the laboratory is very difficult. This difficulty stems from the fact that although the fundamental process is defined for some observed changes – in our experience, for example, the cleavage of ester group by water – it is difficult to define the total environment in the system. Other processes are generally occurring in these systems, such as migration of material into and from the material of interest. Moisture levels are difficult to assess. The potting compound degradation results primarily from moisture in the liner (see Figure 1) that diffuses into the potting compound. In addition, a zinc moiety (from ZnO used as an aid in curing the liner) also migrates into the potting compound that may act as a catalyst for the hydrolytic degradation process. Our limited studies have shown that addition of zinc acetate results in enhancement of the hydrolytic degradation process.

Another aspect that must be considered in using laboratory results to assess service life of materials is the extent of the degradation that must occur to result in a nonserviceable material – 1%, 10%, and 99%. To some degree, it depends on the system requirements for that part. These aspects, as they apply to two polyurethanes discussed above, are briefly considered in the following paragraphs.

Using the kinetic data for degradation of the potting compound, a half-life of four months at 100% relative humidity and 25°C is computed. About 28 months are required for 99% degradation. Observation of aging motors indicates that flow of degraded potting compound was noted as early as 18 months and that most of the motors show flow of potting around 3 months.

Two modifications were made in the motors to provide the potting with longer service life. They were: (1) increased level of NCO/OH and (2) additional barrier coating applied to the liner to decrease transport of moisture into the potting compound. These modifications were shown to decrease the degradation of the potting compound by a factor of four. For this modified family of motors, the service life should be extended to approximately 100 months. The maximum age of these motors is about 72 months. To date, none of these motors has shown any signs of flow of potting degradation.

The kinetic data for the ANP 2969-1 propellant gives a calculated half-life for the binder hydrolysis of about 60 months at 25°C and 75% relative humidity. Here we have no firm knowledge of the extent of the degradation that must occur before the propellant properties are no longer adequate. Part of the difficulty in this case is that we are dealing with a filled system and that the properties are governed not only by the binder but also by the interaction of binder with the filler.

6. REFERENCES

1. J. L. Cohen and J. J. Van Aartsen, "The Hydrolytic Degradation of Polyurethanes," International Symposium on Macromolecules, Helsinki, 1972, Part 3, O. Harva and C. G. Overberger, Eds., pp. 1325-1338, J. Polymer Sci.: Symposium No. 42, 1973
2. Performance of Urethane Vulcanizates in Environments of High Humidity, by F. B. Testroet, Rock Island Arsenal, Report No. 63-2808, 30 Aug 1963
3. Hydrolytic Stability of Polyurethane and Polyacrylate Elastomers in Humid Environments, by F. W. Nieske and F. H. Gahimer, Naval Avionics Facility, Indianapolis, Ind., TR-1772, 27 Feb 1969
4. Hydrolytic Stability of Encapsulants, by F. W. Nieske and F. H. Gahimer, Naval Avionics Facility, Indianapolis, Ind., TR-1778, 1972
5. M. L. Matuszak, "Thermal Degradation of Hydrolysis of Linear Polyurethanes and Model Carbamates," Ph.D. thesis, University of Detroit, 1972
6. Thermoplastic Polyurethane Hydrolysis Stability, by C. S. Schollenberger and F. D. Stewart, B. F. Goodrich Co. Research Center, 19 Aug 1970
7. C. H. Pondracek, "Hydrolytic Stability of Insulating Materials," 31st Annual SPE Technical Conference, Montreal, May 1972, pp. 413-417
8. F. H. Gahimer, "Hydrolytic Stability of Electrical Insulation Materials," 31st Annual SPE Technical Conference, Montreal, May 1973, pp. 403-407
9. Reversion of Polyurethane and Polyacrylate Rubber Encapsulating Compounds in Humid Environments and Development of a Standard Reversion Test, by F. W. Nieske and F. H. Gahimer, Naval Avionics Facility, Indianapolis, Ind., TR-1201, 15 Apr 1968
10. G. L. Welch, "Estimating Service Life of Two Specific Potting Compounds Using Accelerated Hydrolytic Reversion of High Temperatures and High Humidities," National SAMPE Technical Conference (Dallas, Texas), Aerospace Adhesives and Elastomers, 6-8 Oct 1970, Vol. 2, pp. 649-662
11. G. Magnus, R. Dunleavy, and F. Critchfield, "Stability of Urethane Elastomers in Water, Dry Air, and Moist Air Environments," Rubber Chemistry and Technology, Symposium on Elastomers for Unusual Environmental Conditions, Part 2, Vol. 39, No. 4, Sep 1966, pp. 1328-1337
12. Z. Ossefort and F. Testroet, "Hydrolytic Stability of Urethane Elastomers," ibid., pp. 1308-1327
13. L. T. Bellamy, The Infra-Red Spectra of Complex Molecules, New York, John Wiley and Sons, Inc., 1959

14. K. B. Wiberg, Laboratory Techniques of Organic Chemistry, New York, McGraw-Hill Co., Inc., 1960
15. A. Vogel, Elementary Practical Organic Chemistry, Part III, London, Longmans, Green and Co., 1958
16. Handbook of Chemistry and Physics, 44th Edition, Chemical Rubber Publishing Co., 1962-1963, pp. 2595-2596
17. Study of Characteristics and Standard Variability of Composite Solid Propellants, Final Report, E26-69, Thiokol Chemical Corporation, Elkton Division, Ellston, Maryland, 6 Feb 1969
18. R. F. Fedors and R. F. Landel, Determination of Network Density of Filled Composite From Stress-Strain Measurements in the Swollen State, JPL Space Programs Summary 37-43, Vol. IV
19. P. J. Flory, Principles of Polymer Chemistry, Ithaca, New York, Cornell University Press, 1953
20. S. J. Chlystek, Research on Polymeric Materials Suitable for Use as Binders for Solid Propellants, Armstrong Cork Co., ASD Technical Report 61-407, Nov 1961
21. J. H. Hildebrand and R. L. Scott, The Solubility of Nonelectrolytes, New York City, Dover Publications, Inc., 1964
22. E. J. Mastrolia, K. W. Bills, and C. B. Frost, Advanced Technology Studies Under Production Support Program, Report BSD-TR-66-28, Vol. 1, Part 3, Aerojet-General Corp.
23. M. Morton and M. Ohta, Degradation Studies on Condensation Polymers, 1st Quarterly Report, University of Akron, 1958
24. M. Morton and M. Ohta, Degradation Studies on Condensation Polymers, 4th Quarterly Report, University of Akron, 1958
25. M. Morton and M. Ohta, Degradation Studies on Condensation Polymers, 5th Quarterly Report, University of Akron, 1958
26. J. H. Saunders and K. C. Frisch, Polyurethanes: Chemistry and Technology, I. Chemistry, New York, Interscience Publishers, Chapters III and IV, 1962

ACKNOWLEDGMENT

We should like to express our thanks to Hercules, Inc. and to Aerojet Solid Propulsion Co. and many members of their staff for supplying materials required for the study and for many stimulating technical discussions relative to the work presented in this paper.

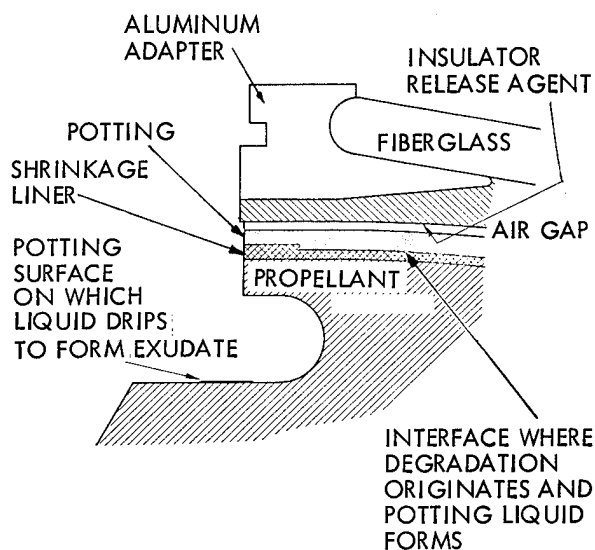


FIGURE 1. SCHEMATIC DIAGRAM OF MOTOR CONFIGURATION SHOWING LOCATION OF POTTING COMPOUND

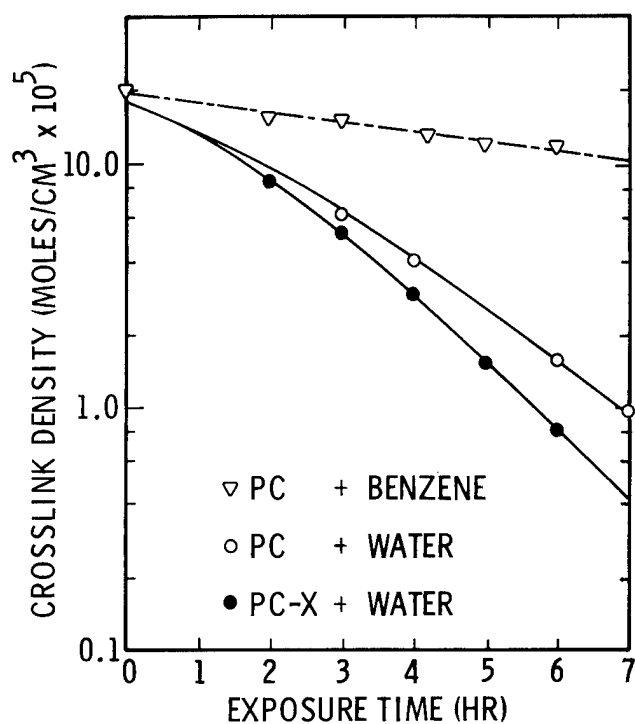


FIGURE 2. FIRST-ORDER PLOT OF CHANGE OF CROSSLINK DENSITY WITH TIME FOR PC AND PC-X REACTED WITH WATER AT 125°C

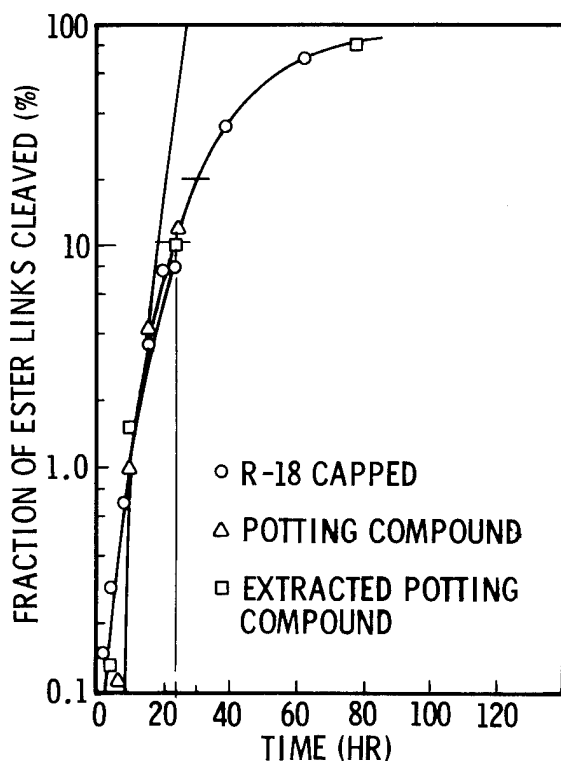


FIGURE 3. HYDROLYSIS OF ESTER LINKS IN VARIOUS MATERIALS AT 125°C

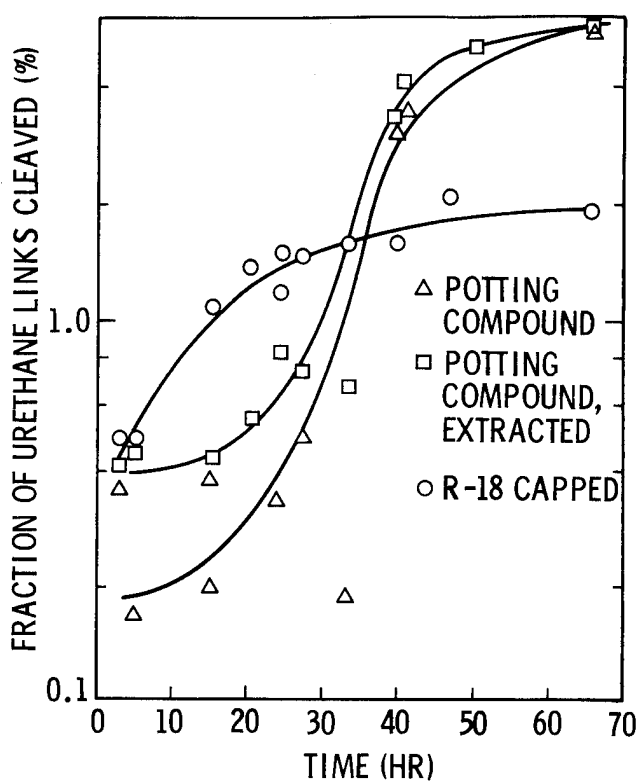


FIGURE 4. HYDROLYSIS OF URETHANE LINKS IN VARIOUS MATERIALS AT 125°C

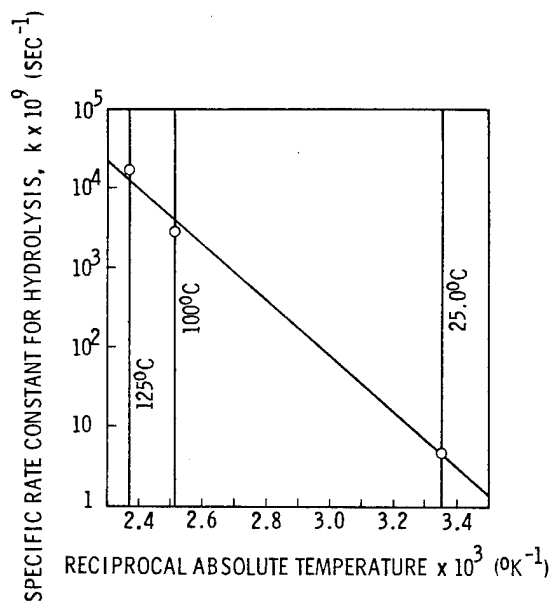


FIGURE 5. ARRHENIUS PLOT OF HYDROLYSIS RATE CONSTANTS FOR NEAT PROPELLANT BINDER

BIOGRAPHIES

L. B. JENSEN received a B.A. in Chemistry from California State University, San Jose, in 1964. Prior to joining Lockheed Missiles & Space Company, Inc. in 1964, he served with Bio-Rad Laboratories in Richmond, California. Mr. Jensen is currently a scientist with the Analytical Chemistry Laboratory of the Lockheed Palo Alto Research Laboratory, where he has worked extensively in the field of materials compatibility. Much of this work has dealt with the kinetics of degradation of polymeric materials. He is currently involved with the degradation of polymeric materials subjected to thermal-vacuum environment.

H. P. MARSHALL, a member of the Lockheed Material Science Laboratory, is the principal investigator in basic and applied physical and organic chemistry and chemical kinetics directed toward understanding the behavior of nonmetallic materials in all types of environments. Much of his recent work has been devoted to investigating the chemical changes induced in propellants upon long-term aging and attempting to associate these changes with propellant physical properties.

Prior to coming to Lockheed, Dr. Marshall spent three years at Stanford Research Institute directing work in polymer chemistry. He had been previously with Celanese Corporation of America, where he worked in vinyl and condensation polymerization. The work at Celanese resulted in three patents.

He is a member of the Joint Motor Life Study Coordination Group, a United States/United Kingdom Polaris team that is reviewing scientific data for the purpose of assessing long-term aging characteristics of the Polaris motor system. In this work, chemical degradation of the polymeric system, as well as gas formation from the propellant binder, has been studied.

Dr. Marshall holds a B.S. in Chemistry from Penn State University in 1947, and a Ph.D. in Physical Organic Chemistry from UCLA in 1952. His 15 technical publications relate to the structure and thermal decomposition of nitro compounds.

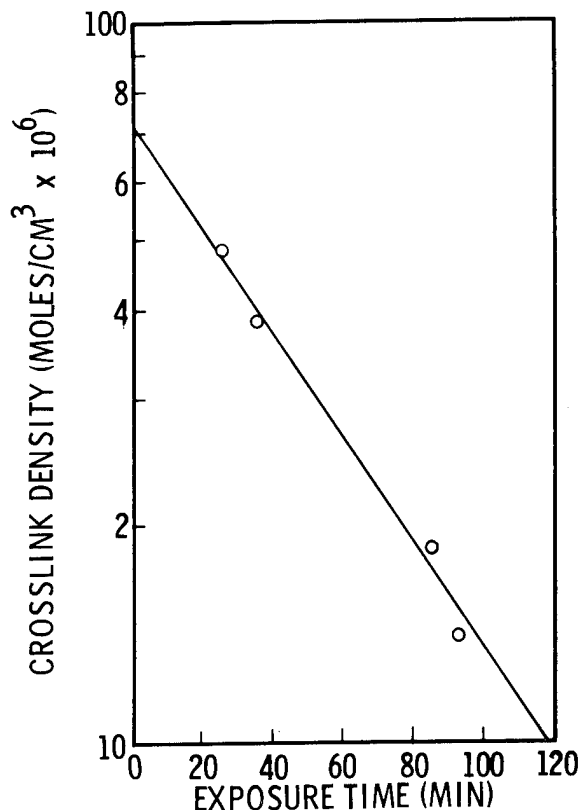


FIGURE 6. CHANGE OF CROSSLINK DENSITY OF NEAT BINDER VERSUS EXPOSURE TIME TO HCl-ACETONE SOLVENT; FIRST-ORDER RATE PLOT

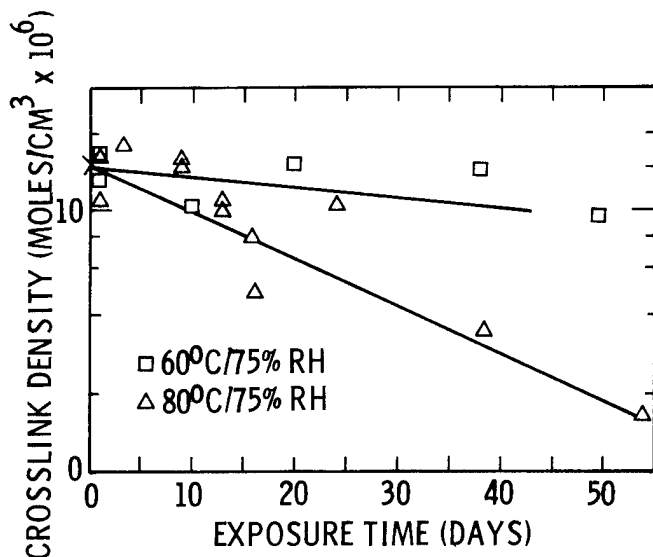


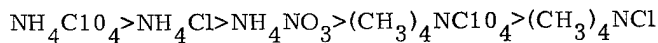
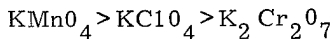
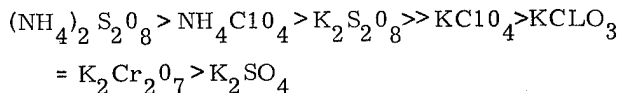
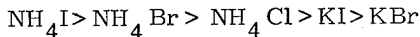
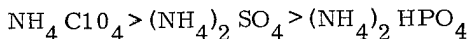
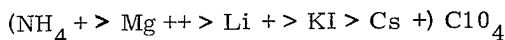
FIGURE 7. CROSSLINK DENSITY VERSUS ENVIRONMENT EXPOSURE TIME AFTER HCl TREATMENT

EFFECT OF ADDITIVES ON POLYACETALS BY TGA

Albert S. Tompa and David M. French

Naval Ordnance Laboratory
Naval Ordnance Station
Indian Head, Md.

An extensive isothermal and dynamic thermogravimetric study of the effect of additives on the thermal decomposition of polyacetals (Delrin, Celcon) has shown that the more acid the character of the cation and anion, the more effective they are in decreasing the thermal stability of polyacetals. However, there is a limitation on the acidity of the cation because if the acidity approaches that of the hydrogen ion as in HCl, then a more thermally stable polymer is produced. Otherwise, it was found that keeping the anion constant, the order with cations increases as you go up a group and across a period in the Periodic Table; keeping the cation constant, the order with anions increases as you go down a group and across a period; with oxidizing agents, keeping the cation constant the order increases with the oxidation potential. Oxyanions are more effective because the presence of additional oxygen atoms increased its acid strength. Peroxyanions are still more effective because when heated they liberate free radicals and oxygen. Methyl substituted cations are less effective because methyl groups are base strengthening. These conclusions are based on the following observations on the effect of ions on polyacetal degradation:



The effect of 11 organic additives yielding free radicals of carbon, nitrogen, oxygen, sulfur, and halogen on the thermal degradation of Delrin was investigated. The more effective additives had exotherms in the melting region of Delrin. N-bromosuccinimide was the most effective and tetranmethyl thiuram disulfide the least.

Our studies indicate that TG offers a novel method for distinguishing the relative acid strength of many inorganic compounds by the single measurement of the relative effect the compound has on lowering the thermal stability of Delrin in an inert atmosphere.

THE COMPATIBILITY OF PBX-9404 AND DELRIN

Donald J. Gould, Thomas M. Massis and E. A. Kjeldgaard
Initiating & Pyrotechnic Component Division 2515
Sandia Laboratories
Albuquerque, New Mexico 87115

ABSTRACT

PBX-9404 (94% HMX, 3% nitrocellulose, 3% tris- β -chloroethyl phosphate) slowly decomposes with the evolution of gases such as NO, NO₂ and N₂O from the nitrocellulose. It has been determined that these gases diffused to a Delrin (polyoxymethylene) part and initiated stress corrosion and decomposition reactions. Experiments utilizing atmospheres containing small partial pressures of various oxides of nitrogen plus those evolved through accelerated aging of PBX-9404 in the presence of Delrin parts showed that these gases were responsible for starting an irreversible depolymerization reaction of the Delrin.

1. INTRODUCTION

In this paper an apparent incompatibility between an injection molded Delrin^{*} part and PBX-9404^{**} will be discussed. Based on the hypothesis that the Delrin was corroded by oxides of nitrogen, which were generated by aging PBX-9404,⁽¹⁾ experiments were designed to determine which of the three oxides of nitrogen evolved (N₂O, NO and NO₂) was the corrosive agent. In addition determination of the roles of oxygen and temperature was desired.

2. BACKGROUND

Delrin is a trade name for the acetal terminated homopolymer of polyoxymethylene. The plastic is highly crystalline (approximately 85%) and has an average molecular weight of 40,000.⁽²⁾ Common manufacturing practice is to include carbon black (approximately 2 wt %) as an ultraviolet screen⁽³⁾ since the plastic is susceptible to photooxidation.⁽⁴⁾ Injection molding of polyoxymethylene usually results in three distinct crystalline regions.⁽⁵⁾ The first region (several mils in depth)

* Delrin is an E. I. DuPont trade name for the acetal terminated homopolymer of polyoxymethylene.

** The explosive PBX-9404 is 94% HMX, 3% nitrocellulose, 3% tris (chloroethyl) phosphate, and 0.1% diphenylamine.

consists of folded-chain lamellae which have bidirectional orientation; the second region (10's of mils depth) consists of lamellae with unidirectional orientation; the third region, which is the interior of the molded piece, contains spherulites which are randomly oriented. The three crystalline regions are a result of the cooling of the part. It is not difficult to conceive of variations in crystalline structure from part to part, let alone batch-to-batch.

Thermal oxidation of the acetal homopolymer is well documented.^(4,6) The degradation does not start at the chain ends but rather at some place along the chain (chain scission). The chains then unzip and release formaldehyde, as well as carbon dioxide, water, and hydrogen. The rate of degradation at a given temperature is accelerated by ultraviolet light and results in the same degradation products. The mechanism is thought to be free radical oxidation, but the exact mechanism has not been determined. A peroxide formation may be involved in the free radical oxidation, but such compounds have not been detected.^(4,6)

Reaction of Delrin with nitrogen dioxide (NO_2) gas in a kinetic gas stream above 150°C has yielded first-order reaction rates with respect to Delrin.⁽⁷⁾ The degradation takes place in molten plastic and proceeds by hydrolysis of the acetal end groups. These kinetics apparently do not apply to a static system below 150°C , such as the case discussed in this paper.

3. EXAMINATION OF CORRODED GEARS

Several gear trains were examined by optical and scanning electron microscopy (SEM). Corrosion was evident in various degrees on all gears. Figures 1 through 3 show a

worst case where the gear teeth are nearly gone. The corrosion has progressed deep into the gear, leaving no trace of the "skin" seen in other gears. Note the tunneling and absence of spherulites. Figures 4 through 7 show a gear with much less damage. The effects of stress corrosion are very evident, and the optical photomicrograph shows very clearly the "skin" effect. Figures 8 through 10 show another gear which has been severely damaged. A powdery residue was found which, when examined, showed numerous spherulites in a fibrous matrix. These three gears cover the degrees of damage found in the corroded gear trains. All these gears were filled with carbon black. Figures 11 and 12 show an unfilled (white) Delrin sleeve found in a gear train from which one of the more severely damaged filled gears had been removed. The damage is extensive but not nearly as bad as in the associated gear. Figures 13 and 14 show an undamaged gear used as a reference. These data were used as models against which compatibility experiments were judged when determining cause and effect.

4. EXPLANATION OF OBSERVATIONS OF CORRODED GEARS

Visible evidence of corrosion conforms very well with what would be expected in view of the multilayer crystalline nature of the plastic. The highly ordered surface surrounding the disordered interior of the gear leaves a highly stressed surface which readily undergoes stress corrosion. The pattern of the cracks corresponds nicely to the expected stress patterns in a molded gear. Once the interior, less ordered part of the gear is exposed to the corroding environment, general decomposition increases; this results in tunneling and decomposition of

the matrix surrounding the spherulites. The spherulites, as stated above, result from uneven cooling of the injection molded part. Thus, some parts may have substantially more spherulites than others, depending on thermal gradients which occur during crystallization of the plastic. The spherulites themselves have a minimum free surface energy as a result of their shape and are much less susceptible to degradation than is the corresponding fibrous matrix.

The fact that the white unfilled sleeve did not show the severity of damage as a corresponding filled gear from the same unit can be explained in one of two ways. First, the carbon in the filled gear could absorb the corroding agent; this would result in the most severe decomposition. Second, the carbon in the filled gears could add to the internal stress and decrease the amount of surface "skin" of highly ordered crystalline plastic. This condition would make the filled gears more susceptible to stress corrosion and subsequent exposure of the interior of the gear to the corroding agent. The unfilled sleeve would be attacked in a similar manner, but the stress corrosion would be less severe and the decomposition would have to progress through a thicker "skin" before reaching the more susceptible interior--a slower process under similar conditions. In view of the results of experiments to be discussed, the second explanation seems more likely.

5. EXPERIMENT DESIGN

The initial experiment was designed to determine the effect of both the presence and amount of dry NO_2 gas on Delrin gears which contained 2 wt % carbon filler. Table I gives the general experiment

summary. All the glass ampoules were sealed in order to maintain a constant gaseous atmosphere. When the ampoules were opened, a weight loss study was initiated. All samples in the weight loss study were maintained in their original thermal environment without the presence of NO_2 gas (Table II).

Isothermal gravimetric analysis (iso-TGA) data of PBX-9404 at varying temperatures and the effect of the decomposition products of PBX-9404 on Delrin in terms of weight loss of the Delrin sample are compiled in Table IV. A second set of ampoules was constructed and filled with various oxides of nitrogen and weighed pieces of filled and unfilled Delrin gears. This experiment was designed as a static test of the long term compatibility of Delrin with the nitrogen oxides. The effects of oxygen and temperature were also studied during this experiment. The experiment and observations are summarized in Table V. The results of qualitative compatibility tests of Delrin with other materials likely to be presented in the component are compiled in Table VI.

6. EXPERIMENTAL OBSERVATIONS

Examination of Table I shows that both increased temperature and increased concentration of NO_2 gas accelerate the decomposition of Delrin. Table II indicates that decomposition, once initiated by NO_2 gas, continues after the NO_2 environment has been removed. Table III and Graph I show that the same continued weight loss is evident in Delrin gears which came from the corroded gear train. Decomposition gases from PBX-9404 do attack Delrin and cause weight loss. Both solid and powdered samples are affected by the gases. Compatibility tests indicate that decomposition

gases from PBX-9404 are incompatible with Delrin at temperatures much above 49°C (120°F). Nitric acid (water saturated vapor phase NO₂) immediately attacks Delrin, whereas an equally strong protonic acid, HCl (wet vapor), has an appreciable induction period before there is evidence of chemical degradation.

Table V tabulates the effects of a long term static environment containing various nitrogen oxides. The conclusions are that NO and N₂O gases have no effect upon Delrin at either ambient temperature or 49°C (120°F). The effect of NO₂ upon the plastic when oxygen is absent is minimal even at 49°C (120°F). When oxygen is added to NO₂ and the ampoule is held at the elevated temperature, the results are typical of those found in the corroded gear trains. The white film observed is formaldehyde which polymerized on the cooled ampoule. There was sufficient NO₂ and oxygen to cause complete decomposition if a mol-per-mol basis is considered. Other structural components in the gear trains do not affect the gears (Table VI).

The observations accompanying Table V indicate that stress corrosion was first seen in the unfilled gear. Observation was possible due to the translucent nature of the unfilled part. No similar observation could be made of the carbon filled gear, but there is no reason to suspect that similar stress corrosion was not taking place in the filled gear. Once obvious stress cracks appeared on the filled gear, the general surface deterioration of the filled part appeared worse than that of the unfilled part.

Figures 15 through 15 show that the experimental gears could indeed be made to reproduce the appearance of the gears from corroded gear trains. If these

photos are compared to the ones taken of the gears from corroded gear trains (Fig. 1-3), there is little doubt that the decomposition of PBX-9404 releases sufficient NO₂ to destroy the Delrin gears.

Figures 19 and 20 show the effects of an ion beam etching process on the surface of a gear. There is no way of determining just how the beam is affecting the plastic structure, but it is interesting to note the connection of fibrous strands to a common point. Perhaps some correlation could be made between the hollowed appearance of the etched surface and the tunneling noted in the corroded gears (compare to Figure 3).

7. CONCLUSIONS AND RECOMMENDATIONS

Decomposition of PBX-9404 results in the evolution of NO₂ gas which chemically attaches itself to parts made of polyoxymethylene. Once the parts (gears in this case) have been impregnated with the NO₂ gas, continued decomposition will occur in the presence of oxygen and heat (thermal oxidation) even if the source of the NO₂ is removed. The fact that both oxygen and heat are necessary in combination with NO₂ gas to cause significant decomposition suggests that the mechanism is similar to that which causes photooxidation by artificial and natural ultraviolet light,⁽⁴⁾ i.e., the NO₂ lowers the activation energy necessary for thermal oxidation to occur. The NO₂ is probably site oriented (stress) on the lamellae and could possibly act as an oxygen exchange medium for chain scission. A tagged experiment (using NO₂)⁽¹⁸⁾, where either the CO₂ or formaldehyde generated during decomposition would be examined for activity, would show how the NO₂ was entering into the thermal oxidative process. Such an experiment was beyond the scope of this investigation.

The fact that nitric acid (aqueous NO_2) has an immediate effect upon the plastic whereas an equally strong protonic acid such as HCl has a prolonged induction period suggests that the HCl is hydrolyzing the acetal end groups rather than causing chain scission. The fact that the activation energy for hydrolysis is two to three times that necessary for free radical oxidation⁽⁷⁾ supports this observation.

If the properties of polyoxymethylene are essential to a particular design, it is suggested that a copolymer (of which there are many) or another material be chosen which is more resistance to oxidation and that close control be exercised over part production. In no case should polyoxymethylene be used in an oxidizing environment even if a copolymer is used.

REFERENCES

1. W. H. Rogers and L. C. Smith, "The Effects of Long-Term Storage at 60°C on Small Cylinders of PBX-9404," LA-4989-MS, Los Alamos Scientific Laboratory, Los Alamos, NM, June 1972.
2. P. G. Kelleher and B. D. Basner, "Oxidation of Ether Linked Thermoplastics," Polymer Eng. & Science, 10, No. 1, January 1970, p. 40.
3. L. Horvath, "Designing for Materials: 2. Acetal Homopolymer," Plastics, 33, May 1968, p. 535.
4. P. G. Kelleher and L. B. Jassie, "Investigations of Thermal Oxidation and Photooxidation of Acetal Plastics by Infrared Spectroscopy," J. of Applied Polymer Science, 9, 1965, pp. 2501-2510.
5. E. S. Clark, "Molecular Orientation in Injection Molding Acetal Homopolymer," Soc. Plast. Eng., 23(7), July 1967, pp. 46-9.
6. V. R. Alishoev, M. B. Newman and B. M. Korvarskaya, "Thermo-Oxidative Degradation and Stabilization of Polyformaldehyde," Plasticheskie Massy (translation), 7, 1962, CA 57, 16847g.
7. C. Arnold Jr., "Delrin Incompatibility-A Summary Report," SLA 74-0051, Sandia Laboratories, Albuquerque, NM (Internal Report).

Table I

EFFECT OF "DRY NO₂" GAS ON DELRIN AS DETERMINED BY MASS SPECTROSCOPY AND ISOTHERMAL TGA

Ampoule No.	Vol. (cm ³)	Total Press (air) (mm Hg)	Partial Press NO ₂ (mm Hg)	NO ₂ (mmol)	Time at 120°F (days)	1st sign of change (days)	Time at ambient temp. (days)	Mass Spec data on gases N ₂ /O ₂	CO ₂	Time at 49°C (hrs) (prior to TGA, 110°F at 1 mm vac. for 18 hrs)	% wt loss
1	33	500	1	1.81×10^{-6}	0	3	47	---	---		
2	33	500	1	1.81×10^{-6}	47	2	0	---	---		
3	33	500	1	1.81×10^{-6}	0	3	12	5.6/1*	5.4 [#]	24	20
4	33	500	1	1.81×10^{-6}	12	2	0	6.2/1	4.9		
5	1000	500	1	5.47×10^{-5}	2	7	10				
6	1000	500	10	5.47×10^{-7}	1	1**	11	4724/1	96.0		
7	33	500	10	1.81×10^{-5}	0	1	47	---	---		
8	33	500	10	1.81×10^{-5}	47	1	0	---	---	24	93
9	33	500	10	1.81×10^{-5}	0	1	12				
10	33	500	10	1.81×10^{-5}	1	1	11				
Control gear	--	Atm. Press.	--	---	--	--	Stored at ambient			7.5	0.0

* Normal ratio = 4/1

Data not relatable to CO₂ concentration in air (uncalibrated); only useful for comparison from sample to sample; e.g., #6 much more than #3.

** Gear completely dissolved after 3 days.

NOTE: Mass spectrometer data on ampoules 1, 2, 7 and 8 was unintelligible.

Table II

WEIGHT LOSS STUDY ON DELRIN GEARS AFTER EXPOSURE TO NO₂ GAS

Accumulated Percent Weight Loss (Zero time weight recorded after removal from ampoules containing NO₂ and heating at 110°F, 1 mm vacuum, for 18 hours)

Ampoule No.	Held at ambient temp.	Held at 120°F	After 7 days	After 14 days	After 24 days	After 35 days	After 45 days	After 62 days
3	x		1.3	3.1	5.6	8.0	9.5	12.5
4		x	12.1	18.0	21.8	23.8	25.0	26.2
5		x	17.8	24.1	27.9	29.9	31.1	32.7
9	x		4.1	7.4	11.1	13.9	15.0	16.7
10	16th to 18th days	x	16.5	19.7	23.1	24.7	25.4	26.4

Table III

PERCENT WEIGHT LOSS OF DELRIN GEARS UNDER ISO-THERMAL CONDITIONS AT 105°C
(No prior vacuum or heat treatment)

<u>Days at 105°C</u>	<u>SN 155755*</u>	<u>SN 142565*</u>	<u>Control Gear</u>
1	6.49%	15.49%	
4			0.87%
6	13.06%	30.81%	
7			0.90%
9	15.73%	25.82%	
11			1.02%
13	18.84%	40.40%	
18			1.35%
20	23.74%	48.03%	
25	26.54%	52.34%	1.59%
32			1.68%
34	30.29%	56.11%	

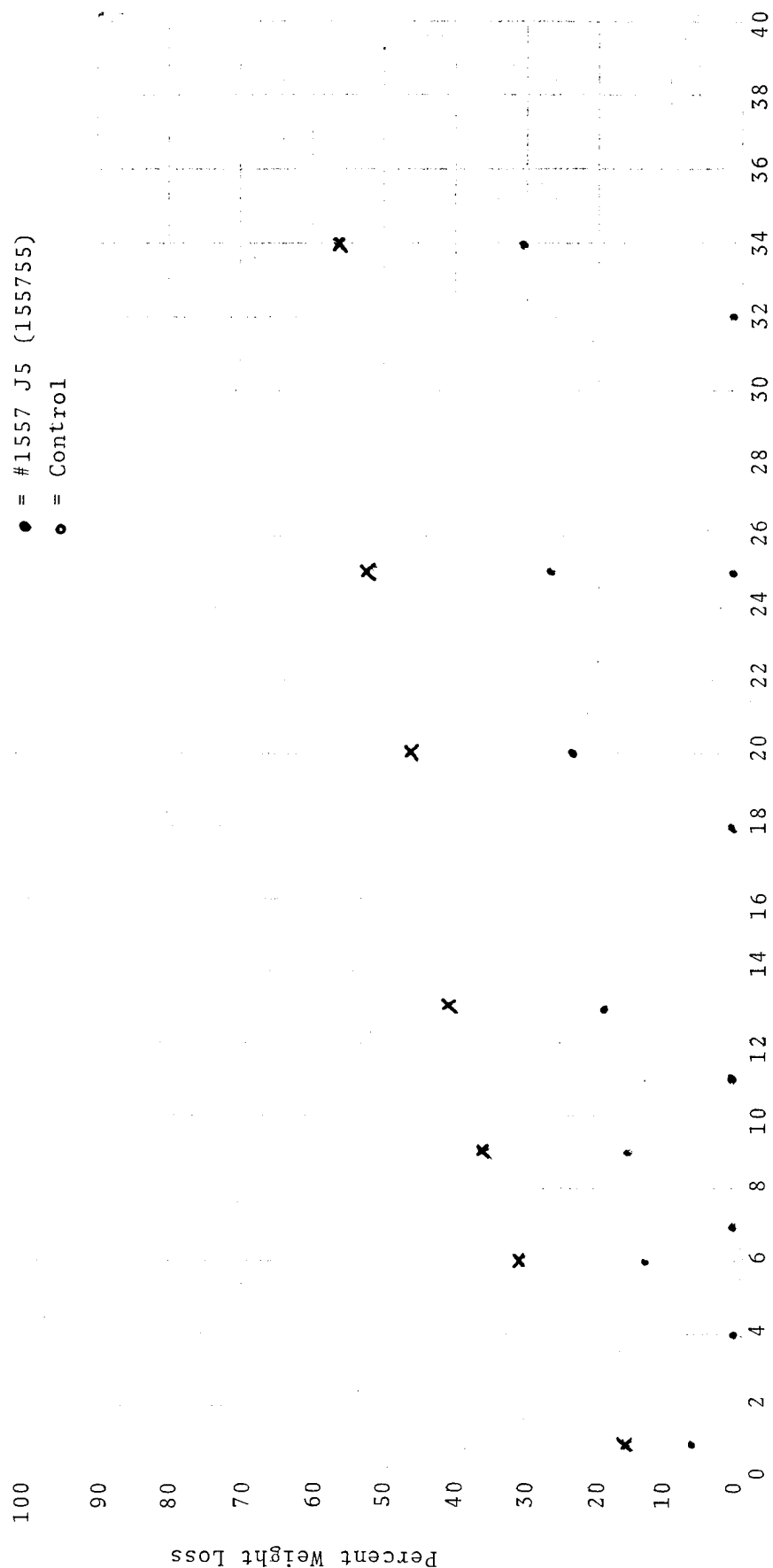
* Gears from corroded gear trains

Graph I

Graphical Representation of

Table III.

- x = #1425 G5 (142565)
- = #1557 J5 (155755)
- o = Control



Time at 105°C (Days)

Table IV

RESULTS OF ISO-THERMAL GRAVIMETRIC ANALYSIS OF DELRIN AND PBX-9404

Material	Experimental Conditions	Percent Weight Loss
Delrin gear/as received/solid	3 hours at 100°C	0
Delrin gear/as received/powdered	7.5 hours at 50°C	0
Delrin gear/from corroded gear train	24 hours at 50°C	0.26
Delrin gear/solid	Preconditioned in 10mm NO ₂ gas (See Table I, ampoule #9). 50°C for 20 ¹ / ₂ hours	93
Delrin gear/solid	Preconditioned in 1mm NO ₂ gas (See Table I, ampoule #3). 50°C for 24 hours	20
Delrin gear/solid	Decomposition gases from PBX-9404 (heated at 120°C) carried in helium gas stream (flow = 15cc/min) passed over gear at 50°C for 4 days	0.14
Delrin gear/powdered	Decomposition gases from PBX-9404 (heated at 120°C) carried in helium gas stream (flow = 15cc/min) passed over gear at 50°C for 4 days	0.17
PBX-9404	130°C for 3 hours	1.90
PBX-9404	140°C for 3 hours	1.98
PBX-9404	160°C for 3 hours	3.89
PBX-9404	180°C for 3 hours	4.59
Delrin gear/solid	Decomposition gases from PBX-9404 (heated at 160°C) carried in helium gas stream (flow = 40cc/min) passed over gear at 100°C for 24 hours	0.18

Table V
RESULTS OF EXPERIMENTS DESIGNED TO DETERMINE THE EFFECT OF NITROGEN OXIDES ON DELRIN AS A
FUNCTION OF TEMPERATURE AND PARTIAL PRESSURE OF OXYGEN (IN SEALED GLASS AMPOULES)

Exp. No.	Nitrogen Oxide Present	P. Press. of NO _x (mm) ^x	Ampoule Vol. (cc)	Mol. of NO _x	P. Press. of Oxygen (mm)	Filled			Unfilled Gear wgt. (mg)	Temp. °C (°F)	Time at Temp. (days)
						Mol. of Oxygen	Gear wgt. (mg)	Mol. of Plastic			
1	N ₂ O	1	50	2.74 x 10 ⁻⁶	0	0	64.49	2.01 x 10 ⁻⁶	25.79	Ambient	800
2	N ₂ O	1	50	2.74 x 10 ⁻⁶	0	0	33.60	1.52 x 10 ⁻⁶	35.08	49 (120) Ambient	550 350
3	NO	1	50	2.74 x 10 ⁻⁶	0	0	33.61	1.27 x 10 ⁻⁶	23.71	Ambient	800
4	NO	1	50	2.74 x 10 ⁻⁶	0	0	33.87	1.35 x 10 ⁻⁶	26.91	49 (120) Ambient	550 250
5	NO ₂	1	50	2.74 x 10 ⁻⁶	0	0	68.22	2.28 x 10 ⁻⁶	34.43	Ambient	800
6	NO ₂	1	50	2.74 x 10 ⁻⁶	0	0	33.96	1.51 x 10 ⁻⁶	34.20	49 (120) Ambient	550 250
7	N ₂ O	1	50	2.74 x 10 ⁻⁶	*133	3.64 x 10 ⁻⁶	38.77	1.56 x 10 ⁻⁶	31.43	Ambient	800
8	N ₂ O	1	50	2.74 x 10 ⁻⁶	133	3.64 x 10 ⁻⁶	42.48	1.52 x 10 ⁻⁶	26.00	49 (120) Ambient	550 250
9	NO	1	50	2.74 x 10 ⁻⁶	133	3.64 x 10 ⁻⁶	24.00	1.51 x 10 ⁻⁶	43.94	Ambient	800
10	NO	1	50	2.74 x 10 ⁻⁶	133	3.64 x 10 ⁻⁶	15.53	1.24 x 10 ⁻⁶	40.18	49 (120) Ambient	550 250
11	NO ₂	1	50	2.74 x 10 ⁻⁶	133	3.64 x 10 ⁻⁶	12.84	1.16 x 10 ⁻⁶	39.54	Ambient	800
12	NO ₂	1	50	2.74 x 10 ⁻⁶	133	3.64 x 10 ⁻⁶	14.45	6.68 x 10 ⁻⁶	15.63	49 (120) Ambient	550 250

* Equal to partial pressure of oxygen in one local atmosphere.

Table V (Continued)

No.	Observations
1	No change.
2	No change.
3	No change.
4	No change.
5	Unfilled (white) gear parts turn yellow with 12 hours. No other change.
6	Unfilled (white) gear parts turn yellow within 12 hours. After 41 days at temperature (49°C), white Delrin showed cracking; however, the cracks were not such as to cause the surface of the part to spread. Cracks are interior and can be seen under bright light as unfilled plastic is translucent. Filled gears showed no change; however, neither are they translucent. After removal from oven, a very faint white film condensed inside ampoule. No other change was observed.
7	No change.
8	No change.
9	NO combined with O ₂ to form NO ₂ which stained unfilled gear parts a bright yellow color within 12 hours. No other change was observed.
10	NO combined with O ₂ to form NO ₂ which stained unfilled gear parts a bright yellow color within 12 hours. After 16 days at 49°C (120°F) the unfilled gear part showed. Cracking similar to #6. After 1 year at temperature, the unfilled gear part is noticeably cracked but the filled part is unchanged. After 15 months at temperature, filled gear part cracked severely. After removal from oven, a noticeable white film condensed on the inside of the ampoule. There has been no further change to date.
11	Same as #9.
12	Same as #10.

Table VI

RESULTS OF QUALITATIVE COMPATIBILITY TESTING ON DELRIN

A. Effect of PBX-9404 on Delrin

PBX-9404/Delrin sheet/cured PR-1221-B2 (Thiokol rubber)/Delrin gear (1)	120°F/sealed tube/50 days	No visible change
PBX-9404/Delrin sheet/Delrin gear (1)	120°F/sealed tube/50 days	No visible change
PBX-9404/cured PR-1221-B2/Delrin sheet/ uncured PR-1221-B2 (1)	120°F/sealed tube/50 days	No visible change
PBX-9404/cured PR-1221-B2/Delrin sheet (2)	120°F/unsealed tube/50 days	No visible change
Delrin sheet/PBX-9404/Delrin sheet/ PBX-9404/Delrin sheet (2)	120°F/sealed tube/27 days	NO ₂ gas evolved, PBX-9404 changed color from blue to yellow, Delrin sheet changed color from white to yellow.
PBX-9404 (10g)/Delrin gear (1)	120°F/sealed tube/15 days	No visible change
PBX-9404 (10g)/Delrin gear (1)	176°F/sealed tube/13 days	Surface cracking
PBX-9404 (10g)/Delrin gear (1)	212°F/sealed tube 7 days	Surface cracking
Fuming nitric acid/Delrin sheet/ PBX-9404/PR-1221-B2 (1)	120°F/unsealed tube/27 days	Incompatible, overnight the color and texture of each ingredient changed.
Delrin gear/fuming nitric acid (1)	Ambient temperature	Immediate chemical attack with surface cracking and flaking off of some parts of the gear
Delrin gear/conc. hydrochloric acid (1)	Ambient temperature	There was a 2-3 day induction period before generalized chemi- cal attack. Prior to decomposi- tion gear surface appears to lose its luster and take on a gray color.

NOTE: Approximately 2 grams of PBX-9404 were used in the above experiments unless otherwise noted.

(1) Materials separated from each other with glass beads.

(2) Materials in intimate contact with each other.

Table VI (Cont'd)

RESULTS OF QUALITATIVE COMPATIBILITY TESTING ON DELRIN

B. Other compatibility experiments were performed to determine the consequences of inadequate curing of the Thiokol rubber (PR-1221-B2) and the presence of a plasticizer in the main charge.

<u>Materials</u>	<u>Experimental Conditions</u>	<u>Results</u>
Component "A" of the PR-1221-B2, a thixotropic rubber like material in approximately 3% solvent/Delrin gear	Immersion/ambient temperature	No visible change
Component "B" of the PR-1221-B2, a catalyst containing lead peroxide in dibutyl phthalate/Delrin gear	Immersion/ambient temperature	No visible change
Tris(2-chloroethyl) phosphate, a plasticizer (3 wt %) used in PBX-9404/Delrin gear	Immersion/ambient temperature	No visible change

SEM PHOTOMICROGRAPHS OF DELRIN GEARS FROM CORRODED GEAR TRAINS
(Figures 1 - 10)

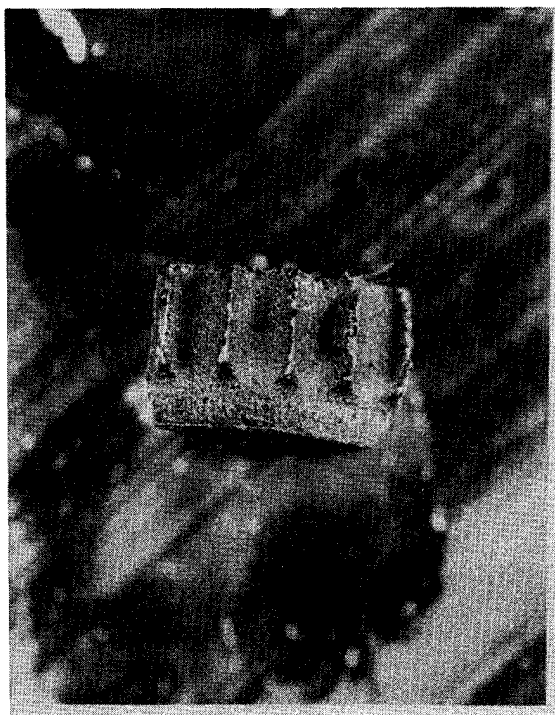


Figure 1
(Gear A)

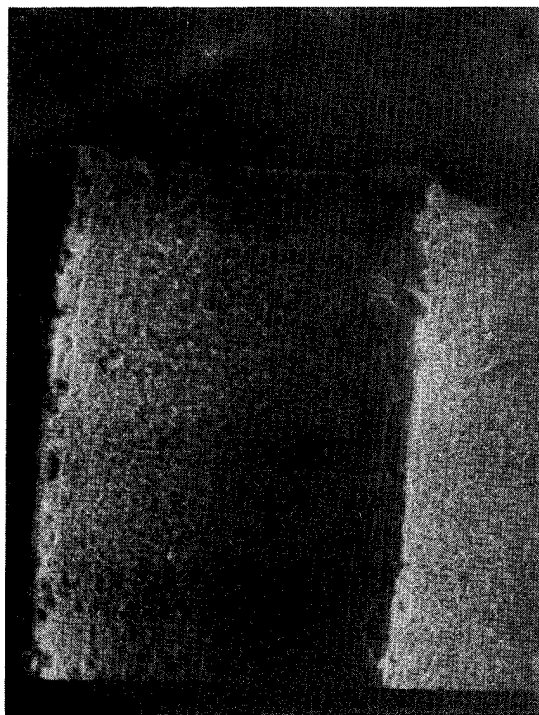


Figure 2
(Gear A, 65X)

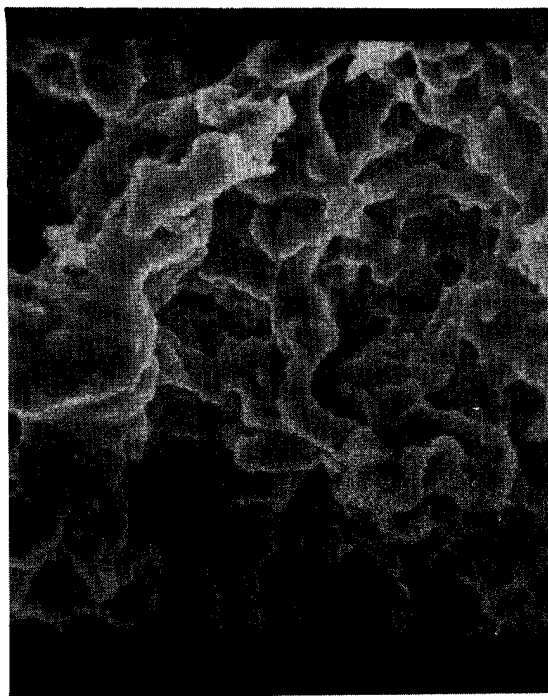


Figure 3
(Gear A, 2000X)

NOTE: Extreme wasting of gear teeth and deep penetration of corrosion into gear body.

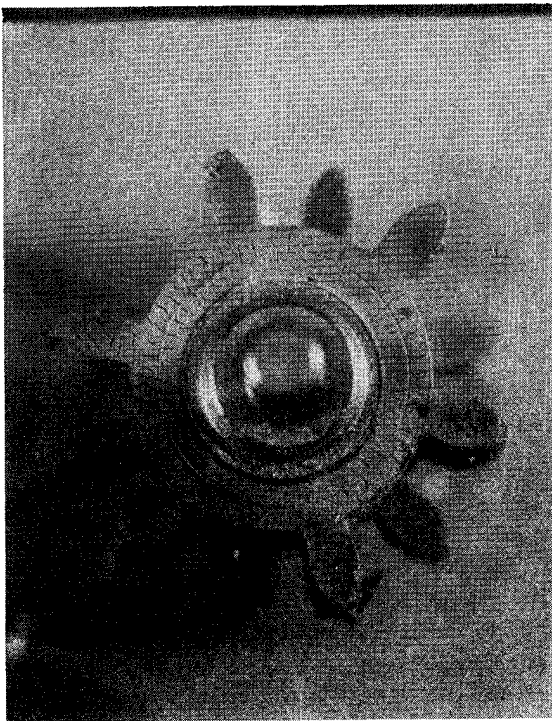


Figure 4
(Gear B)



Figure 5
(Gear B, 65X)

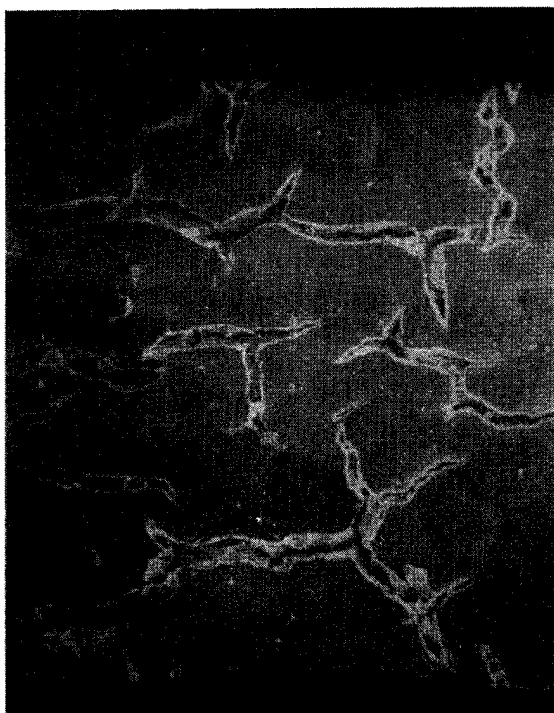


Figure 6
(Gear B, 200X)



Figure 7
(Gear B, 2000X)

NOTE: "Skin" effect and stress cracks on gear. This gear is in the initial stage of decomposition.

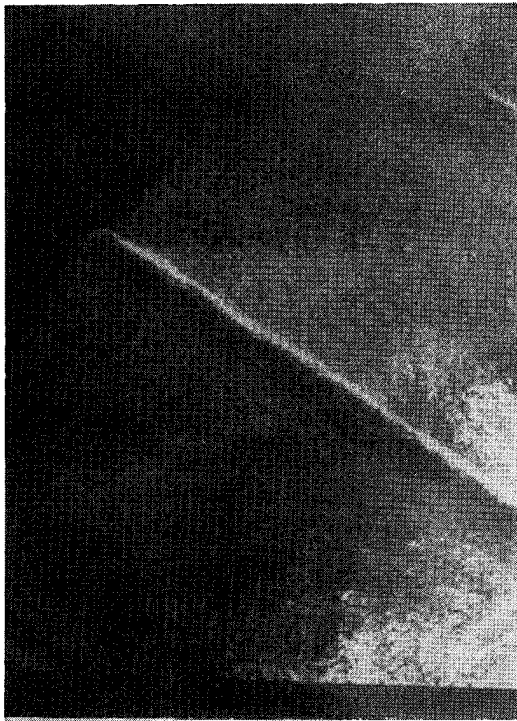


Figure 8
(Gear C, 60X)

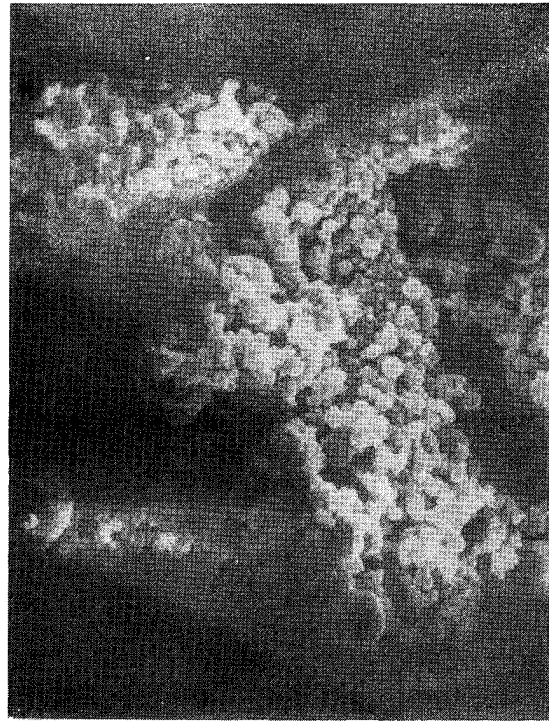


Figure 9
(Gear C, 2000X)

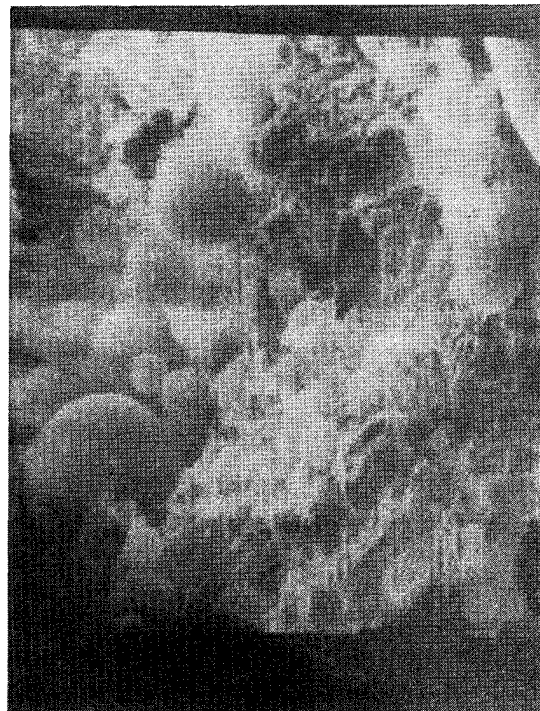


Figure 10
(Gear C, 6000X)

NOTE: Wasting of gear teeth. This gear had a residue which was full of spherulites and is a good example of the effects of cooling during part manufacture.

SEM PHOTOMICROGRAPHS OF AN UNFILLED (WHITE) DELRIN SLEEVE FROM CORRODED GEAR TRAINS
(Figures 11 and 12)

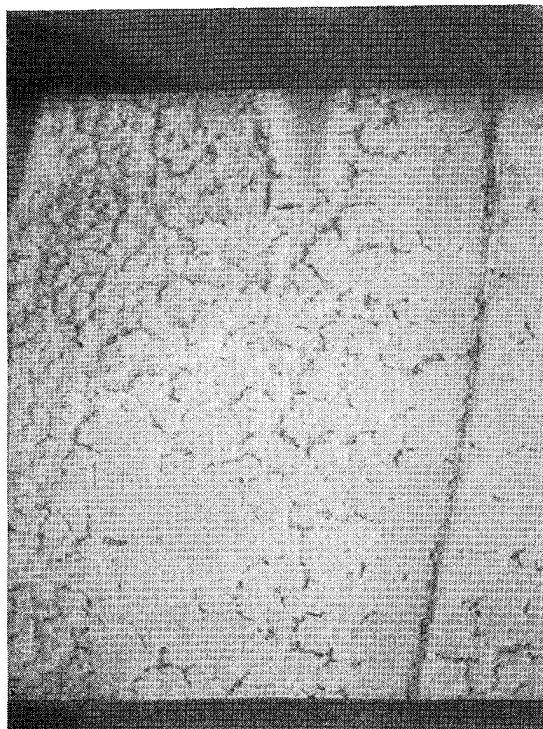


Figure 11
(45X)

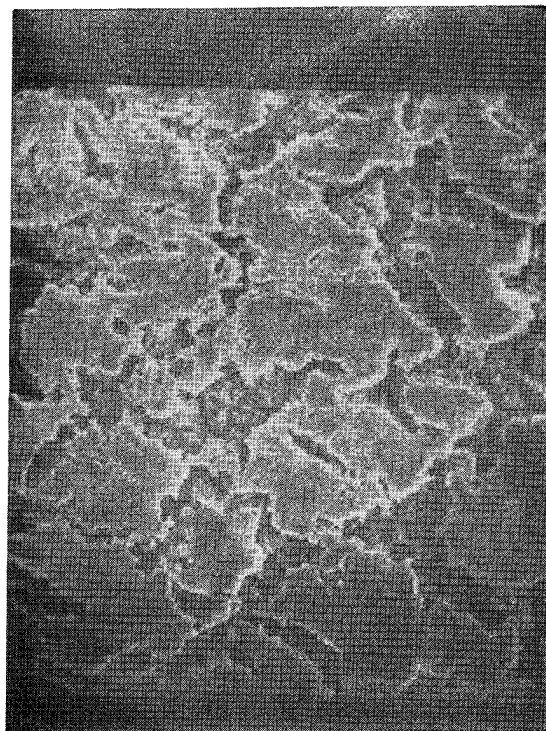


Figure 12
(200X)

NOTE: The unfilled Delrin sleeve is decomposed but to an apparent lesser degree than associated gears; however, the corrosion is still extensive

SEM PHOTOMICROGRAPH OF AN UNCORRODED GEAR

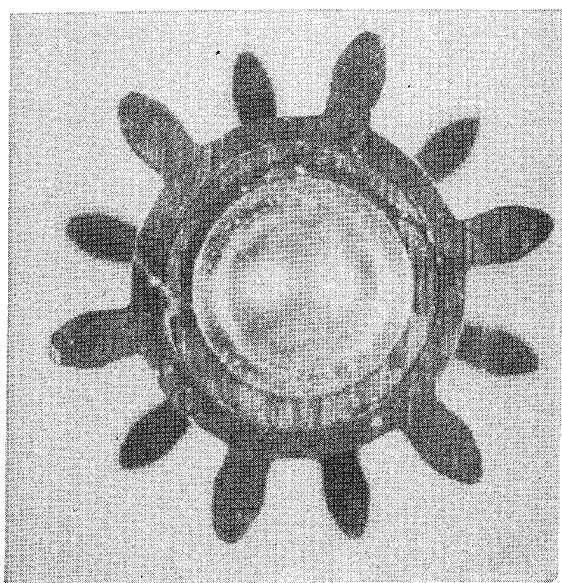


Figure 13

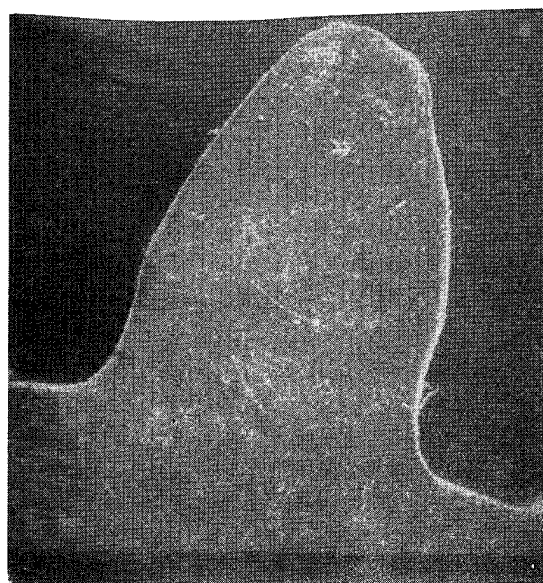


Figure 14
(65X)

NOTE: Smooth surface of an undamaged gear. Compare teeth to those gears with advanced corrosion to gage extent of decomposition.

SEM PHOTOMICROGRAPHS OF A GEAR EXPOSED TO NO₂ GAS FROM 10g OF PBX-9404
AT 80°C FOR 13 DAYS IN A SEALED CONTAINER

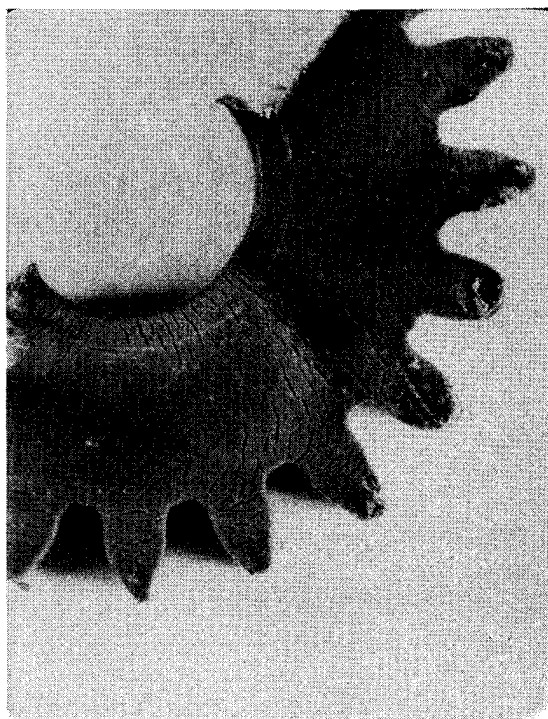


Figure 15

Compare this gear to gear "B" (Figures 4 - 7).
Note how well stress cracks compare.



Figure 16
(65X)

OPTICAL PHOTOMICROGRAPHS OF GEAR PARTS EXPOSED TO 1mm
NO₂ AND 133mm O₂ AT 49°C (120°F)

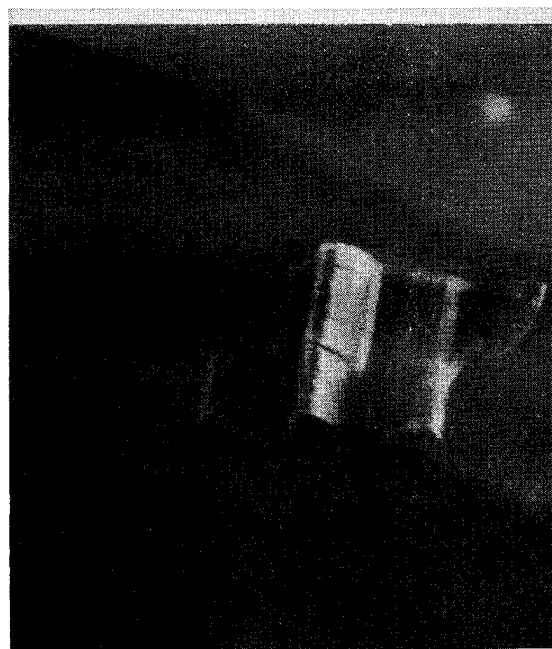
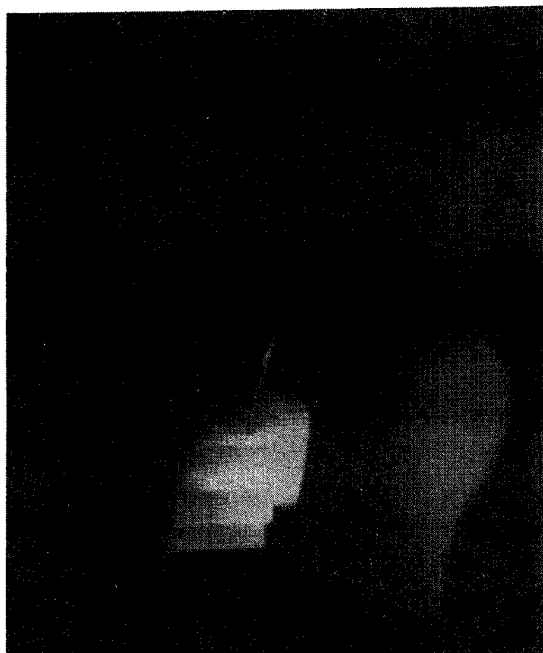
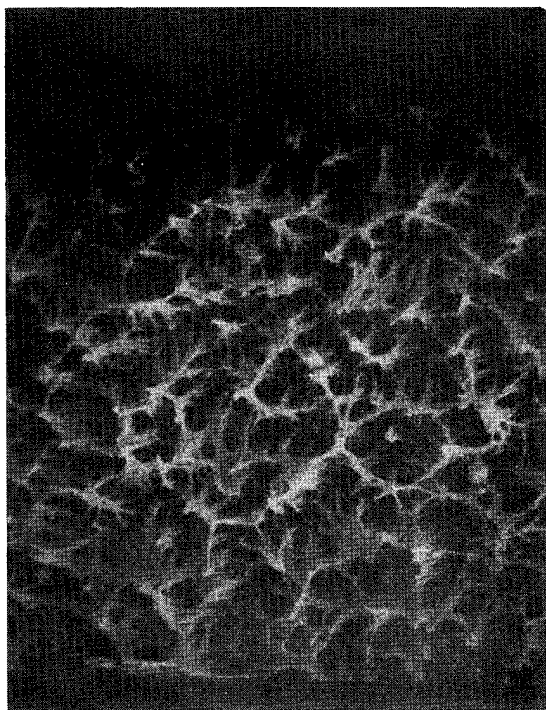


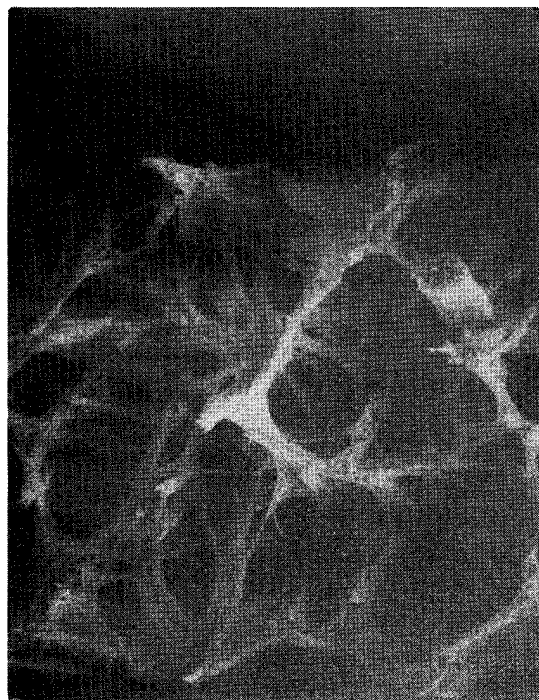
Figure 17
(Unfilled (white) gear exposed for 70 days) Figure 18
(Filled (black) gear exposed for 1 year)

NOTE: Stress cracks in unfilled gear do not split surface as those in filled gear. At the time surface cracks appeared on filled gear unfilled gear surface had separated.

SEM PHOTOMICROGRAPHS OF A DELRIN GEAR SURFACE AFTER ION BEAM ETCH



3 hours exposure
Figure 19
(370X)



3 hours exposure
Figure 20
(1200X)

Compare this gear to gear "A" (Figure 3)

NOTE: Comparable tunneling

LIQUID, HEAVILY-FLUORINATED EPOXY RESINS FOR HIGH ENERGY APPLICATIONS

James R. Griffith
Naval Research Laboratory
Washington, D. C.

ABSTRACT

Some liquid epoxy resins of more than 50% fluorine by weight which possess virtually all the convenient use properties of conventional epoxies have been synthesized at NRL. The fluorine locations within the resin molecules have been carefully selected so that the hybrid materials contain most of the desirable properties of Epon 828 and of Teflon in singular molecular species. The resins can be cured in conventional epoxy fashion, at room temperature if necessary, or at elevated temperatures if maximum strength and chemical resistance are desired. Teflon is wetted unusually well by virtue of the low surface tension of the resins, and compatible suspensions of Teflon powder are easily prepared. Potential applications in the energetic materials area include the use of liquid fluorinated epoxies as propellant binders in the casting of high-energy solid rocket fuels, as filament-winding resins for rocket motor cases, as damage-resistant coatings and plastics for use with high-energy liquid fuels.

1. INTRODUCTION

The NRL C-3 and C-7 fluorinated epoxy resins are liquid diglycidyl ethers which contain 52% and 57% fluorine by weight, respectively.

Polyamines and organic acid anhydrides are effective curing agents which convert the resins into polymers and produce materials similar to cured conventional epoxies except for the properties imparted by the fluorocarbon structure. The convenient use properties, which derive from the liquid epoxy nature in combination with a large quantity of fluorine, make these materials exceptional in their potential for high energy applications.

2. BACKGROUND

During the mid-1960's, there was considerable interest within the Navy concerning the possibility of producing submarine hulls by a filament winding method similar to that employed for the Polaris missile motor case⁽¹⁾. An R & D effort was initiated at NRL with the goal of synthesizing filament winding resins with maximum resistance to the long-term effects of water. This effort became focussed upon a new type of epoxy resin which would contain large quantities of fluorocarbon within the molecular structure while retaining all of the

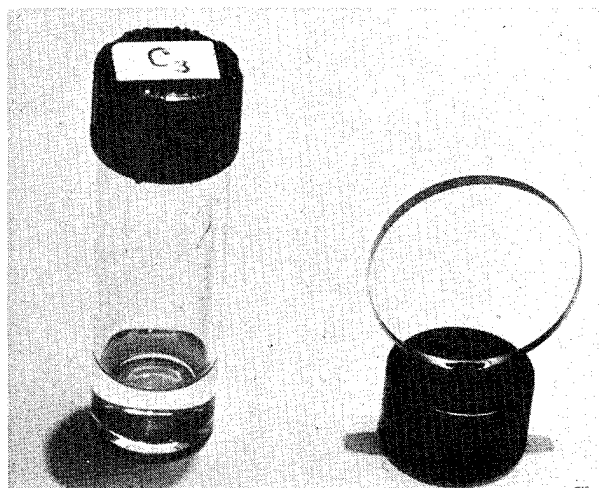


Figure 1. NRL C-3 Fluorinated Epoxy Resin in Precured Liquid State and as Post-Cured, Molded Disc

convenient use properties of liquid epoxies in the precured state and epoxy strength properties after cure^(2,3). The culmination of this effort, after several years of research in organic synthesis, was the NRL C-3 epoxy, which is a liquid diglycidyl ether containing a perfluorinated propyl group. A subsequent resin of the same type contains a perfluorinated heptyl group and is designated the C-7 resin. Synthesis details for these resins have been previously published^(4,5).

3. POTENTIAL HIGH ENERGY APPLICATIONS

Several applications in the high energy area appear particularly promising for the fluorinated epoxies. Certain types of solid propellants for rockets are improved in energy yield by the presence of fluorocarbon, and properly formulated fluoroepoxies would serve the dual function of high-strength binder and fluorine source. In the precured state, the wetting properties of the liquid resins are outstanding, and a wide range of physical properties can be realized which vary from those of elastomer to hard plastic.

Another potential use is that of inert coatings or plastics for contact with high energy fuels. A large quantity of powdered Teflon can be carried in compatible suspension by the fluorinated epoxies, and Teflon-like coatings can be conveniently prepared without the usual difficulties. There are many ramifications of this application which would involve chemical formulation to resist a particular fuel and use conditions.

The projected use of the fluorinated epoxies as filament winding resins remains promising, although interest in the filament-wound submarine hull has diminished. Rocket motor cases which may be subject to high humidity or exposure to liquid water could be filament-wound from the hydrophobic fluoroepoxies with advantage. All of the necessary characteristics of a filament winding resin, such as long pot life, good reinforcement wetting and high composite strengths can be realized.

4. SURFACE TENSION AND WETTING

It had been suggested that fluorinated epoxy resins should have low surface tension which would result in excellent wetting characteristics for "low energy" surfaces, such as that of Teflon⁽⁶⁾. Early syntheses of such resins resulted in products with small amounts of fluorine, and the surface tensions were

in the 35-40 dyne/cm region, which is about the same as that of conventional epoxy resins⁽⁷⁾. In a study of fluorinated monoglycidyl ether liquids of moderate viscosity and high purity, we have shown that surface tension varies inversely with fluorine content and that surface tensions as low as 24 dynes/cm can be obtained⁽⁸⁾. The surface tensions of the C-3 and C-7 diglycidyl ethers are both in this region with values of 24.5 dynes/cm and 23.5 dynes/cm respectively at 25°C. The decrease in surface tension with temperature in the range of 20° to 50°C is about 1 dyne/cm for each 10 degrees rise.

Because of this low surface tension, the fluorinated epoxy resins are excellent wetting fluids, and even Teflon, which has a critical surface tension of about 18 dynes/cm, is wetted exceptionally well. It should be possible to use this property to advantage in the compounding of solid propellant rocket fuels as an aid in dispersal of all the particulate components, such as the oxidizer and metallic powders. In the case-bonded rockets, adhesion of the grain to the liner should also be enhanced in those instances for which good wetting is not obtained with conventional adhesives or binders.

The wetting of Teflon powder by the liquid fluoroepoxies results in highly compatible suspensions which can be used as a paint and cured to give films of a fluorocarbon nature. Some testing of such films for resistance to dimethyl hydrazine and nitrogen tetroxide to assess short term effects has been accomplished. They are resistant to the hydrazine, but liquid N_2O_4 falling directly upon the surface softens a film rather quickly and causes discoloration. This is a very severe test however, and it is not surprising that nitrogen tetroxide liquid would damage the functional group region of the cured epoxy molecule rather rapidly. Resistance to the vapors of this powerful oxidizing agent may be adequate for some short-term uses. The compatibility of such fluoroepoxy-Teflon films with other aggressive chemicals is also of interest.

5. CURE CHARACTERISTICS

Epoxy resins which cure well at room temperatures virtually all employ amines for curing agents, and the temperature-reaction rate dependency is such that violent, exothermic excursions can occur when massive castings are attempted. This is a major reason epoxies have not been used more extensively as binders for

solid propellant rocket fuels.

We have shown previously⁽⁹⁾ that the reaction rate of fluorinated epoxies, closely related to the C-3 type, is about one-half that of common glycidyl ethers with amines in solution. A consequence of this is that aggressive aliphatic polyamines in neat solution with the C-3 resin produce reaction rates that are controllable and convenient for bulk casting. Although sufficient resin has not been available to test the proposition, it should be possible to cast a massive grain of solid propellant without danger of internal exotherm when the fluoroepoxies are employed. A post-cure at moderate temperatures (~40°C) should produce grains which are exceptionally strong mechanically and resistant to environmental influences.

The cure of fluoroepoxies with anhydrides is similar to that of common epoxies. This requires a catalyst, usually a tertiary amine, such as dimethyl benzylamine, and moderate heat. One advantage of anhydride cure versus amine cure is that fluorine can be included within the molecular structure of an anhydride with fewer problems. Fluoroamines are generally not shelf-stable over long periods of time and are greatly diminished in reactivity with epoxies. At NRL a new anhydride curing agent has recently been synthesized which contains 36% fluorine by weight, which is an effective curing agent for fluoroepoxies, and which allows the fluorine content of the total system to remain at a high level.

6. CONCLUSION

Fluoroepoxies are a new class of materials which have potential for contributing to high-energy propellants as well as for resisting other types of aggressive liquid fuels. Because of their newness and limited availability to date, our assessment of the potential is somewhat speculative at this time, but we believe it to be based upon sound technical considerations and expect these materials to be uniquely useful in demanding applications of the future.

7. ACKNOWLEDGEMENT

The author wishes to thank Mr. Joseph Reardon of the Naval Research Laboratory for surface tension measurements.

8. REFERENCES

(1) W. S. Pellini, editor, "Status and Projections of Developments in Hull Structural Materials for Deep Ocean

Vehicles and Fixed Bottom Installations," NRL Report 6167, November 1964.

(2) J. E. Quick and J. R. Griffith, "Fluorocarbon in Epoxy Plastics", NRL Report 6875, April 1969.

(3) J. R. Griffith, J. G. O'Rear and S. A. Reines, Chem. Technol. 2, 311 (1972).

(4) J. G. O'Rear and J. R. Griffith, Coatings and Plastics Preprints, 165th Meeting of the American Chemical Society, Vol. 23, No. 1, 657 (1973).

(5) J. R. Griffith and J. G. O'Rear, Synthesis, No. 7, 493 (1974).

(6) F. R. Dammont, L. H. Sharpe and H. Schonhorn, J. Polymer Sci., B3, 12, 1021 (1965).

(7) H. Lee and K. Neville, "Handbook of Epoxy Resins", McGraw-Hill, New York, Chapter 21, pg. 10 (1967).

(8) J. R. Griffith, J. G. O'Rear and S. A. Reines, Coatings and Plastics Preprints, 161st Meeting of the American Chemical Society, Vol. 31, No. 1, 546 (1971).

(9) S. A. Reines, J. R. Griffith and J. G. O'Rear, J. Org. Chem. 35, 2772 (1970).

9. BIOGRAPHY

Dr. James R. Griffith received the B.S. Degree in Chemistry from Birmingham-Southern College and the Ph.D. Degree in Organic Chemistry from the University of Maryland. His graduate research was in polymer chemistry and concerned carbamates of tertiary alcohols for utilization in polypeptide syntheses. He has been a research organic chemist at the Naval Research Laboratory since 1955 and Head of the Organic Synthesis Section since 1969.

LONG-TERM EFFECTS OF SILICONE OILS ON PETN AND DETONATOR PERFORMANCE

Henry S. Schuldt
Initiating & Pyrotechnic Component Division 2515

Robert J. Burnett
Detonating Components Division 2513
Sandia Laboratories
Albuquerque, New Mexico 87115

and

Billy D. Faubion
Mason & Hanger-Silas Mason Company
Amarillo, Texas 79177

ABSTRACT

In 1970 ~~there~~ were some reasons to believe that oils exuded from silicone rubber were having a deleterious effect on detonator performance in stockpile weapons. These oils were identified and simulated by a mixture of silicone oils. PETN coated with this mixture was stored for two years, after which physicochemical tests in the laboratory and in-detonator test firings showed no long-term adverse interaction or incompatibility between PETN and the silicone oil, and no long-term effects on detonator performance.

1. INTRODUCTION

At the end of 1970, during the course of lot-acceptance testing of PETN (RR5K type), some anomalous detonator firings occurred. These anomalies took the form of increased transmission times and, in a few cases, detonator failures. After considerable investigation⁽¹⁾ the problem was pinpointed as one in which silicone oils from an "O" ring connector were being extruded along the detonator posts and deposited at the bridgewire. This of course constituted an energy barrier. As time passed these oils continued to migrate to coat all available

surface. This reduced the concentration of oil in the critical bridgewire area and the firing times tended to return to normal. Thus with the mechanism of failure and recovery well known, the short-term problem was resolved. However, the long-term effects were not known and such studies constitute the subject of this report. The direction of this endeavor was twofold -- one, basic laboratory experimentation and two, long-term surveillance testing, including test firing.

The "O" rings which exuded the oils under pressure in the connector consisted of

SE 5601 silicone rubber. SE 5601 silicone rubber is made from silicone gum stock by addition of filler and catalysts (2.2 to 2.5 ppm). The gum stock is manufactured by heating and stirring a refined grade of dimethyl silicone oil with a trace of catalyst. For rubbers like SE 5601, with low-temperature flexibility and low compression set, the gums were made by copolymerizing dimethyl siloxane with a small proportion, 5 to 15%, of diphenyl or methylphenyl siloxane and a fraction of a percent of methylvinylsiloxane. Catalysts commonly used to cure the rubber are Varox [2,5-dimethyl-2,5-bis-(tertbutyl-peroxy)] hexane used either as a powder or in solution and Cadox, a peroxide paste catalyst containing 50% 2,4-dichlorobenzoyl peroxide, 37-1/2% GESF-96 and 12-1/2% dibutylphthalate.

2. IN DETONATOR SURVEILLANCE TESTS

The in-detonator surveillance tests will be discussed first since they measure powder acceptability and detonator performance

directly as a function of powder treatment and storage time.

The first test-firing experiment was designed to determine the effect of detonator performance of PETN coated with oil equivalent to that extractable by solvent from one "O" ring. A solution of 20% DC705 and 80% DC200 silicone oil in a hexane carrier was coated on RR5K PETN by a Roto-Vac process. The amount put on was about 150 micrograms or about 0.08% by weight.⁽²⁾ Detonators were loaded with untreated PETN, hexane-stirred PETN, and oil-coated PETN and fired within 5 days. Burst current was 600 amp; test temperature -54°C (-65°F). The data are given in Table I. It is seen that oil coating PETN at this concentration increases threshold only slightly and has no effect on transmission time; these results are very similar to those for PETN merely stirred in the carrier hexane.

Table I

Firing of Detonators Loaded with Silicone-Oil-Doped PETN

Powder Treatment	No. Tested Threshold Burst Current	Est. Threshold Burst Current (amp)	No. Tested at 600 amp	Average Transit Time, t_e (μsec)
No treatment	4	315	5	1.87
Treated with hexane	4	330	5	1.87
Treated with oil solution	5	335	5	1.88

The second firing series experiment was designed to determine if timing improvement as a function of age could be observed in detonators with silicone oil deposited at the bridgewire area. Seventy-five micrograms of silicone oil or approximately one-half of the amount extractable from a single "O" ring⁽²⁾ was introduced onto the header with a syringe. This was then overpressed with RR5K PETN. The units were fired at 54°C (-65°F) with 600 amperes burst current. The test data are given in Table II.

upon aging. No adverse long-term effects were observed.

In the third series of firing experiments detonators were loaded according to production standards with RR5K PETN. Cable connectors, which contained untreated production "O" rings were attached as in normal production. These detonators were stored at room temperature and also 49°C (120°F), 60°C (140°F), and 71°C (160°F). Units were removed periodically and test fired. Uncabled detonators which served

Table II

Firing of Detonators with Silicone Oil Deposited in Bridgewire Area

Number Tested	Days After Loading	Environment If Any	Results (μsec)	Average Transit Time (μsec)
3	6	None	1.89, 2.05	2.00
5	9	None	2.00, 2.00 1.99, 1.91 1.88	1.96
4	9	92 hrs at 140°F	1.98, 1.97	1.95
4	42	None	1.92, 1.92 1.97, 2.06	1.97
4	120	None	1.90, 1.90 1.91, 1.89	1.90
4	250	None	1.85, 1.90 1.85, 1.88	1.87
4	380	None	1.85, 1.84 1.86, 1.89	1.86

As was the case with anomalous detonators in the original lot-acceptance tests, the transmission times were long at first but shortened into the region of acceptability

as controls were included in the test. All units were fired -54°C (-65°F) with 600 amperes burst current. The results are given in Table III. Again long transmission

Table III

Variable Temperature Cable-Time Experiments

Firing Current: 600 amps

Temperature at Firing: -54°C

I. Room Temperature Detonators

Days Cabled	Days at Temperature	No. Tested	Average Transit Time te (μsec)	Timing Range (μsec)
4	4	6	1.99	0.23
8	8	6	2.11	0.25
12	12	6	2.05	0.11
20	20	6	2.01	0.20
28	28	6	2.06	0.28
35	35	8	2.03	0.13
43	43	8	2.00	0.09
50	50	6	2.06	0.13
61	61	6	2.06	0.09
110	110	6	1.99	0.06
124	124	6	2.02	0.12
190	190	6	2.00	0.17
205	205	6	1.98	0.04
266	266	6	2.02	0.05
378	378	6	2.00	0.11
558	558	6	1.97	0.06
744	744	6	1.99	0.12

II. 49°C Detonators

7	7	6	2.09	0.30
14	14	6	2.07	0.24
21	21	6	2.03	0.14
29	29	6	2.03	0.11
40	40	6	2.01	0.11
93	93	6	2.02	0.05
125	125	6	1.99	0.09
149	149	6	2.03	0.09
222	222	6	2.00	0.09
275	275	6	2.00	0.03
392	392	6	2.00	0.04
520	520	6	2.00	0.08
639	639	6	1.98	0.06
758	758	6	1.98	0.05

Table III (Cont'd)

Days Cabled	Days at Temperature	No. Tested	Average Transit Time t_e (μ sec)	Timing Range (μ sec)
III. 60°C Detonators				
7	6	6	2.12	0.27
14	13	6	2.07	0.24
21	20	6	2.03	0.14
Controls	20	5	1.96	0.07
29	28	6	2.03	0.08
40	39	6	2.04	0.07
93	92	6	2.03	0.08
125	124	6	2.01	0.07
176	175	6	2.02	0.04
Controls	175	5	1.98	0.05
251	250	6	2.01	0.10
310	309	6	2.03	0.05
456	455	7	1.95	0.06
Controls	455	4	1.97	0.19
IV. 71°C Detonators				
6	6	6	2.16	0.27
Controls	6	5	1.93	0.03
13	13	6	2.11	0.20
20	20	6	1.95	0.09
Controls	20	5	1.94	0.02
28	28	6	2.00	0.10
39	39	6	2.02	0.10
93	92	5	1.96	0.05
Controls	92	5	1.94	0.02
125	124	5	1.97	0.04
148	148	5	2.01	0.11
175	175	5	2.03	0.07
274	274	5	2.00	0.08
Controls	274	5	1.95	0.05

time ($t_e \geq 2.1 \mu$ sec) are observed after a few days of cable time. It should be noted that uncabled units constantly give short transmission times ($t_e \approx 1.95 \mu$ sec). Within a given series of firings, the range of transmission times after short periods of storage, is also large for cabled units --

indicating significant timing "jitter" -- while that for uncabled units is generally much narrower. Both the transmission times and timing range decrease with increased storage time. Detonators stored at high temperature fired more poorly than those at lower temperature at the early (one week)

part of the testing. As testing continued, units stored at high temperature showed more rapid improvement in firing characteristics than those stored at lower temperature. These observations are consistent with the hypothesis that the oil moves in and out of the bridgewire area more quickly at higher temperatures. At very long times, the detonator times and timing range appear to level out, and at values indicating good detonator performance.

3. LABORATORY EXPERIMENTATION

The in-detonator surveillance tests were complimented by laboratory experiments; such tests are very important since they have often given evidence of a detrimental trend before it becomes severe enough to

appear in firing tests. The laboratory experiments were designed to establish the nature of the oil exuded from the silicone "O" rings, and to determine whether changes occurred in the impregnated powder as a function of time.

Sufficient quantities of oil for analysis were pressed from one each sample of SE 5601 rubber made with Varox and Cadox catalysts. The exuded oils were collected on filter paper layered with 2-inch-diameter by 1/8-inch-thick discs of the rubbers and compressed between stainless steel plates; 4.48 MPa (650 psi) was applied with a hydraulic ram press. The absorbed oil was periodically extracted from the filter paper with spectroquality chloroform. Weight loss of the rubber discs as a function of time is plotted in Figure 1.

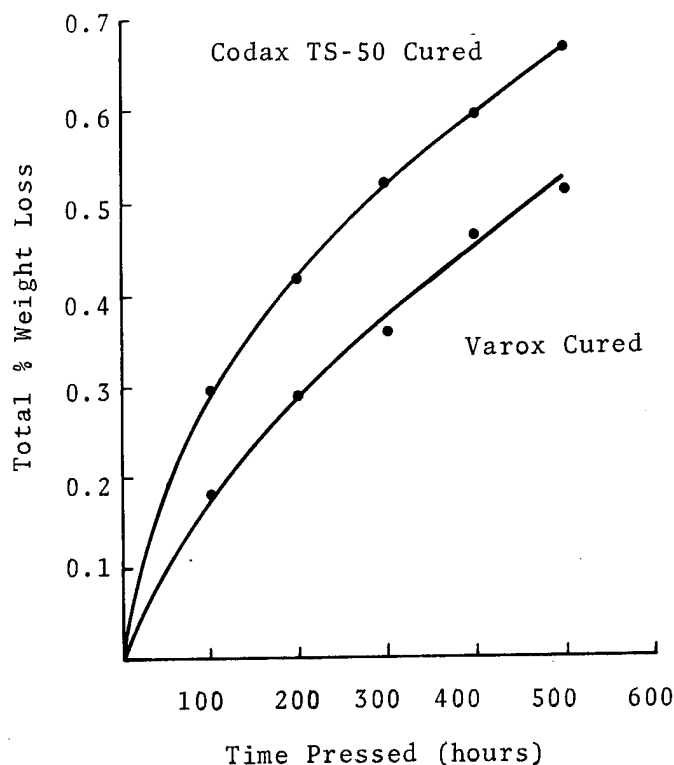


Figure 1. Weight loss of SE 5601 silicone rubber as a function of compression time

The exuded oils were identified primarily by infrared (IR) spectral analysis using a Perkin Elmer Model 21 IR prism spectrophotometer. The samples were run as oil films between two AgCl windows. Characterization of the exuded oils was accomplished by identifying the group frequencies and comparing with spectra of silicone

oils having linkages similar to those in the constituents of SE 5601 rubber--i.e., DC200, which is a dimethyl silicone oil; DC705, a methylphenyl silicone oil; and GE 93-022, a methylvinyl silicone oil. The spectra of the rubber exudates (after 200 hours pressing) and the silicone oils are presented in Figures 2 through 6.

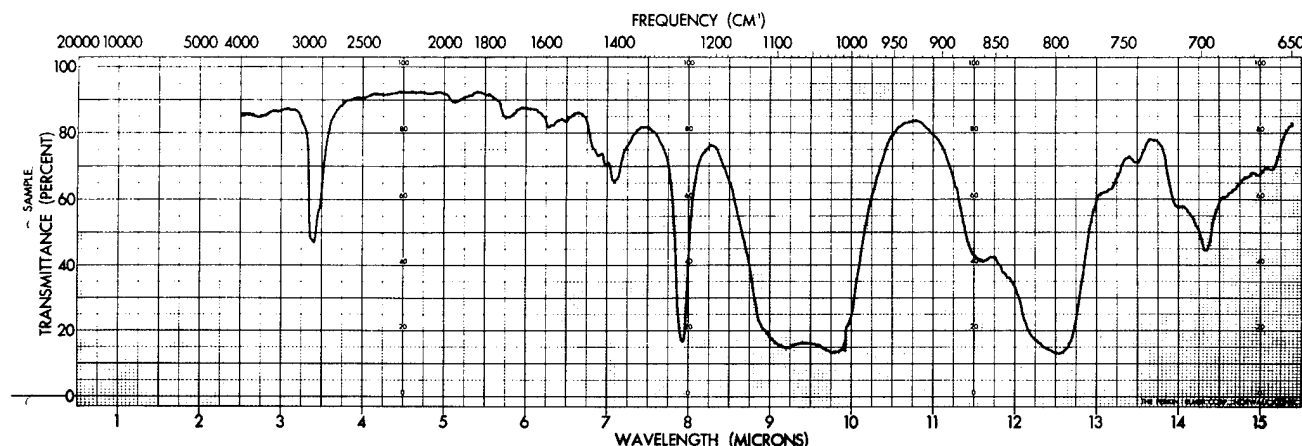


Figure 2. IR spectrum of exudate, Varox, 200 hrs pressing

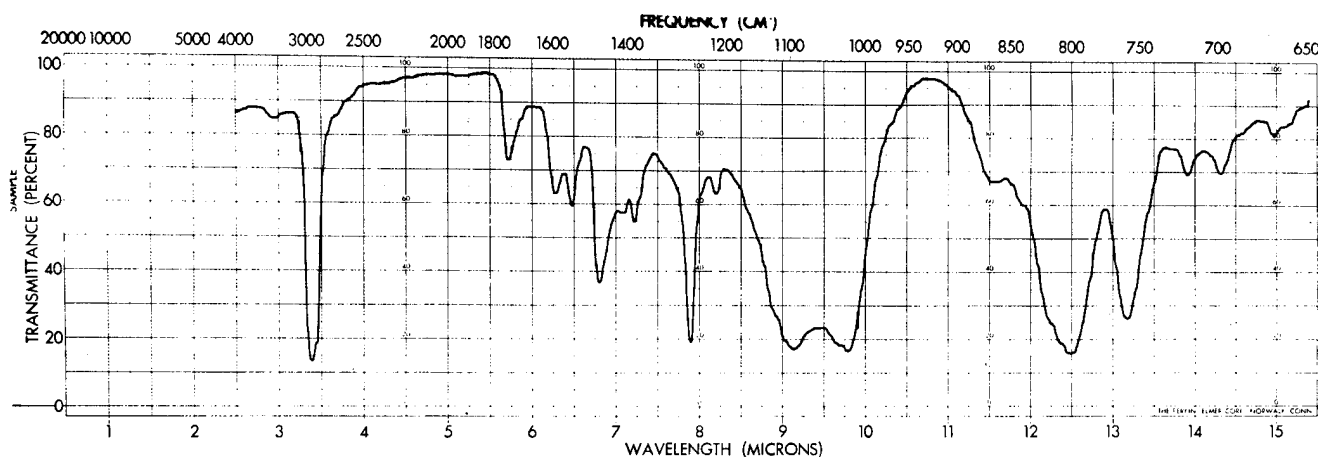


Figure 3. IR spectrum of exudate, Cadox TS-50, 200 hrs pressing

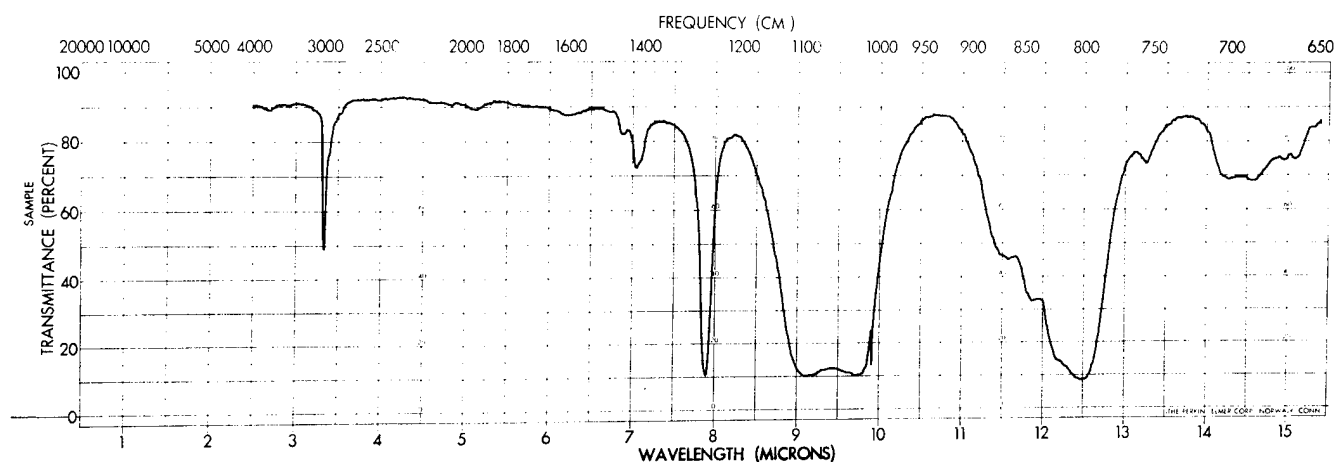


Figure 4. IR spectrum, DC200 (dimethyl silicone oil)

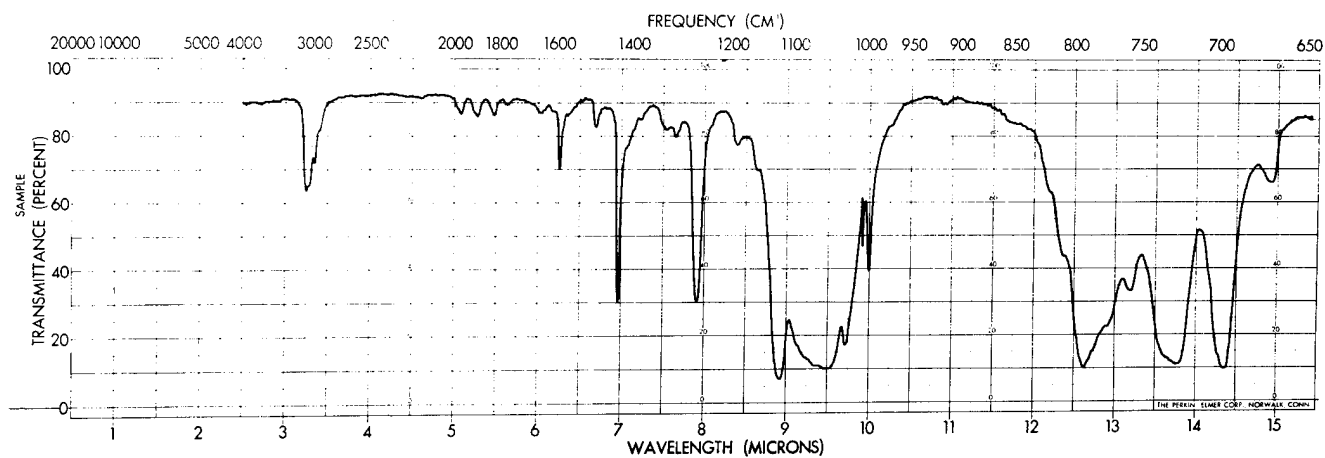


Figure 5. IR spectrum, DC705 (methylphenyl silicone oil)

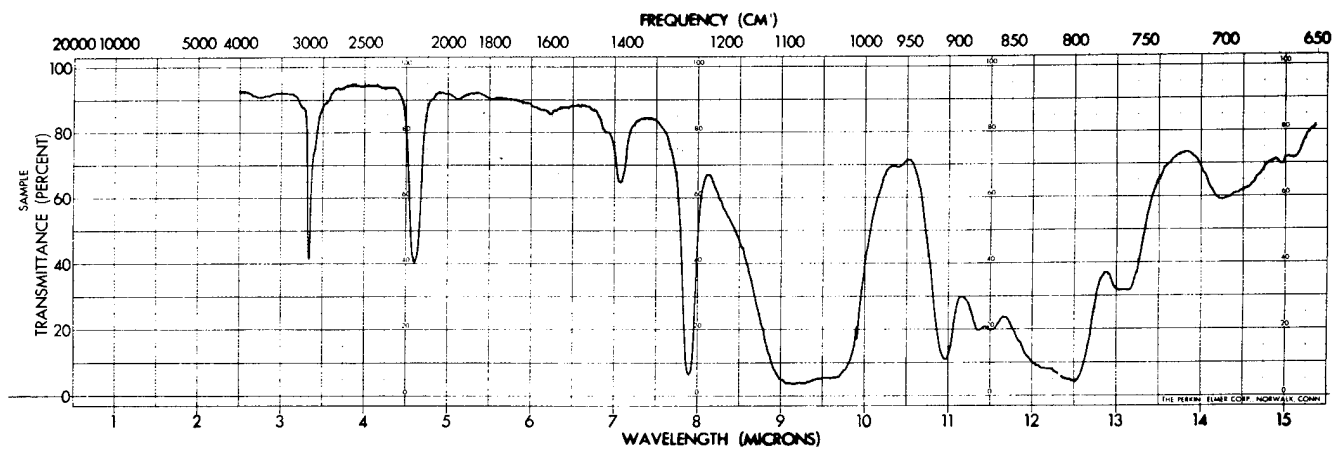


figure 6. IR spectrum, GE 93-022 (methylvinyl silicone oil)

These show the characteristic doublet at 9.2μ and 9.8μ for the Si-O-Si linkage in long-chain siloxanes. The bands at 4.6μ and 11μ observed for methylvinyl silicone oil are not seen in the exuded oils. Also very little vinyl-substituted siloxane should be present according to the rubber formulation unless it was selectively exuded. The sharp peak at 7.9μ and the broad band at 12.5μ are characteristic of the Si-methyl and methyl-Si-methyl groupings, respectively; the peak at 3.4μ and 7.1μ are characteristic of the methyl group. The exuded oils thus appear to contain dimethyl siloxane. The characteristic bands for the Si-phenyl linkage are at 7.0μ , 8.9μ and 10μ and a group of two or three bands between 13.5μ and 14.5μ ; three bands are observed for diphenyl siloxanes.⁽³⁾ The spectra of exuded oils show only the two peaks attributable to methylphenyl siloxane; the other three peaks at 7.0μ , 8.9μ and 10μ are somewhat difficult to detect

with certainty in the exuded oils because of interference with the Si-methyl and O-Si-O absorptions and the instrument slit-interchange perturbation. (In some spectra other than those selected for presentation here, these peaks show up more clearly).

From this analysis of the IR spectra and from knowledge of the manufacturing process, it was concluded that the exuded oils are primarily a mixture of dimethyl siloxane and a methylphenyl siloxane. The ratio of phenyl to methyl groups was determined from the IR intensities.^(3,4) The intensities of the 7.9μ band were used as an indication of the amount of dimethyl siloxane; the 14.3μ band was used to determine the amount of methylphenyl siloxane. Determined in this way the composition of exuded oil from Cadox and Varox cured rubbers as a function of disc-pressing time is given in Table IV. Although the accuracy of this method is limited by the instruments and sampling

Table IV
Composition of Exuded Oil from SE 5601 Rubber

	Time Pressed (hours)	% Dimethyl Siloxane	% Methyl- phenyl Siloxane
Cadox cured	0	78	22
	100	86	14
	200	80	20
	300	83	17
	400	92	8
	500	85	15
Varox cured	0	81	19
	100	85	15
	200	79	21
	300	82	18
	400	87	13
	500	92	8

techniques, the ratio of the amount of the methylphenyl to the dimethyl siloxanes is considered significant, and the results indicate that a reasonable approximation to the ratio of dimethyl to methylphenyl siloxane in exuded oils is 85:15. This is in good agreement with results obtained previously with solvent-extracted oils.⁽²⁾

Gel permeation chromatography (GPC) was used to determine the range of molecular weights of the exuded oils. A DuPont

Model 820 liquid chromatograph was used with five one-meter columns of Corning controlled porosity glass (two each 70 Å, one 175 Å and two each 700 Å). The elutant was a mixture of tetrahydrofuran and ethanol (99:1); the detector was a differential refractometer. By analysis of column retention times (molecular weight decreases with increased time) it was determined that a rather broad range of molecular weights was present (See Figure 7). The molecular weight distribution is also seen to vary as

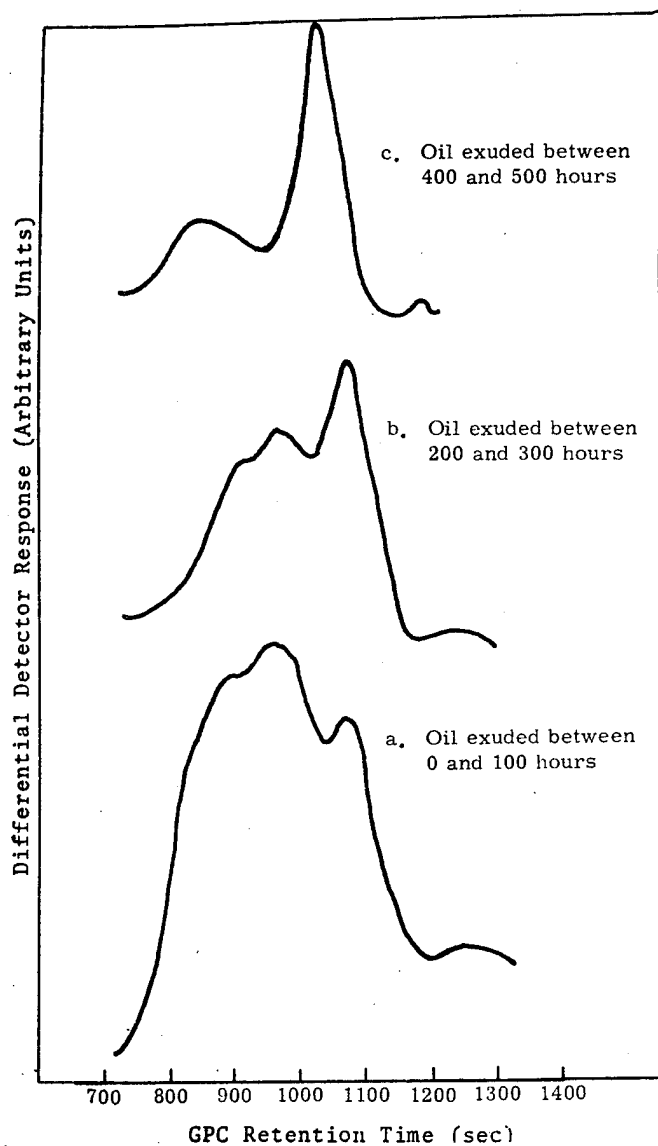


Figure 7. Gel permeation chromatography (GPC) retention times of exuded oils as a function of pressing time.

a function of the pressing time of the rubber discs; the longer the pressing time the higher the molecular weight species. The data suggest that oils for simulating

From considerations of the IR and GPC data, the oil mixture chosen for coating PETN samples for long-term surveillance studies was 85% 1000-centistoke DC200, a high-

Table V

Gel Permeation Chromatography Retention Times of Silicone Oils

Oil	Viscosity (centistoke)	Molecular Weight	Retention Time (sec)
DC200	0	236	1125
DC200	5	700	1130
DC200	50	~4,000	1083
DC200	20	-	1040
DC200	200	11,000	1015
DC200	1,000	-	945
DC200	12,500	-	932
DC705	170	546	1182

the exuded oils should be a mixture of high and low molecular weights. Retention times of selected silicone oils are given in Table V.

molecular-weight dimethyl silicone oil, and 15% 170-centistoke DC705, a low-molecular-weight methylphenyl silicone oil. An IR trace of this silicone oil mixture is shown in Figure 8.

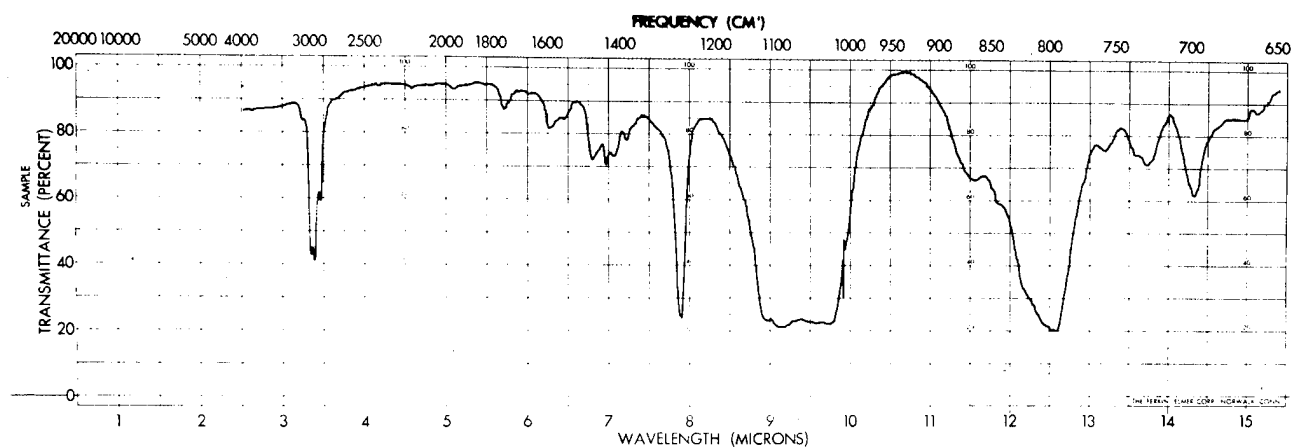


Figure 8. IR spectrum, 85% DC200, 15% DC705

Ten-gram samples of RR5K type PETN (ER-6044 Batch No. 1159) were coated with this mixture in hexane. Hexane was chosen as the slurry vehicle because it dissolves the silicone oils but does not affect the PETN. The oils were slurry deposited with stirring; the stirring action caused some PETN particle comminution. A much larger amount of oil was deposited on the PETN than was exuded onto the PETN in the detonator cavity. This was done in an effort to enhance and/or accelerate any physical or chemical interactions between oil and powder so that potential problems could be detected as soon as possible. Quantitative analysis of the amount of oil deposited on the PETN was performed by neutron activation analysis.⁽⁵⁾ The amount of oil was determined by comparison with a reference sample of DC200 silicone oil. Four randomly picked samples were run in quintuple redundancy. The results are reported in Table VI and show that about 8% by weight

- (1) PETN as received, stored at room temperature,
- (2) PETN as received, stored at 50°C,
- (3) PETN stirred with hexane, stored at 50°C,
- (4) PETN coated with 8% silicone oil, stored at room temperature, and
- (5) PETN coated with 8% silicone oil, stored at 50°C.

The following checks were made on the five samples after 3, 6 and 9 weeks, and 1 and 2 years under the above conditions:

- (1) Differential scanning calorimetry (DSC) was used to measure the heat and temperature of fusion to note any changes in crystal internal energy or chemical degradation.
- (2) Infrared analysis was done to note any chemical interactions.
- (3) X-ray diffraction analysis was

Table VI

Weight Percent Silicone Oil on PETN

	Sample 1	Sample 2	Sample 3	Sample 4
1	6.66	7.94	6.66	8.41
2	7.13	7.35	7.77	8.67
3	8.11	8.57	8.74	5.77
4	9.29	8.77	7.82	6.63
5	8.31	8.24	9.57	9.31
Average at 95% confidence level	7.90±1.24	8.17±0.67	8.11±1.32	7.76±1.79

of oil was coated on the PETN; this compares with a fraction of a percent expected in the detonator cavities.

The PETN samples were subjected to the following treatments.

used to note any chemical interactions or changes in strain patterns of the powder.

- (4) Zeiss particle analysis was made to note any physical changes such as particle size and shape.

4. RESULTS OF LABORATORY TESTING

The Perkin-Elmer DSC-1 was used to measure the temperature and heat of fusion (ΔH_f) of the samples. The ΔH_f was calculated from the peak areas measured with an Ott planimeter. A sample of pure indium ($\Delta H_f =$

6.79 cal g^{-1} , melting point 155°C) was used to calibrate the instrument before each series of runs. The results are shown in Tables VII and VIII. Each value is the average of five runs and the error is reported as the standard deviation. The melting points were taken at the peak

Table VII

Melting Point ($^\circ\text{C}$) of PETN Samples as Function of Storage Time

Sample	3 Weeks	6 Weeks	9 Weeks	2 Years
Control, ambient temperature	141.3 ± 0.2	-	140.3 ± 0.2	140.0 ± 0.3
Control, 50°C	140.3 ± 0.5	140.6 ± 0.5	140.5 ± 0.3	140.9 ± 0.3
Hexane-treated, 50°C	141.1 ± 0.3	141.0 ± 0.2	140.4 ± 0.2	140.0 ± 0.3
Oil-coated, ambient temperature	140.8 ± 0.4	140.6 ± 0.4	140.5 ± 0.2	140.0 ± 0.3
Oil-coated, 50°C	140.8 ± 0.4	140.9 ± 0.3	140.6 ± 0.3	140.0 ± 0.3

Table VIII

Heat of Fusion of PETN Samples as a Function of Storage Time

Sample	ΔH_f (cal/g PETN)			
	1 Week	3 Weeks	1 Year	2 Years
Control, ambient temperature	35.1 ± 1.3	-	36.0 ± 0.4	35.7 ± 1
Control, 50°C	37.6 ± 1.2	37.3 ± 1.6	36.8 ± 1.4	35.9 ± 1
Hexane-treated, 50°C	37.3 ± 1.6	38.0 ± 0.2	36.8 ± 0.9	35.6 ± 1
Oil-coated, ambient temperature	34.9 ± 1.5	35.9 ± 1.2	37.2 ± 0.8	34.5 ± 1.5
Oil-coated, 50°C	36.9 ± 1.5	38.3 ± 1.7	33.0 ± 0.5	34.8 ± 1.5

maxima. There was no significant difference between the melting points of these five samples and the 140°C to 141.5°C literature value for PETN.⁽⁶⁻⁹⁾ The fact that the melting point of PETN was not depressed by the presence of the oil suggests that there is no gross interaction between oil and powder. Also, there is no significant difference in the ΔH_f of the five samples and the values reported by Rogers and Dinegar,⁽⁶⁾ and thus no crystal phase change is indicated.

Infrared spectra were taken on each of the five samples as a function of storage time. The samples were mixed with KBr and run as pressed pellets on the PE21 IR spectrophotometer. Representative spectra of PETN oil-coated PETN and oil-coated PETN stored for two years at room temperature and 50°C are shown in Figures 9 to 12. The spectra are essentially identical except that the oil coated PETN samples display the stronger peaks of the silicone oil. The intensities of these peaks relative to the intensity of

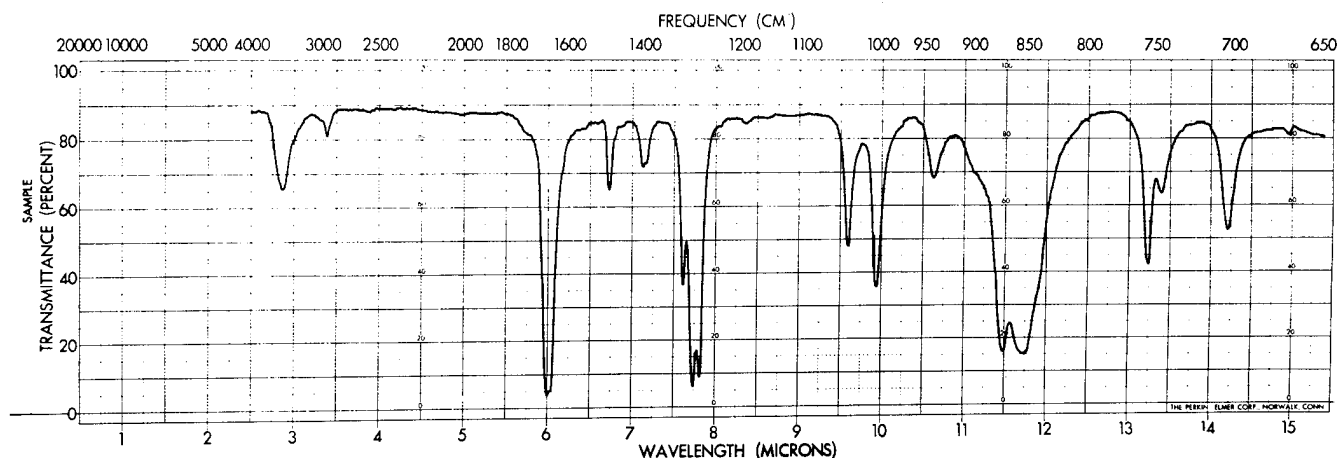


Figure 9. IR spectrum of PETN as received

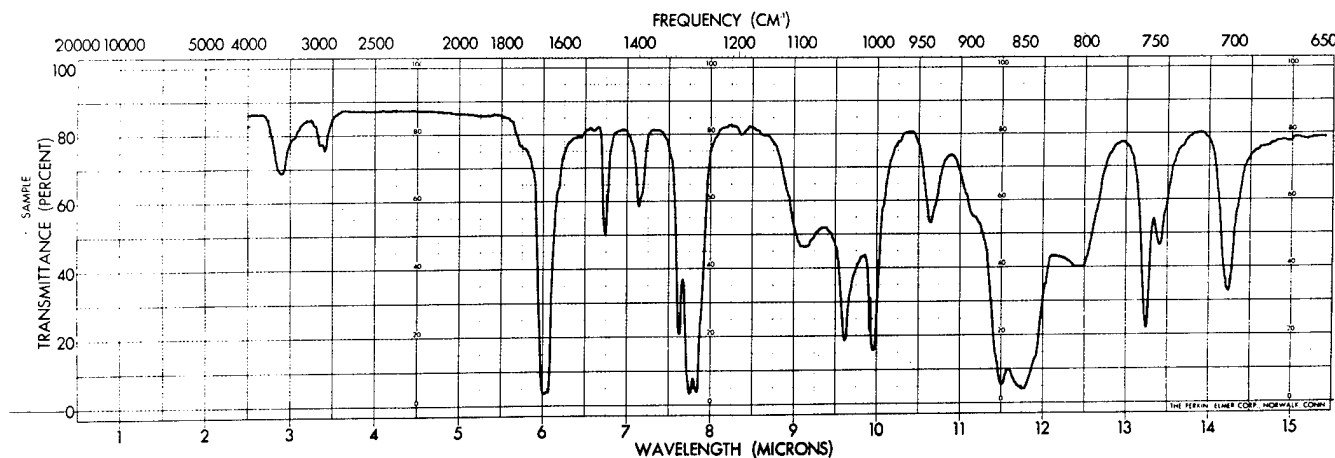


Figure 10. IR spectrum of oil-coated PETN immediately after preparation.

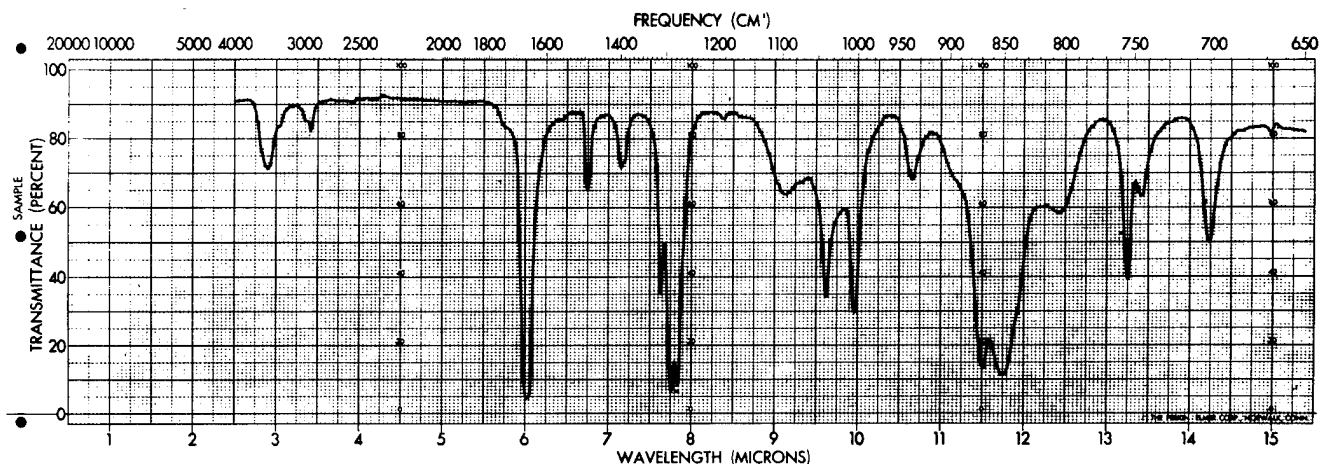


Figure 11. IR spectrum of oil-coated PETN, 2 years at ambient temperature

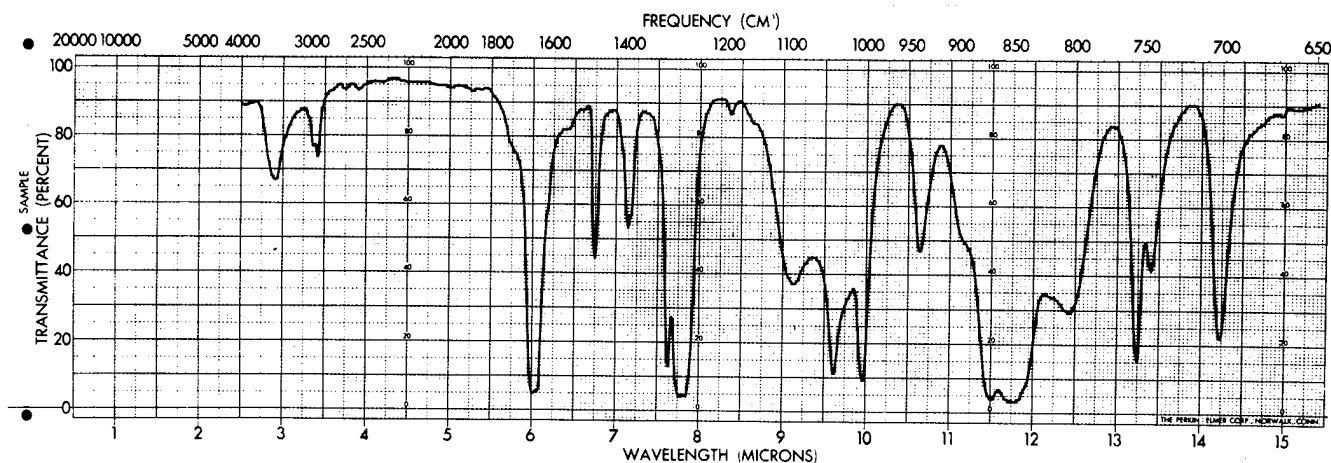


Figure 12. IR spectrum of oil-coated PETN, 2 years at 50°C

peaks due strictly to PETN did not change significantly over the two years.

X-ray powder patterns were taken on each sample of PETN under the conditions stated previously. A Philips Model 12045 diffractometer was used with a copper target. All of the patterns were identical and due entirely to PETN I,^(7,8) the normal phase of PETN

The PETN samples were subjected to Zeiss particle-size analysis. In this tech-

nique photomicrographs of the dispersed crystalline masses are made; a representative number of particles on the film are sized visually and semiautomatically as to length, width, shape factor, etc. These data may be used per se or converted via computation to other forms of particle description such as surface area per unit volume or weight. This latter method reduces the data for a sample to a single number. Photomicrographs of the five samples taken at the start of the experiment and after 2 years are shown in Figures 13



Figure 13. Sample type 1, control, as received (left) and after 2 years at ambient temperature

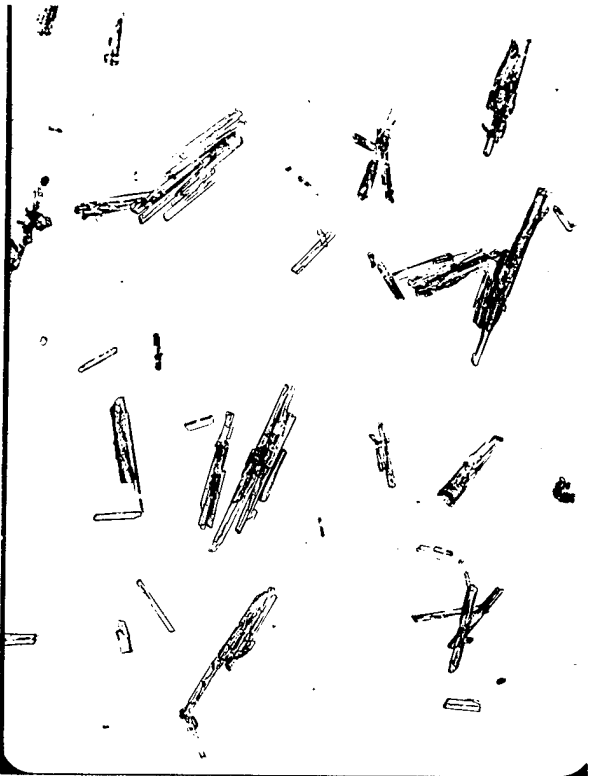


Figure 14. Sample type 2, untreated, as received (left) and after 2 years at 50°C



Figure 15. Sample type 3 when first stirred with hexane (left) and after 2 years at 50°C

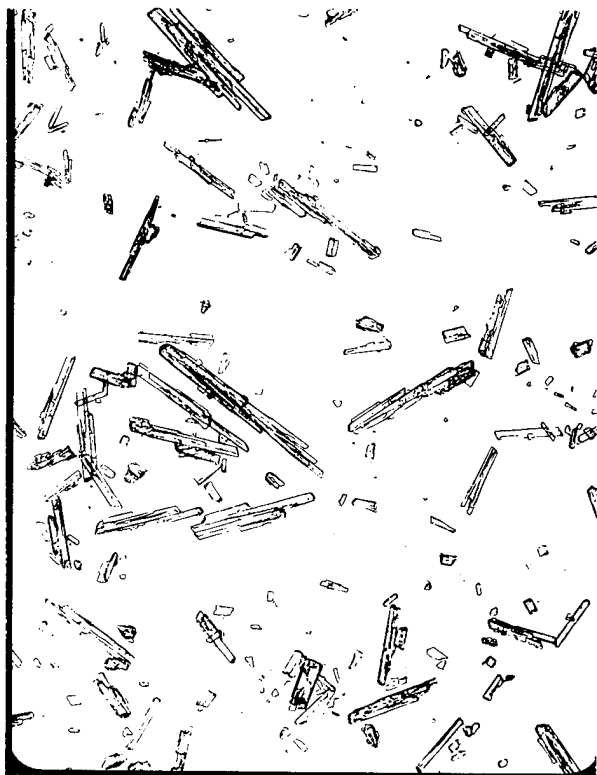


Figure 16. Sample type 4, oil-coated, after 6 weeks (left) and after 2 years at ambient temperature

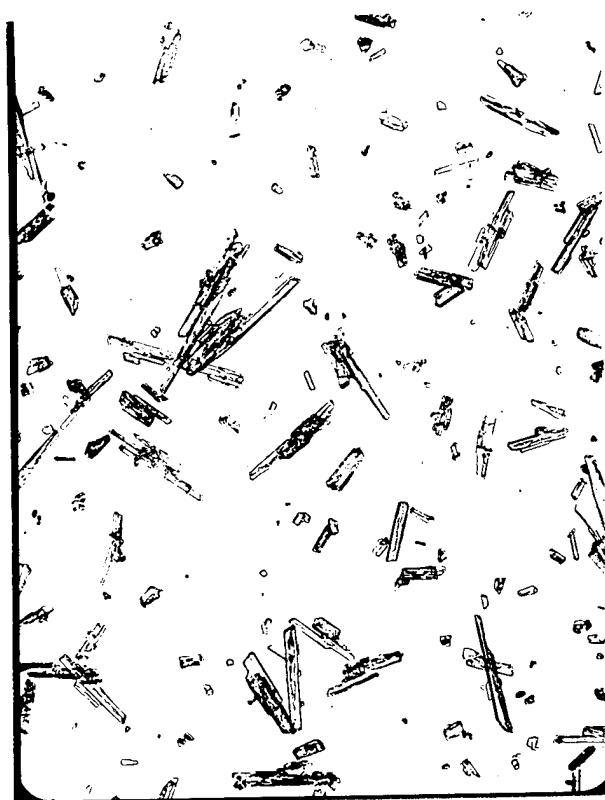


Figure 17. Sample type 5 when first coated with oil (left) and after 2 years at 50°C

to 17. The effect of stirring during slurry coating of the PETN can be seen; particle comminution, and, in particular the formation of small crystalline fragments should be noted. Except for this feature, no particular difference between oil-coated and uncoated PETN is noticeable. No change, either in size or shape, is apparent in any sample after two years of storage. It is particularly noteworthy that even the very tiny fragments persist after two years of storage. Data generated by the Zeiss analysis confirm these visual observations; the calculated specific surface areas are given in Table IX.

These data scatter somewhat because of sampling problems and counting limitations; however, no deleterious changes as a function of time because of oil coating are indicated. The effect of slurry stirring is observed as a larger specific surface area, as expected.

The laboratory experiments thus give no indication of long-range incompatibility between PETN and silicone oils.

Table IX

Zeiss Analysis Specific Area of PETN Samples

	Temperature	Specific Surface Area* at Time Indizted (cm ² /g)				
		Initial	3 Weeks	9 Weeks	1 Year	2 Years
As received	Ambient	1125	--	1350	1250	1000
As received	50°C	1100	1275	1400	1050	1350
Hexane-treated	50°C	1475	1050	1350	1050	1250
Oil-coated, hexane carrier	Ambient	1400	--	1550	1475	1250
Oil-coated, hexane carrier	50°C	1650	1550	1575	1200	1375

* Errors associated with these calculated surface areas are about ± 125 cm²/g.

5. CONCLUSIONS

The results of the laboratory tests of oil-coated PETN show no long-term physical or chemical incompatibility between PETN and silicone oils at the very high levels of 8% oil by weight. The test-firing data confirm the short-term anomalous detonator performance of PETN caused by silicone oil in the powder cavity; no adverse long-term PETN/silicone oil initiations have been observed after two years of testing. Because high temperatures apparently accelerate this phenomenon, no adverse effects are expected for a time period in excess of two years.

interaction or incompatibility between PETN and the silicone oil. Artificially oil-coated PETN as well as cabled production detonators (the cable connector contains the silicone "O" ring from which oil was squeezed into the detonator cavity causing anomalous PETN lot-acceptance firing results) have been test fired after environmental storage. These test firings indicate no deleterious effects in PETN, because of the presence of the oils, after two years of storage. Elevated temperature aging studies indicate that PETN detonators containing small amounts of silicone oil should perform satisfactorily for periods considerably longer than two years.

6. SUMMARY

Oils exuded from silicone rubber have been isolated, identified, and simulated by a mixture of commercial silicone oils. PETN has been coated with this mixture and stored at room temperature and 50°C. A battery of physico-chemical laboratory tests have shown no long-term adverse

REFERENCES

1. CRD Memo, H. M. Barnett to Distribution dtd 12/29/70, subject, Compilation of Data Associated with Cable-Time Effects on Detonators.
2. E. A. Kjeldgaard, personal communication, 12/3/70.
3. J. H. Lady, et al, Anal. Chem. 31, No. 6 (1959), p. 1100.
4. H. H. Willard, et al, Instrumental Methods of Analysis, D. Van Nostrand Company, New York, 1958.
5. R. Daniel, et al, Chimia 21 (1967), p. 554.
6. W. C. McCrone, Microchem. J. 3 (1959), p. 479.
7. R. N. Rogers and R. H. Dinegar, "Thermal Analysis of Some Crystal Habits of Pentaerythritoltetranitrate," LASL, Los Alamos, New Mexico
8. H. H. Cady, "Pentaerythritoltetranitrate II, Its Crystal Structure and Transformation to PETN I," American Crystallographic Association Symposium, Tulane University, March 1970.
9. E. Berlow, R. H. Barth, and J. E. Snow, The Pentaerythritols, Reinhold, New York, 1958.

THE EFFECT OF HUMIDITY ON THE PERFORMANCE OF HNAB

D. J. Gould and T. M. Massis
Actuator and Chemical Component Division 2515
and
W. D. Harwood
Materials and Energy Components Division 9525
Sandia Laboratories
Albuquerque, New Mexico 87115

ABSTRACT

The compatibility of hexanitroazobenzene (HNAB) with the humid atmospheres which can occur in weapons has previously not been directly investigated. In this study HNAB, both as bulk powder and as manufactured into mild detonating fuse (MDF), was subjected to two types of humid environments. After one year of exposure, the HNAB timing performance was essentially unaffected, although some slight decomposition was observed.

A secondary result of this investigation was the development of analytical techniques for detecting the decomposition products of HNAB which exist at less than 2% of the sample weight. Since HNAB is used extensively in precise timing applications, these techniques should prove useful in future compatibility studies of the explosive.

ACKNOWLEDGMENTS

The authors wish to acknowledge the contributing work of G. J. Janser, 2514, for VOD data acquisition; E. E. Ard, 9525, for statistical data reduction; and J. W. Budlong, 9342, for environmental test facilities.

1. INTRODUCTION

In August 1972 an investigation was started to determine the effects of a humidity environment on the explosive hexanitroazobenzene (HNAB) when used in mild detonating fuse (MDF). HNAB in MDF has been incorporated in a design for use in the MC2500 timer. This investigation was based

upon preliminary analyses of a few early prototypes of a weapon gaseous atmosphere which had revealed the presence of substantial quantities of water vapor. In the original design, HNAB-MDF used in the MC2500 would have been directly exposed to this humid weapon atmosphere and thus concern had been expressed about possible environmental effects.

HNAB,* an explosive material of rather recent use at Sandia, has been utilized in a number of components for precise timing applications. As a powder, HNAB has proved to be a reactive compound, and numerous compatibility problems have been found to exist.^(1,2) The HNAB structure is strongly subject to attack by nucleophilic agents such as amine, methoxide, and hydroxyl groups. The azo group and to lesser extent the nitro groups are also subject to reductive degradation.⁽³⁾ Thus, since the chemistry of HNAB in theory and practice has revealed compatibility problems, a potential humidity problem could not be arbitrarily ruled out.

2. PREVIOUS WORK

Past work dealing with the effects of humidity with HNAB and HNAB-MDF was practically nonexistent. Three development reports (plus personal communication with the authors) on aluminum-sheathed MDF utilizing HNAB powder made no mention of the effect of humidity on the powder.^(4,5,6) A comprehensive literature search revealed no direct mention of any work on the effects of water or humidity on HNAB.

Two programs involving HNAB-MDF indirectly studied the effects of humidity.^(7,8) In these programs, full timer assemblies were subjected to a cycled humidity environment. Since the timers contained HNAB-MDF, the environmental humidity cycles gave an indication of the effect of humidity

on the explosive cord. In both studies, however, the MDF in the timer was sealed (though not hermetically) in a silicone rubber. Also, the detonator was exposed to the outside environment, allowing possible permeation and migration of moisture into the MDF. The latter was considered as the more likely path.

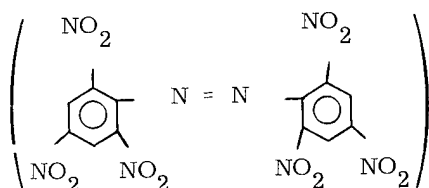
The first program was a factorial experiment which included mechanical shock, thermal shock, and vibration environments, as well as humidity.⁽⁷⁾ Twelve MC2361 timers, fired after environmental conditioning, fell well within the system requirements. The humidity environment was ten 24-hour cycles from 80°F, 100% RH to 110°F, 75% RH.

In the second program, a group of MC2361 and MC2453 timers were subjected to ten 20-day cycles from -36°F to 160°F, at a relative humidity of 100% corrected to room temperature.⁽⁸⁾ Thus the humidity varied as the temperature was cycled. No change in performance of the timers was observed within experimental error.

3. EXPERIMENT

Although the direct programs mentioned above give us confidence in regard to the specific timer performance, the question of the effects of humidity upon HNAB powder and HNAB-MDF remained open. To answer this question an extensive humidity/time study was carried out.

* The structure of HNAB is shown below.



3.1 MATERIALS

Made available for this study were 680 feet of war-reserve-quality, 2-grains/foot HNAB-MDF (Lot 2375) made by the Ensign-Bickford Corporation.⁽⁹⁾ This MDF utilized HNAB powder manufactured by the Northrup-Carolina Corporation (now Chemtronics). From similar powder, previous lots of MDF had been used in the production of such timers as the MC1984, MC2361, and MC2453. Also made available were 500 grams of Northrup-Carolina Lot 36-7 HNAB powder. This powder was the same as that used in the MDF above. Data on the MDF are given in Figure 1.

Of the 680 feet of MDF made available for this study, 190 feet were removed and pressurized to 60,000 psi for 2 minutes (Figure 2). Pressurization of HNAB-MDF increases the velocity of detonation (VOD) slightly and decreases the VOD sigma significantly.

The HNAB powder was used directly as received except that it was subdivided into 50-gram batches and placed in glass recrystallization dishes.

3.2 HUMIDITY PROGRAMS

The two humidity-time programs initiated were as follows:

- A. The first program used an isothermal, constant-humidity environment of 120°F at 90% relative humidity.
- B. The second program used a standard temperature/humidity cycle over a wide range called a "jungle" cycle, as outlined in a Sandia Labs environmental handbook.⁽¹⁰⁾ Details of this 48-hour "jungle" cycle, at a relative humidity of 93% at each temperature, are outlined in Figure 3.

To each humidity environmental chamber the following were added:

- A. Three 50-gram bulk Lot 36-7 HNAB samples in uncovered glass crystallization dishes. Protective tops were placed 2 inches above the dishes to prevent possible water condensation from dripping on the HNAB.
- B. Fifty 15-inch samples of the pressurized Lot 2375 HNAB-MDF.

Sampling periods chosen were 1, 2, 4, 8, 16, 32, and 64 weeks; five MDF samples and 5 grams of the HNAB powder were randomly removed at the end of each exposure period. Three inches of each piece of MDF were removed from one end and retained for chemical and physical analysis; the remaining 12 inches were used for detonation velocity measurements. The 5-gram HNAB powder sample was retained for chemical and physical analyses.

In addition, two of the three 50-gram bulk HNAB samples in the environmental chambers were removed at the end of 16 and 64 weeks. These samples were then blended for uniformity, sampled for historical purposes, and sent to Ensign-Bickford for manufacture into MDF in accordance with the original Sandia specification (which was used for the Lot 2375 HNAB-MDF). After their return, the humidity-conditioned HNAB-MDF was to be tested for its explosive, chemical and physical properties.

The 16-week sample has been manufactured and returned to Sandia for testing, but the 64-week sample has been sent only recently to Ensign-Bickford. After return to Sandia for testing, sometime in the future, the 64-week bulk sample results will be given later in an addendum to this report.

THE ENSIGN-BICKFORD COMPANY
QUALITY CONTROL DEPARTMENT
CERTIFICATE OF COMPLIANCE AND ANALYSIS

To: Sandia Corporation Igloo Receiving Area 2315 Weinmaster, Sandia Base Albuquerque, New Mexico 87115		Lot No. 2371, 2372, 2374, 2375, 2376.		Partial No. 2	
		QUANTITY			
Consigned to: Same Customers P.O. No. 58-8501 Item No. 1		Ordered 300' to UMC 700' to Sandia		Shipped 300' to UMC Part. 1 680' to Sandia " 2	
Material 2 gr/ft HNAB AL MDF		Dwg No. & Rev. No.		Spec No. & Rev. No. SS209838 Rev. C	
Method of Packing Straight Lengths in Tubes, Wood Box		E. B. Co. Spec. No.		Invoice No. 5388-B	
		Contract No.		E. B. P/Request No. 5388	
Ship Via: Commercial Truck				Date Shipped 9/16/70	
It is Certified that the following are the results of tests prescribed for the above Item as required by the applicable specification. _____					
SS209838 Rev. C, and Contract 58-8501.					
Applicable Authorized waivers or changes _____					
TEST REQUIRED	SPEC. LIMITS OR REQUIREMENTS	NO. OF PCS. TESTED	TEST RESULTS		
Velocity of Det.	6200 Meters/sec. Min.	5/lot	See Page 2, acceptable		
Coreloads	2.0 ± 0.2 gr/ft.	5/lot	See Page 2, acceptable		
Type H Explosive Lot #36-7 (N.C.)	Core Material (HNAB) was supplied by Sandia Corporation.				
Sheath-Aluminum Lot #P-30182	Aluminum Content 99.95% Pure (Min.)		Vendor Certified, acceptable.		
Radiographic	MIL-STD-453 and E-B Co. Spec. PS0001/A Class II	100%	Shippable Lengths acceptable.		
Diameter	0.041" ± 0.001"	100%	0.040" acceptable.		
Wall Thickness	0.007" Min.	1/lot	0.008" Min., acceptable.		
#2375-	20 Lengths 200 ft.	2.06 gr/ft	6723 Meters per sec.		
		2.16 " "	6724 " " "		
		2.02 " "	6709 " " "		
		1.98 " "	6750 " " "		
		2.03 " "	6698 " " "		

Figure 1. MDF data
IV-B-4

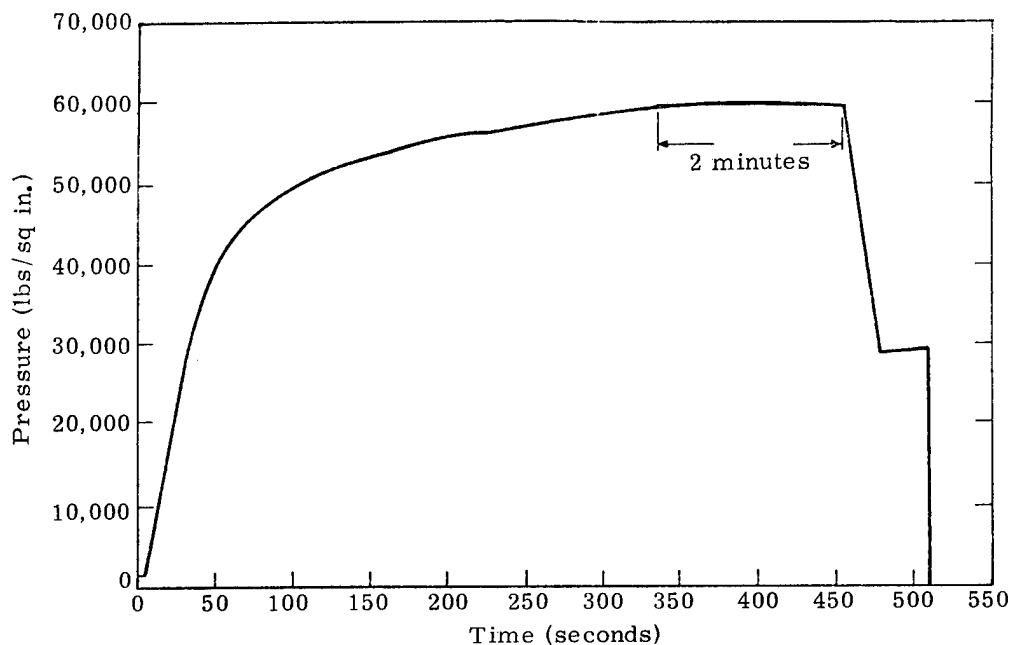


Figure 2. MDF pressurization curve for Lot 2375 HNAB-MDF

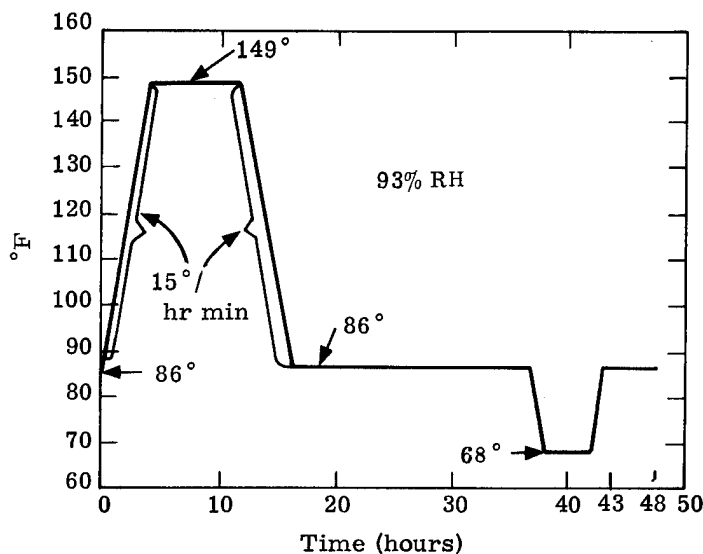


Figure 3. "Jungle" cycle temperature/time profile⁽¹⁰⁾

3.3 EXPLOSIVE TESTING

Two explosive testing procedures were used to evaluate the exposed MDF samples:

- 1. Function time or velocity of detonation (VOD) over a given distance.
2. Output measurements utilizing the plate dent test.

Function-time and VOD measurements were made over a distance of 10 ± 0.002 inches, using a standard MDF test fixture. The MDF was initiated from the environmentally exposed end with a Reynolds Corporation RP-2 PETN-loaded detonator. The function time was measured between lacquer-coated copper wire ionization switches on a Nano-fast counter and a raster oscilloscope trace (as a

back-up). After firing of the five MDF samples from each exposure and environmental conditions, a statistical analysis was performed on the samples of that time period. This analysis was compared to nonconditioned baseline VOD measurements of the pressurized HNAB-MDF, and the comparison was followed by a complete analysis of variance for the study as a whole.

The explosive output measurements were performed with the use of the standard plate dent test for energy released by the detonating MDF. A number of the 3-inch pieces of MDF removed from the original 15-inch exposure samples were fired with a Reynolds Corporation RP-2 detonator, with the environmentally exposed end in contact with the plate dent test block. After firing, standard techniques were used to measure the extent of the dent from the detonated MDF, and the results were then compared with those from other tested samples.

3.4 CHEMICAL AND PHYSICAL ANALYSIS

To measure the possible changes occurring in the environmentally conditioned samples (both the HNAB powder and MDF samples), three analytical techniques were utilized:

1. thermal analysis,
2. thin-layer chromatography (TLC), and
3. scanning electron microscopy (SEM).

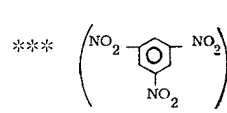
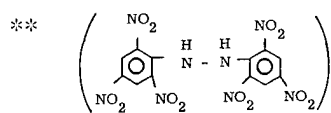
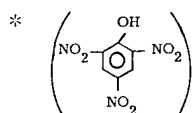
Thermal analysis -- Thermal analyses using a duPont 900 thermal analysis system were performed with the Differential Scanning Calorimeter (DSC) and Thermogravimetric Analyzer (TGA) modules on both the HNAB powder and MDF. It

was hoped that the various techniques used would provide data on thermal decomposition rates, on variations in the HNAB polymorphic transition and melting-point temperature, and on the presence of decomposition impurities.

The DSC (quantitative DTA as used by the duPont thermal analysis system) was chosen over the DTA module because the MDF samples could be run without removing the explosive from the aluminum sheath. Past results on numerous MDF samples left intact have shown that there is little loss in sensitivity due to the presence of the large mass of sheath material relative to the mass of HNAB powder present.

Thin-layer chromatography (TLC) -- If changes were occurring in the HNAB and HNAB-MDF, the likely cause would be decomposition of the explosive. Thus an analysis, both qualitative and quantitative, of the HNAB was necessary. Two methods for doing this were considered, liquid chromatography and thin-layer chromatography (TLC). Equipment for liquid chromatography, though available at Sandia, was not operational at the time of the analysis. Thus TLC procedures were developed to separate, identify, and measure semiquantitatively the impurities of decomposition products in the HNAB.⁽¹¹⁾

All TLC separations and analyses were performed on prepared Kodak fluorescent silica-G-coated mylar plates and development apparatus. The subsequent separations of picric acid* and hexanitrohydrazobenzene** and HNAB were conducted with a solution of one part absolute ethanol to nine parts ethyl acetate; the separation of trinitrobenzene***



from HNAB was conducted with a solution of one part acetic acid, one part ethyl acetate, and four parts n-heptane. All chemicals were of reagent grade quality or better. Hexanitrohydrazobenzene was detected visually; the picric acid and trinitrobenzene were determined with a Chromato-Vue ultraviolet source (made by Ultra Violet Products, Inc.) with either the long- or short-wave sources.

All the bulk HNAB powders have been analyzed by TLC, with a representative number of MDF samples also analyzed. Because of the difficulty in removing the HNAB from the aluminum sheath, only representative MDF samples were analyzed by TLC.

Scanning electron microscopy (SEM) -- Recently an extensive program at Sandia with MDF materials (other than HNAB-MDF) involved an investigation of possible crystal growth of the explosive material within the sheath. A technique was developed in which the MDF sheath could be carefully cut and separated, exposing the explosive with little or no disturbance to the structure. The exposed explosive surfaces were then examined with an SEM, at various magnifications, to determine whether the crystal growth had occurred. This study revealed a close correlation between the degree of crystal growth and the occurrence of detonation problems.

This technique was used to compare the baseline and environmentally conditioned HNAB-MDF samples to detect crystal changes which might have occurred within the explosive core of the MDF.

4. RESULTS AND DISCUSSION

Visual observations of the HNAB powder and the MDF as they were removed from the humidity

chambers indicated that the isothermal/constant-humidity condition was a less severe environment than the jungle cycle for both the powder and the MDF. These observations were based on the corrosion of the high-purity aluminum sheath as well as the apparent decomposition of the exposed HNAB powder surfaces.

Extensive corrosion of the high-purity aluminum sheath material was evident on the MDF samples. SEM photomicrographs (~ 300X) of MDF samples which were not exposed, and of MDF samples exposed for 32 weeks, dramatically show the extent of the corrosion taking place (Figure 4). Note the nearly complete disappearance of the mechanical drawing marks on the exposed aluminum sheath. Although the isothermal/constant-humidity environment appeared to have been more detrimental to the aluminum than the jungle cycle, in reality it was not. The oxide coating on the jungle-cycle sheath is a hard, durable oxide surface, while that on the isothermal/constant-humidity sample is one that can be easily removed. During the cooling cycle of the jungle environment there is considerable condensation of the water vapor, with subsequent disturbance and removal of the nondurable oxide areas (such as those that exist on the isothermal/constant-humidity MDF samples). Thus the observed hard oxide coatings were left. In the isothermal/constant-humidity environment this "cleansing" action did not occur.

During sampling periods of the jungle cycle, portions of the HNAB powder were observed to be turning black near the walls of the glass recrystallization dishes. Upon removal of the 16-week, 50-gram bulk HNAB sample for MDF manufacture, a more careful examination of the black areas revealed that this black material occurred in the vicinity of white residues on the glass (Figure 5).

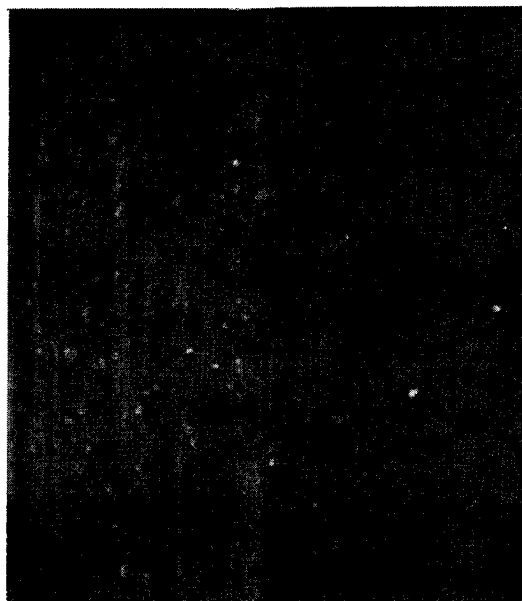
The white residues were quite similar to those observed when hard water is allowed to dry on glass surfaces.



0 weeks: baseline



32 weeks: isothermal/constant-humidity cycle



32 weeks: "jungle" cycle

Figure 4. Effects of humidity on aluminum sheating
(Lot 2375 HNAB-MDF) (300X)

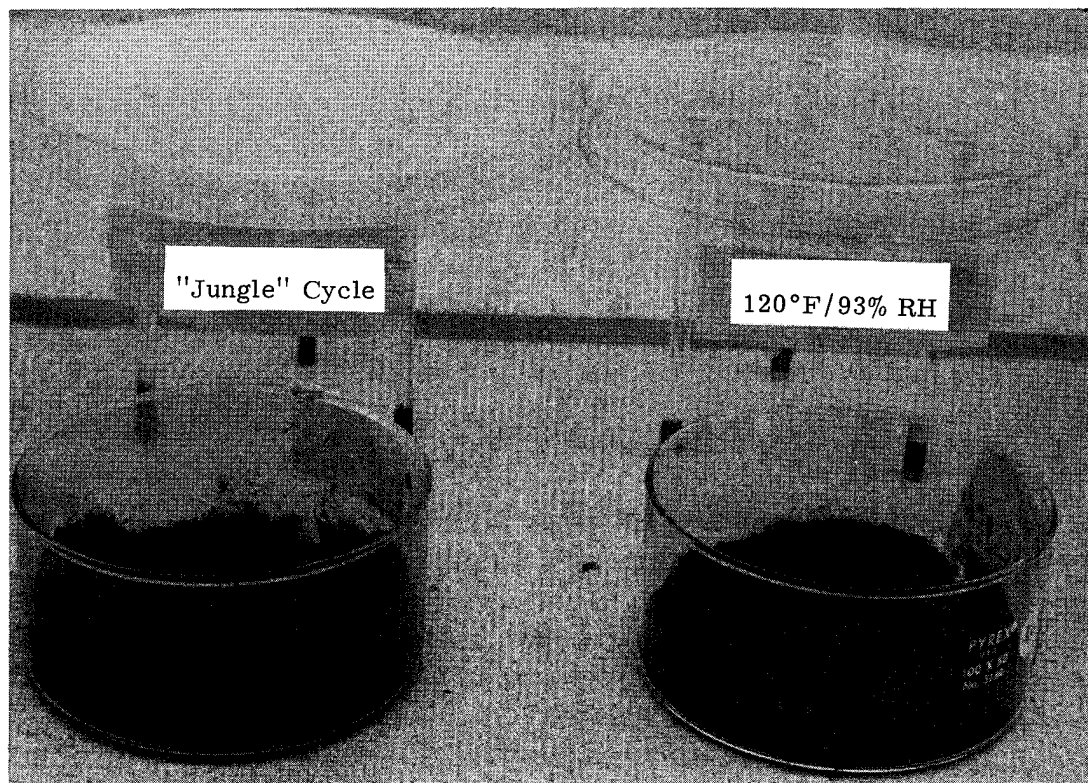


Figure 5. Effects of humidity on Lot 36-7 HNAB powder (16 weeks)

An analysis by emission spectroscopy of the white residues indicated that the major elements present were calcium, magnesium, aluminum, copper, and sodium, with minor amounts of strontium, iron, and silica. From this analysis, the two major sources of the residue were concluded to be the products of the corrosion of the aluminum tray holding the containers and impurities from the addition of humidity from untreated water in the chambers. Corrosion of the aluminum tray, which was quite evident, would account for the presence of the aluminum and copper; the other elements are those commonly found in the water supplies of the Albuquerque area.

The decomposition noted, which occurred only on the surfaces near the walls of the glass containers, can be explained by examining the cooling cycle. Condensation and subsequent dripping from the protective glass tops deposited small quantities of the

decomposing aluminum tray and water-hardness residues onto the HNAB surfaces near the walls. This alkaline solution resulted in the decomposition of the HNAB powder. Thin-layer chromatographic analysis of this deposit revealed the following materials and semiquantitative results: 0.8% picric acid, 0.2% trinitrobenzene, and 0.1% hexanitrohydrazobenzene, with the major portion remaining as HNAB.

If the presence of the hard water residues had been completely responsible for this decomposition, it would have been present over the complete HNAB surface, rather than only at the edges. (Introduced through the humidity inlets, these materials would have been spread by the oven fans equally throughout the chamber.) Furthermore, no evidence of corrosion was observed on the isothermal/constant-humidity samples or containers.

4.1 FIRING DATA

As described above, the MDF samples (both exposed and unexposed) were initiated for measurement of function time or detonation velocity over a 10-inch distance. Firing data were considered the prime diagnostic measurement for evaluating the MDF after exposure to both humidity environments. The determination of whether the HNAB-MDF was still within acceptable limits for use as a precise timing material was the primary objective of the humidity/time study. Table I and Figures 6 and 7 present the pertinent MDF firing data for the unexposed (or baseline MDF) and the exposed samples.

The general reaction of the samples to humidity was a small but rapid change to a slower detonation velocity than baseline through the first 4 weeks followed by a period of little change through the next 32 weeks. This trend in the data occurred for the MDF samples exposed to both the jungle-cycle and isothermal/constant-humidity environments. A noticeable but small increase in detonation velocity then appeared between 32 and 64 weeks. Both environmental exposures give the same general pattern, but greater fluctuations were observed in the jungle-cycle exposure.

In the past, this relatively rapid change to a slower detonation velocity through the first 4 weeks has been observed in both timers and HNAB-MDF which had been subjected to only thermal environments. Thus the reduction in detonation velocity was apparently not a result of the humidity environments.

Although this initial reduction in detonation velocity occurred, the change was quite small (with the maximum slowdown being 0.123 microsecond or

26 meters per second): Only a 0.35% decrease from baseline. Timing or detonation-velocity variations of this order are well within the values specified for MDF use in precise timing applications.

No entirely satisfactory explanation has been postulated to explain the slight but immediate lowering of the detonation velocity in HNAB-MDF when subjected to thermal environments. A lowering in the detonation velocity without the presence of decomposition is usually the result of a density reduction in the explosive materials, although no direct evidence exists to support this postulation.

The increases observed in the detonation velocity for the long-exposure MDF samples correspond quite closely to physical and chemical changes measured in the MDF HNAB with such diagnostic tools as thermal analysis, thin-layer chromatography and scanning electron microscopy (see later discussion).

Over the full test interval, the effects of exposure on velocity of detonation were somewhat different for the isothermal/constant humidity environment than for the jungle cycle. As shown in Figure 8A for the isothermal/constant-humidity environment, the positive slope of the regression line indicates increasing function time over the exposure period, which represents a decrease in velocity. Figure 8B presents the same data except with the test results for the base line samples removed. The confidence limit lines placed around the regression line show that there is no change of identifiable magnitude after the initial decrease in detonation velocity discussed above.

Figure 9A is the linear regression showing the effects of jungle cycle exposure on function time.

TABLE 1

"Jungle" Cycle Statistical Firing Data

	Baseline	One Weeks	Two Weeks	Four Weeks	Eight Weeks	Sixteen Weeks	Thirty-two Weeks	Sixty-four Weeks
Range (μsec)	0.098	0.082	0.054	0.037	0.075	0.103	0.075	0.127
Minimum (μsec)	34.198	34.311	34.277	34.326	34.329	34.243	34.292	34.249
Maximum (μsec)	34.296	34.393	34.331	34.363	34.399	34.346	34.367	34.376
σ (μsec)	0.028	0.032	0.021	0.018	0.029	0.045	0.029	0.039
\bar{N} (μsec)	34.245	34.342	34.303	34.347	34.368	34.309	34.323	34.294
Number	13	5	5	5	5	4 [*]	6	9

*One of the five shots failed to initiate due to fixturing.

Isothermal/Constant-Humidity Statistical Firing Data

	Baseline	One Weeks	Two Weeks	Four Weeks	Eight Weeks	Sixteen Weeks	Thirty-two Weeks	Sixty-four Weeks
Range (μsec)	0.098	0.038	0.061	0.072	0.083	0.070	0.028	0.092
Minimum (μsec)	34.198	34.288	34.274	34.300	34.281	34.304	34.322	34.220
Maximum (μsec)	34.296	34.326	34.355	34.372	34.364	34.374	34.350	34.312
σ (μsec)	0.028	0.016	0.030	0.033	0.031	0.028	0.011	0.031
\bar{N} (μsec)	34.245	34.308	34.300	34.338	34.313	34.337	34.337	34.227
Number	13	5	5	5	5	5	5	10

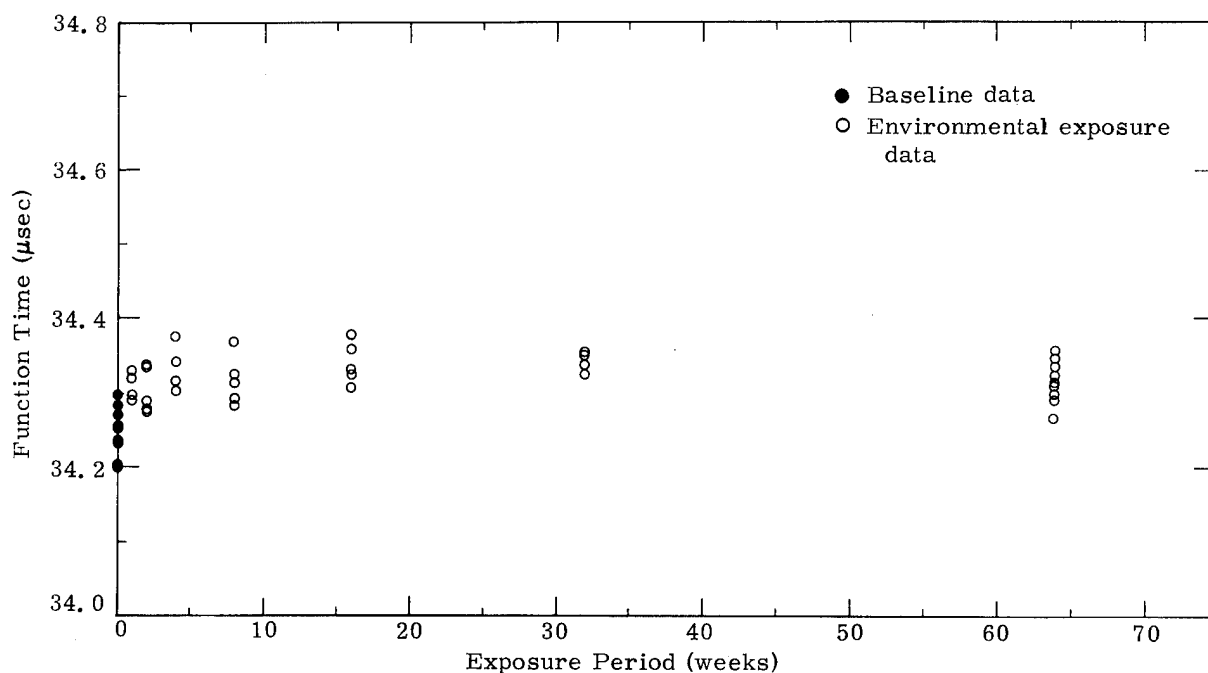


Figure 6. MDF function time vs isothermal/constant-humidity exposure period

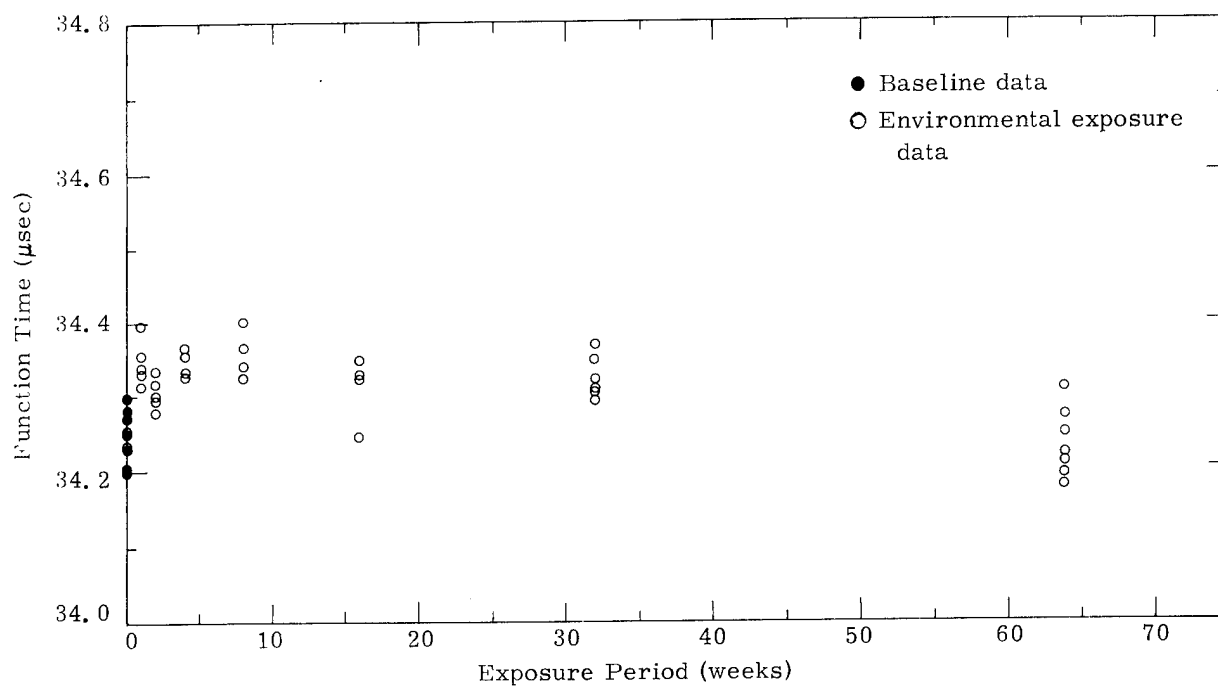


Figure 7. MDF function time vs "jungle"-cycle exposure period

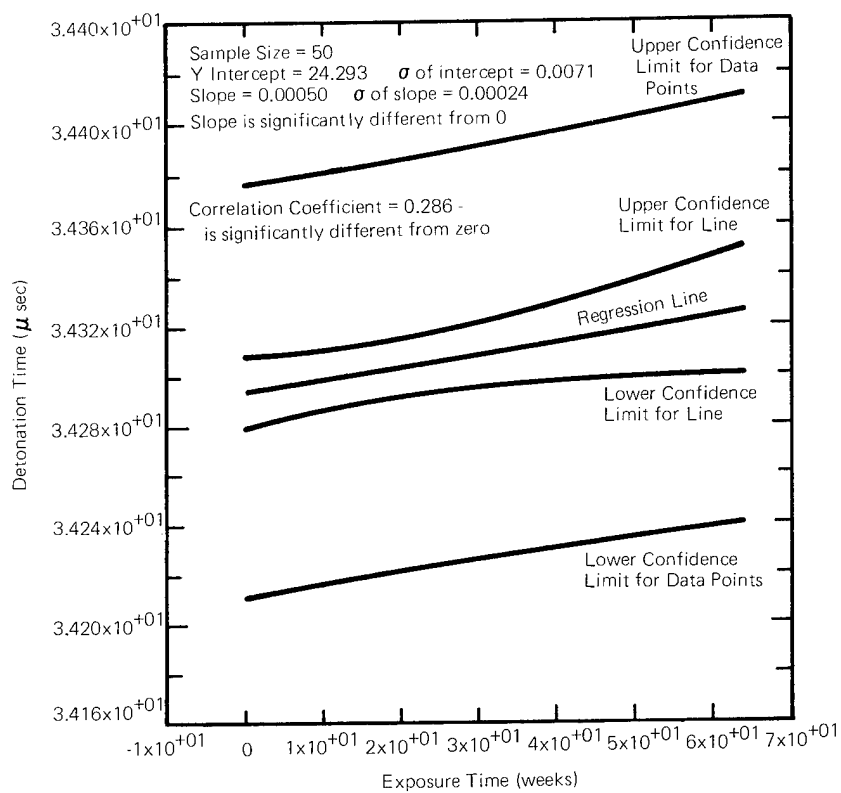


Figure 8A. Isothermal/constant-humidity firing data, linear response

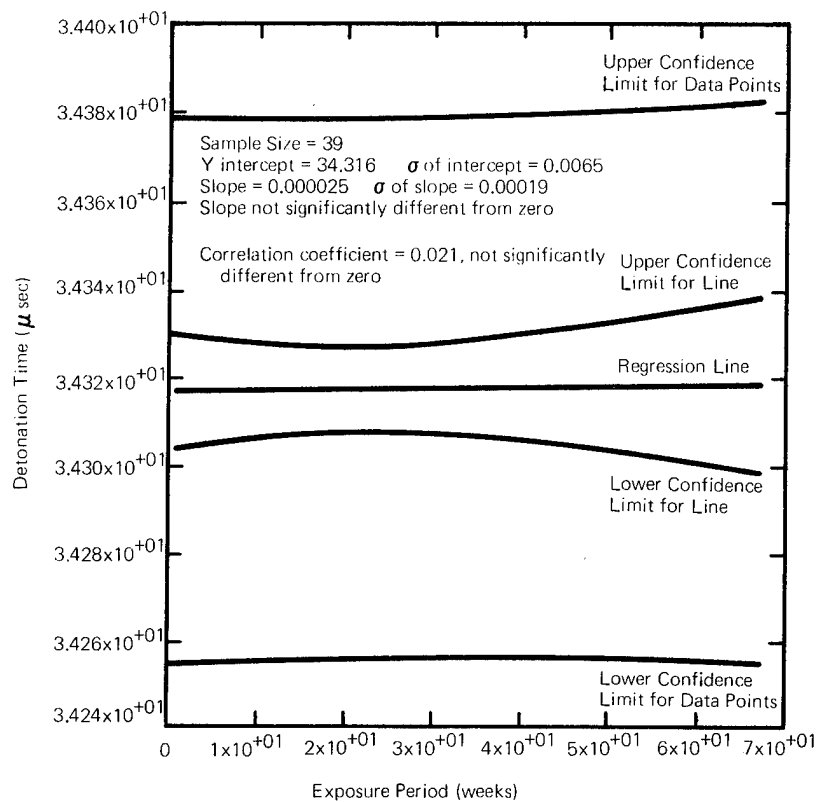


Figure 8B. Isothermal/constant-humidity firing data, linear response baseline data removed

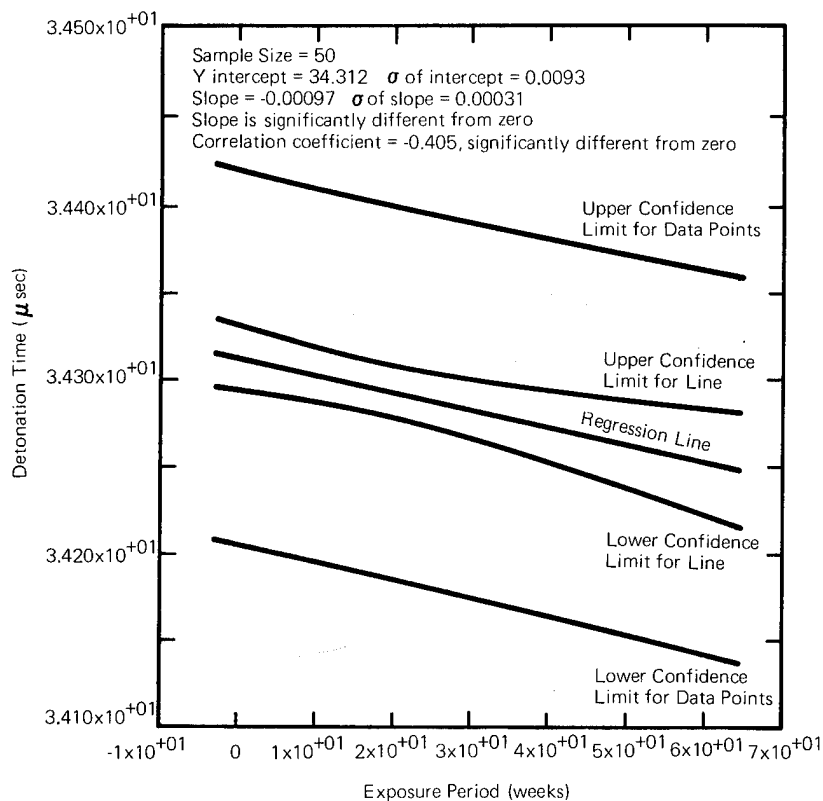


Figure 9A. "Jungle"-cycle firing data, linear response

The function time is seen to become slower with increasing exposure, which corresponds to faster detonation velocities. In Figure 9B, the regression is calculated with the baseline data removed. In this figure, the closeness of the limit lines to the regressing line gives good confidence that the indicated changes truly exist. The change in the Y intercept of the regression line between Figures 9A and 9B represents the effect of the initial slow up in detonation velocity discussed above.

Linear regression models with the baseline data removed to minimize the effects of the initial slow-up were found to provide the best description of sample performance. For the jungle cycle, the samples are shown to have an initial velocity of $7.395 \text{ mm}/\mu\text{sec}$ with a velocity increase of $1.87 \times 10^{-2} \text{ mm}/\mu\text{sec}/\text{year}$. The isothermal/constant humidity samples, with baseline data removed, show an initial velocity of $7.40 \text{ mm}/\mu\text{sec}$ with no discernible change with time, since the slope cannot be shown to be significantly different from zero. This observation for the isothermal/constant humidity is in keeping with other Sandia work in which no appreciable changes in detonation velocity could be recognized after 30 months storage at 110°F .⁽¹²⁾ Fitting the data to higher degree polynomial or exponential regressions does not appear to yield models that better describe the performance.

In summary, the test data were generally characterized by a slight slowing up of the detonation velocity during the early weeks of exposure followed by a plateau of no discernible change through 32 weeks. There was an identifiable increase in detonation velocity by 64 weeks that was more evident in the jungle cycle data than in the isothermal/constant humidity data. This portion of the data accounts for the significant slope seen

in the linear regression of the jungle cycle data that is not seen in the similar regression for the isothermal/constant humidity.

A failure of the MDF to initiate was noted for one of the 16-week jungle-cycle samples. This failure has been attributed to a fixture problem and not an MDF problem. Plastic particles from the detonator holder can be released during assembly operations and, by lodging between the detonator and MDF, can prevent initiation of the materials. This type of failure has been observed in the past. The fact that no failures were noted in the 32-week and 64-week exposure samples is additional evidence that the one 16-week failure was not an MDF problem.

Timing data for the bulk HNAB powders which were manufactured into MDF after 16 weeks' exposure to both humidity environments show that the difference between the original baseline data and the two samples is very small (Table II). For the MDF from the jungle-cycle-exposed powder, the change from original baseline data was not large enough to be recognizable as statistically different. For the MDF from the isothermal/constant-humidity powder the difference was slight but statistically significant. In both cases, the MDF made from both exposed powders propagated faster than the original baseline MDF. The variability (σ) within the group was almost exactly the same for each. It thus can be concluded that the initial performance of the MDF from both exposed powders is very close to the reference material.

To obtain additional timing information on both conditioned samples (after environmental exposure of the bulk powders), a number of MDF samples were subjected to similar humidity conditioning for 5 and 14 days and initiated afterwards. Data from

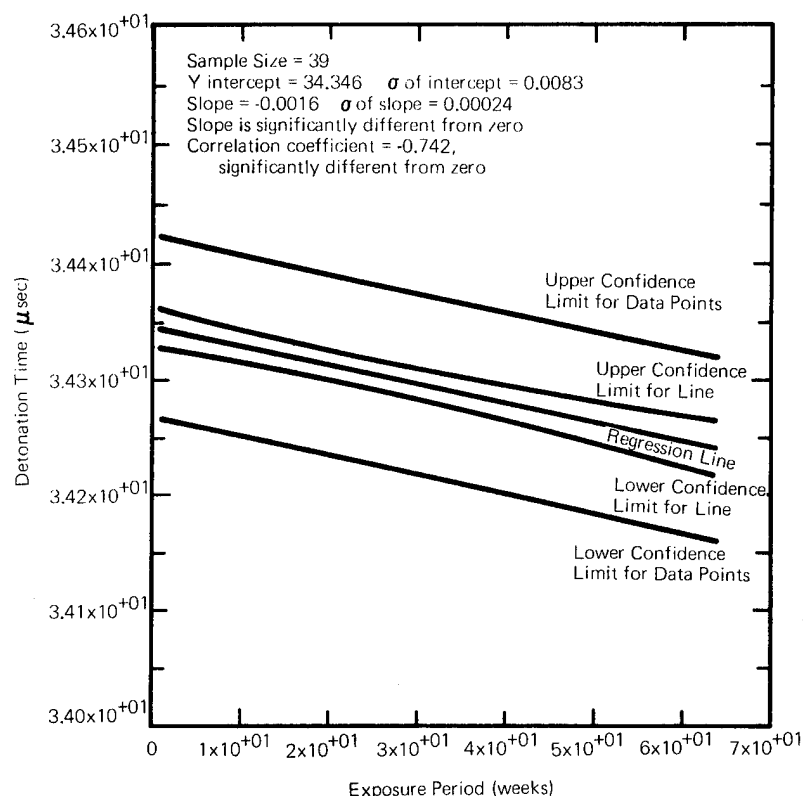


Figure 9B. "Jungle"-cycle firing data, linear response baseline data removed

TABLE II

Statistical Firing Data for HNAB Powder Manufactured Into MDF 16-Week Exposure

	Lot 2375 Baseline	Isothermal/Constant Humidity	"Jungle" Cycle
Range (μ sec)	0.098	0.136	0.138
Minimum (μ sec)	34.198	34.113	34.170
Maximum (μ sec)	34.296	34.249	34.308
σ (μ sec)	0.028	0.030	0.033
\bar{X} (μ sec)	34.245	34.186	34.220
Number	13	14	14
VOD (mm/ μ sec)	7.417	7.430	7.423

both environments show the usual decrease in velocity of detonation (VOD) between zero and 5 days' exposure, paralleling the original firing information obtained for the Lot 2375 baseline MDF (Table III and Figures 10 and 11). This was then

followed by a leveling off of the decrease between 5 and 14 days, again paralleling the original pattern. Thus the 16-week exposed HNAB powders, when manufactured into MDF, behaved similarly to the original Lot 2375 MDF.

TABLE III

Statistical Firing Data for 16-Week HNAB Powder Manufactured
Into MDF Reexposure to "Jungle" Cycle

	Zero Days	Five Days	Fourteen Days
Range (μsec)	0.138	0.127	0.136
Minimum (μsec)	34.170	34.249	34.266
Maximum (μsec)	34.308	34.376	34.402
Stand. Dev. (σ - μsec)	0.033	0.039	0.039
Mean (\bar{X} μsec)	34.220	34.294	34.339
Number	14	9	10
VOI (mm/ μsec)	7.423	7.407	7.397

Reexposure to Isothermal/Constant Humidity-Environment

	Zero Days	Five Days	Fourteen Days
Range (μsec)	0.136	0.092	0.123
Minimum (μsec)	34.113	34.220	34.226
Maximum (μsec)	34.249	34.312	34.349
Stand. Dev. (σ - μsec)	0.030	0.031	0.034
Mean (\bar{X} μsec)	34.186	34.277	34.269
Number	14	10	10
VOI (mm/ μsec)	7.430	7.410	7.412

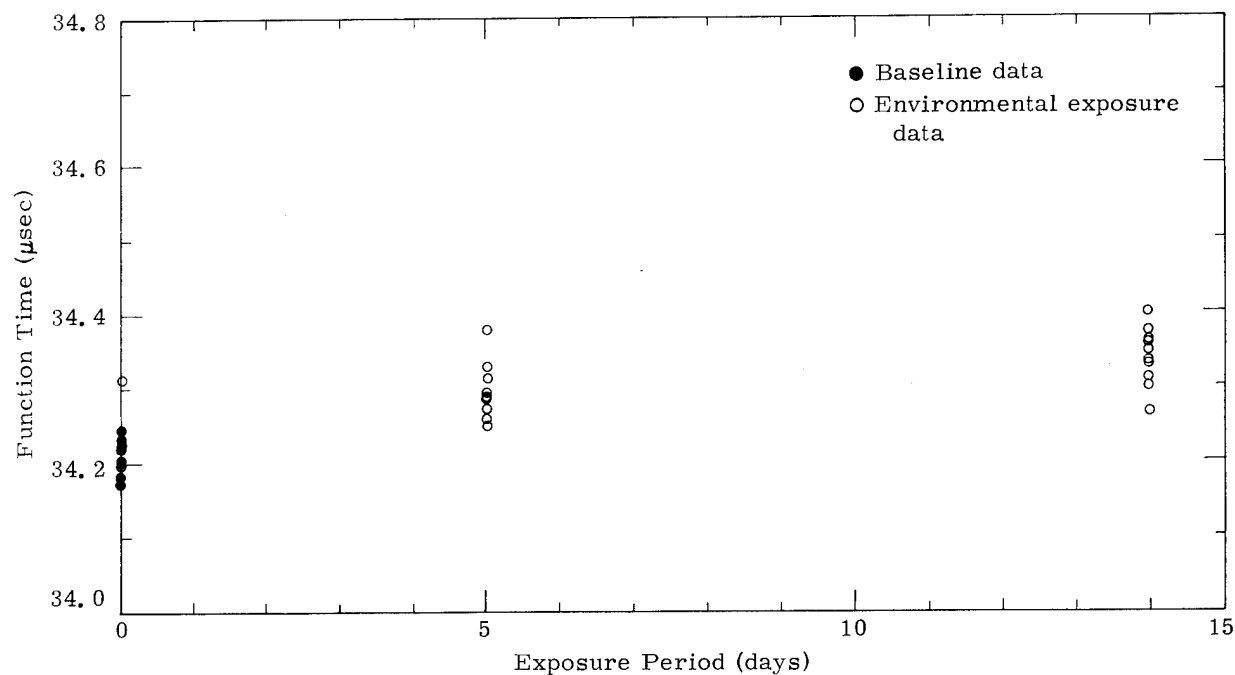


Figure 10. Function time vs exposure period for "jungle" cycle
(MDF manufactured from bulk powder exposed for
16 weeks)

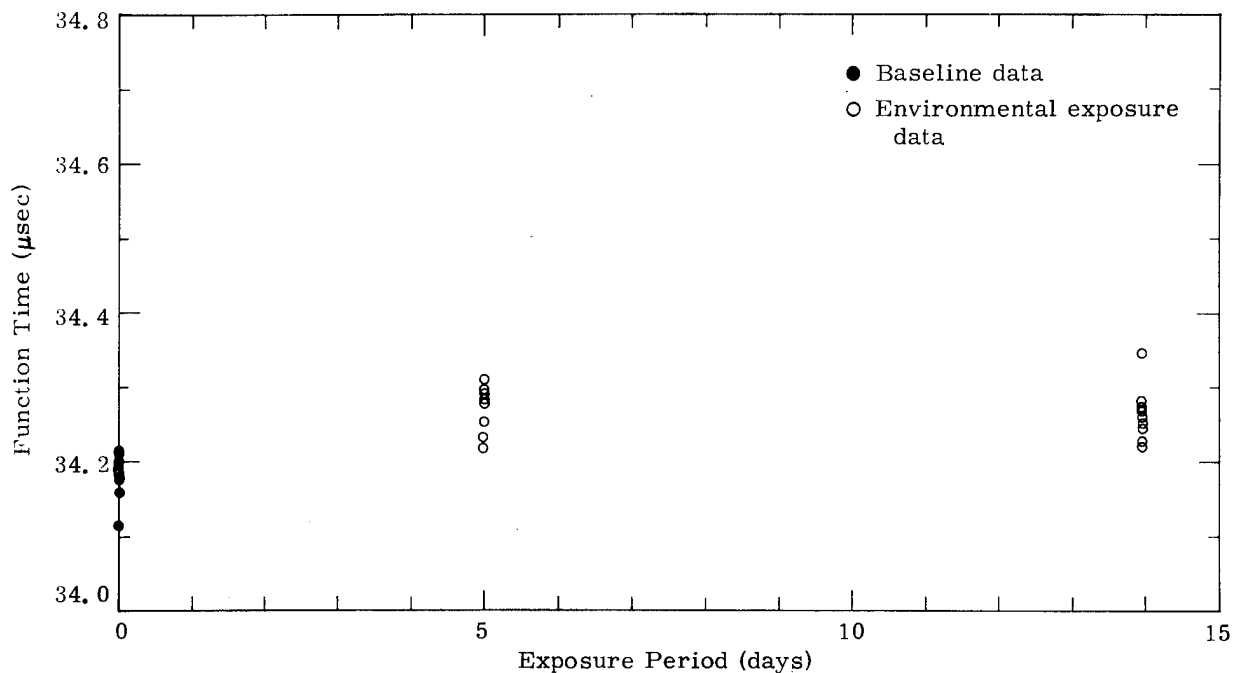


Figure 11. Function time vs exposure period for isothermal/constant humidity (MDF manufactured from bulk powder exposed for 16 weeks)

Because the testing time intervals were so short, little confidence could be assigned to mathematical exercises designed to fit the various data points to those of the original exposures, with subsequent comparison of long-term performance and parallel variations.

The manufactured MDF prior to heating did not behave at all like the 16-week exposed MDF samples. Instead, it behaved like the original unexposed Lot 2375 MDF. Thus the HNAB powder apparently manifested no "memory" of its original environmental conditioning.

Another comparison will be made in the future when the 64-week bulk powders are manufactured into MDF and returned for further testing.

4.2 PLATE DENT TESTS

By firing a number of the remaining ends of the environmentally exposed MDF samples, it was hoped that some measurement of the energy output could be obtained, and possibly that this energy output could then be related to any variations in timing data obtained for the MDF. The plate dent test was initially used to attempt to measure changes in energy output.

After a series of three shots from each exposure period and environment with the humidity-exposed end in contact with the witness block, the depth of each dent was measured. The depths ranged from 1 to 4 mils, and no correlation could be found between the depth of the dent and the exposed period.

The only conclusion from this work was that an energy output was obtained from each exposed sample. A better correlation would have been obtained if the end of the MDF in contact with the witness plate had been trimmed and trued, as is normally done. However, this would have removed the environmentally exposed explosive and invalidated the experiment.

4.3 THERMAL ANALYSIS STUDIES

Results of the thermal analysis testing program on both HNAB powder and MDF, as they were removed periodically from the two humidity/time studies, conclusively indicate that changes in the HNAB did occur. When these data are compared to those obtained from thin-layer chromatography and scanning electron microscopy, an excellent correlation with probable explanations as to what had occurred during conditioning was obtained.

Thermal analysis measurements of the HNAB-MDF samples from period to period indicated the following changes in the MDF HNAB:

1. A polymorphic reversion of the HNAB powder occurred in the MDF.
2. There was a slight lowering and broadening of the HNAB melting-point transition.
3. The extent of decomposition occurring in MDF HNAB was not as great as that which occurred in the HNAB powder samples.

Five polymorphs of HNAB have been found to occur, of which three can exist at room temperature: Forms I, II, and III.⁽¹³⁾ During the manufacture and purification of HNAB, any of the three polymorphic forms of mixtures thereof can be isolated, depending upon procedures used. Form II

is the desirable polymorph to use because it exists over the broadest range of temperatures.⁽¹⁴⁾ The densities of the three stable forms are:

Form I: 1.795 gm/cc

Form II: 1.794 gm/cc

Form III: 1.72 gm/cc

DSC data (Figure 12) show that Lot 36-7 HNAB exists primarily as Form II, with small amounts of Form III present. But during the manufacture of HNAB into MDF, a partial reversion of Form II HNAB to Form III has occurred (Figure 12). This partial reversion, attributed to a pressure-induced phase transformation of the HNAB resulting from the mechanical drawing operation, has been observed in the past during MDF manufacture of pure Form II.⁽¹⁵⁾ A mixture of Forms II and III resulted. The two DSC curves in Figure 12 clearly show that this reversion occurred.

As a note, the ratio of Form III to Form II in the MDF is small; therefore, the density difference between the forms will have little or no effect on the VOD.

As the two humidity/time programs commenced, a shift of the polymorphic transition temperature to a higher value resulted (Figures 13 and 14). Because of the thermal environments (in addition to the humidity) in which the MDF samples were placed, the original pressure-induced phase transformation (Form II to Form III HNAB) reversed itself. Through 64 weeks this thermally induced polymorphic transition had reversed itself to the point of approaching that of the original Lot 36-7 HNAB. Given enough time, Forms II and III HNAB would arrive at an equilibrium. The jungle-cycle rate of reversion to Form II was found to be much greater than that of the isothermal/constant-humidity environment, as would be expected

Figure 12. DSC thermogram showing HNAB polymorphic transformation during MDF manufacture

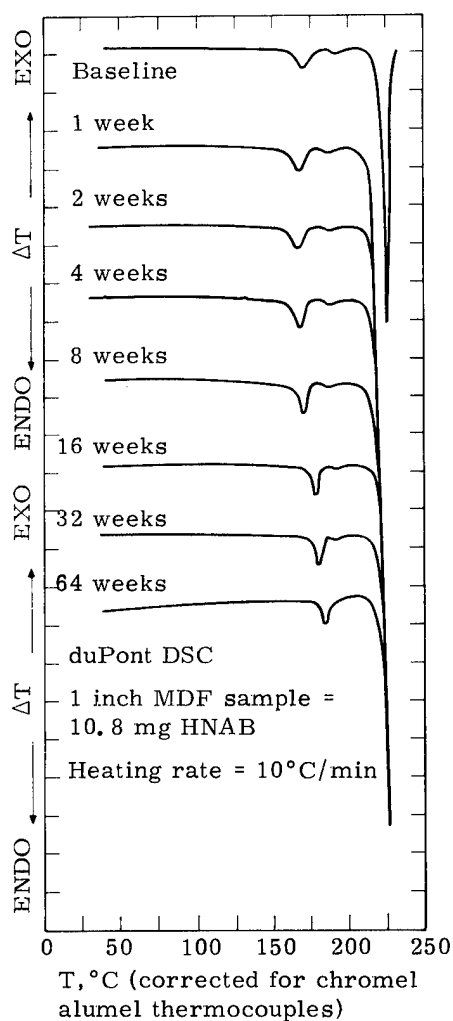
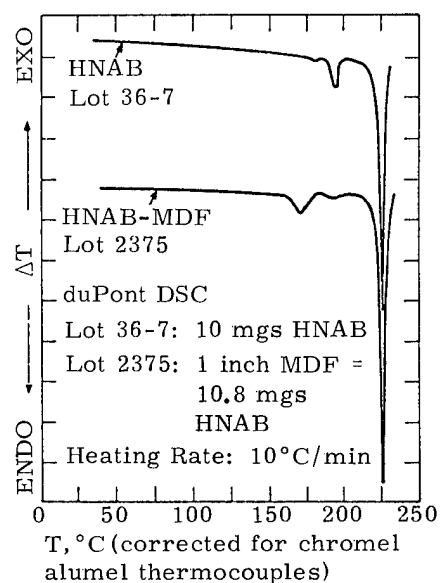


Figure 13. DSC thermogram showing HNAB-MDF polymorphic reversion during 64-week "jungle" cycle

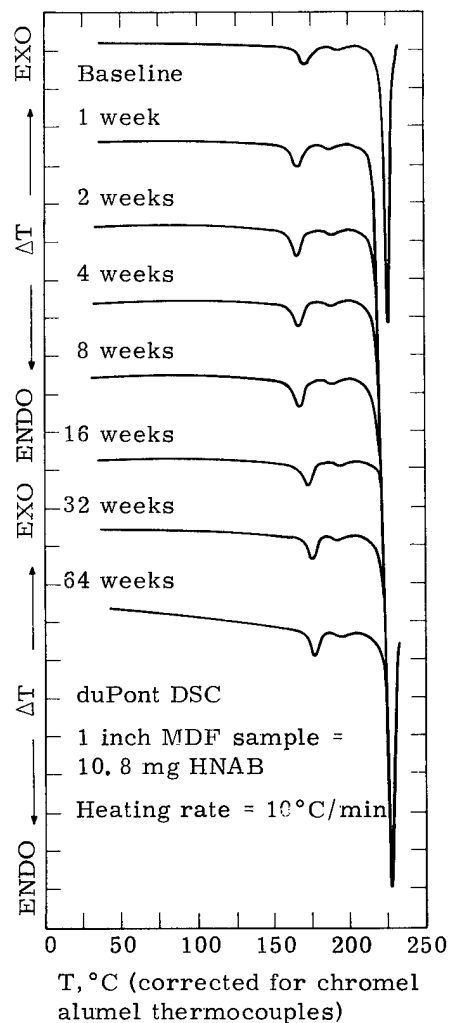


Figure 14. DSC thermograms showing HNAB-MDF polymorphic reversion during 64-week isothermal/constant-humidity

because of the higher temperature reached (149°F versus 120°F) during portions of the cycle. Table IV is a tabulation of the onset temperature shifts as they varied with the exposure period through the 64 weeks for both humidity programs.

If the HNAB melting-point transitions for the unexposed and 64-week-exposure MDF samples in both programs are compared (Figures 15 and 16), a slight lowering and broadening of this transition is noted.

A lowering and broadening of a melting-point transition along with a curved or sloping onset in a DSC trace is indicative of the presence of impurities in a material. The more extensive the occurrence, the more impure the sample is. Because of the presence of impurities, a broad range of melting will result due to varying solid solution melts of the impurities and main constituent.

This characteristic effect on the melting transition due to impurities is not very pronounced in the MDF materials and indicates that no significant decomposition has occurred in the HNAB. However, when correlated with subsequent TLC data (see later discussions), an excellent comparison results. The TLC data on the MDF HNAB shows small increases in concentrations of impurities. These data can be compared to those of the bulk HNAB powders, where significantly more decomposition occurred. As expected, the bulk samples showed the most significant change in the melting-point transition.

The lowering and broadening of the melting transition is much more pronounced for the unexposed (or baseline) Lot 2375 HNAB-MDF when compared to Lot 36-7 HNAB powder (see Figure 12). This

can be attributed to the increased concentration of the impurity hexanitrohydrazobenzene resulting from MDF manufacture (see discussion beginning on page 37).

Considerably more variations in the thermal analysis measurements were observed for the Lot 36-7 HNAB powder than for the MDF, suggesting that the actual humidity environments in addition to the thermal effects were affecting the exposed powdered material. Though variations were noted, none were considered catastrophic, and in all cases the performance of the HNAB was not affected adversely.

Four observations were noted in the thermal analysis data of the conditioned HNAB powder samples:

1. The small amounts of the HNAB polymorph, Form III, originally present in the unexposed powder slowly reverted to Form II HNAB in both programs.
2. An immediate lowering of the melting-point transition occurred after only 1 week of exposure.
3. A gradual but significant broadening accompanied by a curved or sloping onset of the melting-point transition was measured for the long-exposure (especially the jungle-cycle) powders.
4. TGA data showed an increasing rate of weight loss as a function of length of time in the humidity environments.

As with the MDF samples from both environments, polymorphic reversion of the Form III HNAB to Form II resulted (Figures 17 and 18).

TABLE IV

Variations in the HNAB-MDF Polymorphic Reversion
Onset Temperature as a Function of Exposure Time

Exposure Period (weeks)	Temperature	
	"Jungle" Cycle (°C)	Isothermal/Constant Humidity (°C)
0	158	158
1	158	158
2	158	158
4	161	158
8	163	159
16	173	164
32	175	166
64	178	170

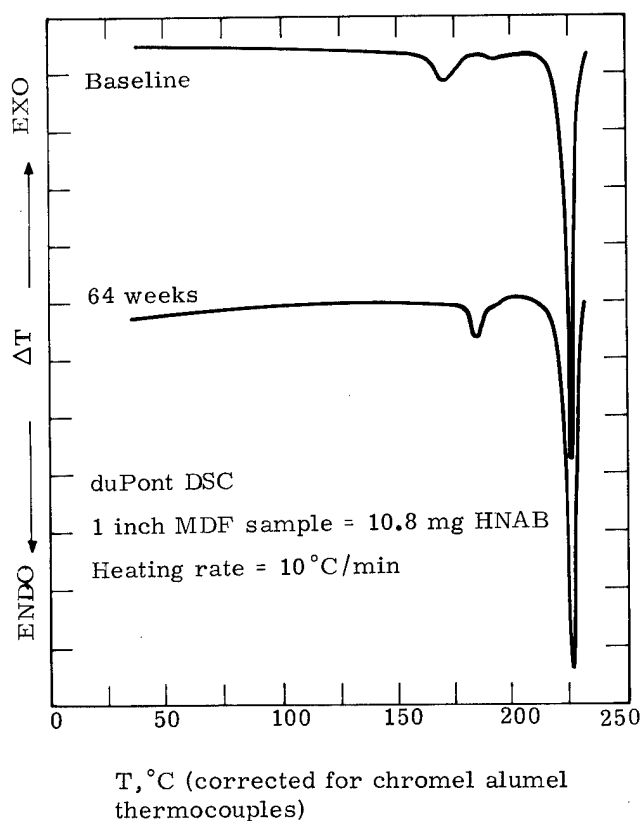


Figure 15. Effects of "jungle" cycle on
Lot 2375 HNAB-MDF melting-
point transition

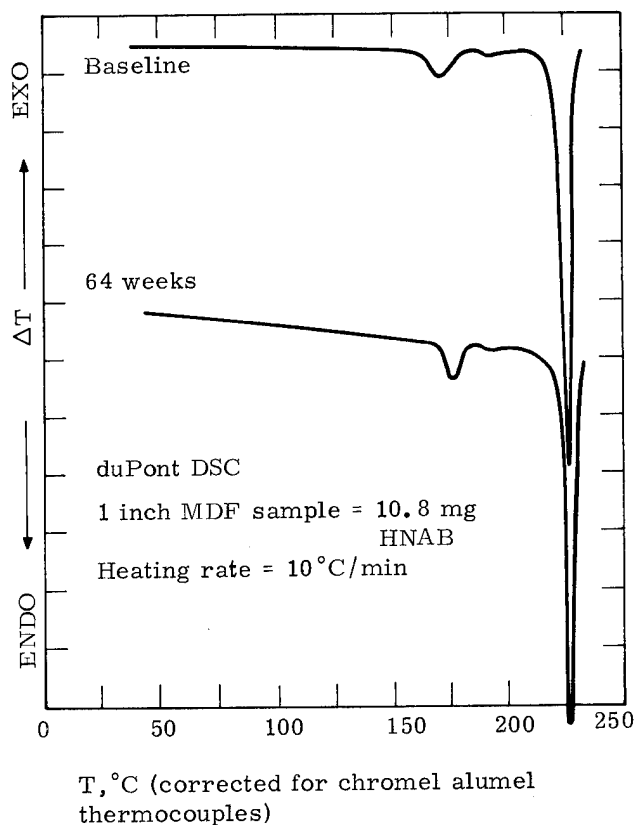


Figure 16. Effects of isothermal/constant-
humidity environment on
Lot 2375 HNAB-MDF melting-
point transition

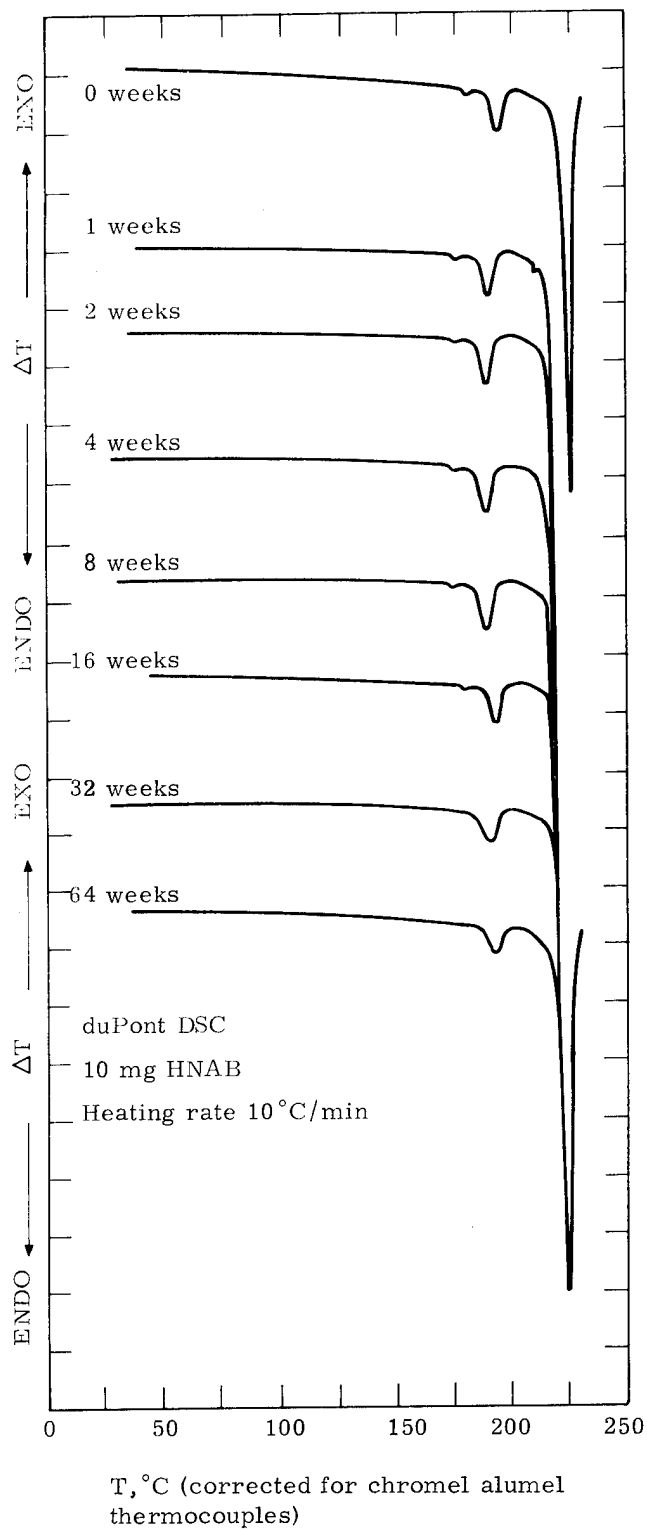


Figure 17. DSC thermograms of Lot 36-7 HNAB powder throughout 64-week "jungle"-cycle environment

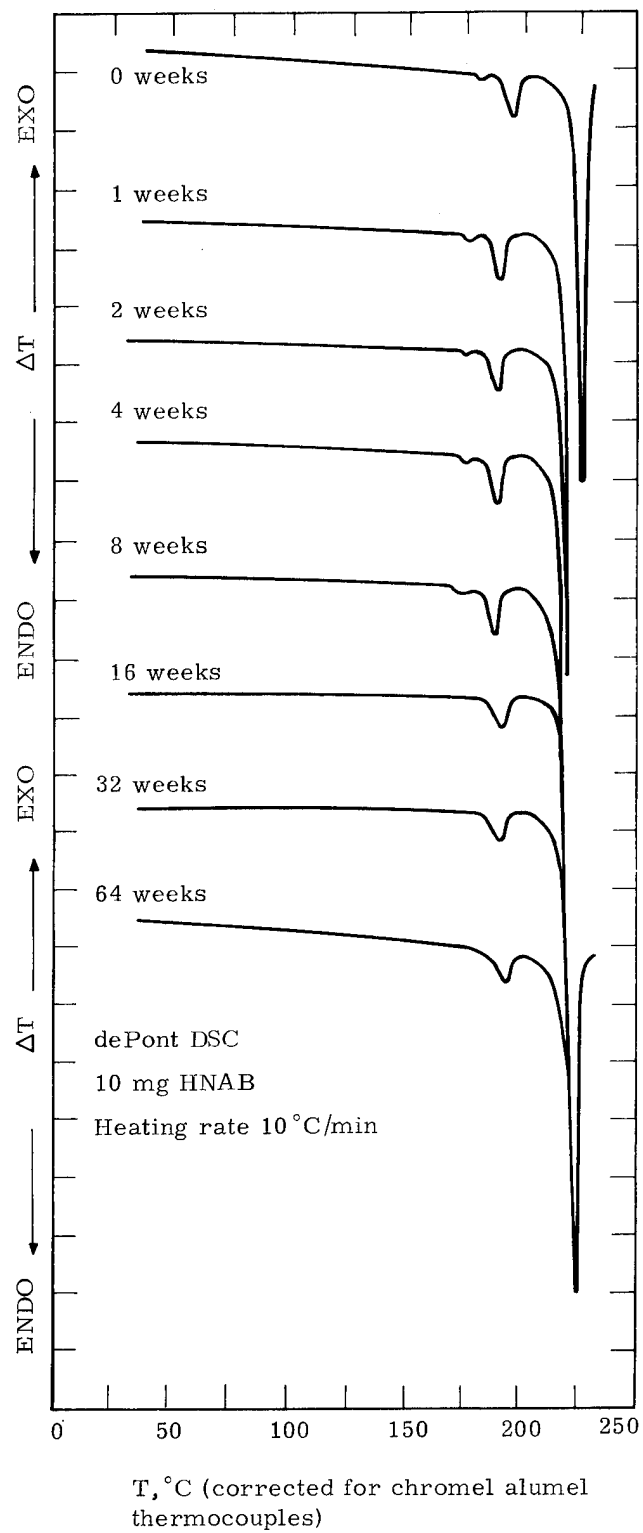


Figure 18. DSC thermograms of Lot 36-7 HNAB powder throughout 64-week isothermal/constant-humidity environment

Since nearly all the bulk HNAB existed as Form II, the magnitude of this reversion was not as great as that observed in the MDF samples. As previously discussed for the MDF samples, this reversion progressed most rapidly in the jungle-cycle environment. By the end of 64 weeks, the polymorphic reversion to Form II was nearly complete.

Again, a lowering and broadening of the HNAB melting-point isotherm was evident in the DSC data. When the original unexposed Lot 36-7 HNAB DSC data are compared directly to those of the 64-week-exposure powders from both studies, this change in the melting transition is quite apparent (Figures 19 and 20). Thus the change in the shape of this transition suggests that measur-

able decomposition in the HNAB had occurred. When again compared to the TLC data (see later discussions), the measured increased concentrations of picric acid and trinitrobenzene correspond closely to the observed DSC data.

Likewise, the immediate lowering of the melting point of HNAB after only 1 week of exposure to both environments corresponds quite closely to the increases in the measured quantities of hexanitrohydrazobenzene present.

As previously mentioned, TGA measurements on the bulk powders show a greater rate of decomposition in the HNAB with increasing exposure time (Figures 21 and 22). Of many possible explanations, the following is considered to be the most likely:

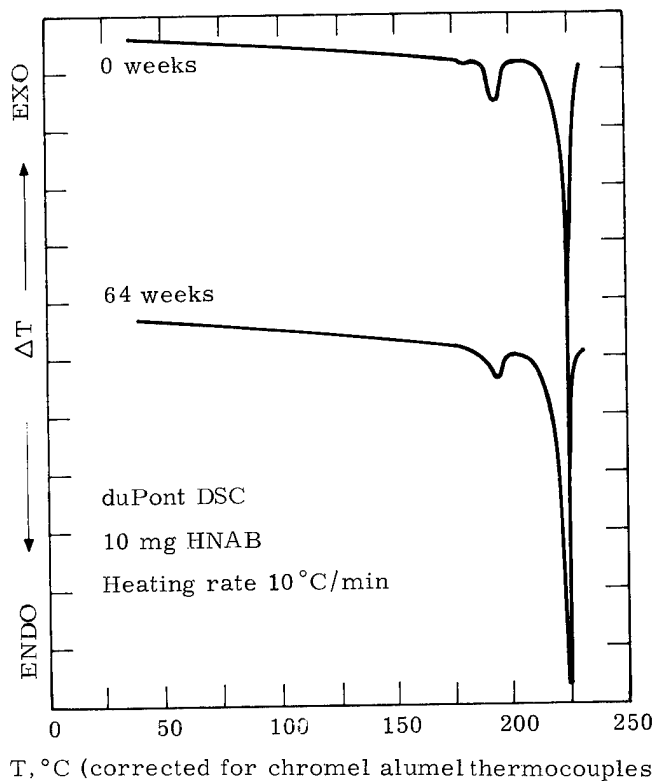


Figure 19. DSC thermograms showing the effect of "jungle" cycle on melting-point transitions of Lot 36-7 HNAB powder

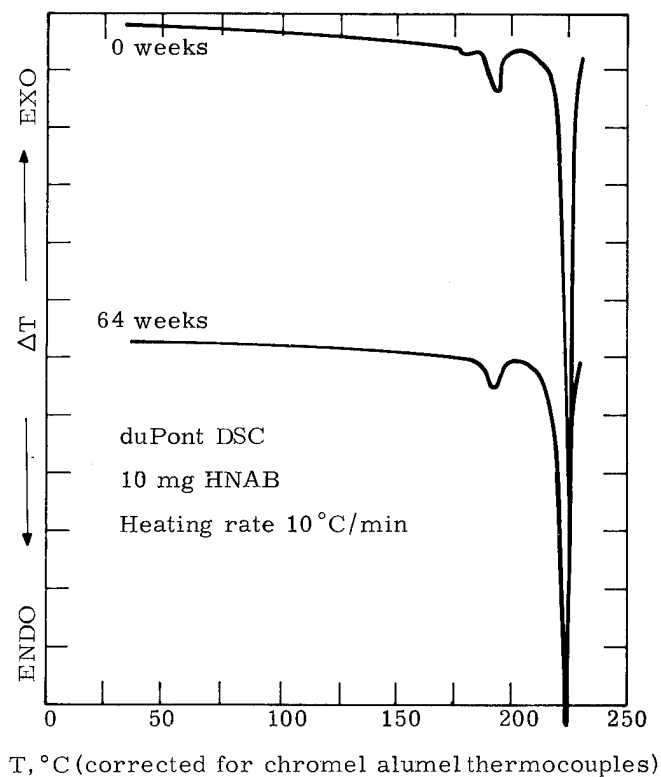


Figure 20. DSC thermograms showing the effect of isothermal/constant-humidity environment on melting-point transition of Lot 36-7 HNAB powder

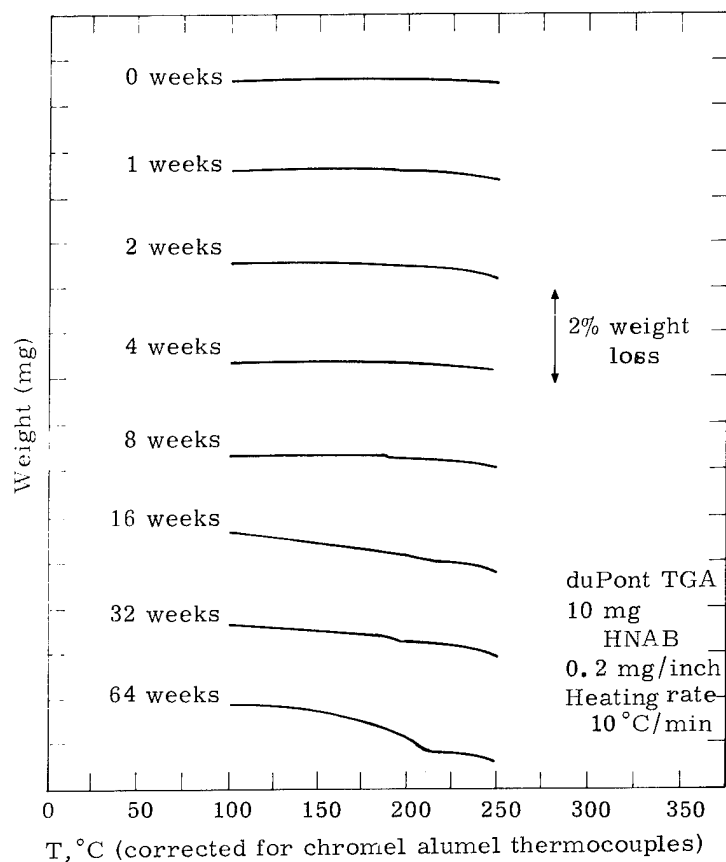
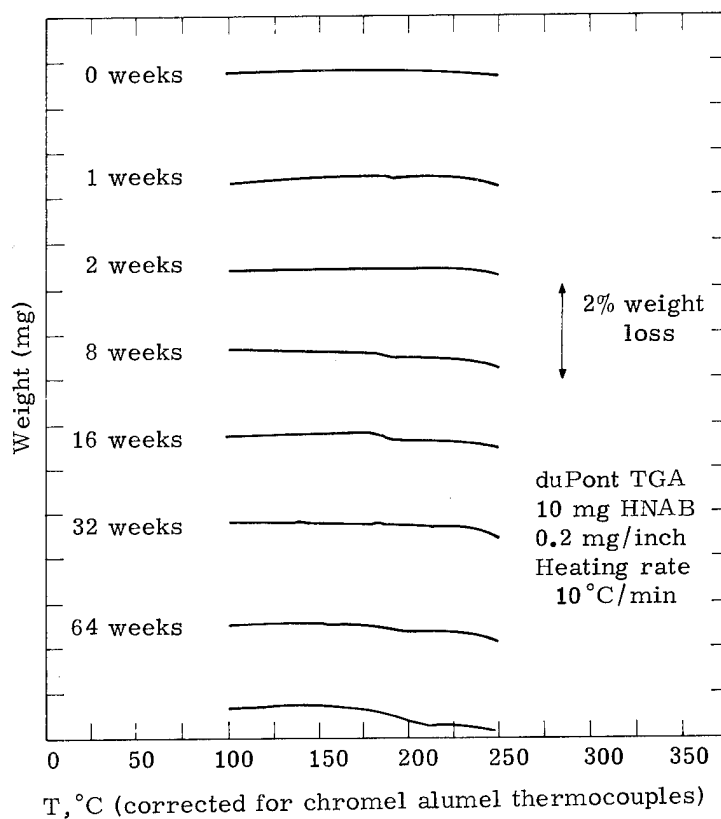


Figure 21. TGA measurements on Lot 36-7 powders subjected to "jungle"-cycle environment

Figure 22. TGA measurements on Lot 36-7 HNAB powders subjected to isothermal/constant-humidity environment



The melting points of picric acid and trinitrobenzene are 121°C and 122°C, respectively.⁽¹⁵⁾ TGA measurements on both materials show that vaporization takes place rapidly after melting (Figure 23). TLC data also show increasing concentrations of picric acid and trinitrobenzene with exposure time. If decomposition of the HNAB is a surface phenomenon (and it would be if water vapor were reacting with the HNAB), the increasing amounts of picric acid and trinitrobenzene could account for the increased rates of weight loss measured for the HNAB powders. The magnitude of the weight losses between 125°C and 220°C correspond closely to the total amounts of both materials present when measured by TLC.

4.4 TLC DATA

Originally, if changes in both the HNAB powder and MDF were to occur, it was felt that decom-

position of the explosive material would be one of the more probable causes. These impressions were further enhanced by the slight variations previously noted in both the detonation velocity and thermal analysis data--thus the interest in determining the identity and quantity of the decomposition products present in the HNAB.

A large number of TLC plate development solutions and materials were tested during development of satisfactory analytical techniques for the various decomposition products.⁽¹¹⁾ As mentioned in the introduction, of the many systems chromatographed, the following three compounds besides HNAB were found to occur in the powders: hexanitrohydrazobenzene, picric acid, and trinitrobenzene.

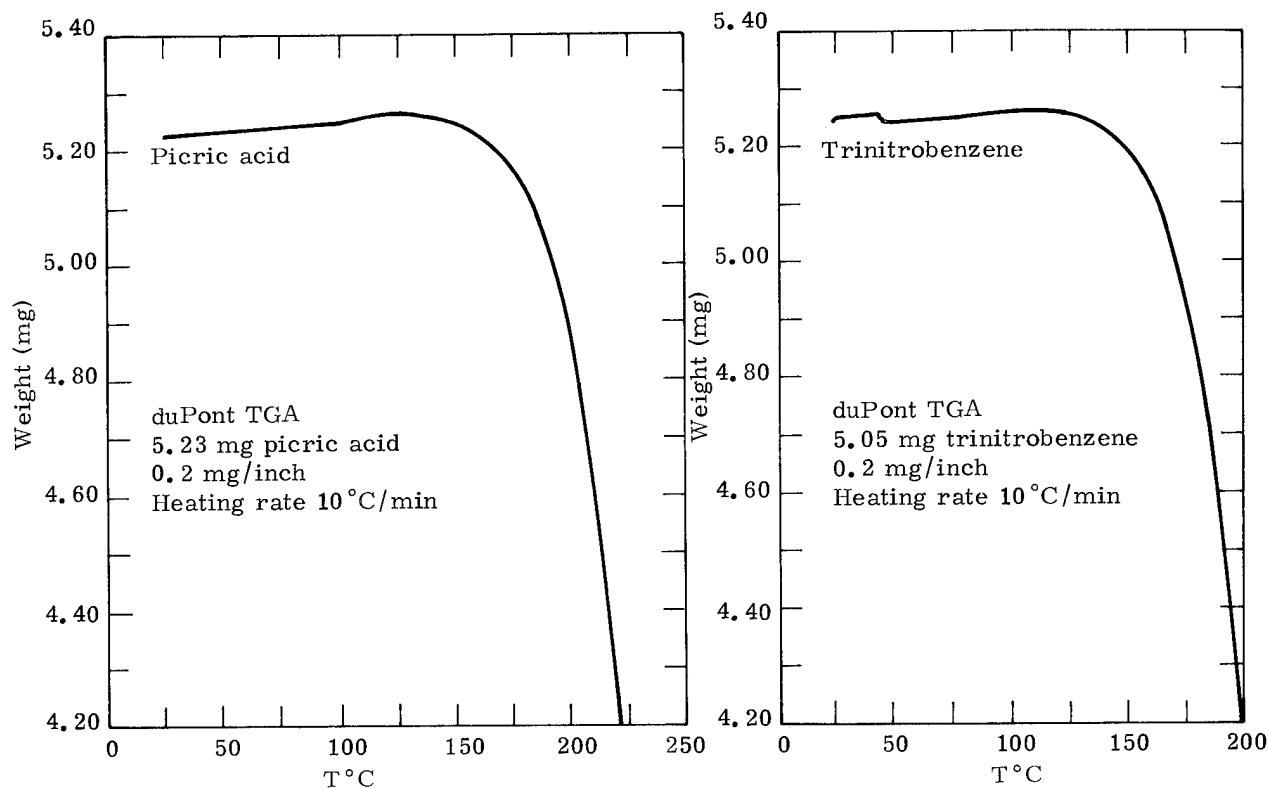


Figure 23. TGA's of trinitrobenzene and picric acid

The two plate development solutions described earlier provided the best separation and subsequent semiquantitative analysis of the decomposition products of HNAB. Tables V through

VIII are the semiquantitative analysis results for the various conditioned HNAB powder and MDF samples.

TABLE V

TLC Analysis of the Isothermal/Constant Humidity (120 °F/90% RH)
Lot 36-7 Bulk HNAB Powders

Exposure Time	Hexanitrohydrazobenzene	Picric Acid	Trinitrobenzene
Baseline	0.08%	Not detected	~0.05%
1 Weeks	0.3 %	<0.1 %	0.1 %
2 Weeks	0.3 %	<0.1 %	0.1 %
4 Weeks	0.3 %	0.1 %	0.15%
8 Weeks	0.4 %	0.1 %	0.15%
16 Weeks	0.4 %	0.15%	0.15%
32 Weeks	0.4 %	0.15%	0.15%
64 Weeks	0.7 %	0.3 %	0.3 %

TABLE VI

TLC Analysis of the "Jungle" Cycle
Lot 36-7 HNAB Powders

Exposure Time	Hexanitrohydrazobenzene	Picric Acid	Trinitrobenzene
Baseline	0.08%	Not detected	~0.05%
1 Weeks	0.07 - 0.8%	<0.1 %	0.1 %
2 Weeks	0.7 - 0.8%	0.1 %	0.15%
4 Weeks	0.7 - 0.8%	0.15%	0.15%
8 Weeks	0.8 %	0.15%	0.2 %
16 Weeks	0.8 %	0.2 %	0.2 %
32 Weeks	0.8 %	0.3 %	0.25%
64 Weeks	0.8 %	0.6 - 0.7%	0.6 %

TABLE VII

TLC Analysis of Isothermal/Constant Humidity (120 °F/90% RH)
Lot 2375 HNAB-MDF

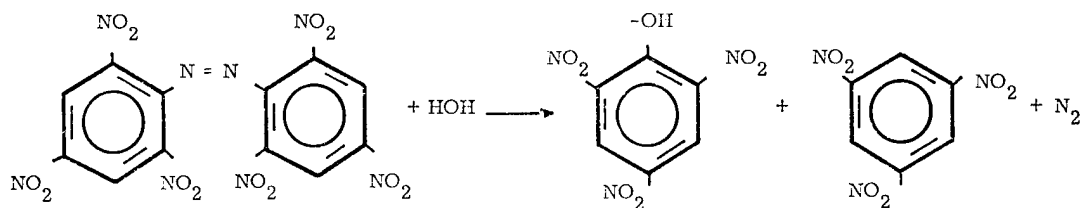
Exposure Time	Hexanitrohydrazobenzene	Picric Acid	Trinitrobenzene
Baseline	0.6 - 0.7%	<0.1 %	0.1 %
2 Weeks	0.7 %	<0.1 %	0.1 %
32 Weeks	0.7 %	0.15%	0.15%
64 Weeks	0.6 %	0.2 - 0.3%	0.15 - 0.2%

TABLE VIII
TLC Analysis of "Jungle" Cycle Lot 2375 HNAB-MDF

Exposure Time	Hexanitrohydrazobenzene	Picric Acid	Trinitrobenzene
Baseline	0.6 - 0.7%	<0.1%	0.1%
2 Weeks	0.8%	<0.1%	0.1%
32 Weeks	0.7%	0.15 - 0.2%	0.1%
64 Weeks	0.4 - 0.5%	0.3 - 0.4%	0.35 - 0.4%

The TLC results of the Lot 36-7 HNAB powder samples show a gradual and nearly equal increase with exposure time in the percentages of picric acid and trinitrobenzene present (Tables V and VI). From these results it is evident that exposure of the HNAB powder to both humidity environments has resulted in a gradual breakdown of the HNAB structure to picric acid and trinitrobenzene (this

can be compared with the MDF TLC analysis results in Tables VII and VIII). The jungle cycle has had a more detrimental effect on the HNAB than the isothermal/constant-humidity condition. The probable decomposition reaction to obtain both picric acid and trinitrobenzene from HNAB is as follows (intermediate reactions being ignored):⁽¹⁶⁾



As mentioned in the thermal analysis results and discussion section, the measured increased concentration of the above corresponds quite well to the measured changes in the HNAB melting transition. For example, the increase in picric acid and trinitrobenzene concentrations from 32 weeks to 64 weeks during the jungle-cycle environment showed a corresponding lowering and broadening of the HNAB melting transition (see Figure 17). This is quite apparent also in Figure 19, which compares the original Lot 36-7 HNAB melting transition to that of the 64-week jungle-cycle sample. Very little trinitrobenzene and no picric acid were detected in the original HNAB. Likewise, a TLC and thermal analysis comparison of the other conditioned samples from both humidity studies show similar correlations, although these are less

evident because the amount of decomposition was not as large.

More difficult to explain is the rapid increase in concentration of hexanitrohydrazobenzene in the exposed HNAB powders, especially that of the jungle-cycle samples. After only 1 week in the jungle environment, the concentration of hexanitrohydrazobenzene increased from a baseline measurement of 0.08% to 0.7 - 0.8%. Soon thereafter, an equilibrium concentration was reached at about 0.8% and remained there for the rest of the 64-week program. This may be contrasted with the effect of the isothermal/constant-humidity environment, in which there was a rapid increase to 0.3% hexanitrohydrazobenzene after 1 week of exposure, followed by a gradual increase to 0.7%

after 64 weeks. A number of possibilities have been suggested to explain this rapid increase followed by equilibrium of the hexanitrohydrazobenzene concentration such as:

1. An impurity in the original Lot 36-7 HNAB reverted to hexanitrohydrazobenzene.
2. Noncontrol of the water purification step prior to vaporization for humidity control to the chamber resulted in the introduction of an inorganic compound which reacted with the HNAB.
3. An equilibrium reaction between HNAB and hexanitrohydrazobenzene occurred.
4. Least likely but still possible is the decomposition of a finite amount of the cis-isomer of HNAB.

Since no other impurities beside those previously mentioned could be isolated in HNAB (and those present existed in small quantity), Number 1 as a possible explanation is considered doubtful. In addition, the DSC measurements suggest a rather pure original compound.

During the water purification step prior to vaporization for humidity control, tap water was supposedly passed through a metered deionization system; subsequently refuted by emission spectroscopy data (see previous discussion). A reducing condition would have had to result from the presence of these materials to form hexanitrohydrazobenzene. Most water impurities, being alkaline, would decompose HNAB rather than reduce it to hexanitrohydrazobenzene. Since small increases were noted for picric acid and trinitrobenzene, significant decomposition apparently did not occur because of an inorganic impurity. This basically reiterates what was earlier found for the dark residues observed on the jungle-cycle glass containers.

Though the stereoisomerism in HNAB has not been studied, the actual occurrence of the cis-isomer is considered doubtful. Studies on the cis-isomer for azobenzene found that a coplanar or true cis arrangement of the molecule was not possible because of steric effects.⁽¹⁷⁾ The addition of nitro groups to the benzene ring to form HNAB would result in additional steric hindrance; thus the possibility of the cis-isomer existing for HNAB is considered doubtful. X-ray data of the molecule also have shown that the trans-isomer is the sole structure for HNAB though this does not preclude small quantities of the cis-isomer being present which X-ray would not detect.⁽¹⁴⁾

Discussions about this sudden increase in the hexanitrohydrazobenzene concentration to a constant level of 0.8% suggested that an equilibrium condition between the two materials might exist. Hexanitrohydrazobenzene is an intermediate compound produced during the manufacture of HNAB and thus could revert back in equilibrium with HNAB. However, to further elucidate the mechanism is considered beyond the original intention of this paper.

This definite increase in hexanitrohydrazobenzene concentration was also indicated by the DSC results. Previous discussions mentioned that an immediate lowering of the HNAB melting transition (see Figures 17 and 18) was observed and was attributed to the sudden increased appearance of this impurity. This was quite evident in the jungle-cycle samples, corresponding more closely to higher concentrations of hexanitrohydrazobenzene in these environmental samples than in those from the isothermal/constant-humidity environment.

TLC analysis of some of the MDF HNAB materials indicated that decomposition which occurred in the explosive cord was considerably different, as

would be expected, for the actual effect of humidity or water must be quite minimal. Because the explosive packing density in the MDF is in the vicinity of 95% crystal density or better, the amount of water migrating any appreciable distance up the ends of the small diameter MDF must be exceedingly small. Thus the primary mechanism for decomposition very probably consisted of the thermal environments to which the MDF samples were exposed during each humidity condition.

Originally, the hexanitrohydrazobenzene concentration present in Lot 36-7 HNAB was 0.08%. After manufacture into MDF and pressurization the concentration of this impurity had increased to a level of 0.6 - 0.7%. These data possibly suggest the existence of an equilibrium between HNAB and hexanitrohydrazobenzene. The MDF drawing and subsequent pressurization operations appear to have provided the necessary driving force to cause the reversion of HNAB to hexanitrohydrazobenzene to occur.

Small increases in the picric acid and trinitrobenzene concentration levels also were measured in the HNAB after manufacture into MDF (Table IX).

Environmental conditioning caused a slight additional increase in the amount of hexanitrohydrazobenzene present in the MDF HNAB. Two-week concentration levels were 0.8% and 0.7% for the jungle-cycle and isothermal/constant-humidity conditions, respectively. Again the upper level of this impurity was similar to that previously measured in the bulk HNAB powders.

But instead of remaining constant at this level for the whole of the program, the concentration of

hexanitrohydrazobenzene dropped after long exposure to both environments (Table X). If the equilibrium hypothesis for HNAB and hexanitrohydrazobenzene is valid, then this should not have occurred unless the presence of air, water, or some other occluded material is required to maintain the equilibrium concentration of the two materials. This was followed by a nearly equal increase in the concentrations of picric acid and trinitrobenzene (see Tables VII and VIII). In MDF, the primary result and mechanism of decomposition appear to be hexanitrohydrazobenzene forming picric acid and trinitrobenzene.

The MDF TLC results agree quite closely with those obtained by thermal analysis. Decomposition of the HNAB within the MDF is quite small compared to that measured in the bulk HNAB powders; thus only small thermal analysis differences from time period to time period were noted. In most cases these differences could not even be measured.

Table XI presents the TLC results for the 50-gram bulk samples removed from each environment after 16 and 64 weeks for MDF manufacture. The results vary slightly from those previously discussed, which were obtained by analyzing the 5-gram samples taken from a separate container at the end of each exposure period. These variations were not large and they basically confirm the original HNAB powder results in Tables V and VI. As previously noted, firing data obtained on the exposed 16-week bulk samples made into MDF (from both environments) were not statistically different from similar exposed MDF samples. Thus the small increase in decomposition of the HNAB has not affected its performance in MDF.

TABLE IX

Increases in Picric Acid and Trinitrobenzene
After Manufacture Into MDF

<u>Sample</u>	<u>Picric Acid</u>	<u>Trinitrobenzene</u>
Lot 36-7 HNAB	Not detected	0.05%
Lot 2375 MDF	< 0.1%	0.1 %

TABLE X

Hexanitrohydrazobenzene Concentration Versus Exposure Time

<u>Environment</u>	<u>Baseline</u>	<u>Two Weeks</u>	<u>Thirty-two Weeks</u>	<u>Sixty-four Weeks</u>
"Jungle" Cycle	0.6 - 0.7%	0.8%	0.7%	0.4 - 0.5%
Isothermal/Constant Humidity	0.6 - 0.7%	0.7%	0.7%	0.6%

TABLE XI

TLC Analysis of 50-Gram HNAB for MDF Manufacture

<u>Environment</u>	<u>Hexanitrohydrazobenzene</u>	<u>Picric Acid</u>	<u>Trinitrobenzene</u>
16 Weeks - "Jungle" Cycle	0.7 - 0.8%	0.2 %	0.2 %
64 Weeks - "Jungle" Cycle	0.9%	0.7 %	0.5 - 0.6%
16 Weeks - Isothermal/ Constant Humidity	0.8 - 0.1%	0.15%	0.15%
64 Weeks - Isothermal/ Constant Humidity	0.7 - 0.8%	0.5 %	0.3 %
Lot 36-7 HNAB (Unexposed)	0.08%	Not detected	~ 0.05%

4.5 SCANNING ELECTRON MICROSCOPY

Scanning electron microscopy (SEM) of the unexposed and exposed MDF samples indicated that little or no crystal growth had occurred in the HNAB cores (Figures 24 and 25); this agrees with the small variations noted in the timing data. If crystal growth had occurred, significant timing data variations would also have been noted as a result of the higher core density. SEM analyses of MDF materials other than HNAB have shown significant crystal growth in the cores which correlated quite well with major variations in the explosive timing data.

Though crystal growth within the cores was not observed, other changes were observed. After long exposure, microholes or cavities occurred in the HNAB (see the 2000X photographs in Figures 24 and 25). Their presence was noted after 8 and 16 weeks, respectively, in the jungle-cycle and isothermal/constant-humidity environments. Diameters of the microholes were as large as 1 micron, with the large majority under 0.3 micron. After onset of microhole formation, the number per unit area increased with progressively longer exposure periods. In addition, the jungle-cycle samples had proportionally more microholes than the isothermal/constant-humidity samples for the same time period.

The presence of the microholes in the HNAB cores can be explained in the following manner: Two previous changes, polymorphic reversion and small amounts of decomposition were noted in the MDF HNAB. Decomposition resulting in the formation of picric acid and trinitrobenzene also would be accompanied by a gaseous product (possibly N_2) from the hydrazo or azo linkage (depend-

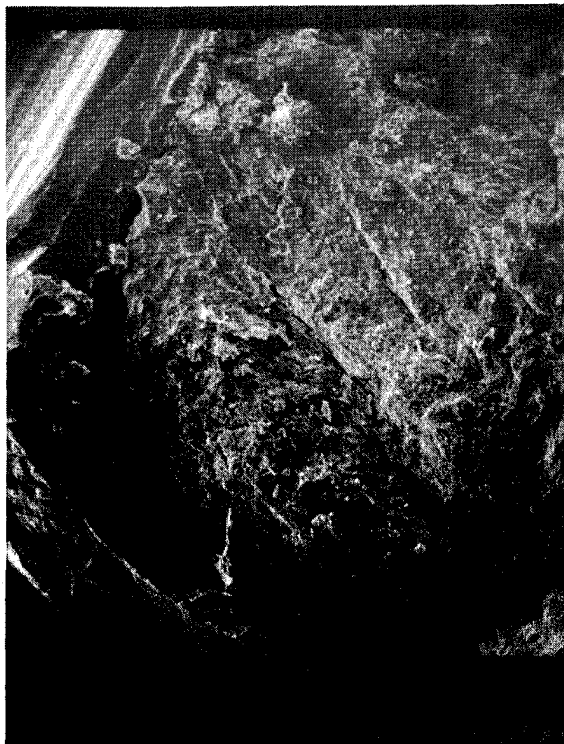
ing upon the decomposition mechanism employed). In conjunction with the polymorphic reversion, the decomposition gases would be released from the crystals, generate a pressure, and eventually escape from the HNAB core, forming the observed microholes or cavities. The increasing population of microholes correlates quite closely with the increasing percentages of picric acid and trinitrobenzene present.

Basically, the small changes observed in the SEM MDF analysis corresponded in magnitude with those observed in analyses performed with the other diagnostic techniques.

5. SUMMARY AND CONCLUSIONS

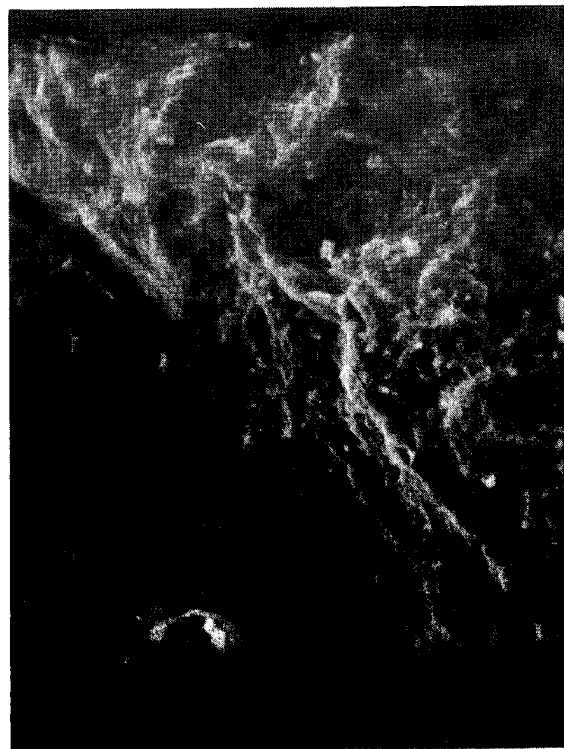
The diagnostic test data showed that some changes in the HNAB powder and MDF did occur during exposure to the two humidity/time environments. However, the magnitude of these changes were small. Such changes, in either the MDF or the bulk powder, would not be significant enough to preclude the use of these materials in precise timing applications.

MDF timing or velocity of detonation data showed that an immediate slowdown occurred soon after the humidity studies commenced. This was followed by a period of little change and then by a period of increasing detonation velocity. However, in all cases, the data fell well within the limits allowed for HNAB-MDF for precise timing applications. This initial slowdown has been observed in the past for HNAB-MDF which was subjected to thermal environments. The long time exposure periods in which increases in detonation velocity occurred were also considered to be a result of thermal, rather than humidity conditions. Also,



Baseline - 0 Weeks

200X



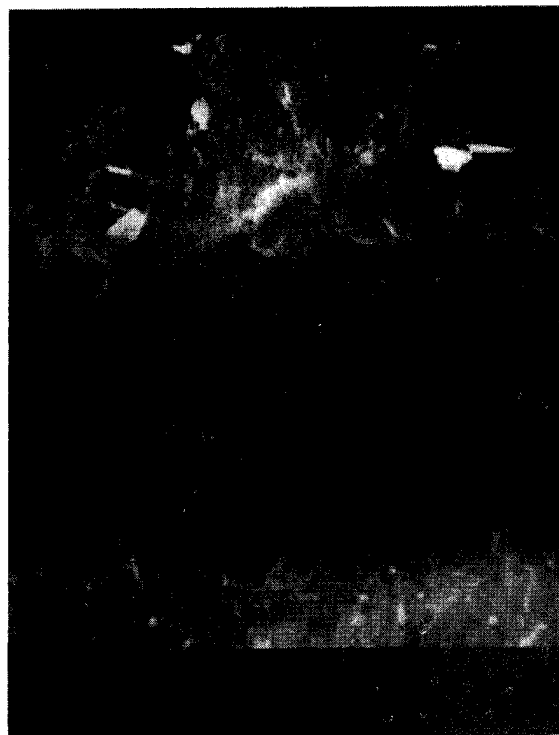
Baseline - 0 Weeks

2000X



1 Week

200X



1 Week

2000X

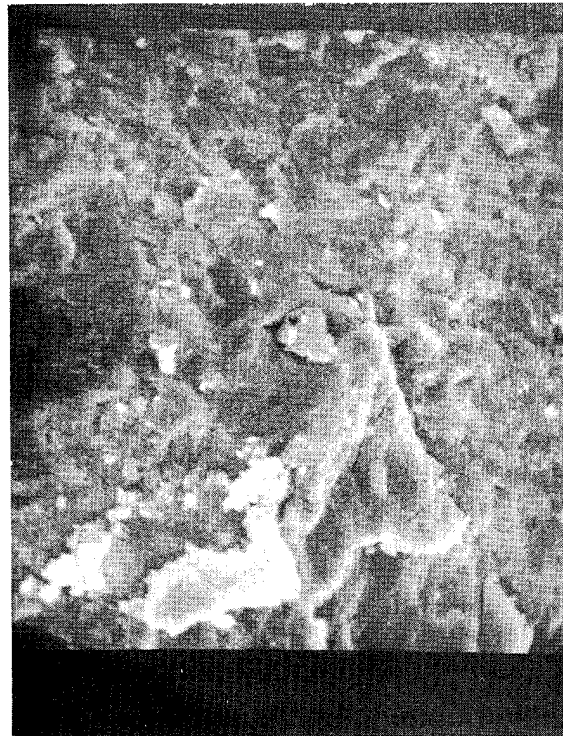
Figure 24. SEM photomicrographs of Lot 2376 HNAB-MDF:
"jungle"-cycle exposure

(continued)



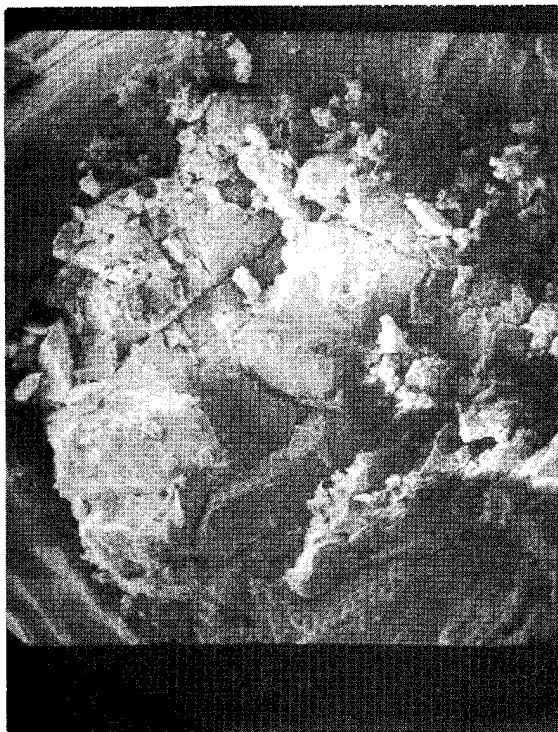
2 Weeks

200X



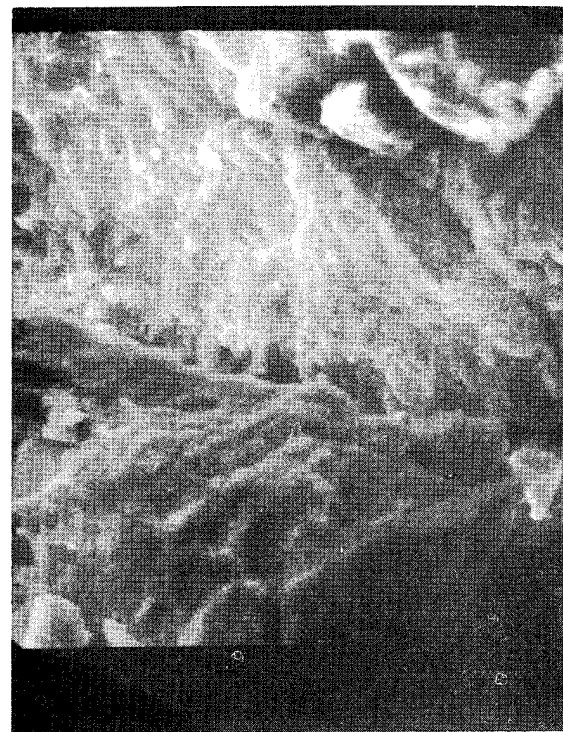
2 Weeks

2000X



4 Weeks

200X



4 Weeks

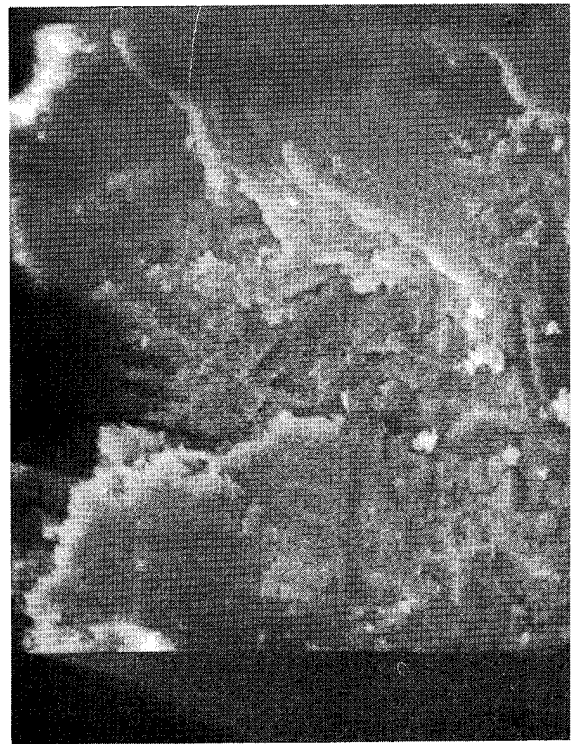
2000X

Figure 24. (continued)



8 Weeks

200X



8 Weeks

2000X



16 Weeks

200X



16 Weeks

2000X

Figure 24. (continued)



32 Weeks

200X



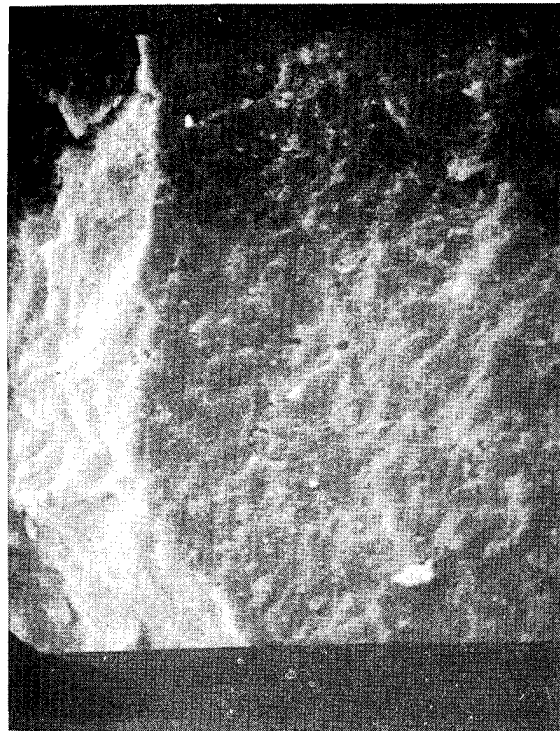
32 Weeks

2000X



64 Weeks

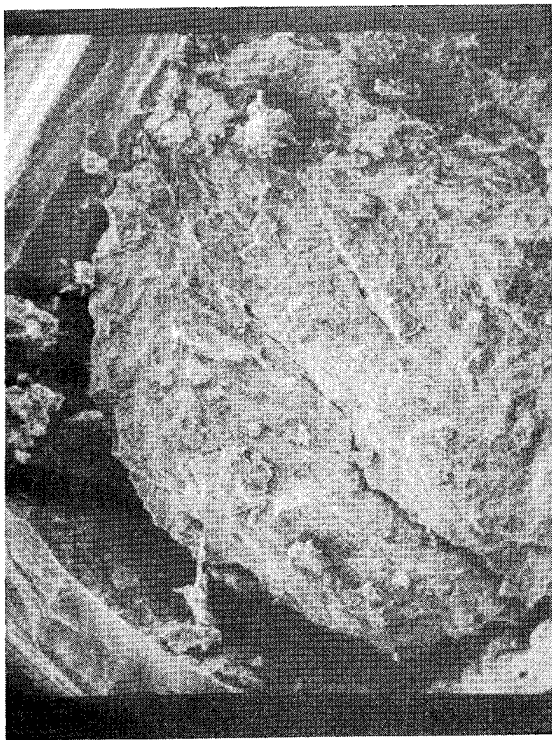
200X



64 Weeks

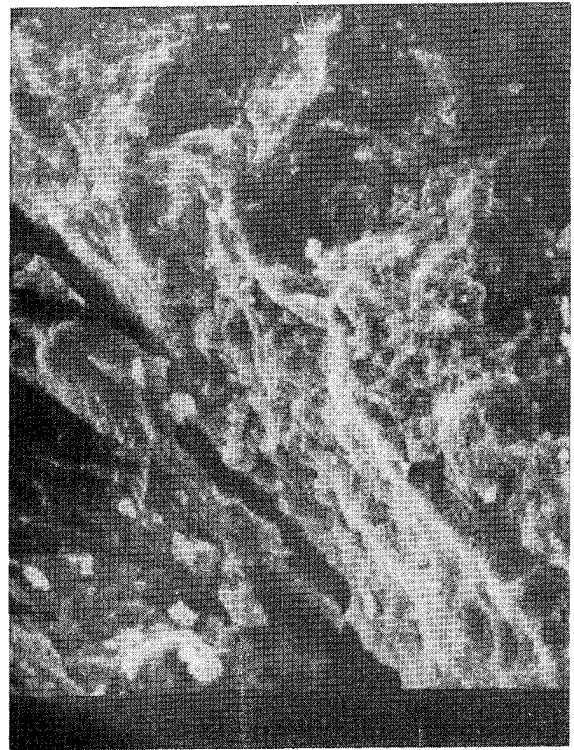
2000X

Figure 24. (concluded)



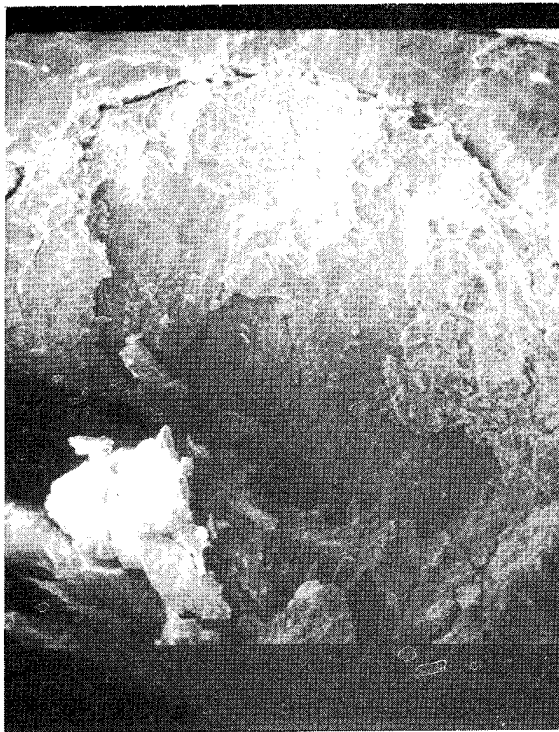
Baseline - 0 Weeks

200X



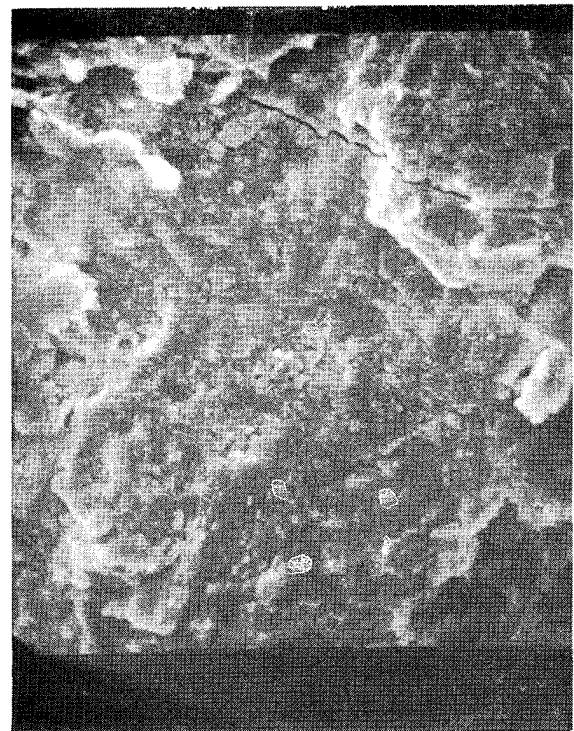
Baseline - 0 Weeks

2000X



1 Week

200X

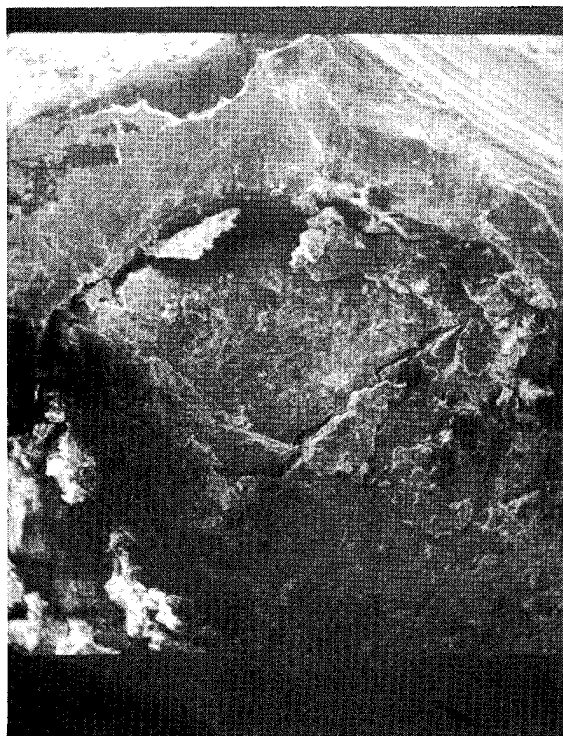


1 Week

2000X

Figure 25. SEM photomicrograph of Lot 2375 HNAB-MDF:
isothermal/constant-humidity exposure

(continued)



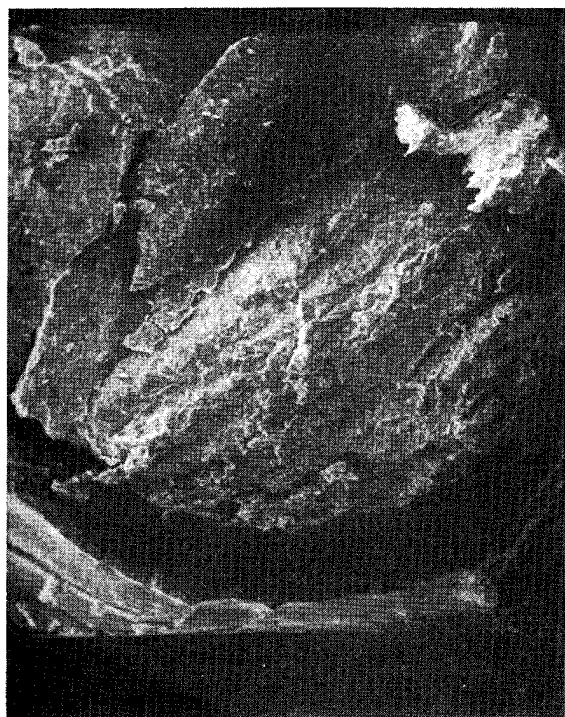
2 Weeks

200X



2 Weeks

2000X



4 Weeks

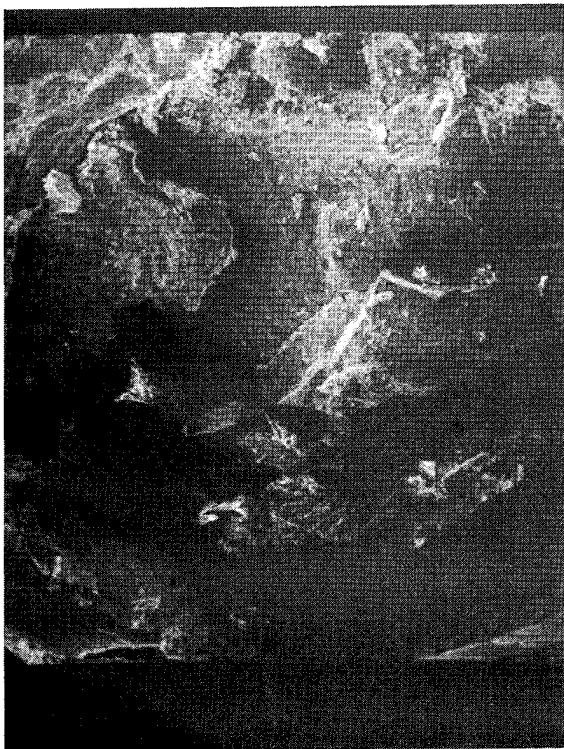
200X



4 Weeks

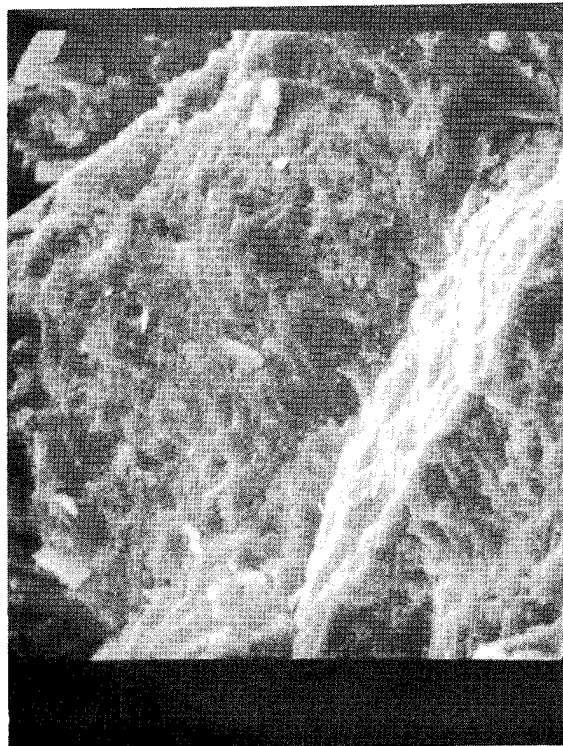
2000X

Figure 25. (continued)



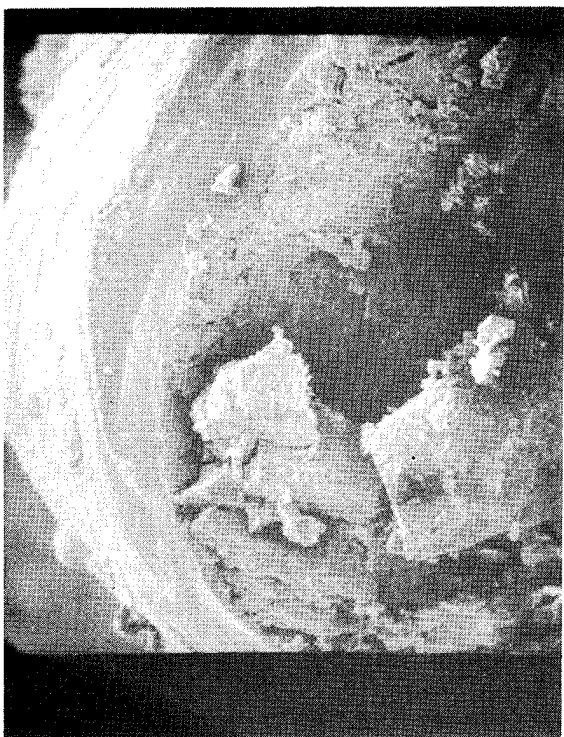
8 Weeks

200X



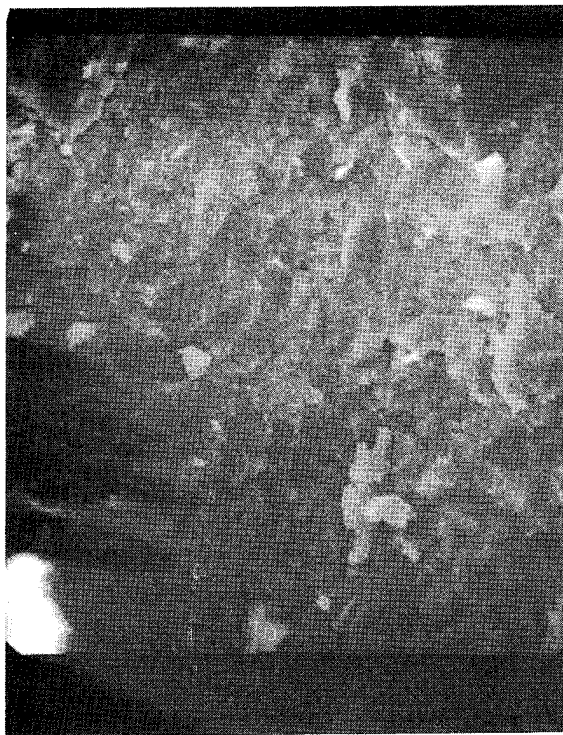
8 Weeks

2000X



16 Weeks

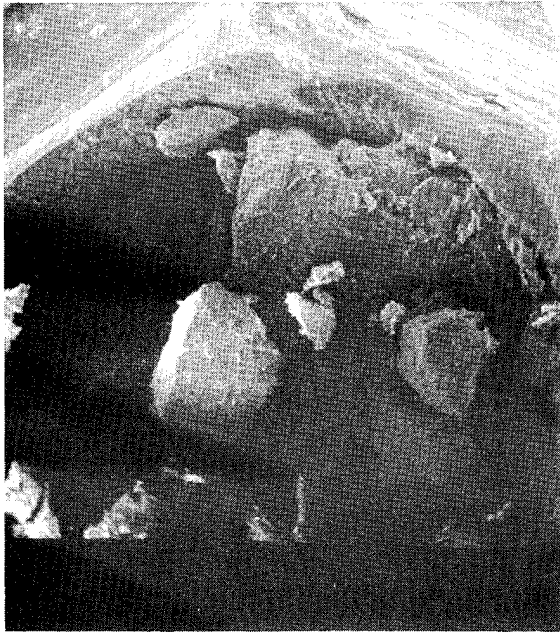
200X



16 Weeks

2000X

Figure 25. (continued)



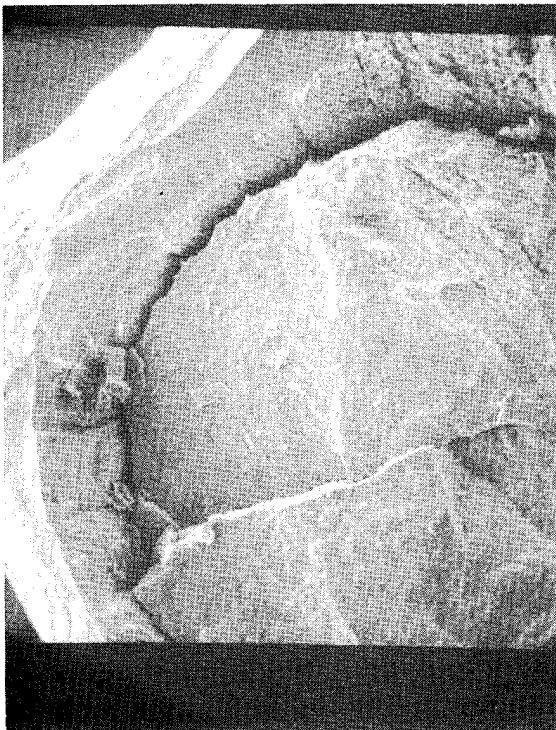
32 Weeks

200X



32 Weeks

2000X



64 Weeks

200X



64 Weeks

2000X

Figure 25. (concluded)

the chemical analysis data of the bulk HNAB powder and MDF do not provide the same general trends in the results, suggesting different mechanisms of decomposition.

Thermal analysis, thin-layer chromatography, and scanning electron microscopy all measured small changes within the MDF HNAB. These changes suggested, directly or indirectly, that some decomposition was occurring within the HNAB-MDF cores. Again, in each case the change (decomposition) measured was small, with the jungle cycle a more severe environment than the isothermal/constant-humidity exposure.

The detonation velocity data can be related to an extent to the decomposition noted within the MDF HNAB. All three decomposition products measured are energetic materials and thus would contribute to the detonation phenomenon. During the decomposition reactions, changes in the MDF (either chemical or physical) could have occurred, thus altering the detonation characteristics. An increased detonation velocity was noted only after similar increases in decomposition occurred. During the early exposure periods, little decomposition and corresponding small changes in the detonation velocity were measured.

Changes in the bulk HNAB powders also occurred. By comparing similar time exposures of the HNAB powders and the MDF, the effect of both humidity environments was shown to be significantly greater in the bulk powders than in the MDF. Both the thermal analysis (DSC) and the thin-layer chromatography (TLC) analysis indicated that greater amounts of decomposition occurred in the bulk powder. In addition, the TLC data suggested that different mechanisms for decomposition were

involved. In the bulk, the reaction of HNAB with humidity (or water) was the primary decomposition mechanism; in MDF geometry, hexanitrohydrazobenzene (as an impurity), and not the HNAB, apparently was primarily involved in the decomposition. In both cases the products of decomposition were picric acid and trinitrobenzene.

Reversion of the Form III HNAB polymorph to Form II was observed in both the bulk and MDF HNAB materials. Because greater amounts of Form III existed in the MDF, the magnitude of this reversion appeared to be greater. However, similar patterns of change occurred in both cases; thus a similar mechanism (thermal effects) apparently caused this reversion.

Bulk HNAB powder which was subjected to a given humidity environment for 16 weeks was manufactured into MDF and tested. Data from this aspect of the humidity/time study showed very little change from the baseline data. Thus a 16-week exposure to a humidity environment did not affect the HNAB powder adversely. The 64-week bulk samples, as previously noted, have not been manufactured into MDF for evaluation purposes and will be discussed later in an addendum to this report.

Although the primary purpose of this program was to determine the effects of a humid environment on HNAB, a secondary useful result occurred: the development of sensitive analytical techniques for detection of decomposition products in HNAB. These tools may prove very useful in the study of potential compatibility problems concerning HNAB and other explosive materials.

From this study, the overall conclusion is that humidity will not affect the performance of the HNAB significantly and thus does not preclude its use as a timing material in humid environments. Though some changes were noted by the various diagnostic techniques, the materials performed within the allotted performance spec-

ifications. Within reasonable limits HNAB-MDF, when subjected to humidity environments, requires no special storage considerations. Based on usual observations of the MDF, it appears that the aluminum sheathing material probably degrades faster than the HNAB cores.

REFERENCES

1. R. J. Buxton and T. M. Massis, "Compatibility of Explosives with Structural Materials of Interest," SC-M-70-355, Sandia Laboratories, Albuquerque, N. M., August 1970.
2. R. J. Buxton and T. M. Massis, "Compatibility of Explosives with Structural Materials of Interest," SC-M-70-355, Vol. II, Sandia Laboratories, Albuquerque, N. M., June 1972.
3. Personal communication between D. K. McCarthy, 2516, and authors.
4. J. C. Bagg, "Aluminum-Sheathed Mild Detonating Fuse (U)," SC-TM-67-632, RS 3410/1046, Sandia Laboratories, Albuquerque, N. M.
5. A. C. Schwarz, "Aluminum-Sheathed Mild Detonating Fuse (U)," Progress Report No. 2, SC-TM-68-211, Sandia Laboratories, Albuquerque, N. M.
6. J. C. Bagg and R. R. Weinmaster, "Aluminum-Sheathed Mild Detonating Fuse (U)," Progress Report No. 3, SC-TM-710859, Sandia Laboratories, Albuquerque, N. M.
7. R. R. Weinmaster and J. C. Bagg, "Characteristics and Development Report for MC1984 and MC2361 Timers (U)," SC-DR-710860, RS 3150/2158, Sandia Laboratories, Albuquerque, N. M.
8. Personal communication between R. R. Weinmaster, 2314, and T. M. Massis, 2515.
9. Manufactured according to Sandia Specification SS209838 Rev. C.
10. "Sandia Corporation Standard Environmental Test Levels," SC-4451A(M), p. 13.
11. T. M. Massis and D. J. Gould, "Separation and Analysis of Decomposition Products in Hexanitroazobenzene (HNAB) by TLC," unpublished report.
12. W. D. Harwood, "Light Load MDF," Quality Engineering Report Cycle 2 of BB293014, September 1973.
13. W. C. McCrone, "Crystallographic Study of SC-101," Project 883, Chicago, Ill., (1967).
14. E. J. Graeber and B. Morosin, "The Crystal Structures of 2, 2', 4, 4', 6, 6' - Hexanitroazobenzene (HNAB), Form I and Form II," Acta. Cryst. B30 310 (1974).
15. Handbook of Chemistry and Physics, Edition 46, C-172 & C-478, The Chemical Rubber Co., Cleveland, Ohio, (1966-1967).
16. D. M. O'Keefe, "Synthesis and Properties of HNAB," SAND-74-0239, Sandia Laboratories, Albuquerque, N. M.
17. G. C. Hampson and J. M. Robertson: J. Chem Soc., 409, (1941).

COMPUTER COMPATIBILITY DATA RETRIEVAL PROGRAM

Julian L. Davis, George Brincka and David W. Levi

1. INTRODUCTION

A computer program called IECOMPAT was developed for storage and retrieval of compatibility data on inert-energetic systems. An inert-energetic system is defined as a binary system consisting of a polymer (inert material) and explosive or propellant (energetic).

Some 2500 system combinations are permanently stored in the data bank in the CDC 6600 computer located at Picatinny Arsenal. They represent information from the literature to the end of 1973. The data bank may be updated. The user may currently run the program on any of Picatinny's INTERCOM 3 (teletype) or batch terminals. The program is so constructed that, by a dialogue with the computer, the user may receive answers to a variety of questions: he may obtain information about a given system stored in the data bank, or may obtain various combinations of cross-reference information such as all inert materials in data bank compatible with a given energetic material. The user is presented with specific instructions and a series of codes relating to the questions he wants answered. This will be described below:

2. COMPUTER DIALOGUE

In addressing the computer terminal, the user engages in a dialogue with the computer in the following sense: After logging in, the user will get a message from the computer asking if he wants a list of the codes for the type of information desired. If he already knows the codes, he

types "No", then the number of the code corresponding to the question he wants answered. If he doesn't know the codes he types "Yes" and obtains the codes shown in Fig. 1.

It is worth noting that Codes 6 and 7 give the new user a current list of all the inert and energetic materials (respectively) in the data bank. This information can also be helpful in giving him the terminology that is used. Suppose the user wants information about the system:

POLYPHOSPHAZENE + MINOL-2. He types the number "1" (corresponding to Code 1). He then receives instructions on how to type in the system. Having done so he will then get a computer printout of the information in the data bank on this system as shown in Fig. 2.

Note the format:

System: inert + energetic

Compatibility: yes, no or marginal

Method: type of test used to determine compatibility such as VAC STAB (vacuum stability), DTA

Remarks: identification of materials and other pertinent remarks

Reference: Source of information (available from PLASTEC)

Note that the spelling must be precise. For example, neither MINOL2 nor MILOL 2 are in the data bank. Thus, if such a variant of MINOL-2 is typed in, the following message is obtained: Inert Material MINOL2 (MINOL 2) Not In Data Bank.

Suppose the user wants to know all the energetic materials compatible with a given inert material, say ABS. He types "2" and gets instructions and a printout of the appropriate energetic materials as shown in Fig. 3 (upper part). If he then wants those energetic materials incompatible or marginal with inert material ABS, he types "4" and gets instructions and a printout as shown in Fig. 3 (lower part).

In a similar manner, if the user wants all the inert materials compatible with a given energetic material, he types "3". If he wants those that are incompatible or marginal with a given inert material, he types "5". For example, if he wants those inert materials compatible with energetic material M5, or those inert materials incompatible or marginal with M5 he will get instructions and printouts as shown in Fig. 4.

As an example of a multiple listing of a given system conflicting results depending on test conditions, consider the system EPOXIDE + M5, (Fig. 5). There are three different printouts for this system giving compatibility: YES, MARGINAL, NO. The user is invited to study the appropriate literature given in the references for further information. The point here is that there is sometimes conflicting results depending on test conditions, material differences such as different structures of resins or curing agents, different commercial additives, impurities, different curing conditions, etc. The user must use his best engineering judgement (based on information in the available literature) in the selection of the system for his particular use.

In addition to the short term effects illustrated in the above printouts, the data bank contains long term storage data, where available. This effect

is usually on the polymer. As an example, consider the system: POLYESTER + M7. The appropriate printouts show three sets of information for this system, (Fig. 6). The first printout represents the short-term effect (VAC STAB) whereas the others show that the long-term storage effect is to make the system marginal or incompatible.

Figs 7 and 8 show printouts for the system EPOXIDE + RDX where rather extensive compatibility testing has been carried out. The comments made above are further illustrated by this example.

DO YOU WANT A STATEMENT OF THE CODES REPRESENTING THE TYPE OF INFORMATION DESIRED.

TYPE YES OR NO, PRESS RETURN KEY- YES

-CODES FOR TYPE OF INFORMATION DESIRED-

1. INFORMATION ABOUT A SPECIFIC SYSTEM.
2. LIST OF ENERGETIC MATERIALS COMPATIBLE WITH A GIVEN INERT MATERIAL.
3. LIST OF INERT MATERIALS COMPATIBLE WITH A GIVEN ENERGETIC MATERIAL.
4. LIST OF ENERGETIC MATERIALS INCOMPATIBLE OR MARGINAL WITH A GIVEN INERT MATERIAL.
5. LIST OF INERT MATERIALS INCOMPATIBLE OR MARGINAL WITH A GIVEN ENERGETIC MATERIAL.
6. LIST OF INERT MATERIALS IN DATA BANK.
7. LIST OF ENERGETIC MATERIALS IN DATA BANK.
8. NO MORE INFORMATION DESIRED. STOP PROGRAM.

UNDER CODES 2-5, A PREFIX IS ADDED TO AN ANSWER WHEN TESTS PRODUCED CONFLICTING RESULTS, OR TO MAKE ANSWER MORE COMPLETE--

- C IN THE PREFIX SIGNIFIES AT LEAST ONE TEST INDICATED THE SYSTEM IS COMPATIBLE.
- I IN THE PREFIX SIGNIFIES AT LEAST ONE TEST INDICATED THE SYSTEM IS INCOMPATIBLE.
- M IN THE PREFIX SIGNIFIES AT LEAST ONE TEST INDICATED THE SYSTEM IS MARGINAL.

FIG. 1 INFORMATION THAT MAY BE OBTAINED FROM THE DATA BANK

ENTER NEXT INERT MATERIAL OR CODE. 1

TYPE THE SPECIFIC SYSTEM - THE INERT MATERIAL ON FIRST LINE.
PRESS RETURN KEY, THE ENERGETIC MATERIAL ON NEXT LINE,
PRESS RETURN KEY

POLYPHOSPHAZENE
MINOL-2

SYSTEM: POLYPHOSPHAZENE + MINOL-2
COMPATIBILITY: YES
METHOD: VAC STAB (100 DEG. C; 40 HRS)
REMARKS: POLYPHOSPHAZENE RUBBER (AMMRC); POLYPHOSPHAZENE
RUBBER (AMMRC) (IN ACETONE)
REFERENCE: ANAL. CHEM. BR., REPORT NO. AL-S-82-71, 1971
(AVAILABLE MED, FRL)

FIG. 2 COMPATIBILITY OF POLYPHOSPHAZENE + MINOL-2

ENTER CODE--USE NO BLANKS--2
ENTER INERT MATERIAL, PRESS RETURN KEY
ABS

THE FOLLOWING ENERGETIC MATERIALS ARE COMPATIBLE WITH INERT
MATERIAL ABS

M6	M9
M26	NH
COMP B	M15
M1	M17
M80	

ENTER NEXT INERT MATERIAL OR CODE. 4
ENTER INERT MATERIAL, PRESS RETURN KEY. ABS

THE FOLLOWING ENERGETIC MATERIALS ARE INCOMPATIBLE OR MARGINAL
WITH INERT MATERIAL ABS

M *TNT	M *RDX-TNT
I *NQ	

FIG. 3 LISTS OF ENERGETICS ^(a)COMPATIBLE AND ^(b)INCOMPATIBLE
OR MARGINAL WITH ABS

THE FOLLOWING INERT MATERIALS ARE COMPATIBLE WITH ENERGETIC MATERIAL M5

SILICONE
MI * EPOXIDE
CELLULOSE NITRATE
NITRO CELLULOSE
POLYSTYRENE
POLYESTER
MI * ADHESIVE
COSTING
I * LOCTITE

ENTER NEXT ENERGETIC MATERIAL OR CODE. 5

ENTER ENERGETIC MATERIAL, PRESS RETURN KEY. M5

THE FOLLOWING INERT MATERIALS ARE INCOMPATIBLE OR MARGINAL WITH ENERGETIC MATERIAL M5

M * POLYURETHANE
CMI * EPOXIDE
CMI * ADHESIVE
CI * LOCTITE
M * RUBBER
MI * SEALANT

FIG. 4 LISTS OF INERTS (a) COMPATIBLE AND (b) INCOMPATIBLE OR MARGINAL WITH ENERGETIC MATERIAL M5

ENTER NEXT SYSTEM OR CODE.

EPOXIDE

M5

SYSTEM: EPOXIDE + M5
COMPATIBILITY: YES
METHOD: DTA; VAC STAB (90 DEG. C; 40 HRS)
REMARKS: EPON 815 + DMA; EPOXY H-1863
REFERENCE: HONEYWELL REPORT MARCH 1971 (AVAIL MED, FRL);
PLASTEC REPORT 33, 1968

SYSTEM: EPOXIDE + M5
COMPATIBILITY: MARGINAL
METHOD: DTA
REMARKS: EPON 815 + VERSAMID 140; EPON 828 + VERSAMID 140
UNCURED
REFERENCE: HONEYWELL REPORT MARCH 1971 (AVAIL MED, FRL)

SYSTEM: EPOXIDE + M5
COMPATIBILITY: NO
METHOD: VAC STAB (90 DEG. C; 40 HRS)
REMARKS: EPON 828; EPOXY 437
REFERENCE: PLASTEC REPORT 33, 1968

FIG. 5 COMPATIBILITY OF EPOXIDE + M5

SYSTEM: POLYESTER + M7
COMPATIBILITY: YES
METHOD: VAC STAB (90 DEG. C; 40 HRS)
REMARKS: LAMINAC 4116 (CYANAMID) - MEK PEROXIDE CURED AND
UNCURED;
LAMINAC 4116, 4134 (CYANAMID); PHTHALIC ALKYD
(DRYING OIL MF-884) (APG); STYRENATED ALKYD MF-882
(APG); VINYL TOLUENE ALKYD (APG)

REFERENCE: PLASTEC REPORT 40, 1971; PLASTEC NOTE 22, 1970

SYSTEM: POLYESTER + M7
COMPATIBILITY: MARGINAL
METHOD: STORAGE (50 DEG. C; 26 WKS)
REMARKS: LAMINAC 4116, WGT CHANGE
REFERENCE: PA TECH REPORT 2595, 1959

SYSTEM: POLYESTER + M7
COMPATIBILITY: NO
METHOD: STORAGE (50 DEG. C; 26 WKS)
REMARKS: LAMINAC 4116, WGT CHANGE
REFERENCE: PA TECH REPORT 2595, 1959

ENTER NEXT SYSTEM OR CODE. POLYESTER

M8

NO DATA FOR THIS SYSTEM.

FIG. 6 COMPATIBILITY OF POLYESTER + M7 AND POLYESTER + M8

ENTER CODE--USE NO BLANKS--1
TYPE THE SPECIFIC SYSTEM - THE INERT MATERIAL ON FIRST LINE.
PRESS RETURN KEY, THE ENERGETIC MATERIAL ON NEXT LINE,
PRESS RETURN KEY

EPOXIDE

RDX

SYSTEM: EPOXIDE + RDX
COMPATIBILITY: YES
METHOD: VAC STAB (100 DEG C; 40 HOURS) (ROOM TEMP); STORAGE
(76 DEG. C; 36 WKS); DTA
REMARKS: EPON 828 (SHELL) (MALEIC ANHYDRIDE CURED); EPON 810
(3 PART SYSTEM) UNCURED; ECCO BOND PDQ (4%1)
(EMERSON AND DUMING) QUICK SET MATERIAL, UNCURED;
EPON 914 CURED; EPOWELD XL9141 (A+E+ HARDMAN)
UNCURED; DSL A1, DSLA2, EPIKOTE 828-VERSAMID 140
CURED; DSLB1, DSLB2, EPIKOTE 828-SYNOLID 960 CURED;
DSL 01, EPIKOTE 828-EPIKURE LVU CURED; DSL D1,
EPIKOTE 828-GENAMID 2000 CURED; 555-1011, MIL-C-52232;
DEVCON (CHEM DEVEL CORP); EPON 31-59 CURED AND
UNCURED; EPON 31-59, PART B, UNCURED; EPON 934,
CURED; EPOXY-PHENOLIC, MIL-C-52232; HYSOL CAKE
(HOUGHTON LABS), CURED; BAKELITE BRR-18795; EPON 828
W Z WGT CHANGE; EPON 828 AMINE CURED.
REFERENCE: ANAL CHEM BR, REPORT NO. AL-S-74-72, 1972 (AVAIL
MED, FRL); SANDIA CORP REPORT SC-M-70-355 1970;
PLASTEC REPORT 40, 1971 PLASTEC REPORT 33, 1968;
PLASTEC NOTE 22, 1970; PA TECH REPORT 2595, 1959;
THERMOCHIM ACTA 5, 433, 1973.

FIG. 7 COMPATIBILITY OF EPOXIDE + RDX

SYSTEM:	EPOXIDE + RDX
COMPATIBILITY:	MARGINAL
METHOD:	VAC STAB (100 DEG. C; 40 HRS)
REMARKS:	EPON 820-VERSAMID 140, ADH A; EPOXY-POLYAMIDE, MIL-C-22750; TRA-BOND BB-2129 (TRA-CON INC)
REFERENCE:	PLASTEC REPORT 33, 1968

SYSTEM:	EPOXIDE + RDX
COMPATIBILITY:	NO
METHOD:	VAC STAB (150 DEG C; LESS THAN 1 HOUR) (250 DEG F); STORAGE (76 DEG. C; 36 WKS); DTA
REMARKS:	BONDMASTER M-777 EPOXY (RUBBER AND ASBESTOS CORP) UNCURED: ALUMINA, EPOXY, VERSAMID (54-45-33) CURED; EPON 914 UNCURED; ECCO BOND (EMERSON AND CUMING) 45LV-CAT. 15LV (CURED 1-1 BY WGT) (CURED 66-34 BY WGT); A1177B (GOODRICH) CURED; BROLITE (EPOXY A423 + THINNER 0252); DEVCON MIX (CHEM DEVEL CORP); EPON 31-59, PART A, UNCURED; EPON 820-VERSAMID 140; EPON 934 UNCURED; EPON 934, PART A, UNCURED; EPON 934, PART B, UNCURED EPOXY/POLYAMIDE, MIL-C-22750; FIBERITE 5430 (EPOXY-GLASS); HYSOL (HOUGHTON LABS), UNCURED; ARMSTRONG A-4; EPON 828 W Z APPEARANCE; EPON 828 ANHYDRIDE CURED.
REFERENCE:	SANDIA CORP REPORT SC-M-70-355, 1970; PLASTEC REPORT 33, 1968; PLASTEC NOTE 22, 1970; PA TECH REPORT 2595, 1959; THERMOCHIM ACTA 5, 433, 1973.

FIG. 8 COMPATIBILITY OF EPOXIDE + RDX

COMPATIBILITIES OF PLASTICS AND ENERGETIC MATERIALS IN SMALL CALIBER AMMUNITION

by

Wilmer White

Pyrotechnic Development Branch, MD
Frankford Arsenal
Philadelphia, Pa.

ABSTRACT

Two examples of polymer (plastics) utilized with high energy materials are presented.

1. Propellant compositions with priming mixtures.
2. Radiation activated polymers as binders in external tracers.

In addition, a discussion on the use of hypergolic materials with tracer compositions is presented.

1. PROPELLANT COMPOSITIONS WITH PRIMING MIXTURES

A most familiar example of incompatibility between plastics and pyrotechnics is the problem of volatile agents from the plastic impregnating and reacting with priming mixtures, causing loss of sensitivity or functioning capability in primers. In high temperature, PAD applications nitroglycerine migration from double base propellant charges was determined to be the cause of a number of misfires. This problem was solved by placing an integral web between the primer and propellant charge. A similar situation arose with the use of the hybrid or jet flame primer shown in Figure 1. Here, thin sheets of double-base, high nitroglycerine content propellant are placed inside the primer cup with a small amount of primer mix added to a center perforation to initiate the reaction. It was found that these hybrid primers lost sensitivity on storage due to the reaction of the nitroglycerin with the antimony sulfide, a gritty material added to enhance the impact sensitivity and to supply fuel to the mix.

mixes is continuing, with emphasis on reducing or eliminating volatiles from the propellants in the hybrid arrangement and also certain highly reactive fuels in the primer mix. Some of the advantages of hybrid primer are:

1. Reduced brisance.
2. Uniform charge weight is more easily achieved.
3. Improved ignition efficiency at low temperature.

Recent test results of hybrid primer/ignition systems, using propellant discs, continue to offer promise in the field of propellant ignition both in performance and improved production efficiency. Current emphasis is on improving ignition for cannon caliber ammunition.

The truly novel aspect of this hybrid arrangement is the fact that a propellant-type, miniature gas generator is made to react within a response time comparable to that achieved by standard primers.

The development of stable, high-energy propellant sheet and compatible percussion-sensitive

2. RADIATION ACTIVATED POLYMERS AS BINDERS IN EXTERNAL TRACERS

An example where compatibility of energetic materials with radiation environments had to be considered occurred in the radiation-polymerization of pyrotechnics. The Serial Flechette Rifle (SFR) is a micro-caliber weapon firing a projectile of very small diameter ($\sim 0.075''$). A tracer round of conventional design for such micro-caliber ammunition (i.e. a pyrotechnic mix compacted into a cavity in the base of the projectile), would present serious production and cost problems. However, a tracer projectile with a cavity of $0.060''$ diameter was mass-produced, with feasibility tests proving only partially successful. Enlarging the body of the flechette was not a practical solution; this suggested the application of an external tracer composition, closely bound to the surface of the shaft.

One coating approach attempted was using an epoxy binder with standard pyrotechnic compositions. This procedure produced an acceptably performing tracer with 30% ignition reliability; complications arose, however, due to inadequate bonding around the projectile body, resulting in a bright muzzle flash (from tracer mix burning inside the barrel).

It was determined by subsequent experimentation that a more successful method of increasing bonding strength was through the use of radiation-induced polymerization. Available sources of radiation have energies far in excess of normal chemical bond energies, which are typically in the range of 10 eV. These energy and intensity levels, however, cause concern that degradation of pyrotechnic compositions will occur during the subsequent to the radiation process. Experience has shown, however, that doses required to yield 100% conversion of monomer to polymer are usually less than 10M rads (one rad corresponds to the absorption of 100 ergs/gm of material). Degradation of common explosives and pyrotechnic formulations is not significant below 10^3 Mrads. Hence

no change in characteristics were detectable in the pyrotechnic mix from radiation doses required to effect 100% cure of the polymeric binder.

All irradiations in this investigation were performed in a nominal 10,000 curie, cobalt-60 facility. Five projectile/coating configurations were evaluated. These are shown in Figure 2, which offers a comparison of the internal tracer (item a) with several different external tracer configurations. Projectiles (b) and (c) represent the tracer formulations in which thermally-cured epoxy resin was used. For projectile (b), the pyrotechnic composition was applied by hand, cured, and then hand-filed to the final configuration. For projectile (c), the tracer mixture was fabricated in a transfer mold and then cured. Projectile (c), appears here in the "as molded" configuration. Samples (d) through (f) represent various radiation polymerized configurations. Projectile (d) was unsatisfactory due to the dimensional limitations of the sabot, which is a molded fiberglass shoe used to hold the projectile in place as it travels along the barrel of the weapon. Projectiles (e) and (f) represent two configurations of projectiles having externally applied pyrotechnics; these were used in the majority of the lots which were further tested.

The feasibility of utilizing radiation processing techniques to produce external tracer rounds has been demonstrated. Results indicate that systems which produce highly cross-linked binders with resulting resilient properties will give optimum performance. The quantity of material applied to the fin area is critical, however, with a balance existing between trace characteristics and bonding strength required for retention of the pyrotechnic charge during firing. No compatibility problems were encountered which would preclude the use of irradiation as a tool in casting or curing pyrotechnics.

In another application, the use of radiation-polymerized binders is currently under investigation in primers. With the introduction of high speed

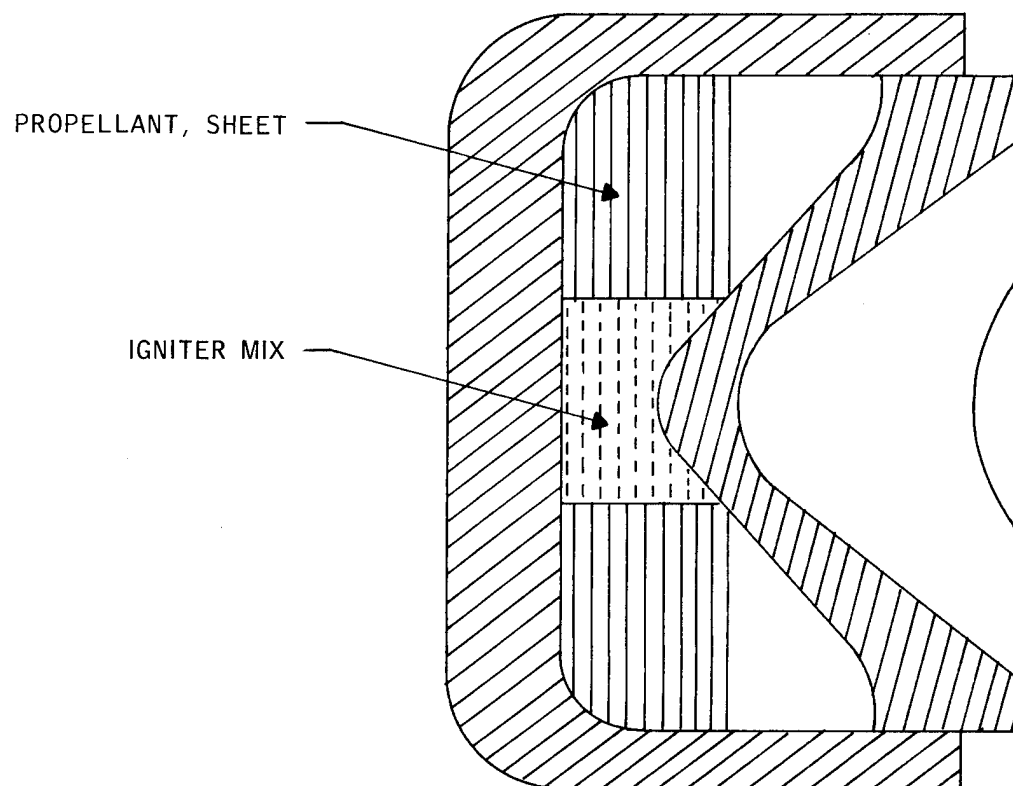


Figure 1. The Jet Flame Primer

primer insertion machines, primer dusting, a common occurrence, has received considerable attention. Although only several granules of priming composition dust per primer, a large quantity of primer dust can accumulate on the equipment through-out daily production. During "debugging" operations on the primer insertion machines, sufficient quantities of priming mixture were collected at several locations to identify this as a hazardous situation.

One of the many suggested solutions to this problem was the improved binding capability of the radiation-treated, polymer-bound pellet. Results to date indicate that a strong, hard, primer pellet is obtained, which has a slight decrease in drop test sensitivity. Once the pellet is cured, the loss of mixture through dusting should be greatly minimized.

3. HYPERGOLIC MATERIALS WITH TRACER COMPOSITIONS

Another example where compatibility was a consideration involved the use of hypergolic compounds in tracer compositions. Such materials are useful largely because of one outstanding characteristic, that of spontaneous ignition on exposure to air; naturally the materials must also possess significant pyrotechnic capability.

In any tracer compound, ignition is the primary concern, and compositions containing hypergolic compounds are no exception. However, since these compounds react vigorously with oxygen either from the atmosphere or from water, it is imperative that careful evaluations be made as to their reactivity or stability when admixed with conventional tracer mixtures containing strong oxidizing agents.

The hypergolic chemicals most commonly used in these tests were triethyl aluminum (TEA), trimethyl aluminum (TMA), and mixtures thereof.

The properties of TEA are shown in Figure 3. Note that it is a liquid at normal environmental temperatures. Its chemical stability in the presence of various oxidizers is shown in Figure 4, which represents results of a series of compatibility tests. The compatibility test was accomplished by adding two milliliters of TEA to 2 to 3 grams of each oxidizer indicated, and observing the combination for signs of smoking or fuming (which are indicative of reaction). The mixtures were handled in a glove box under a positive nitrogen atmosphere.

As can be determined from the results shown here, there were two categories of combinations determined from this qualitative experiment -- compatible and incompatible. It is also apparent that while all the nitrate salts tested were compatible, only some of the perchlorate and chlorates successfully passed the test. Furthermore, the sodium salts used were all compatible. It should be noted that this compatibility experiment was short term only, involving a three-day monitoring period; the long term stability of TEA/oxidizer combinations has not been determined.

The next step employed in this study was that of evaluating the characteristics of what we believed were complete pyrotechnic mixtures, which include TEA/oxidizer/meter or metal hydride. This phase of testing was accomplished using a similar procedure to that previously described. The experimental compositions contained three grams of oxidizer, two grams of powdered metal and two milliliters of TEA. The results (Figure 5) show that compositions containing sodium chlorate and magnesium, or sodium chlorate and boron with TEA produce brighter flames and have shorter ignition delay times. As can be seen, long ignition delay times were obtained on many of the compositions evaluated. It was found that the ignition delay times could be greatly reduced

by using a 50/50 mole percent mixture of TEA / TMA (trimethyl aluminum). This finding was quite helpful to us, since it meant that we could direct attention to other oxidizers and metals previously ruled out because of the long ignition delay times of their mixtures. Figure 6 lists the hypergolic tracer formulations which provided the best laboratory results obtained during our investigation.

The objectives of this investigation were to evaluate hypergolic, pyrotechnic compositions for fuse in tracer or spotter ammunition. This involved hazards in storing and handling these same materials. Optimized systems were selected from the standpoint of performance as well as a low ignition risk while in components.

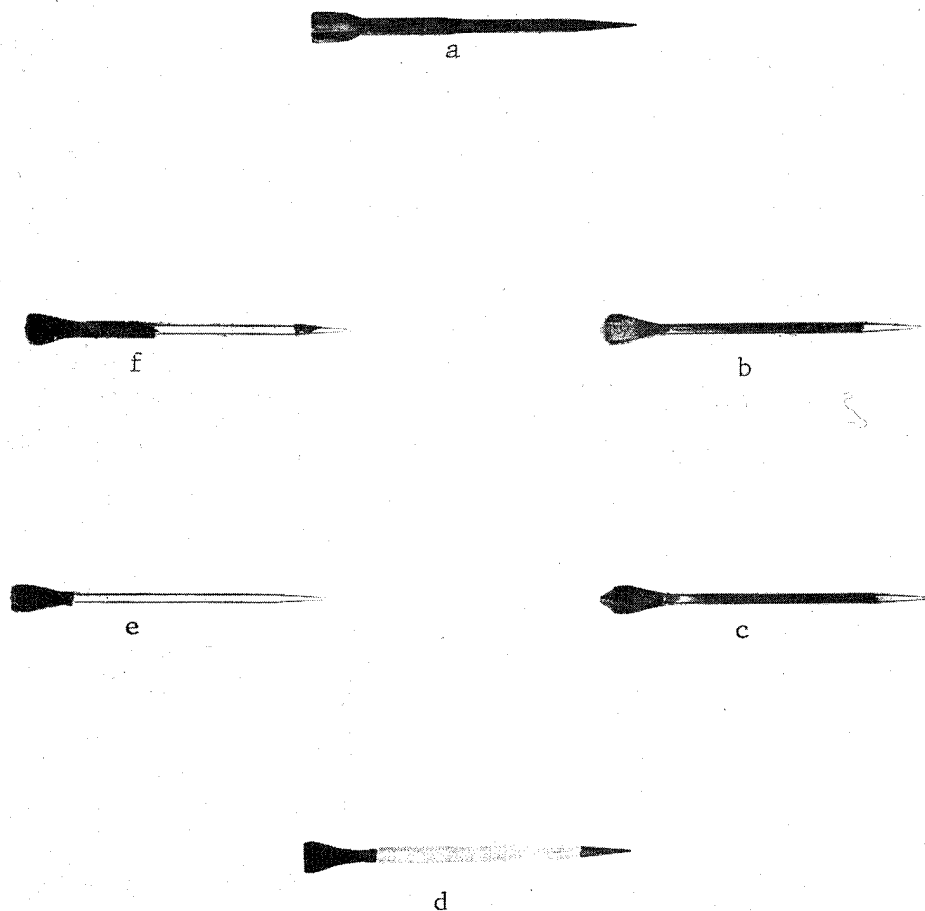


Figure 2 SFR Tracer Projectiles: a) Type 10 Internal;
b) External-hand fabricated and filed (epoxy);
c) Molded (epoxy); d) Radiation Polymerized
(shaft only); e) Radiation Polymerized (fins
only); f) Radiation Polymerized (fins and shaft)

<u>Description:</u>	Colorless Liquid
<u>Formula:</u>	Al (C ₂ H ₅) ₃
<u>Constants:</u>	MW 114.15
	BP 194°C
	MP <-18°C
<u>Fire Hazard:</u>	Spontaneous Reaction With Air Violent Reaction With Water
<u>Explosion Hazard:</u>	Moderate (Presence of Ethane)

Figure 3. Properties of Triethyl Aluminum (TEA)

<u>Compound</u>	<u>Compatible</u>	<u>Incompatible</u>
Sodium Nitrate	X	
Chlorate	X	
Iodate	X	
Chromate	X	
Peroxide	X	
Fluoride	X	
Potassium Nitrate	X	
Chromate	X	
Dichromate	X	
Permanganate	X	
Iodate		X
Chlorate		X
Bromate		X
Strontium Peroxide	X	
Nitrate	X	
Perchlorate	X	
Barium Peroxide	X	
Nitrate	X	
Iron Chloride		X
Bismuth Pentoxide		X
Ammonium Perchlorate		X
Copper Oxide	X	
Manganese Oxide	X	
Boron Trioxide	X	

Figure 4. Compatibility Of Oxidizers With TEA

Oxidizer/Metal	Ignition Delay (Short, Long)	Burning Rate (Fast, Slow)	Brightness (Bright, Very Bright)
NaClO_3/Mg	S	F	VB
NaClO_3/B	S	F	VB
$\text{NaClO}_3/\text{LiAlH}_4$	L	F	B
$\text{Na}_2\text{O}_2/\text{ZrH}_2$	L	F	B
$\text{Na}_2\text{O}_2/\text{Al}$	L	F	B
$\text{Na}_2\text{O}_2/\text{Mg}$	L	F	B
$\text{Na}_2\text{O}_2/\text{B}$	L	F	B

Figure 5. Burning Characteristics of TEA/Oxidizer/Metal Mixtures

Mixture	Composition (Wt %)				TEA/TMA*
	Mg	Zr	NaClO_3	$\text{Sr}(\text{NO}_3)_2$	
TI-3A	50		30		20
TI-3B		60	25		15
TI-3C	30	30	25		15
TI-6A	45			30	25
TI-6B	50			30	20

* 50:50 mole %

Figure 6. Final Hypergolic Tracer Formulations

COMPATIBILITY TESTING TECHNIQUES FOR GASLESS PYROTECHNICS

Thomas M. Massis and David K. McCarthy
Explosive Materials Division 2516

Donald J. Gould
Initiating & Pyrotechnic Component Division 2515
Sandia Laboratories
Albuquerque, New Mexico 87115

and

Bruce D. McLaughlin
Los Alamos Scientific Laboratory
Los Alamos, New Mexico 87544

ABSTRACT

Renewed interest in pyrotechnic compositions has caused a re-examination of compatibility test techniques. This has led to the application of several new methods to evaluate potential compatibility problems involving gasless pyrotechnic compositions. These two methods are scanning electron microscopy and electrochemical techniques (corrosion cell potentials and potentiokinetic sweep procedures). This paper describes the use of these techniques to evaluate compatibility between pyrotechnics and structural materials.

ACKNOWLEDGMENTS

The authors wish to acknowledge the contributions of W. H. Smyrl, 5831, for electrochemical data acquisition and helpful discussion, and T. Minchow for assistance in manuscript preparation.

1. INTRODUCTION

In the past, compatibility testing of energetic materials has primarily involved measuring the volume of gas evolved at elevated temperatures when two materials are in contact. The amount of gas produced by the reacted materials is then compared to that evolved by the individual materials. From these data, an evaluation of the materials is made as to whether

they are compatible, with some prediction made as to the compatibility of the materials in a component over its stockpile life.

Compatibility data obtained on most of the energetic materials have been on organic explosives. Generally when organic explosives react with other materials,

gaseous products are evolved. Thus gas evolution has been considered to be a standard measurement of compatibility for organic materials.

The primary technique to obtain these data has been the vacuum stability test and, more recently, the chemical reactivity test (CRT)^(1,2) The chemical reactivity test at Sandia Laboratories is currently favored over the vacuum stability test because it provides both qualitative and quantitative data about the gases evolved during reactivity testing. These two techniques in combination with rapid screening procedures (such as visual and thermal analysis techniques) are used to eliminate incompatible combinations prior to further development. Several documents regarding the chemical compatibility between energetic materials and component structural materials have been published.^(3,4)

About 1973, Sandia's interest in pyrotechnic materials for components began to increase. This interest was related to a desire to decrease the use of primary explosives wherever possible and to substitute less sensitive pyrotechnics or secondary explosives. Generally, the main uses of primary explosives have been in detonators, switches, igniters and valve actuators.

With the advent of the expanded use of pyrotechnics came the problem of testing these materials for compatibility with their corresponding structural materials. Gas evolution techniques were originally utilized, but it soon became evident that some of the potential reactions would be gasless. Thus, in many of these cases, gas evolution techniques were found to be of limited value in compatibility testing.

For example, a number of Sandia components utilize B/CaCrO₄, Ti/KClO₄, and AlA (Zr/Fe₂O₃). The reactions with such materials as kovar (header posts) and nichrome (bridgewires) would most likely not evolve gases. Corrosion of the metallic interfaces and decomposition of the pyrotechnic formulation could take place without gas formation and not be detected by normal compatibility procedures.

Thus questions arise as to what should be used for the compatibility testing of materials that do not necessarily evolve gaseous products.

This paper describes a study that was undertaken to provide compatibility information for a pyrotechnic formulation--potassium hexacyanocobaltate (K₃ [Co(CN)₆]) -- and potassium perchlorate (KClO₄) with various component structural materials for an actuator application. Data have been obtained on this pyrotechnic composition using short term screening tests. These in turn have been related to relatively long term testing procedures.

2. EXPERIMENTAL

In the attempt to anticipate compatibility problems which may arise in pyrotechnic systems, the measurement of electrochemical potentials has been useful. This is particularly true if the pyrotechnic composition contains soluble or hygroscopic materials because manufacturing procedures usually do not exclude moisture from pyrotechnic assembly areas. Two types of measurement that yield relevant information are the potentiokinetic sweep and the measurement of mixed, or corrosion potentials, which result when two or more metals or alloys are interfaced by an electrolyte while in electrical contact.

A potentiokinetic sweep is performed by immersion of an electrode of the metal in a saturated solution of the appropriate soluble substance, together with a standard electrode, in our case a saturated calomel electrode (SCE). A potential is imposed upon the couple, and this potential is varied over a range of values. A record of current versus electrode potential is obtained. The polarization curve reflects the behavior of the electrode-electrolyte system in a general sense; it may reveal active-passive behavior, the passive potential range, if any, and the critical current density required to break down passivation. It may also reveal anodic hysteresis, often noted in metals subject to electrochemical pitting.

The corrosion potential is also measured against a standard electrode but in a different fashion. An electrode of the metal of interest is immersed in water, or a saturated solution of a suitable soluble phase, and allowed to come to equilibrium with the solution. The potential difference developed between it and a standard electrode is then measured with a high impedance voltmeter. If two or more metals are in electrical contact with one another, the one showing the highest negative potential (referenced to the standard) may be expected to function as the anode of a cell when exposed to a conductive solution. The corrosion potential results from the interaction of the work functions of the metals present with the thermodynamic and kinetic properties of the specific solvent-electrolyte environment. Measurements of this type enable the investigator to determine whether the conditions necessary to develop corrosion exist; determination of rates of reaction must depend upon other methods.

A pyrotechnic composition produced by coprecipitation of potassium perchlorate, (KClO_4), and potassium hexacyanocobaltate (III), $\text{K}_3[\text{Co}(\text{CN})_6]$, was being considered for an actuator having a nichrome bridge-wire welded to kovar pins which passed through a metallized ceramic header. The absence of data concerning the compatibility of this pyrotechnic with the proposed structural materials required an investigation into possible degradative interactions. A quantity of $\text{K}_3[\text{Co}(\text{CN})_6]$ was prepared, twice recrystallized from water and air dried.⁽⁵⁾ This material, which is very soluble in water, was found to gain 4.6% in weight at room temperature over a three day period when exposed to a relative humidity of 50%. Further investigation revealed that this material would gain about 0.9% in weight when exposed to 50% relative humidity for four hours. Given the hygroscopic nature of the potassium hexacyanocobaltate(III) and the fact that the device employing it must operate over a range of temperatures, the corrosion potentials of kovar and two types of nichrome in solutions of potassium hexacyanocobaltate(III), potassium perchlorate, and the mixture were measured. The two types of nichrome utilized were tophet A and tophet C, which could not be distinguished from one another in the potentiokinetic sweep.

Potentiokinetic sweeps were made by exposing strips of nichrome ($\sim .25 \text{ cm}^2$) and lengths of kovar wire ($\sim .60 \text{ cm}^2$) to $\sim 50 \text{ ml}$ of solution each. Starting from minus 500 mv referenced to a saturated calomel electrode (SCE) (or minus 1000 mv in some cases), the potential was increased linearly at a rate of 5 mv/sec to plus 1200 mv SCE, and linearly decreased back to minus 500 SCE. Current was recorded versus electrode potential.

Corrosion potentials were recorded for each system one half hour after the immersion of freshly cleaned metal samples.

3. RESULTS AND DISCUSSION

3.1 POTENTIOKINETIC SWEEP

Both nichrome and kovar exhibit regions of activity and passivity in all three of the solutions examined. The results for nichrome are essentially the same in solutions of potassium hexacyanocobaltate and the pyrotechnic, and the results for kovar are likewise essentially the same in these solutions.

The polarization curve for kovar in the pyrotechnic exhibits a pronounced active region extending from about minus 650 mv, SCE to minus 350 mv SCE, and exhibits pronounced anodic hysteresis.

3.2 CORROSION POTENTIALS

When corrosion potentials were measured as discussed above, the values given in Table 1 were obtained.

may be due to a reduction in solubility due to the common ion effect between the two potassium salts.

When each of the corrosion potentials is located on the corresponding polarization diagram, it is found that all six fall within regions of passivity. Kovar, however, falls very near the border of its active region, and it is likely that the potential could drift by as much as 100 mv as a result of temperature changes or changes in the amount of dissolved O_2 in the solution. Such a drift in the cathodic direction would probably activate kovar to galvanic attack.

3.3 SEM ANALYSIS

The metallic samples were examined for evidence of corrosive attack by scanning electron microscopy (SEM). The SEM examination of the kovar samples subjected to the potentiokinetic sweep did indeed confirm that an active region exists. Extensive pitting on the kovar surface occurred (Figure 1). Therefore, compatibility problems should be readily detected by

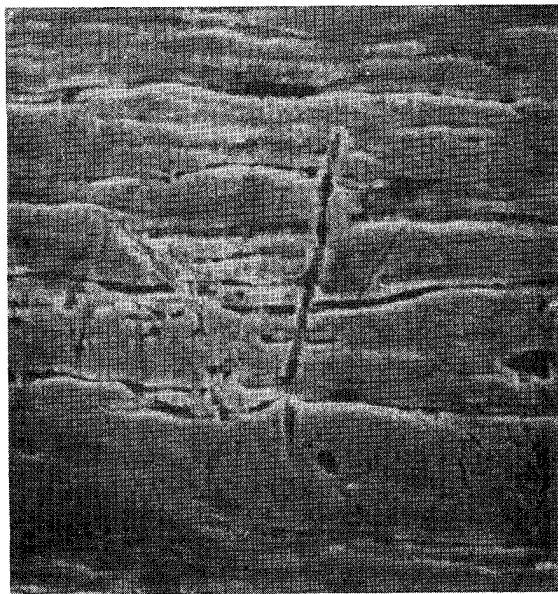
Table 1

	Potential (mv SCE)		
	<u>KClO₄</u>	<u>K₃[Co(CN)₆]</u>	<u>Pyrotechnic</u>
Kovar	-150	-250	-350
Nichrome	-150	-350	-280

In view of the apparent insensitivity of these metals to the presence of potassium perchlorate as evidenced by the potentiokinetic sweep data, the reversal of position exhibited by kovar and nichrome when potassium hexacyanocobaltate is replaced by the pyrotechnic is not understood. It

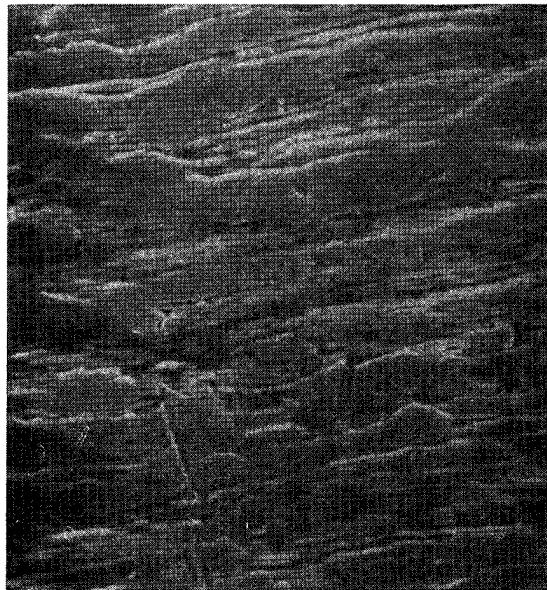
inspection of the kovar provided enough time is given to cause this pitting to occur.

Similar SEM examination of the nichrome samples subjected to the potentiokinetic sweep also show activity on the surfaces.



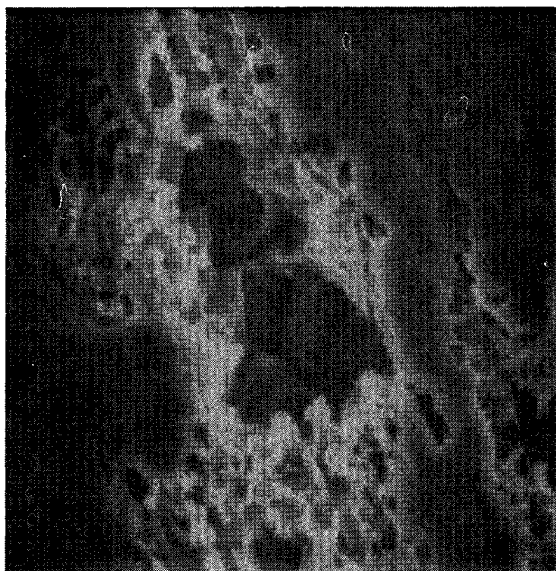
Kovar-Control

1000X
SEM



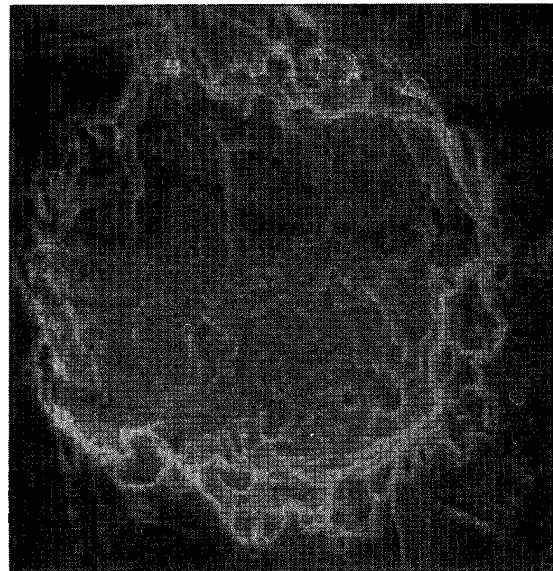
Kovar/KC10₄

600X
SEM



Kovar/K₃[Co(CN)₆]

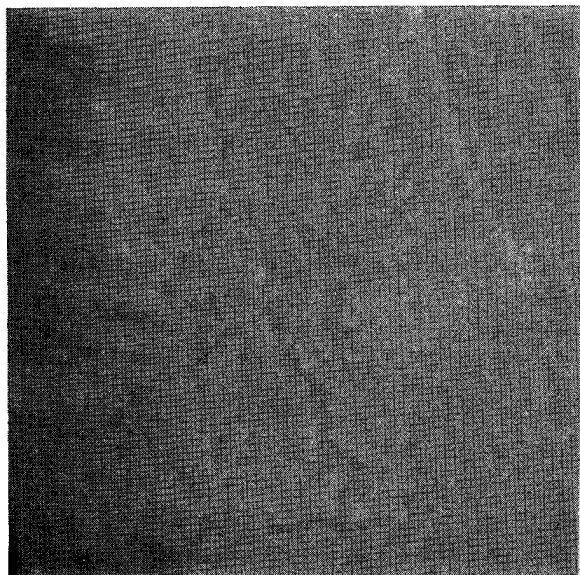
1800X
SEM



Kovar/Pyrotechnic

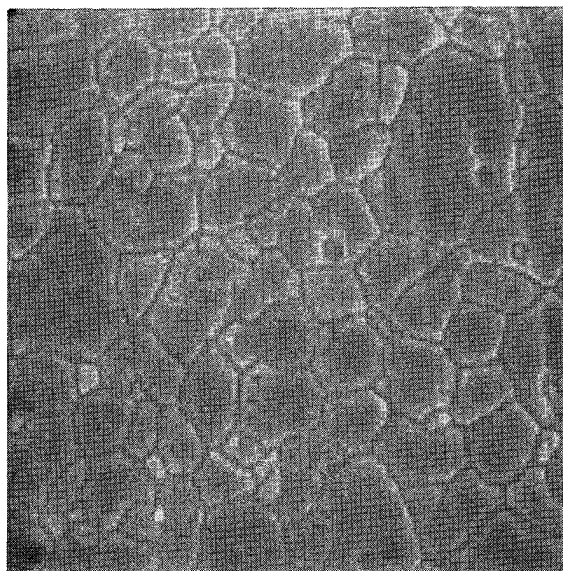
900X
SEM

Figure 1: Kovar samples subjected to potentiokinetic sweep



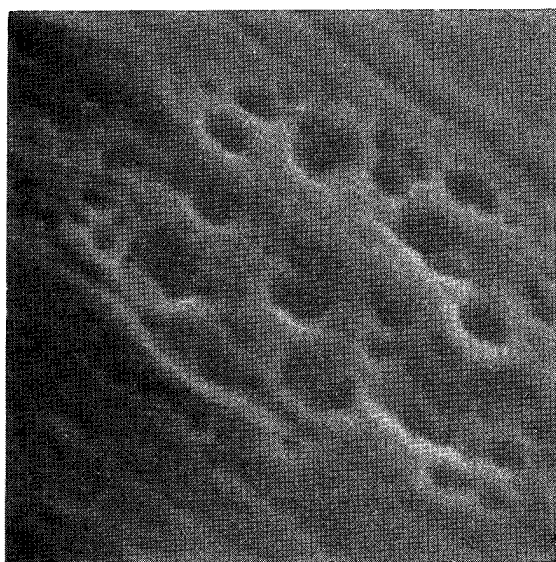
Nichrome Control

1800X
SEM



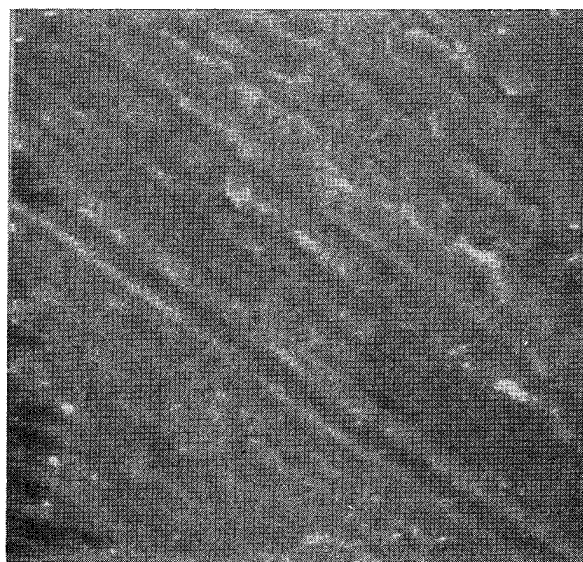
Nichrome/KClO₄

1800X
SEM



Nichrome/K₃[Co(CN)₆]

3000X
SEM



Nichrome/Pyrotechnic

1800X
SEM

Figure 2: Nichrome samples subjected to potentiokinetic sweep

Photomicrographs show grain boundary etching, pitting, and surface corrosion occurring during this test procedure (Figure 2). As with kovar, these characteristics should be easily observed by inspection during actual use.

The distinct advantage of utilizing the potentiokinetic sweep is that the technique permits the possible creation of an accelerated incompatible environment which can be used as a model for further studies of compatibility of materials. Phenomena observed with this technique which provides a severe overtest of storage conditions will very likely be observed during actual stockpile of similar materials, but after a longer time. Tests such as thermal aging or humidity storage should also accelerate surface activity of the samples and could be used as short or long term compatibility tests to confirm previous findings.

4. ACCELERATED AGING STUDIES

Given the evidence of possible incompatibility presented in the previous section, a long term thermal/humidity aging study was initiated to look for evidence of incompatibility. Accordingly, samples of kovar, tophet A, and tophet C were placed in separate containers, one type of metal to a container, for exposure to potassium hexacyanocobaltate or the pyrotechnic mixture. These samples were isothermally aged at 50°C, 75°C, and 100°C. Control samples of metal were also maintained in the same thermal environments. A similar set of samples was maintained at room temperature in a 75% relative humidity environment. Samples were removed for examination at 18 days, 100 days, and 260 days and examined with the SEM for possible corrosion (Tables 2 through 5). Any signs of corrosion on the wires during this test would then preclude consideration of these combinations for Sandia components.

Table 2

Sample	100°C Environmental Exposure		
	Time Period		
	18 Days	100 Days	260 Days
Kovar $K_3[Co(CN)_6]$	No change	No change	No change
Pyrotechnic	No change	No change	No change
Tophet A $K_3[Co(CN)_6]$	No change	Some pitting, slight surface corrosion	Some pitting, general corrosion and grain boundary etching in both materials
Pyrotechnic	No change	Slight corrosion	
Tophet C $K_3[Co(CN)_6]$	No change	Some pitting, slight corrosion	Some pitting, general corrosion and grain boundary etching in both materials
Pyrotechnic	No change	Slight corrosion	

Table 3

<u>Sample</u>	75°C Environmental Exposure		
	<u>Time Period</u>		
	<u>18 Days</u>	<u>100 Days</u>	<u>260 Days</u>
Kovar $K_3[Co(CN)_6]$	No change	No change	No change
Pyrotechnic	No change	No change	No change
Tophet A $K_3[Co(CN)_6]$	No change	Some pitting, slight surface corrosion	Pitting, general surface corrosion and grain boundary etching in both materials
Pyrotechnic	No change	Very slight sur- face corrosion	
Tophet C $K_3[Co(CN)_6]$	No change	Some pitting, slight surface corrosion	Pitting, general surface corrosion and grain boundary etching in both materials
Pyrotechnic	No change	Very slight sur- face corrosion	

Table 4

<u>Sample</u>	50°C Environmental Exposure		
	<u>Time Period</u>		
	<u>18 Days</u>	<u>100 Days</u>	<u>260 Days</u>
Kovar $K_3[Co(CN)_6]$	No change	No change	No change
Pyrotechnic	No change	No change	No change
Tophet A $K_3[Co(CN)_6]$	No change	No change	Some pitting, slight surface corrosion
Pyrotechnic	No change	No change	Some pitting, slight surface corrosion
Tophet C $K_3[Co(CN)_6]$	No change	No change	Some pitting, slight surface corrosion
Pyrotechnic	No change	No change	Some pitting, slight surface corrosion

Table 5

50% RH Environment

Sample	Time Period		
	18 Days	100 Days	260 Days
Kovar $K_3[Co(CN)_6]$	No change	No change	No change
Pyrotechnic	No change	No change	No change
Tophet A $K_3[Co(CN)_6]$	No change	No change	General to extensive corrosion
Pyrotechnic	No change	No change	General corrosion
Tophet C $K_3[Co(CN)_6]$	No change	No change	General to extensive corrosion
Pyrotechnic	No change	No change	General corrosion

After 18 days in the thermal and humidity environments, the samples showed no evidence of corrosion or activity on the surface.

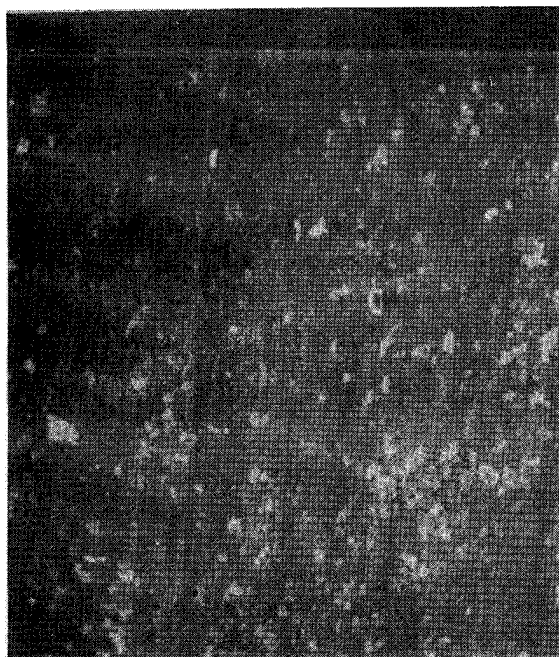
After 100 days in all environments, the kovar samples still showed no signs of surface activity or corrosion, but the tophet A and tophet C samples subjected to the 75°C and 100°C environments for 100 days showed indications of surface activity. Little or no activity was observed on the 50°C or relative humidity samples.

A definite increase in the number of pits was observed in the tophet wires with time and temperature (Figure 3). This increase was not observed in the control samples. The number of pits in the wires in contact with the potassium hexacyanocobaltate were observed to be greater than those with the pyrotechnic. This suggests that potassium hexacyanocobaltate(III) is more reactive than the pyrotechnic, that $KClO_4$ passivates the material, or that a concentration effect is in evidence. One wire subjected

to the 100°C/100 day environment with potassium hexacyanocobaltate revealed a large area of significant corrosion (Figure 3).

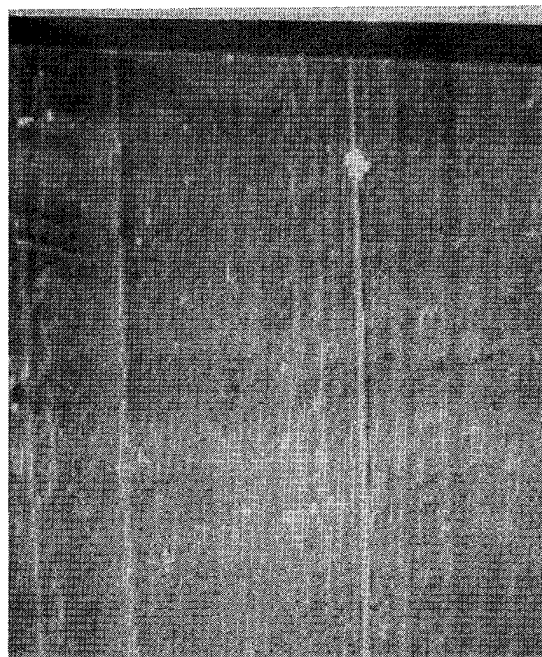
The tophet C wires with both the potassium hexacyanocobaltate(III) and the pyrotechnic showed a slight fading of the mechanical drawing marks with time, which indicates some surface corrosion was starting to occur. If alteration of the surface characteristics and the increased number of pits is compared to findings from the potentiokinetic sweep data, a correlation is observed between the two techniques for tophet A and C within 100 days.

Samples removed after 260 days for the tophet A and tophet C materials agree very closely to observations made after 100 days (Figure 4). Besides the continued surface activity observed in the 75°C and 100°C samples during this additional time period, a similar type of activity was observed in the 50°C and humidity samples.



Tophet A/ $K_3[Co(CN)_6]$
75°C/100 days

1000X
SEM



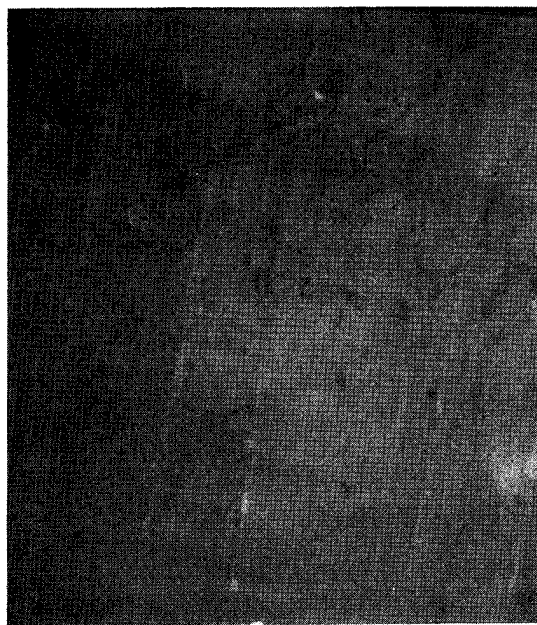
Tophet A/Pyrotechnic
75°C/100 days

1000X
SEM



Tophet A/ $K_5[Co(CN)_6]$
75°C/100 days

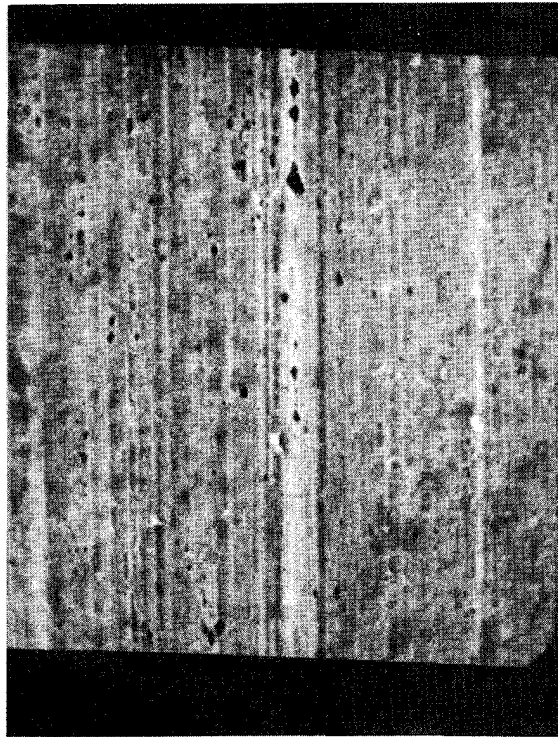
750X
SEM



Tophet A Control
75°C/100 days

1000X
SEM

Figure 3: Tophet wires after 100 days environmental exposure



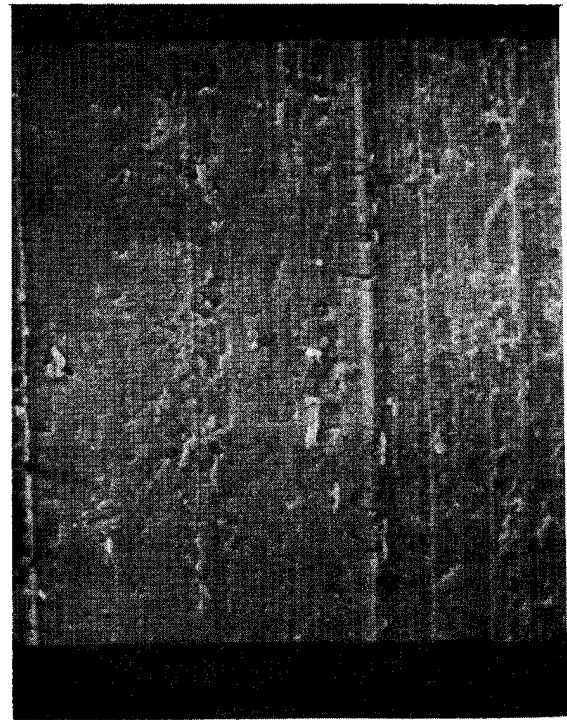
Tophet A - Control
75°C/260 days

1000X
SEM



Tophet A/Pyrotechnic
75°C/260 days

1000X
SEM



Tophet A/Pyrotechnic
75°C/260 days

1000X
SEM

Figure 4: Tophet A wires after environmental exposure (260 days)

In addition, the tophet A samples aged at 75°C and 100°C for 260 days in the pyrotechnic are starting to show the faint grain boundary etching phenomena that occurred in nichrome samples during the potentiokinetic sweep work (Figure 5). Both tophet A and C exposed to the potassium hexacyanocobaltate for 260 days in the 75% relative humidity environment had general to extensive surface corrosion on the surfaces, which again was similar to that observed in the potentiokinetic sweep study (Figure 6).

The greater observed surface corrosion for the tophet C with the pyrotechnic and potassium hexacyanocobaltate(III) combinations at both 75°C and 100°C for 260 days indicates continued surface corrosion beyond that observed for 100 days (Figure 7). Fading of the tophet C wire drawing marks was also noted in the 75% relative humidity samples.

Aging studies with the kovar after 260 days and under all conditions did not show surface changes. Some possible pitting may be starting, but the numbers per unit area are not significantly above that observed for the blanks. In no case was extensive surface activity observed like that found during the potentiokinetic sweep study. It appears that kovar requires longer exposures to thermal and humidity environments with these pyrotechnic materials to cause the phenomena observed during a potentiokinetic sweep.

Thus, in the case of nichrome (tophet A or C), it can be stated that an excellent correlation exists between the results of the short term potentiokinetic sweep or corrosion potential studies and long term SEM examinations, leading to the conclusion that an incompatibility exists for the

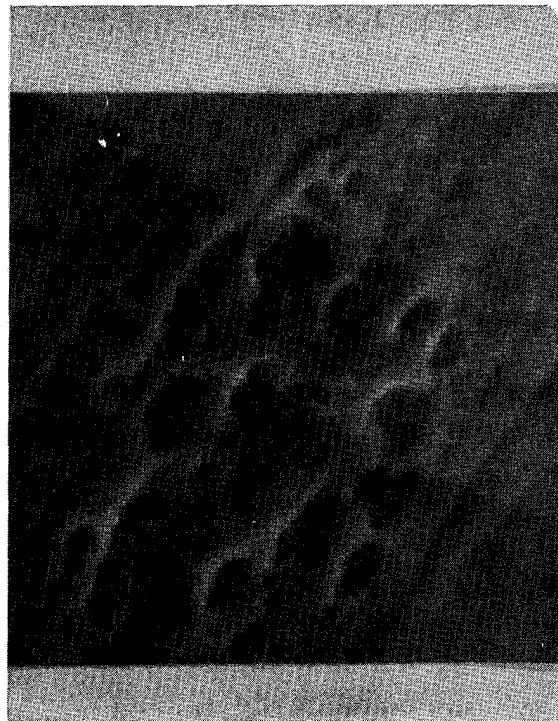
pyrotechnic-bridgewire combination.

5. CONCLUSIONS

Through the use of the corrosion potentials or the potentiokinetic sweep surface reaction as a short term or screening test, an incompatibility between structural materials and a pyrotechnic has been revealed. The long term aging studies of the metal samples tophet A and tophet C with potassium hexacyanocobaltate and the pyrotechnic confirmed that the screening tests were valid tests. The SEM revealed these changes long before the calssical compatibility tests would have revealed their presence. Based upon normal prediction criteria, changes in components within two to three years would be expected. This is far short of the stockpile life expected for Sandia components.

REFERENCES

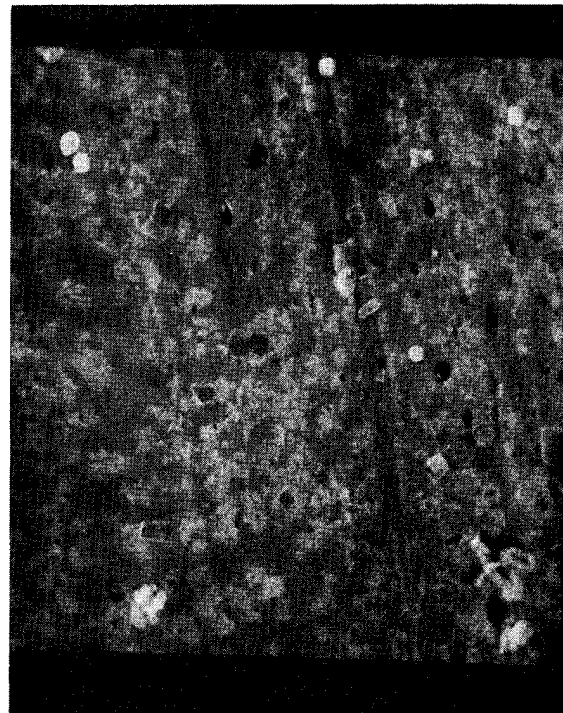
1. Military Explosives, Depts. of the Army and the Air Force, TM-9-1910, April 1955.
2. Personal communication between T. M. Massis and D. L. Seaton of the Lawrence Livermore Laboratory (LLL), who developed this gas chromatographic technique for compatibility testing.
3. Buxton, R. J. and Massis, T. M., "Compatibility of Explosives with Structural Materials of Interest," SC-M-70-355, August 1970.
4. Buxton, R. J. and Massis, T. M., "Compatibility of Explosives with Structural Materials of Interest," SC-M-70-355, Vol. II, June 1972.
5. Fernelius, W. C. (ed.), Inorganic Synthesis, McGraw-Hill, New York, 1946, p. 225.



Nichrome/ $K_3[Co(CN)_6]$ 3000X
 Potentiokinetic Sweep SEM
 Note appearance of grain boundary etching

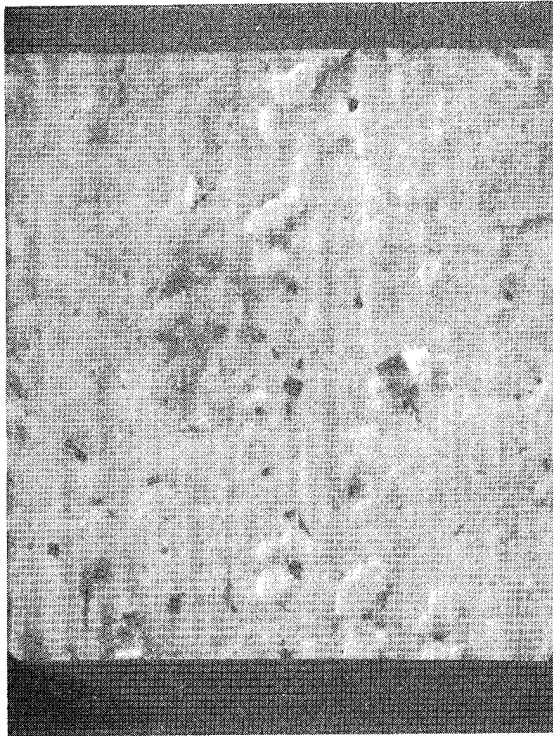


Tophet A/Pyrotechnic 3000X
 75°C/260 days SEM
 Note appearance of grain boundary etching

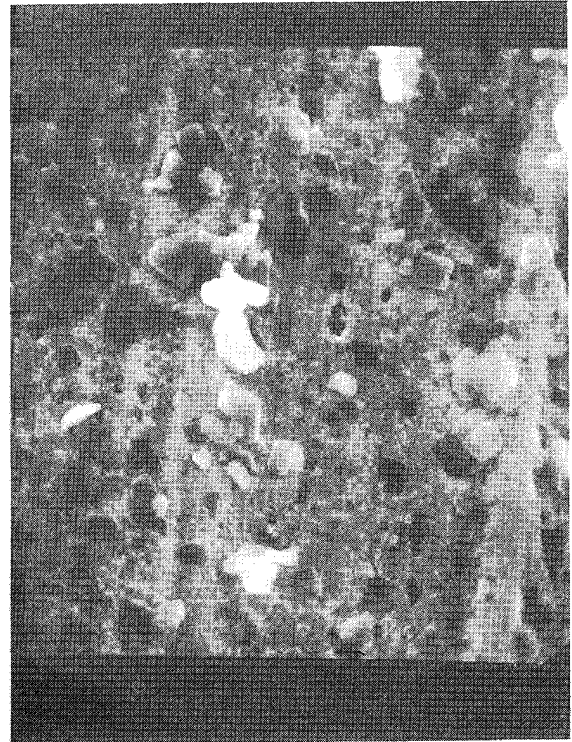


Tophet C/Pyrotechnic 3000X
 75°C/260 days SEM

Figure 5: Tophet wires after environmental exposure

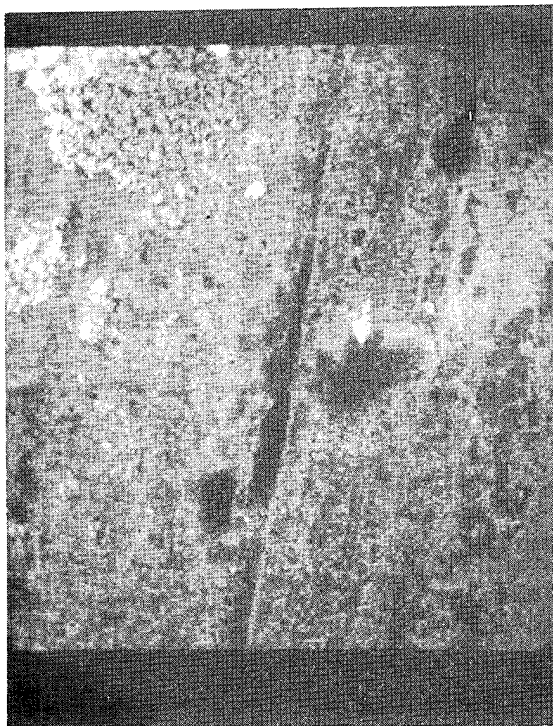


Tophet A/ $K_3[Co(CN)_6]$ 3000X
50% RH/260 days SEM



Tophet C/ $K_3[Co(CN)_6]$ 3000X
50% RH/260 days SEM

Figure 6: Tophet wires exposed to 50% RH environment



Tophet C/ $K_3[Co(CN)_6]$ 1000X
75°C/260 days SEM



Tophet C/Pyrotechnic 1000X
100°C/260 days SEM

Figure 7: Tophet C wires after environmental exposure

Cleared for public release by
Naval Sea Systems Command
Public Affairs - OOD2
/s/ R. C. Bassett, Case #136
November 8, 1974

A NEW, HIGHLY STABLE AND COMPATIBLE SMOKELESS ROCKET PROPELLANT

A. T. Camp, E. R. Csanady, and P. R. Mosher
Naval Ordnance Station, Indian Head, Md.

ABSTRACT

A smokeless, plateau-burning double-base rocket propellant has been developed without lead or nitroglycerin. This offers major improvements over conventional double-base in stability, safety, compatibility with typical rocket materials and environmental impact during manufacture and use. Energy is ten percent higher than that of N-5 double-base propellant, widely used in the 2.75-inch aircraft rocket Shillelagh, and ASROC missiles since 1954. Scale-up studies are being done at the Radford Army Ammunition Plant under sponsorship of the Army's 2.75 project office.

1. INTRODUCTION

Double-base rocket propellants have served many of the nation's military needs since 1943 and are still in widespread use today. Several new rockets and improvements of existing ones use double-base propellants in preference to ammonium perchlorate/rubber-base compositions. The reasons for this include lower system cost, high production capacity in government-owned, contractor-operated plants, low signature of exhaust under most atmospheric conditions, insensitivity to oxygen and water, very long shelf life, very low dependence of performance on conditioned rocket temperature, and non-corrosivity of exhaust. In spite of these several good features smokeless double-base propellants have several disadvantages in comparison with rubber-base composites. Among these are lower volumetric efficiency, (unless aluminum and Class A materials such as HMX are used), migratory tendencies of nitroglycerin, incompatibility of migrated NG with many materials, and moderately toxic effects of the lead compounds ordinarily used to provide temperature insensitive ballistics (plateau and mesa burning).

2. DISCUSSION

This paper deals with a plateau-burning propellant system of moderate energy which has all the attractive features of Class B, Class 2 types of double-base but contains no migrating plasticizers and no

lead compounds. This propellant is being scaled-up with Army funding for evaluation in the world-renowned 2.75-inch Folding Fin Aircraft Rocket as a potential replacement for the twenty-year-old N-5 double-base "leaded" propellant. Although it contains only ten percent more energy, it will be used at sufficiently higher pressure and higher burn rate than N-5 to be much more effective, and will have more nearly constant ballistics over long periods of aging. Thus, it affords very substantial improvements over existing double-base systems in typical tactical rockets. In typical hot storage tests at 80°C (176°F) AA-10 lasted 237 days, nearly twice as long as N-5 and four times as long as the principal World War II, U. S. rocket propellant, designated JPN.

The composition of NOSIH AA-10 propellant is not yet fully optimized. However, its primary nitrate, energetic plasticizers have been available commercially for 15 years and are less volatile than nitroglycerin by as much as two orders of magnitude. Hence, they do not cause appreciable headaches to operators. With common rocket seals and typical inhibitors such as cellulose acetate and ethyl cellulose these plasticizers show less than one-tenth the migration tendencies of NG or the inert plasticizers normally used to desensitize NG. One problem noted in scale-up is the apparently critical nature of the condition of the fibrous nitrocellulose prior to its incorporation in propellant.

The ballistic modifier content of AA-10 is about one-fifth that required formerly to produce plateau or mesa burning rate-pressure relationships in propellants of this energy level. The modifier is water-insensitive and does not increase the human toxicity of the typical smokeless exhaust products produced by nitrate esters: namely N_2 , CO_2 , H_2O , CO and H_2 .

Compatibility of NOSIH AA-10 with typical components of rocket and gun propulsion designs is expected to be outstanding, based on usage of other energetic compositions which contain the same plasticizers. Although safe, useful lives for double-base propelled ordnance such as the 2.75 FFAR and 5-inch ZUNI rockets, often exceed ten or fifteen years, it is expected that modern ordnance using NOS AA-10 propellant will reach technological obsolescence long before the propellant degrades below the rigorous standards of ballistic performance imposed on tactical weapons.

Modifications of AA-10 are also being evaluated as gun propellants, identified as NOSOL's. Such propellants offer in guns many of the same advantages identified for AA-10 in rockets.

3. BIOGRAPHIES

A. T. CAMP: Born in Jamestown, New York, January 6, 1920. Received his B.E. in Chemical Engineering from Yale in 1941, & M.S. in Industrial Management from MIT in 1956. Employed as research associate at Hercules, Inc. 1941-1950; Naval Ordnance Test Station, China Lake, CA, 1950-1959, ultimately as Head, Propellants Division; Lockheed Propulsion Company 1959-1964 as Director of Propellant Development; Naval Ordnance Station, Indian Head, MD, 1964 to present, in several senior capacities. Presently Special Assistant to the Technical Director for Propellant Technology. Inventor of several propellants and devices widely used in U. S. ordnance.

E. R. CSANADY: Born in Cleveland, Ohio, September 18, 1915. Attended New River State and received his BSChE from West Virginia University in 1940. Employed in various capacities by E. I. DuPont, Jones & Laughlin Steel Corp., Pittsburgh Ordnance District before entering Military service in 1942; Served with Army Air Corps during World War II; Chemist with American Rolling Mill Company 1946-1947; Naval Ordnance Station 1947 to present as a Chemical Engineer in various capacities. Presently Consultant for Double Base Propellants. Inventor of propellants used by U. S. Navy. Holder of several patents in propellant technology area.

P. R. MOSHER: Born in Dillon, Montana, November 17, 1916. Received his bachelors degree in Chemical Engineering in 1938 from CCNY, and Masters from Columbia in 1940. Also attended University of Delaware and George Washington University. Employed in various capacities in private industry-Hercules, General Chemical, General Motors, before joining Naval Ordnance Station in 1956. Presently Chemical Engineering supervisor of a branch in the NOS Pilot Plant. Holder of patents in fields of gun propellants, paints, soaps, rocket powder, and torpedo fuel.